Homological Invariants of Strongly Invertible Knots

Michael Snape

Submitted in fulfilment of the requirements for the
Degree of Doctor of Philosophy

School of Mathematics & Statistics
College of Science & Engineering
University of Glasgow

December 2018

Abstract

This thesis explores the relationship between Khovanov homology and strongly invertible knots through the use of a geometric construction due to Sakuma. On the one hand, new homological and polynomial invariants of strongly invertible knots are extracted from Sakuma's construction, all of which are related to Khovanov homology. Conversely, these invariants are used to study the two-component links and annular knots obtained from Sakuma's construction, the latter of which are almost entirely disjoint from the class of braid closures. Applications include the problem of unknot detection in the strongly invertible setting, the efficiency of an invariant when compared with the η-polynomial of Kojima and Yamasaki, and the use of polynomial invariants to bound the size of the intrinsic symmetry group of a two-component Sakuma link. We also define a new quantity, $\varkappa_A$, and conjecture that it is an invariant of strongly invertible knots.

Acknowledgements

Just as no knot is complete without its ambient space, no thesis is created in a vacuum. I would therefore like to thank the following people for their assistance in making this work possible.

Firstly, this thesis owes a huge amount to the guidance of Liam Watson. I would like to thank him for sharing with me his infectious enthusiasm for low-dimensional topology and for being a constant source of inspiration, not to mention his fantastic blackboard artwork (which is well worth a view [93]).

I would also like to thank Brendan Owens for his support throughout my PhD, especially for helping me prepare for my Cecil King presentation, and for keeping an eye on my progress here in Glasgow after Liam moved back to Canada. I would also like to thank him for his assistance during the corrections stage, and in particular for making time to go through the alterations I made to the definition of $\varkappa_A$.

I would like to thank Eli Grigsby for her interest in my work, and for answering my questions about annular Khovanov homology, the d_t invariant, and sutured Floer homology.

Thanks too should go to my office mate, Andy Monk, who has been a massive help in getting me through the existential crises that inevitably accompany a pure maths PhD. I'm not quite sure how it's happened, but we've done it!

In the summer of 2016 I spoke at the ECSTATIC conference at Imperial College, which was a fantastic experience. I would like to thank Tom Hockenhull and Marco Marengon, the organisers, for inviting me to give a talk and for running such a great conference.

For the last four months of 2017 I visited Liam at the Université de Sherbrooke in Québec, Canada, which was funded by a Jim Gatheral travel scholarship. I would like to thank to Lise Charbonneau at UdeS who was invaluable in helping me with the necessary paperwork — especially when I had to reapply for a work permit at the last minute due to general incompetence! I would also like to thank the staff and students of the mathematics department at UdeS for making me feel welcome, especially Noémie Leymonerie and Denis Langford. I also want to thank Clementina Bouche, Jean-Simon Caunter, and Emilie Simard for the hours of bouldering and belaying at Lac Larouche and Vertige; and thanks to Clem for the invites to the pot lucks at Tierra del Fuego. You all helped a homesick Anglophone feel much less lonely — merci beaucoup à tous!

I also want to thank all my friends in Glasgow and the rest of the UK for helping take my mind

off mathematics, especially during the painful writing up process. Thanks also to the Glasgow University Mountaineering Club and all its members, past and present, at home and abroad, for all the fantastic memories, and for giving me the opportunity to learn to trad climb.

I want to thank my family for their support, especially Mary, who showed me that it could be done!

Lastly, I want to thank Tor for all her love and support during these past four years. I look forward to starting the next journey with you!

Declaration

I declare that, except where explicit reference is made to the contribution of others, this thesis is the result of my own work and has not been submitted for any other degree at the University of Glasgow or any other institution.

Contents

List of Figures

List of Tables

List of Symbols

$\cong$	Homeomorphic, isomorphic, link equivalent
$\simeq$	Filtered quasi-isomorphic
$\mathbb{C}, \mathbb{R}, \mathbb{Q}, \mathbb{Z}, \mathbb{F}$	Complex numbers, reals, rationals, integers, general number field
Z_n, D_n, S_n	Cyclic group of order n, dihedral group of order $2n$, permutation group on n objects
S^3, B^3	3-sphere, 3-ball
S^1	1-sphere
D^2	2-disc
I	Unit interval $[0, 1]$
A	Annulus, $S^1 \times I$
$\mathcal{U}$	Unknot
D_L	Link diagram
RI, RII, $RIII$	Reidemeister moves
$Wr(D_L)$	Writhe of a link diagram
$\mathrm{lk}(L)$	Linking number of a link
$SWr(D_L)$	Self-writhe of a link diagram
$L_1 \sqcup L_2$	Disjoint union of links L_1, L_2
$K_1 \# K_2$	Connect sum of knots K_1, K_2
$T(p, q)$	Torus knot of type (p, q)
$Sat(P, C)$	Satellite link with pattern P and companion knot C
$\mathcal{N}(L)$	Tubular neighbourhood of a link L
$E(L)$, $S^3 \backslash \mathcal{N}(L)$	Link exterior
$-L$	Inverse of the link L
$\overline{L}$	Mirror image of the link L
$Sym(L)$	Symmetry group of the link L
$MCG(X)$	Mapping class group of manifold X
$Sym^*(L)$	Intrinsic symmetry group of link L
$\Gamma(L)$	For an n-component link L the group $\mathbb{Z}/2\mathbb{Z} \times (\mathbb{Z}/2\mathbb{Z}^n \rtimes S_n)$
(K, h)	Strongly invertible knot with involution h
$(\mathcal{U}, h_0)$	Strongly invertible unknot
$D(K)$	The knot $K \# -K$ for some oriented knot K
$(\overline{K, h})$	Strongly invertible mirror of (K, h)

$S(\alpha, \beta)$	2-bridge knot of type (α, β)
$\mathbb{L} = \mathcal{B} \cup \mathcal{L}$	Sakuma link with branch-set component $\mathcal{B}$ and longitude component $\mathcal{L}$
(K, h, n)	Framed strongly invertible knot
$\mathbb{L}_n$	Framed Sakuma link
$\Sigma(S^3, L)$	Double branched cover of S^3 over the link L
(B^3, τ)	n-string tangle
$(D^2 \times I, \tau)$	n-string sutured tangle
B_n	n-strand braid
$\widehat{B_n}$	Closure of B_n
$\widehat{T}$	Braid-like closure of sutured tangle T
$H_n(X; R)$	The nth homology group of X with coefficients in R
$\eta(L)$	η-polynomial of a link L
$\Delta(K)$	Alexander polynomial of a knot K
$J(L)$	Jones polynomial of a link L
$\widehat{J}(L)$	Unnormalised Jones polynomial of a link L
$\langle D_L \rangle$	Kauffman Bracket of link diagram D_L
$AJ(L)$	Annular Jones polynomial of annular link L
$\langle D_L \rangle_A$	Annular Kauffman bracket of an annular link diagram D_L
ω	Wrapping number of an annular link L
$[\![D_L]\!]$	Khovanov bracket of link diagram D_L
CKh	Khovanov chain complex
Kh	Khovanov homology
$\widetilde{CKh}$	Reduced Khovanov chain complex
$\widetilde{Kh}$	Reduced Khovanov homology
$CAKh$	Annular Khovanov chain complex
AKh	Annular Khovanov homology
SFH	Sutured Floer homology
$\widehat{HFK}$	Knot Floer homology
$\varkappa$	Watson's $\varkappa$ invariant
$\varkappa_A$	$\varkappa_A$ invariant
TKh	Tangle Khovanov homology

Introduction

The study of knot and link symmetry has its roots in the very beginning of knot theory. Indeed, ever since the first knot tables were being complied by Tait in the 19th century [85] questions about their symmetry properties were raised. For example, a natural query that arises is which knots are *amphicheiral*; that is, which are equivalent to their mirror images. Also of interest is the question of knot invertibility; if we consider the orientation of a knot curve, an *invertible knot* is one which equivalent to itself with the orientation reversed. It was unclear for a time whether or not a non-invertible knot existed, a problem which wasn't resolved until the 1960s when Trotter [89] found an infinite family of non-invertible knots. Today, the study of knot symmetry is still an active area of research; for example a recent result of Paoluzzi and Sakuma [67] has answered a longstanding open question regarding the existence of amphicheiral prime knots with free periodic symmetries of period 2.

The principal objects of study appearing in this thesis are *strongly invertible knots*. These are knots paired with a particular symmetry, known as a strong inversion, which is an involution of S^3 that reverses the orientation of the knot. All strongly invertible knots are invertible by definition, but there are examples of invertible knots which are not strongly invertible [26] [98]. For knots with a small number of crossings, strongly invertible knots are particularly prevalent; as Sakuma notes [79], about 85% of the prime knots with 10 crossings or less admit strong inversions. In addition, strongly invertible composite knots are easily constructed by taking the connect sum of any oriented knot with its inverse.

In addition to strongly invertible knots we will be concerning ourselves with a geometric construction, first developed by Sakuma [79], which allows us to associate to every strongly invertible knot a unique two-component link with both components unknotted. The link should be viewed as an auxiliary object of the strongly invertible knot — an invariant of the link is by construction an invariant of the strongly invertible knot. Indeed, Sakuma's motivation for his construction was to apply the η-polynomial of Kojima and Yamasaki [46] to strongly invertible knots.

While strongly invertible knots may appear to be a relatively unassuming class of objects, they make appearances in the wider field of low-dimensional topology, perhaps most notably in the *Berge conjecture*. In an unpublished work Berge [6] produced a list of knots which admit lens space surgeries; it was then conjectured is that this list is exhaustive, that is, if a knot admits a lens space surgery it must be one of knots in Berge's list. Interestingly, as Watson notes in the introduction of [91], the Berge conjecture can be restated in terms of strongly invertible knots.

Berge knots are genus 2, so by a result of Osborne [63] are strongly invertible; the conjecture then comes down to first showing that any knot admitting a lens space surgery is strongly invertible, then showing that a strongly invertible knot admitting a lens space surgery is a Berge knot. However, not all strongly invertible knots admit lens space surgeries. Watson constructs for each strongly invertible knot a certain quotient tangle, which we shall call the *Watson tangle*, and proves that surgeries on strongly invertible knots correspond to double branched covers of S^3 over certain closures of the associated quotient tangle. Using this fact he developed obstructions for strongly invertible knots to admit lens space surgeries using *Khovanov homology*, our other main protagonist.

The development by Khovanov of a homology theory for links [40] in the late 1990s resulted in a explosion of new algebraic tools available to knot theorists. Khovanov homology was the first of what became known as 'categorified' knot invariants, by which we mean homological invariants whose Euler characteristics return a classical polynomial invariant. In the case of Khovanov homology, it is the categorified version of Jones polynomial — a polynomial invariant first constructed by Jones in the 1980s [34]. The advantage of working with categorified invariants over polynomial ones is that they contain more stucture, which allows for more applications. Perhaps the most archetypal example of this is Rasmussen's s invariant [73], which is defined using the Lee spectral sequence from Khovanov homology to Khovanov-Lee homology [48]. Using the s invariant Rasmussen was able to come up with a purely combinatorial proof of the Milnor conjecture.

The use of spectral sequences converging from Khovanov homology to other homology theories has become a standard technique for knot theorists, and has led to a number of celebrated discoveries. An important example is Kronheimer and Mwroka's proof that Khovanov homology detects the unknot [47], which exploited a spectral sequence from Khovanov to instanton Floer homology. Another came from Ozsváth and Szabó [66], who exhibited a spectral sequence between the Khovanov homology of a link and the Heegaard-Floer homology of its double-branched cover. In fact, the connection between Khovanov-style homology theories and Heegaard-Floer-style theories is so widespread that a collection of sequences have been uncovered; see, for example, papers by Roberts [76], and Grigsby and Wehrli [22] [23]. A variation of Khovanov homology of particular interest in this thesis is *annular Khovanov homology*, which is an invariant of links in the thickened annulus $A \times I$, instead of the usual 3-sphere. Annular links are a naturally occurring set of objects, appearing, for example, in the construction of satellite knots; as closures of braids; and as quotients of periodic knots by their symmetry, when viewed as lying in the exterior of the axis of rotation.

In recent years attempts have been made to understand the interplay between Khovanov homology and knot symmetries. For example, Watson [92] has defined a homological invariant of strongly invertible knots, $\varkappa$, using Khovanov homology. His invariant provides compelling evidence that quantum topological invariants can be a source of powerful new tools for studying strongly invertible knots. Another important set of examples have as their motivation work of Murasugi [61], who used the Jones polynomial to rule out the periodic symmetries a knot can

have. In particular, *equivariant* Khovanov homology theories have been defined — see papers of Cibili [13], Politarczyk [69], and Borodzik and Politarczyk [8] — which use the extra structure coming from a the presence of a periodic symmetry. In addition, Zhang [100] has studied the annular setting, and proved a rank inequality between the annular Khovanov homology of a periodic link and its quotient link. This thesis is best viewed in the context of all these recent works.

0.1 Summary of main results

Following in the spirit of Sakuma, the results in this thesis come as a consequence of constructing invariants of strongly invertible knots from invariants of related auxiliary objects. In addition to Sakuma's links and Watson's tangles mentioned above, it is possible to associate a pair of annular knots and a further tangle to every strongly invertible knot, which allows for a wide range of new invariants. The relationships between the auxiliary objects and their parent strongly invertible knot are exhibited by the following schematic:

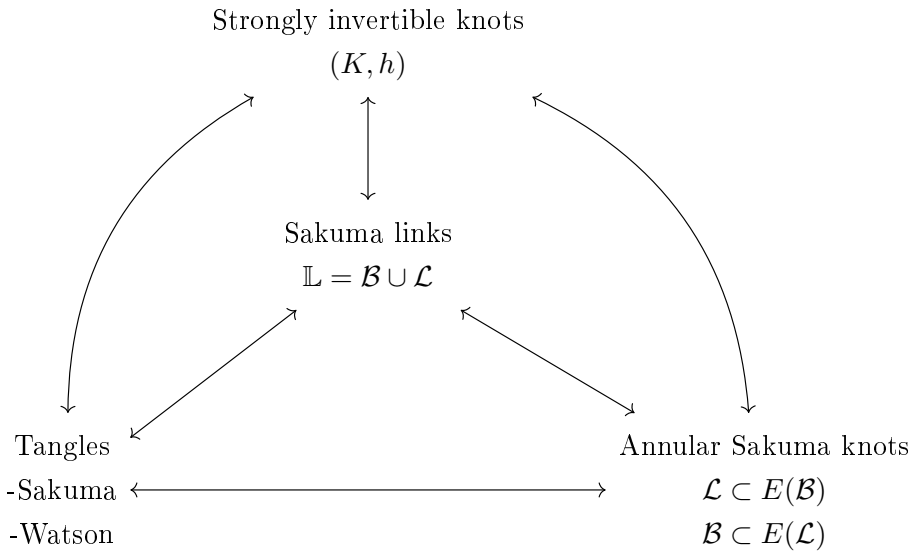

In actual fact, we do a little more. Sakuma's construction begins by taking a pair of equivariant longitudes of a strongly invertible knot (K, h) which have zero linking number with K. We expand upon Sakuma's construction by changing the framing of the pair of longitudes — this allows us to build an infinite family of quotient objects for each (K, h). We label a strongly invertible knot with a non-zero framing n by (K, h, n), and call it a *framed strongly invertible knot*.

We apply to the families of auxiliary objects a number of invariants, which by construction give us invariants of strongly invertible knots. In addition to the η-polynomial we investigate seven other invariants: the Jones polynomial, the annular Jones polynomial, Khovanov homology, annular Khovanov homology, tangle Khovanov homology, Watson's $\varkappa$ invariant, and $\varkappa_A$, a conjectured new invariant which is best viewed as an annular offshoot of $\varkappa$. We find that some invariants are sensitive to changing the longitude framing in Sakuma's construction, whilst other are not, and

return the same value for all framings.

We assess the different invariants, following three main lines of inquiry:

1. Ability to detect the strongly invertible unknot.
2. Ability to distinguish pairs of strongly invertible knots.
3. Ability to detect the cheirality of the underlying knot.

Unknot detection

One of the first questions one should ask of any knot invariant is whether or not it gives a unique value on the unknot. In our setting, we are interested in the *strongly invertible unknot* $(\mathcal{U}, h_0)$, which is simply the unknot equipped with its standard inverting involution. It is known that the η-polynomial does not detect the unknot [79], whilst Watson proves [92, Theorem 1] that $\varkappa$ does detect it. We prove the following three theorems:

Theorem 0.1.1. *Let (K, h) be a strongly invertible knot with Sakuma link $\mathbb{L}$. Then,*

$$(K, h) \cong (\mathcal{U}, h_0) \iff dim_{\mathbb{F}}(Kh^*(\mathbb{L})) = 4.$$

That is, Khovanov homology detects the strongly invertible unknot.

Theorem 0.1.2. *Let $\mathbb{L} = \mathcal{B} \cup \mathcal{L}$ be a Sakuma link, and let $\mathcal{U}$ be the homologically trivial unknot in $A \times I$.*

1. *Suppose $AKh^*(\mathcal{L}) \cong AKh^*(\mathcal{U}) \cong \mathbb{F}[0,1,0] \oplus \mathbb{F}[0,-1,0]$. Then $\mathbb{L}$ is the two-component unlink and $\mathcal{L} \cong \mathcal{U}$.*
2. *Suppose $AKh^*(\mathcal{B}) \cong AKh^*(\mathcal{U}) \cong \mathbb{F}[0,1,0] \oplus \mathbb{F}[0,-1,0]$. Then $\mathbb{L}$ is the two-component unlink and $\mathcal{B} \cong \mathcal{U}$.*

Theorem 0.1.3. *Let (K, h) be a strongly invertible knot, and let $T_{(K,h)}$ be its Watson tangle. Suppose $TKh^*(T_{(K,h)}) \cong TKh^*(T_{(\mathcal{U},h_0)})$, where $T_{(\mathcal{U},h_0)}$ is the Watson tangle associated to $(\mathcal{U}, h_0)$. Then $(K, h) \cong (\mathcal{U}, h_0)$.*

The following theorem relies on the fact that $\varkappa_A$ is an invariant of strongly invertible knots — something we have only been able to conjecture.

Theorem 0.1.4. *Let L_m be a family of annular Sakuma knots associated to a strongly invertible knot (K, h). Suppose $\varkappa_A(K, h, L) = 0$. Then $(K, h) \cong (\mathcal{U}, h_0)$.*

Effectiveness of invariants

We also compare the invariants' ability to distinguish strongly invertible knots. As the η-polynomial has been determined for the largest number of examples (see the appendix to [79]), we use it as the benchmark invariant.

We prove a result about the η-polynomials of a family of torus knots.

Proposition 0.1.5. *$\eta_{(T(-m,2),h)}(t) = \eta_{(T(-m-2,2),h)}(t)$ for $m = 4k-1$, $(k \geq 1)$.*

On the other hand, we show that the annular Jones polynomial can distinguish every member of the family.

Proposition 0.1.6. *$AJ(\mathcal{L}_{T(-m,2)})(q,t) \neq AJ(\mathcal{L}_{T(-m-2,2)})(q,t)$ for all $m \geq 3$. Hence, the annular Jones polynomial distinguishes every member of the family of strongly invertible torus knots $(T(-m,2),h)$, $m \geq 3$.*

Sensitivity to cheirality

One interesting facet of the η-polynomial is its ability to determine whether the underlying knot of a strongly invertible knot is cheiral [79, Proposition 3.4]. Since the remaining invariants all have their roots in Khovanov homology, which is known to be sensitive to the cheirality of a knot [40], we obtain similar results. A particular instance is the following result for the Jones polynomial:

Proposition 0.1.7. *Let (K,h,n) be a framed strongly invertible knot and suppose K is hyperbolic and amphicheiral.*

1. *Suppose that K does not have a free or cyclic period of period 2, and let h be the unique inverting involution. Then $(K,h,n) \cong (\overline{K,h,n})$, and so $J_{(K,h,n)}(q) = J_{(\overline{K,h,n})}(q)$ for all n. In particular, when $n=0$ we have $J_{(K,h)}(q) = J_{(\overline{K,h})}(q) = J_{(K,h)}(q^{-1})$.*
2. *Suppose K does have period 2, and let h_1 and h_2 be its two inequivalent inverting involutions. Then $(K,h_1,n) \cong (\overline{K,h_2,n})$, and so $J_{(K,h_1,n)}(q) = J_{(\overline{K,h_2,n})}(q)$ for all n. In particular, when $n=0$ we have $J_{(K,h_1)}(q) = J_{(\overline{K,h_2})}(q) = J_{(K,h_2)}(q^{-1})$.*

It is also possible to apply the invariants to Sakuma's links, and this can have some interesting implications when considering their symmetry properties. In particular, there exists a related, but subtly different, symmetry group of a link, originally defined by Whitten [97], called the *intrinsic symmetry group*. As noted by Berglund et al. in [11], from one point of view the intrinsic symmetry group is a more natural object to study than the standard symmetry group of the link as every element is easy to explicitly describe. We use polynomial invariants to provide restrictions on the size of the intrinsic symmetry group of the two-component links. For example, an element of the intrinsic symmetry group that exchanges the two components is referred to as a *pure exchange* symmetry; and it turns out that the η-polynomial can determine when one of Sakuma's two-component links cannot have a pure exchange symmetry.

We also focus on the class of annular knots as objects in their own right. Most of the current literature on annular knots deals with annular knots obtained from braid closures; however we show that the class of knots obtained using Sakuma's construction is almost completely disjoint from this class.

Proposition 0.1.8. *Let $K \subset A \times I$ be an annular Sakuma knot that is not associated to $(\mathcal{U}, h_0, \pm 1)$. Then K is not equivalent to a braid closure.*

0.2 Overview

Chapter 1 covers the necessary background material on knot symmetries. Explicit knot symmetries and their role as elements in the symmetry group and intrinsic symmetry group of a knot are explained.

Chapter 2 introduces Sakuma's and Watson's constructions, and constructs the families of auxiliary objects we attach to each strongly invertible knot.

In **Chapter 3** we turn our attention to polynomial invariants of strongly invertible knots. In particular, Sakuma's work on applying the η-polynomial of Kojima and Yamasaki to strongly invertible knots is covered, as well as the Jones polynomial and its annular counterpart. We end with a discussion regarding the use of polynomial invariants to study the intrinsic symmetry group of a Sakuma link.

In **Chapter 4** we define and study homological invariants of strongly invertible knots. We look at five invariants: Khovanov homology, annular Khovanov homology, $\varkappa$, $\varkappa_A$, and tangle Khovanov homology.

Finally, in **Chapter 5** we provide a final evaluation of the invariants covered, and list some directions for future work.

Appendix A is a user manual for the Mathematica package '$AKh.m$', which was written by the author in order to obtain explicit calculations for the annular Khovanov homology of annular Sakuma knots.

Chapter 1

Symmetries of knots and links

In this first chapter we will provide the necessary background on the symmetry properties of knots and links, with a particular emphasis on strongly invertible knots. Along the way we will come across different types of finite symmetries, and will see two differing concepts of a link's symmetry group. We will end by returning to strongly invertible knots and their properties.

1.1 Symmetry groups of knots and links

1.1.1 Properties of knots and links

Much of the following discussion and definitions are taken from Cromwell's book [15, Chapters 1 & 3] or Kawauchi's [38, Chapter 3]. We begin with the formal definition of a link in the 3-sphere. There are two equivalent ways in which links are defined: using subsets of S^3, or using embeddings into S^3. We choose the latter.

Definition 1.1.1. An *n-component link* L is an embedding of a disjoint union of n copies of S^1 in S^3. A *knot* is a link with one component.

Knots and links come with notions of equivalence, which are of varying flavours and strengths. The most commonly used one is *ambient isotopy*.

Definition 1.1.2. Two links L and L' are said to be *ambient isotopic* if there exists an isotopy $h : S^3 \times [0,1] \to S^3$ such that $h(L,0) = L$ and $h(L,1) = L'$.

Ambient isotopy forms an equivalence relation on the set of links: we say an equivalence class of a link is its *link type*. In this thesis we will always use this notion of link equivalence. An example of a stronger equivalence relation is if we were to number the components of $L = K_1 \cup \ldots \cup K_n$ and $L' = K'_1 \cup \ldots \cup K'_n$ from 1 to n, and further demand that an ambient isotopy also preserve the numbering — that is, $h(K_i) = K'_i$ for all i.

Remark. An equivalent alternative to ambient isotopy can be defined when links are considered as subspaces of S^3. In this case, two links L and L' are equivalent if there is an orientation

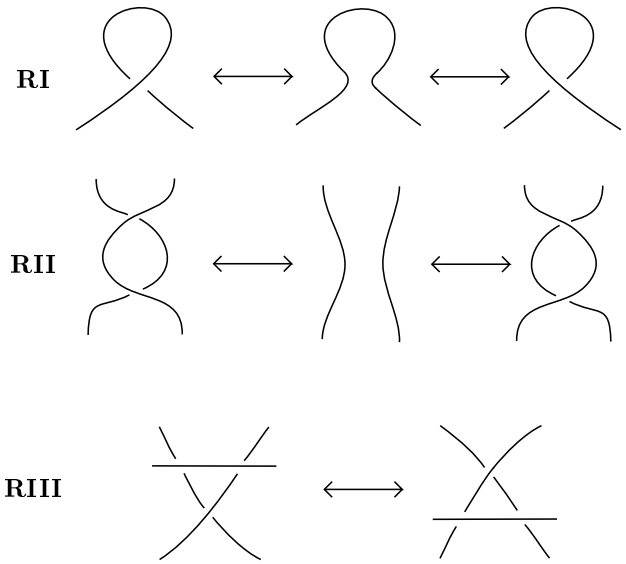

Figure 1.1: The three Reidemeister moves

preserving homeomorphism of S^3 to itself that takes L to L'. In this thesis we will use both notions interchangeably.

Determining when two links are of the same type is not a straight-forward task, since an explicit isotopy is required. Instead, knot theorists often find it easier to attack the problem from another angle, by determining when two links are not of the same type. The standard way to do this is to cook up a *link invariant*, which is a quantity which is the same on all equivalent links. Therefore, if the link invariant of two links L and L' is not the same, we know the links cannot possibly be equivalent.

Now, knots and links are 3-dimensional objects, but since mathematics is done on paper, we would like to be able to represent them accurately as a drawing in the plane $\mathbb{R}^2$. This can be done by projecting a link onto a chosen plane in such a way that there are a finite number of singular points and there are exactly two points in the preimage of each one — such a projection is called a *regular projection*. A link diagram is obtained from a regular projection by including crossing information — this is done by putting in a break to indicate which strand is passing over and which is passing under at each crossing. There are an infinite number of ways to represent a given link, and, as Cromwell notes [15, Chapter 3.3], in general there is no 'correct' or 'best' diagram — different diagrams of the same link can be used to exhibit different characteristics. This is an important point to remember when we start viewing the different symmetries of a link. Another instance of this point are the link diagrams of *alternating links*.

Definition 1.1.3. A link diagram is *alternating* if, when travelling along each component, the crossings alternate between over-crossings and under-crossings. A link is said to be *alternating* if it possesses an alternating diagram.

The crucial theorem which allows us to work with link diagrams is due to Reidemeister [74].

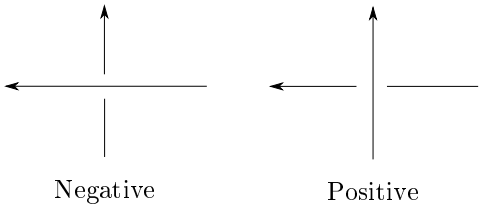

Figure 1.2: Crossing conventions

Reidemeister's Theorem (Reidemeister, 1927)**.** *Let L_1 and L_2 be two links in S^3, and let D_1 and D_2 be diagrams of them in $\mathbb{R}^2$. Then L_1 and L_2 are equivalent if and only if D_2 can be obtained from D_1 by applying a finite series of the Reidemeister moves shown in Figure 1.1, as well as some ambient isotopies of the plane.*

Many of the link invariants we come across are defined using link diagrams. In order to prove that such quantities are link invariants we must show that they are invariant under each of the three Reidemeister moves. It is important to stress, however, that not all link invariants are diagrammatic; some can only be defined on the link when it is viewed as a subspace of S^3.

Given a knot we can equip it with an *orientation*. There are two possible choices available and we depict a choice in a knot's diagram by placing an arrow on a strand. The same idea naturally extends to links.

Definition 1.1.4. Let $L = K_1 \cup \ldots \cup K_n$ be a link in S^3. An *orientation* on L is a choice of orientation on each of its components K_i. We say a link equipped with an orientation is an *oriented link*.

Once a link diagram D has been oriented we can divide the crossings into two sets, which we call the *positive crossings* and the *negative crossings*. Given a crossing p in an oriented link diagram, we define the *sign* of p to be either $+$ or $-$, depending on whether p is positive or negative. The most common convention for them is shown in Figure 1.2 — unfortunately some mathematicians have been known to use the opposite convention.

Definition 1.1.5. Let $L \subset S^3$ be an oriented link, and let D_L be a choice of diagram with n_+ positive crossings and n_- negative crossings. The *writhe* of D_L is defined to be

$$Wr(D_L) = n_+ - n_-.$$

The writhe is an invariant of the diagram, but is not an invariant of the link it depicts. The reason for this is that the writhe is not preserved under Reidemeister I moves. However, for alternating links Thistlethwaite [87], Kauffman [36], and Murasugi [60] independently proved that *reduced* diagrams of the link always have the same writhe — a result which was originally conjectured by Tait in the 19th century.

Definition 1.1.6. Let $L \subset S^3$ be a link with diagram D_L. We say a crossing p in D_L is *nugatory* if there is a circle in $\mathbb{R}^2$ meeting p transversely which does not meet the diagram at any other

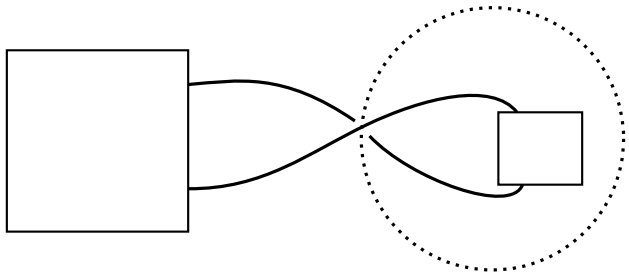

Figure 1.3: A nugatory crossing in a link diagram

point. If D_L has no nugatory crossings it is said to be *reduced*.

See Figure 1.3 for an example of a nugatory crossing in a link diagram. Nugatory crossings can clearly be removed by flipping one half of the diagram over — this motivates the use of the phrase 'reduced diagram'.

Building upon the idea of the writhe, for links with two or more components we have the notion of *linking number*. We state the definition for two-component links:

Definition 1.1.7. Let $L = K_1 \cup K_2$ be an oriented two-component link, and D_L be a diagram. Suppose there are n_+ positive crossings between K_1 and K_2, and n_- negative crossings. The *linking number* of L is:

$$\mathrm{lk}(L) = \mathrm{lk}(K_1, K_2) := \frac{n_+ - n_-}{2}.$$

The linking number is an invariant of two-component links — that is, it is invariant under Reidemeister moves. A related concept is that of *self-writhe*.

Definition 1.1.8. Let $L = K_1 \cup K_2$ be an oriented two-component link, and D_L be a diagram. Suppose there are n_+ intra-component positive crossings, and n_- intra-component negative crossings. The *self-writhe* of D_L is:

$$SWr(D_L) = n_+ - n_-.$$

The three concepts of writhe and linking number are related as follows:

$$Wr(D_L) = 2\mathrm{lk}(L) + SWr(D_L).$$

As a consequence of the above, for alternating links the self-writhe is also an invariant of reduced diagrams.

Next, we define precisely a sense of 'primeness' for knots and links.

Definition 1.1.9. Let L_1 and L_2 be two links. The *disjoint union*, denoted $L_1 \sqcup L_2$, is the link formed by placing L_1 and L_2 inside disjoint balls B_1, $B_2 \subset S^3$.

Definition 1.1.10. A link L is *split* if L can be expressed as a disjoint union of two sub-links L_1, L_2.

Definition 1.1.11. Let $L \subset S^3$ be a link, and suppose there exists a 2-sphere S which meets L transversely in exactly two points. Let $\alpha \subset S$ be an arc that connects the two points of $L \cap S$, and let U_1 and U_2 be the two components of $S^3 \backslash S$. Define $L_i = (L \cap U_i) \cup \alpha$ for $i \in \{1, 2\}$. Then L is a *product* link with *factors* L_1 and L_2, and we say S is a *factorising sphere* for L. We write $L = L_1 \# L_2$.

Definition 1.1.12. A factor of a link is a *proper factor* if it is not the unknot, nor the link itself. A link with proper factors is called a *composite link*. A link with no proper factors is a *locally trivial* link.

Definition 1.1.13. A link is *prime* if it is non-trivial, non-split, and locally trivial.

Now we will outline the main types of links. Due to a result of Thurston we can neatly divide links into one of three categories: hyperbolic, satellite, and torus.

First, the torus links. As their name suggests, these are a class of links which can be embedded in a torus $T \subset S^3$.

Definition 1.1.14. Let T be a trivially embedded torus in S^3 and let (m, l) be the standard meridian-longitude pair of curves on T. Let (p, q) be a pair of coprime integers. We say a *torus knot* on T is of type (p, q), and denote it $T(p, q)$, if it is homologous to the curve $pm + ql$ in $H_1(T; \mathbb{Z})$. A *torus link* $T(np, nq)$ is simply n copies of $T(p, q)$ in parallel, all oriented in the same direction.

Now, the satellite links.

Definition 1.1.15. Let $K \subset S^3$ be a knot, and l be a longitude of K. We say l is *preferred* if the linking number $\mathrm{lk}(K, l) = 0$.

Definition 1.1.16. Let $C \subset S^3$ be a knot, and $\mathcal{N}(C)$ be a regular neighbourhood of C. Let $P \subset V$ be a link in a solid torus such that P is not contained in any 3-ball in V. Now let $\phi : V \to \mathcal{N}(C)$ be a homeomorphism mapping the standard meridian-longitude pair on V to a meridian and *preferred* longitude on $\mathcal{N}(C)$. A *satellite link* is the link $\mathrm{Sat}(P, C) = \phi(P)$. We say that $\mathrm{Sat}(P, C)$ has *pattern* P and *companion* C.

A particular type of satellite link are the *cable links*.

Definition 1.1.17. An *n-parallel cable link* of a knot C is the satellite link $\mathrm{Sat}(P, C)$, where P is the n-component torus link $T(0, n)$.

Finally, the hyperbolic links. In order to understand their definition we will first briefly describe the statement of Thurston's Hyperbolisation Theorem. This ground-breaking theorem is concerned with the different geometric structures we can equip 3-manifolds with. In particular, the motivation behind it was to determine which 3-manifolds can be equipped with a hyperbolic structure.

An interesting class of 3-manifolds are the *link exteriors*, which are obtained from S^3 by removing the interior of a regular neighbourhood of a link: we denote them by $S^3 \backslash \mathcal{N}(L)$, or $E(L)$ for short.

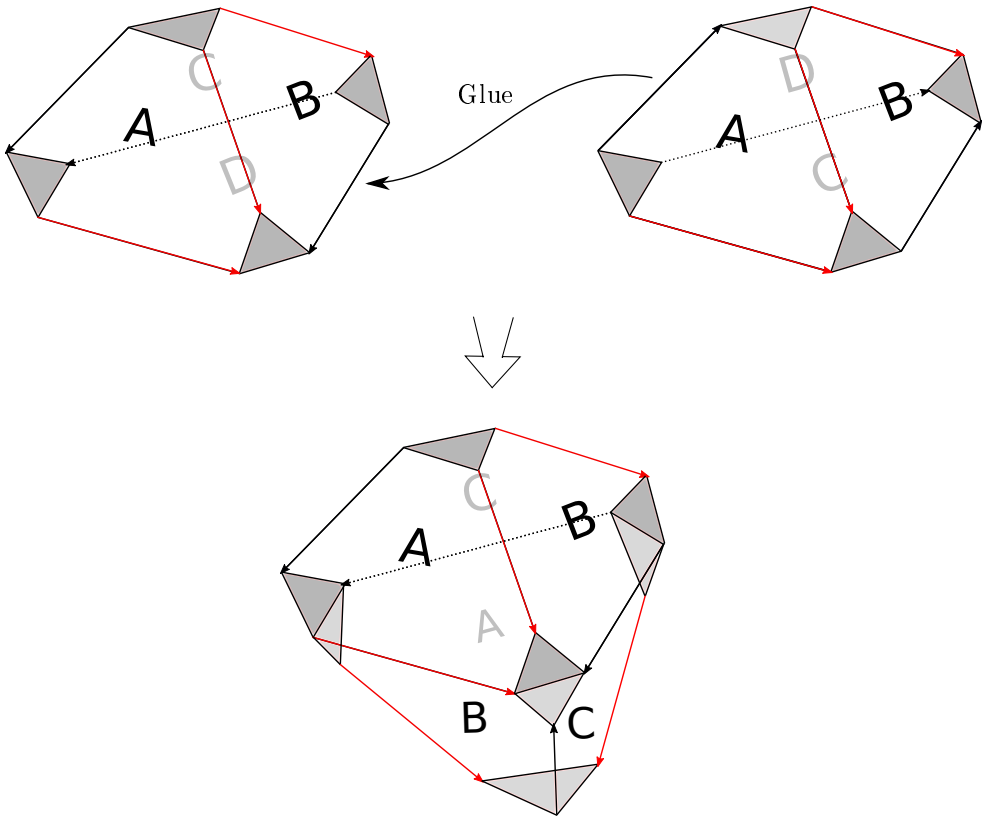

Figure 1.4: Building the Figure-8 knot exterior from tetrahedra

When applied to link exteriors links Thurston's theorem allows us to classify links into one of the three sets mentioned above. Those links whose exteriors permit a hyperbolic structure are the *hyperbolic links*. The exteriors of hyperbolic links have a finite hyperbolic volume, and this is a powerful link invariant — in fact, the hyperbolic volume is an example of a non-diagrammatic invariant. The other two sets have properties which prevent a hyperbolic structure being attached to their exteriors: it turns out these are precisely the torus links and the satellite links.

We will now state the theorem as it appears in [15, Chapter 4], then will provide the necessary definitions.

Hyperbolisation Theorem (Thurston)**.** *Let L be a non-split link. Then the exterior of L, $S^3\backslash\mathcal{N}(L)$, is a manifold with a hyperbolic structure if and only if L is atoroidal and anannular. Furthermore, $S^3\backslash\mathcal{N}(L)$ has finite volume if and only if L is not the trivial knot or the Hopf link.*

Definition 1.1.18. Let T be a torus embedded in $E(L)$ for some $L \subset S^3$. We say T is said to be *boundary parallel* if there is a continuous map $h\colon T \times [0,1] \to E(L)$ such that $h(T \times \{0\}) = T$ and $h(T \times \{1\})$ is a component of $\partial E(L)$.

Definition 1.1.19. Let A be an annulus properly embedded in $E(L)$ for some $L \subset S^3$. We say A is *boundary parallel* if there is a continuous map $h\colon A \times [0,1] \to E(L)$ such that $h(A \times \{0\}) = A$ and $h(A \times \{1\})$ is a subset of a component of $E(L)$.

Next, we define the notion of a compressible surface in a 3-manifold. Given a surface F, we say

a loop in F is *essential* if it represents a non-trivial element of $H_1(F)$.

Definition 1.1.20. Let F be a surface in a connected 3-manifold M. We say a disc $D \subset M$ is a *compressing disc* for F in M if $D \cap F = \partial D$ and ∂D is essential in F.

Definition 1.1.21. Let F be a properly embedded compact surface in a compact connected 3-manifold M. If F is not a sphere or a disc, we say F is *compressible* in M if there exists a compressing disc for F in M. Otherwise, we say F is *incompressible* in M.

We can think of an incompressible surface as being one which has been simplified as much as possible whilst remaining 'non-trivial' inside the 3-manifold. There are also notions of compressibility for spheres and discs, but we omit these for brevity.

Definition 1.1.22. A link $L \subset S^3$ is *atoroidal* if any torus T in the interior of $E(L)$ is compressible or boundary parallel.

Definition 1.1.23. A link $L \subset S^3$ is *anannular* if any annulus A properly embedded in $E(L)$ is compressible or boundary parallel.

Informally, the problem with a link exterior containing an embedded annulus or torus that cannot be compressed away is that these pieces cannot be given a hyperbolic geometric structure. Satellite links contain such a torus — the regular neighbourhood of its companion curve — and so their exteriors are not atoroidal. As for torus links, they fail the anannular condition.

How is the exterior of a hyperbolic link given a hyperbolic structure? Thurston [88, Chapter 3] describes the general method: "one divides the complement into a union of ideal polyhedra, then attempts to realize these polyhedra as ideal hyperbolic polyhedra and glue them together to form a hyperbolic manifold". By a hyperbolic tetrahedra we mean tetrahedra as they appear in hyperbolic 3-space, equipped with the hyperbolic metric.

Example 1.1.24 (Figure-8 knot exterior)**.** As an example of how we might go about gluing together tetrahedra to make a link complement we will show what happens without proof for the Figure-8 knot (this example can be found in Thurston's book [88, Example 1.4.8]). Consider Figure 1.4: the Figure-8 exterior can be obtained from gluing two truncated tetrahedra together so that face labels, edge colours, and edge arrows match up. The eight shaded triangles are glued together pairwise along their edges to make the boundary of the exterior, which is a torus. Note that this diagram does not actually show the Figure-8 knot in any way — to see this a couple more diagrams are needed (see Thurston [88, Figure 1.26]).

In practice this method is much too complicated to do by hand, but fortunately there exists a computer program that will find the hyperbolic triangulation for us. Written by Jeffrey Weeks in the 1980s, SnapPea is an incredibly powerful and useful tool for low-dimensional topologists interested in hyperbolic 3-manifolds. Its latest iteration is as SnapPy [16], which is an extension of the original SnapPea to the Python programming language. The algorithm SnapPy uses to find a triangulation of a link exterior is also due to Weeks [94].

1.1.2 Symmetries of knots and links

We will now describe some of the basic symmetry properties of knots and links. We begin with invertible links and amphicheiral links.

If L is an oriented link, we say the link in which all orientations are reversed is its *inverse*, and denote it by $-L$. It is immediate that another stronger notion of link equivalence can be obtained if we also specify the orientations on link components be preserved by our ambient isotopies. In particular, if L is ambient isotopic to its inverse we say it is *invertible*.

Next, view S^3 as $\mathbb{R}^3 \cup \{\infty\}$. Let $r : S^3 \to S^3$ be the orientation reversing homeomorphism which sends a point (x, y, z) to $(-x, -y, -z)$ and $\{\infty\}$ to itself — we say r is a *reflection of S^3 through two points*. The image of a link under r is called its *mirror image*, and is denoted by $\overline{L}$. If an unoriented link is ambient isotopic to its mirror image we say it is *amphicheiral*; otherwise it is *cheiral*.

Remark. As Cromwell notes in [15, Chapter 1], we should really call $-K$ the *reverse* of K — and so this thesis should really be about strongly *reversible* knots! The definition was changed when K and $-\overline{K}$ were found to be inverse elements in the concordance group of knots, however many other definitions have not been updated, and so the old label is still canon in many circumstances. Therefore, to prevent unnecessary confusion, we will retain the old term.

We can choose to differentiate between those ambient isotopies that send a link to its mirror. For $L = K_1 \cup \ldots \cup K_n$ an oriented link we can form 2^n related links by reversing some orientations of its components. We will refer to a related link by L_ϵ, where the n-tuple $\epsilon \in \{+, -\}^n$ indicates whether the orientation of each K_i is preserved or reversed. If $\overline{L}$ is equivalent to L_ϵ, we say that L is *ϵ-amphicheiral*.

For knots things are simpler: if $\overline{K} = K$ we say K is (+)amphicheiral, and if $\overline{K} = -K$ we say K is (−)amphicheiral. In homeomorphism language, if there exists an orientation reversing homeomorphism of S^3 that preserves (reverses) the orientation of K then K is (+)amphicheiral ((−)amphicheiral).

Following Cromwell, if we denote the operation that sends K to $-K$ as s, and let $t = rs$ be the operation sending K to $-\overline{K}$ we obtain a group G (which is isomorphic to the Klein 4-group).

	1	r	s	t
1	1	r	s	t
r	r	1	t	s
s	s	t	1	r
t	t	s	r	1

A knot K then must have one of the following five symmetry types, depending on which subgroup of G is realised in the knot type of K.

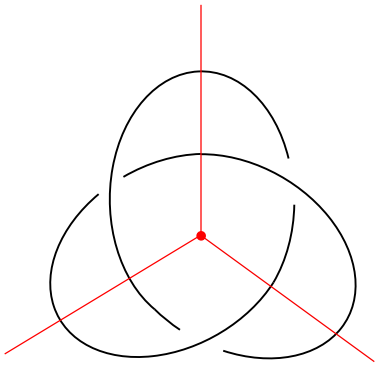

Figure 1.5: The trefoil admits a periodic symmetry of period 3

G	fully symmetric
$\langle s \rangle$	invertible
$\langle r \rangle$	(+)amphicheiral
$\langle t \rangle$	(−)amphicheiral
$\langle 1 \rangle$	no symmetry

We will now outline some of the most common examples of symmetries of knots and links. They are sometimes known as 'rigid' symmetries due to the fact they can all be described by the action of a rotation or reflection of the 3-sphere. The reference for the upcoming definitions and results is Kawauchi's excellent book [38, Chapter 10].

Definition 1.1.25. A knot $K \subset S^3$ is a *periodic knot* of period n if there is a periodic map f of (S^3, K) of period n such that $\mathrm{Fix}(f) \cong S^1$ and $\mathrm{Fix}(f) \cap K = \emptyset$.

The standard way to draw periodic symmetries is to view the fixed point set of the map to be an axis passing straight through the plane of a knot diagram. As we can see from Figure 1.5 it is clear that the trefoil admits a periodic symmetry of period 3. When we specify our knots be oriented we see that periodic symmetries preserve the orientation of K. This means they do not feature at all in the symmetry type group defined above, showing the group's limitations at capturing all the symmetry information of a knot.

Definition 1.1.26. A knot $K \subset S^3$ is a *freely periodic knot* with free period n if there is a periodic map f of (S^3, K) of period n such that $\mathrm{Fix}(f^i) = \emptyset$ for all $1 \leq i \leq n-1$.

Free symmetries are much harder to visualise than periodic symmetries; perhaps the most intuitive set of examples are those on torus knots — whose exteriors are *Seifert fibred*.

Definition 1.1.27. Let $D^2 \subset \mathbb{C}$ be the unit disc in the complex plane, and $\rho\colon D^2 \to D^2$ be a homeomorphism given by $\rho(x) = xe^{\frac{2\pi i a}{b}}$, where a and b are coprime integers. Consider the product manifold $D^2 \times I$, and form the quotient under the relation $(x, 0) \sim (\rho(x), 1)$. The resulting torus, T, can be expressed as a union of *fibres*, namely as the collection of circles $(\{x\} \times I)_\sim$. We say

that T is a *standard fibred torus*.

Definition 1.1.28. Let M be a closed 3-manifold. A *Seifert fibration* of M is a decomposition of M into a disjoint union of fibres such that each fibre has a tubular neighbourhood equivalent to a standard fibred torus.

Given a Seifert fibration on the exterior of a torus knot we can obtain a free symmetry by pushing each point along its fibre. To get a symmetry of period n imagine identifying each fibre with the unit circle in the complex plane, then send each point x in the fibre to $e^{\frac{2\pi i}{n}}x$.

Sakuma has proved [80], [81] that the presence of free periodic symmetries is inconsistent with a knot being amphicheiral.

Theorem 1.1.29 (Sakuma, 1986). *Let $K \subset S^3$ be an amphicheiral, prime knot. Then K does not have any free periodic symmetries of period > 2.*

Theorem 1.1.30 (Sakuma, 1987). *Let $K \subset S^3$ be an amphicheiral hyperbolic knot. Then K has no free periodic symmetries.*

It was an open question for a time about whether or not there existed an amphicheiral prime knot with free period 2. Recently, however, Paoluzzi and Sakuma [67] have resolved this question in the affirmative:

Theorem 1.1.31 (Paoluzzi-Sakuma, 2018).
1. *There are infinitely many prime knots with free period 2 that are $(+)$amphicheiral but not $(-)$amphicheiral; in particular, they are not invertible.*
2. *There are infinitely many prime knots with free period 2 that are (ϵ)amphicheiral where $\epsilon \in \{+, -\}$; in particular, they are invertible.*

We now arrive at the main set of objects featuring in this thesis — the strongly invertible knots.

Definition 1.1.32. A knot $K \subset S^3$ is *strongly invertible* if there is an involution of (S^3, K) which preserves the orientation of S^3 and reverses the orientation of K.

We note the subtle difference between the definitions of invertible knots and *strongly* invertible knots: in order for an invertible knot to be strongly invertible the homeomorphism which takes K to $-K$ must be an *involution*. From the definition it is immediate that all strongly invertible knots are invertible, though it turns out that the converse is not true (see papers by Hartley [26] and Whitten [98] for examples of invertible knots which are not strongly invertible). For hyperbolic knots, however, more can be said [38, Proposition 10.3.3].

Proposition 1.1.33. *Let K be an invertible, hyperbolic knot. Then K is strongly invertible.*

Definition 1.1.34. A knot $K \subset S^3$ is *strongly $(+)$amphicheiral* or *periodically $(+)$amphicheiral* if there is an involution or a periodic map respectively of (S^3, K) which reverses the orientation of S^3 and preserves the orientation of K. Likewise, K is *strongly $(-)$amphicheiral* or *periodically*

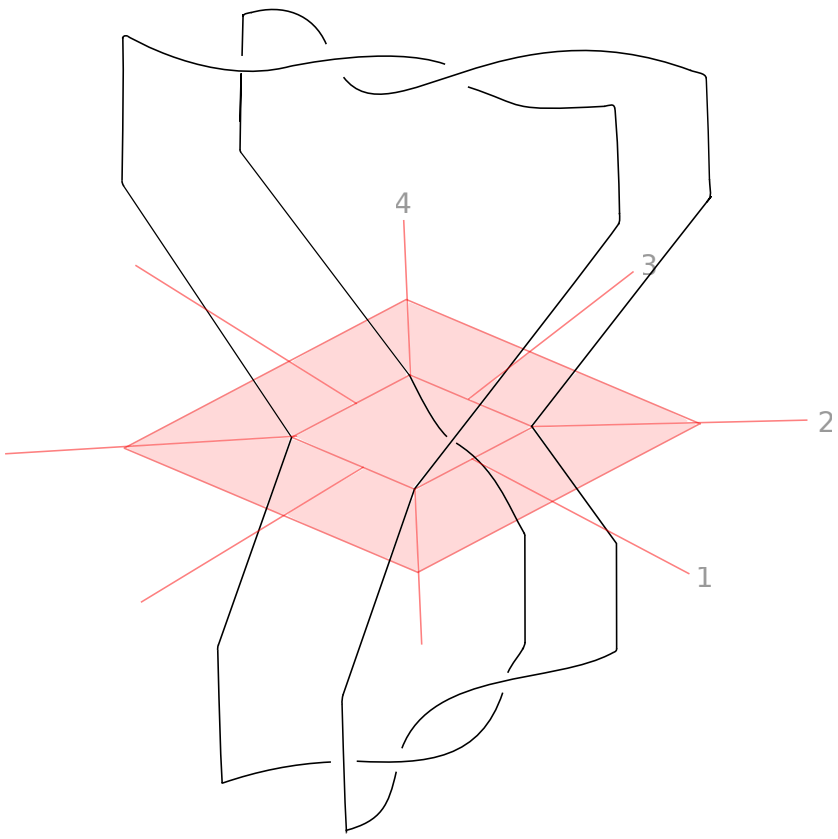

Figure 1.6: A highly symmetrical diagram of the Figure-8 knot

$(-)$*amphicheiral* if there is an involution or periodic map of (S^3, K) which reverses the orientations of both S^3 and K.

A particular instance of a map that realises the periodically $(+)$amphicheiral symmetry is a *twisted rotation*. The following construction appears in a paper of Luo [51]: view S^3 as $(\mathbb{R} \times \mathbb{C}) \cup \{\infty\}$ and f be the map that takes a point (x, z) to $(-x, -e^{\frac{2\pi i}{n}} z)$ and $\{\infty\}$ to itself. Then f is said to be a *twisted* $\frac{2\pi}{n}$*-rotation* of S^3.

Analogously to the strongly invertible setting, there is an example of an amphicheiral knot which is not periodically amphicheiral [26], but for hyperbolic knots this can be ignored [38, Proposition 10.4.3].

Proposition 1.1.35. *Let K be an amphicheiral, hyperbolic knot. Then K is periodically amphicheiral.*

Example 1.1.36. We will now see some of the above symmetries in action, by considering a particular diagram of the Figure-8 knot. The Figure-8 is a highly symmetrical, hyperbolic knot: it is strongly invertible, periodically $(+)$amphicheiral, strongly $(-)$amphicheiral, and admits a

periodic symmetry of period 2. However, if we turn to perhaps its most well known diagram (the right hand knot diagram in Figure 1.7, which appears in Rolfsen's table of knots [77, Appendix C]), only a strong inversion is present. This highlights a fundamental difficulty in studying the symmetries of a knot or link — even if the existence of a certain symmetry is known, actually finding a diagram exhibiting it is often a difficult task!

Consider now the diagram of the Figure-8 knot in Figure 1.6 ([38, Figure 4.2.2]) . This has been drawn in such as way as to be more suggestive of its 3-dimensional nature; in particular it lies above and below the red plane, passing through it in four points. We claim that all of the symmetries mentioned above can be exhibited in this diagram. Firstly, the periodic symmetry can be seen by rotating the knot π radians about an axis passing through the centre of the red plane. The $(+)$amphicheiral symmetry is exhibited by rotating $\frac{\pi}{2}$ radians about the same axis, then reflecting in the red plane. There are two strong inversions in the diagram too: rotate the knot π radians about the axes labelled 2 and 4. Finally, two $(-)$amphicheiral symmetries can be obtained by rotating π radians about axes 1 and 3 respectively, then reflecting in the red plane.

1.1.3 The symmetry group

The symmetry group of a link is a classic invariant, which, like the hyperbolic volume, is non-diagrammatic. As Kodama and Sakuma remark in the opening to [44], the symmetry group of a link essentially codifies information about its cheirality and invertibility. For knots, the explicit 'rigid' symmetries introduced previously are all contained within the symmetry group — although, as we will see, not every symmetry appears as a non-trivial group element. We stay with Kawauchi [38, Chapter 10.6] for the following definitions.

For a link $L \subset S^3$ let $Aut(S^3, L)$ be the group of homeomorphisms from the pair (S^3, L) to itself, and let $Aut_0(S^3, L)$ be the subgroup consisting of those homeomorphisms which are ambient isotopic to the identity.

Definition 1.1.37. Let $L \subset S^3$ be a link. The *symmetry group of* L, $Sym(L)$, is defined to be the quotient group $Aut(S^3, L)/Aut_0(S^3, L)$.

The symmetry group of L is therefore just the mapping class group of the pair (S^3, L). For knots, $Sym(K)$ can also be identified with the mapping class group of the knot exterior $E(K)$, which we will denote by $MCG(E(K))$, and the outer automorphism group of its knot group $\pi(K) := \pi_1(E(K))$. The proof of the following appears in Kawauchi [38, Theorem 10.6.2].

Theorem 1.1.38. *Let $K \subset S^3$ be a prime knot. Then we have the following natural isomorphisms:*

$$Sym(K) \cong MCG(E(K)) \cong Out(\pi(K))$$

The symmetry group has been extensively calculated. For hyperbolic links $Sym(L)$ is isomorphic to the group of isometries on $E(L)$, when $E(L)$ is viewed as a hyperbolic manifold (c.f. [44]). Using this fact Weeks was able to use his SnapPea program to calculate the symmetry groups

of hyperbolic links, since, as Henry and Weeks state in [30] "the potentially difficult topological question of finding the symmetries of the link complement is reduced to the computationally trivial combinatorial question of finding the symmetries of the canonical triangulation". Using the SnapPea computer program Henry and Weeks [30] calculated the groups of hyperbolic knots up to 10 crossings and links up to 9 crossings.

Working independently to Henry and Weeks, Kodama and Sakuma [44] computed the symmetry group of all but three of the prime knots up to ten crossings by using a combined approach of theorems and a computer program written by Kodama, which calculated symmetries of a certain θ-graph. An example of one of their supporting theorems is given below for the hyperbolic case. Let $Sym^+(K)$ be the subgroup of $Sym(K)$ in which all elements preserve the orientation of S^3, and $Sym'(K)$ be the subgroup in which elements preserve the orientations of both S^3 and K.

Proposition 1.1.39 (Kodama-Sakuma, 1992). *Let $K \subset S^3$ be a hyperbolic knot.*

1. *$Sym'(K)$ is a finite cyclic group Z_n for some positive integer n.*
2. *$Sym^+(K)$ is isomorphic to the dihedral group D_n of order $2n$, or to Z_n, according to whether K is invertible or not.*
3. *If K is cheiral, then $Sym(K) \cong Sym^+(K)$.*
4. *Suppose K is amphicheiral. If K is invertible, then $Sym(K) \cong D_{2n}$. If K is non-invertible, then $Sym(K) \cong Z_{2n}$ or D_n according to whether K is positive or negative amphicheiral.*

Example 1.1.40 (Figure-8 revisited). Using SnapPy it can be easily verified that the symmetry group of the Figure-8 knot is isomorphic to the dihedral group D_4, which is generated by an element r, of order 4 and an element s of order 2. Returning to the decomposition of $E(4_1)$ into tetrahedra in Figure 1.4 we can intuitively see how the two generators must act on the tetrahedra: r cycles through the 4 faces, and s exchanges the two tetrahedra.

Furthermore, the symmetry group of 4_1 can be viewed completely in terms of its rigid symmetries. We have

$$D_4 = \{e, r, r^2, r^3, s, sr, sr^2, sr^3\}$$

Where r are r^3 are $(+)$amphicheiral symmetries of order 4, r^2 is a periodic symmetry of period 2, s and sr^2 are two strong inversions, and sr and sr^3 are $(-)$amphicheiral symmetries of order 2. Compare this with Figure 1.6: some of the elements of the group are present in the diagram. As we will see later, two strong inversions are considered equivalent if they are conjugate (c.f. [44]) — which is the case for the two strong inversions exhibited in Figure 1.6.

For torus knots, the symmetry group is not quite as useful a tool to describe its symmetries, as it is always isomorphic to $\mathbb{Z}/2\mathbb{Z}$.

Theorem 1.1.41 (Schreier, 1924). *Let $K \subset S^3$ be a torus knot $T(p, q)$, then $Out(\pi(K)) \cong \mathbb{Z}/2\mathbb{Z}$.*

Corollary 1.1.42. *Let $K \subset S^3$ be a torus knot $T(p, q)$, then $Sym(K) \cong \mathbb{Z}/2\mathbb{Z}$.*

From the point of view of symmetries, the above result is in part due to the fact that all torus knots are cheiral, but also because, as Kawauchi notes, torus knots admit a circle action. We define the circle group $\mathbb{T}$ to be the points of the unit circle $S^1 \subset \mathbb{C}$ under multiplication. Let $T(p,q)$ be a torus knot of type (p,q); then $\mathbb{T}$ acts on $(S^3, T(p,q))$ by sending a point $x \in S^3 \subset \mathbb{C}^2$ to $e^{i\theta}x$. This action includes any periodic symmetries. In order to see that free periodic symmetries are embedded within an action of $\mathbb{T}$ consider a Seifert fibration of the exterior of $T(p,q)$. An action of $\mathbb{T}$ consists in sending a point x on each fibre to $e^{\frac{2\pi i}{n}}x$ on the same fibre. Now, since all homeomorphisms given by a circle action are ambient isotopic to the identity, all homeomorphisms realising free and cyclic periods of $T(p,q)$ must also be ambient isotopic to the identity, and so their images in $Sym(T(p,q))$ are trivial.

As a result, "there are finite group actions which are not detected by the symmetry group" (Kawauchi). The symmetry group says nothing about how many free and cyclic periods a torus knot has; we must use other methods for this task.

So far all the examples of symmetry groups have been finite groups. However, intuitively, the number of homeomorphisms of (S^3, L) is very large, perhaps even infinite. Even after we quotient out by those homeomorphisms ambient isotopic to the identity we may still wonder whether $Sym(L)$ is necessarily a finite group. It turns out that this is not always the case, as the following result of Sakuma [82] shows.

Proposition 1.1.43 (Sakuma, 1989)**.** *A link L has a finite symmetry group if and only if L is a hyperbolic link, a torus link, or a cable of a torus link.*

In general, satellite links have an infinite symmetry group. Sakuma in [82] shows this by exhibiting a family of Dehn twists on the exterior of a satellite link. Given a satellite link L with companion knot K we can decompose its exterior $E(L)$ into a union of three pieces $M_0 \cup T \times [0,1] \cup M_1$, where $M_0 = \mathcal{N}(K) \backslash \mathring{\mathcal{N}}(L)$, $T = \partial\mathcal{N}(K)$, and $M_1 = S^3 \backslash \mathring{\mathcal{N}}(K)$. Then *Dehn twists* (a type of homeomorphism of a surface we leave undefined, see [77]) along T belong to the mapping class group of $E(L)$, and so also to $Sym(L)$. Recall that cable links are a class of satellite links which have a torus link as their pattern, which means they sit on the surface of the neighbourhood of the companion knot. Intuitively, this property will cause problems if we try to perform Dehn twists on the exterior of a cable link (see [82] for further details).

In the next section we will encounter another type of symmetry group which is always finite for all knots and links.

1.1.4 The intrinsic symmetry group

We will now detail a related, but subtly different, symmetry group. This group was developed by Whitten [97] in the late 1960s, and is known as the *intrinsic symmetry group*. The primary reference for this section is a paper by Berglund et al. [11].

Let $L \subset S^3$ be a link with symmetry group $Sym(L)$. Consider the homomorphism given by

$$\pi : Sym(L) = MCG(S^3, L) \to MCG(S^3) \times MCG(L)$$

where $f \in MCG(S^3, L) \mapsto (f|_{S^3}, f|_L)$.

Definition 1.1.44. Let L, $Sym(L)$ and π be as above. The intrinsic symmetry group, $Sym^*(L)$, of L is the image of the map π in $MCG(S^3) \times MCG(L)$.

Now, $MCG(S^3) \cong \mathbb{Z}/2\mathbb{Z}$, with the non-zero element generated by an orientation reversing homeomorphism. This means that $Sym^*(L)$ contains explicit homeomorphisms on L — the only thing about the ambient S^3 it sees is its orientation. The main difference between $Sym(L)$ and $Sym^*(L)$ is that $Sym^*(L)$ is always a finite group — as Berglund et al. remark, for the satellite links not covered by Sakuma's theorem (Proposition 1.1.43) there are infinitely many elements which act non-trivially on the complement of L, but fix the link itself. These elements are contained in the kernel of π, so are safely ignored. In addition, there are known examples of links with a non-empty kernel even when $Sym(L)$ is finite [11, Table 13]. Berglund's group give the following as the main motivation for working with $Sym^*(L)$ over $Sym(L)$: "it is often difficult to describe an element of $Sym(L)$ in $\ker \pi$ exactly, but it is always simple to understand the exact meaning of the statement $\gamma \in Sym^*(L)$".

The intrinsic symmetry group can be described in a more explicit way. For an n-component link L the group $MCG(S^3) \times MCG(L)$, denoted by $\Gamma(L)$ for short, can be expressed as a product and semi-direct product of copies of $\mathbb{Z}/2\mathbb{Z}$ as follows:

$$\Gamma(L) = \mathbb{Z}/2\mathbb{Z} \times (\mathbb{Z}/2\mathbb{Z}^n \rtimes S_n),$$

where S_n is the permutation group on n objects. The proof of this statement can be found in Berglund [11, Proposition 4.9]. Informally, the group $\Gamma(L)$ encodes the orientations of the components of L, the order in which they are labelled, and the orientation of the ambient S^3. We express elements $\gamma \in \Gamma(L)$ by the shorthand $(\epsilon_0, \epsilon_1, \ldots, \epsilon_n, p)$, where $\epsilon_i \in \{-1, 1\}$ and $p \in S_n$; an element of $\Gamma(L)$ acts on L to produce a new link L_γ. We then specify that $\gamma \in \Gamma(L)$ is contained in $Sym^*(L)$ if and only if there is an ambient isotopy which takes L to L_γ.

Remark. In fact, the intrinsic symmetry group was defined originally by Whitten [97] using the above terminology; the definition we gave above comes from a result of Berglund et al [11, Proposition 4.9].

For knots $\Gamma(K)$ is none other than the group of knot symmetry types defined earlier! That is, for $K \subset S^3$, $\Gamma(K) \cong \mathbb{Z}/2\mathbb{Z} \times \mathbb{Z}/2\mathbb{Z}$. Hence, $Sym^*(K)$ is isomorphic to one of the five subgroups of $\Gamma(K)$ outlined previously. The following result follows almost immediately.

Lemma 1.1.45. *Let $K \subset S^3$ be a knot. Then the map $\pi : Sym(K) \to Sym^*(K)$ is surjective.*

Proof. The result comes from the following three implications:

- K (+)amphicheiral $\iff$ $(1, 0) \in Sym^*(K)$.
- K invertible $\iff$ $(0, 1) \in Sym^*(K)$.
- K (−)amphicheiral $\iff$ $(1, 1) \in Sym^*(K)$.

□

Example 1.1.46. The Figure-8 knot has full symmetry, so its intrinsic symmetry group is $\mathbb{Z}/2\mathbb{Z}\times\mathbb{Z}/2\mathbb{Z}$. From earlier we know that $Sym(4_1) \cong D_4$. We will now describe explicitly the map $\pi : Sym(4_1) \to Sym^*(4_1)$:

$$\begin{array}{llllll} e & \mapsto & (0,0) & s & \mapsto & (0,1) \\ r & \mapsto & (1,0) & sr & \mapsto & (1,1) \\ r^2 & \mapsto & (0,0) & sr^2 & \mapsto & (0,1) \\ r^3 & \mapsto & (1,0) & sr^3 & \mapsto & (1,1) \end{array}$$

Note that π has a non-trivial kernel: periodic symmetries do not feature in the intrinsic symmetry group.

For links, $\Gamma(L)$ is more interesting. For example, for two-component links $\Gamma(L)$ is a 16 element non-abelian group isomorphic to $\mathbb{Z}/2\mathbb{Z} \times D_4$. Berglund et al. note that for an element $\gamma \in \Gamma(L)$ the intrinsic symmetry group of the link L_γ is the conjugate subgroup $\gamma Sym^*(L)\gamma^{-1}$. Thus, the number of possible distinct intrinsic symmetry groups is the number of non-conjugate subgroups of $\Gamma(L)$. For two-component links, there are 35 subgroups of $\Gamma(L)$, and 27 of them are non-conjugate. Exactly how many of these 27 subgroups actually appear as the intrinsic symmetry group of some two-component link is an open question; Berglund et al. have found that only 6 are realised by prime links with 8 or fewer crossings.

A specific type of symmetry for two-component links of interest to us is the *pure exchange symmetry*, which is the symmetry corresponding to the element $(1, 1, 1, (1, 2)) \in \Gamma(L)$. It should be clear that a two-component link can only have pure exchange symmetry if both of its components are of the same knot type.

1.2 Strongly invertible knots revisited

We will now return to strongly invertible knots, which were briefly touched upon earlier. Much of the following is taken from Sakuma's paper [79].

1.2.1 Properties of strongly invertible knots

We will start by providing an equivalent definition to that given earlier (Definition 1.1.32). This alternative definition of a strongly invertible knot is really just a consequence of Definition 1.1.32, but it is in some respects more illuminating.

Definition 1.2.1. A knot K in S^3 *admits a strong inversion* if there is an orientation preserving involution h on S^3 such that the following are satisfied:

1. $h(K) = K$
2. $\mathrm{Fix}(h)$ is a circle that meets K in two points

We can think of our involution as a half rotation about some axis in the 3-sphere which meets K in two places. It proves useful to think of the axis as a copy of S^1 which passes through the point

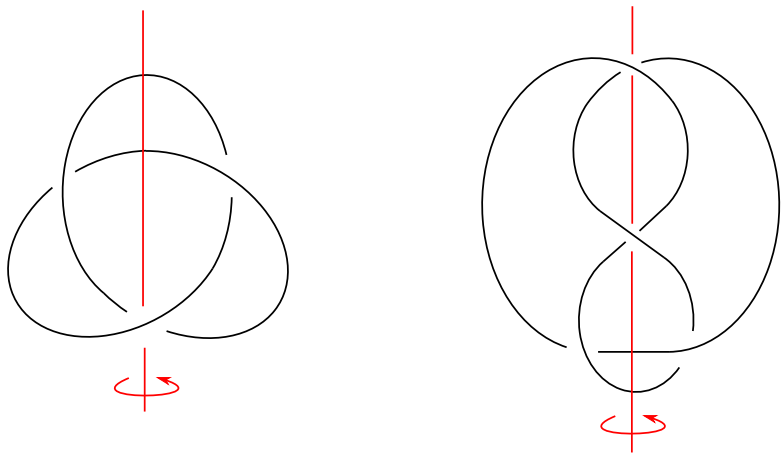

Figure 1.7: Two strongly invertible knot diagrams

at infinity. This is possible due to the affirmation of the Smith conjecture [58], which states that the fixed point set of any homeomorphism of finite order on the 3-sphere is always an unknotted S^1.

We consider the pair (K, h), where K is strongly invertible and h satisfies the criteria above. Such a pairing (K, h) is called a *strongly invertible knot* and there exists an equivalence relation on the set of such pairs. Namely, $(K, h) \cong (K', h')$ if and only if there is an orientation-preserving homeomorphism f on S^3 such that $f(K) = K'$ and $fhf^{-1} = h'$. As we saw earlier, a strong inversion is an element of the symmetry group of a knot, $Sym(K)$. From the above definitions, it immediately follows that an equivalence class of a strongly invertible knot corresponds to the conjugacy class of a strong inversion in $Sym(K)$ (cf. [92, Definition 8]).

For an example of two equivalent strong inversions we return to the Figure-8 example in Figure 1.6: if we take the conjugate of one strong inversion with the periodic symmetry we obtain the other. On the other hand, Figure 1.8 displays two distinct strong inversions.

Remark. When we draw diagrams of strongly invertible knots $D_{(K,h)}$ as in Figure 1.7 we invariably end up with instances where the fixed point set of the involution interacts with a crossing of the diagram. By this we mean that in S^3 the fixed point set passes in between the two strands that comprise the crossing. It is also important to remember that (K, h) is an equivalence class, meaning that when we depict strongly invertible knots diagrammatically we have implicitly chosen a member of the class ahead of time.

Definition 1.2.2. Suppose (K, h) is a strongly invertible knot. Then (K, h) is said to be *trivial* if it is equivalent to $(\mathcal{U}, h_0)$, where $\mathcal{U}$ is the unknot and h_0 is its standard inverting involution.

Marumoto in [54, Proposition 2] proved that detecting the trivial strongly invertible knot ultimately amounts to detecting the unknot.

Proposition 1.2.3 (Marumoto, 1977)**.** *Let (K, h) be a strongly invertible knot. Then (K, h) is trivial if and only if K is trivial.*

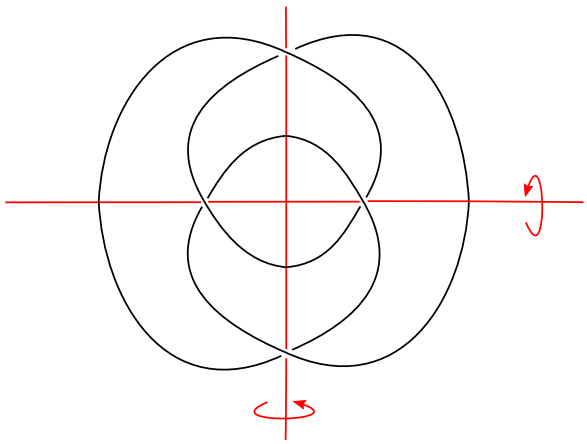

Figure 1.8: Two distinct strong inversions on the Figure-8 knot

It is also possible to define a notion of 'primeness' for strongly invertible knots. Given two strongly invertible knots (K_1, h_1), (K_2, h_2) Sakuma shows us how to form their equivariant connect sum $(K_1, h_1)\#(K_2, h_2)$. In order for the connect sum to be well defined, however, we need some additional information about the pair of strongly invertible knots (K_1, h_1), (K_2, h_2).

1. An orientation of $\mathrm{Fix}(h_i)$.

2. A marked base point ∞_i of $\mathrm{Fix}(h_i)$, which lies in one of the two components of $\mathrm{Fix}(h_i)\backslash K_i$.

We call a strongly invertible knot equipped with the above information a *directed* strongly invertible knot. The connect sum operation then proceeds as follows. Let z_i be a point of $\mathrm{Fix}(h_i) \cap K_i$ and B_i be an equivariant regular neighbourhood of z_i (so that $h_i(B_i) = B_i$ set-wise). Let also f be an orientation reversing equivariant homeomorphism from $\partial(B_1, B_1 \cap K_1)$ to $\partial(B_2, B_2 \cap K_2)$. Then f can be used as a gluing map between $(S^3, K_1)\backslash(\mathring{B}_1, \mathring{B}_1 \cap K_1)$ and $(S^3, K_2)\backslash(\mathring{B}_2, \mathring{B}_2 \cap K_2)$, which gives us a manifold homeomorphic to $(S^3, K_1\#K_2)$. Furthermore, the involutions h_1 and h_2 combine to determine a strong inversion h of $K_1\#K_2$.

In order to make this operation precise we use the directed information: in order to form $(K_1, h_1)\#(K_2, h_2)$ we specify that z_1 be the second point we come to following the orientation from ∞_1, and z_2 be the first point from ∞_2 (see [79, Figure 1.1]). Sakuma proves that the directed information also determines the gluing map, by showing another choice of gluing map returns an equivalent strongly invertible knot. We can now formally define the equivariant connect sum of (K_1, h_1) and (K_2, h_2) to be the strongly invertible knot $(K_1\#K_2, h)$.

Definition 1.2.4. A strongly invertible knot (K, h) is *prime* if it is not trivial and is not equivalent to an equivariant connect sum of two non-trivial strongly invertible knots.

Definition 1.2.5. Given an oriented knot $K \subset S^3$ define the *double* of K, $D(K)$ to be the knot $K\# - K$.

As Watson remarks in [92], while not every knot K admits a strong inversion, it is always the case that $D(K)$ does. Indeed, we can define the strongly invertible double of K to be $(D(K), h)$, where h is an inverting involution that exchanges K and $-K$ (c.f. [79, Definition 1.1]). It is important

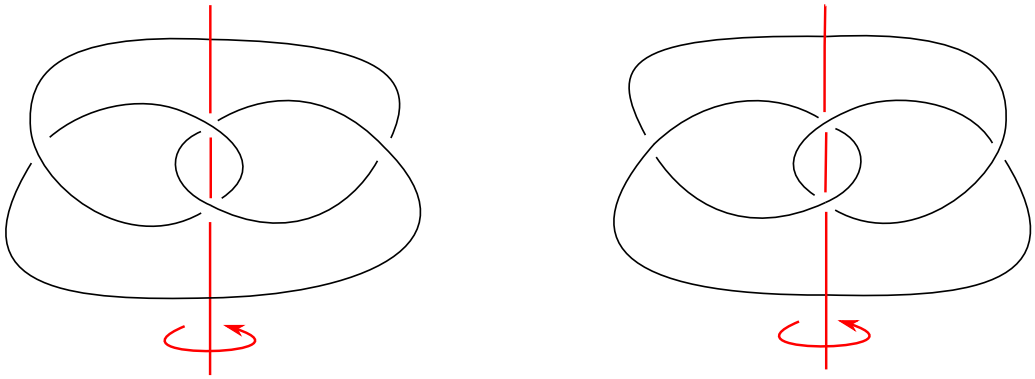

Figure 1.9: Two more views of the strong inversions on the Figure-8 (Left: $(4_1, h_1)$, Right: $(4_1, h_2)$)

to note that $(D(K), h)$ is not formed from the *equivariant* connect sum of two strongly invertible knots — in fact, as stated above, K need not admit a strong inversion at all. This point motivates the presence of strongly invertible doubles in the following result [79, Lemma 1.2(2)].

Lemma 1.2.6 (Sakuma, 1985). *A strongly invertible knot (K, h) is prime if and only if K is prime or $(K, h) \cong (D(K'), h')$ for some prime knot K'.*

Building on the connect sum operation, Sakuma also proved a decomposition theorem [79, Theorem 1] for a general directed strongly invertible knot into its prime pieces.

Theorem 1.2.7 (Sakuma, 1985). *Let (K, h) be a non-trivial, directed, strongly invertible knot.*

1. *(K, h) has an equivariant prime decomposition. Any prime decomposition is equivalent to a decomposition*
$$(K, h) \cong \{\#_{i=1}^{r}(K_1, h_1)\}\#\{\#_{j=1}^{s} D(\hat{K}_j)\}$$
where K_i and $\hat{K}_j$ are prime knots.

2. *Let $\{\#_{i=1}^{r}(K_1, h_1)\}\#\{\#_{j=1}^{s} D(\hat{K}_j)\}$ and $\{\#_{i=1}^{r'}(K_1', h_1')\}\#\{\#_{j=1}^{s'} D(\hat{K}_j')\}$ be two prime decompositions of (K, h). Then*

   (a) $r = r'$ and $(K_i, h_i) \cong (K_i', h_i')$ for each $1 \leq i \leq r$.

   (b) $s = s'$ and after a permutation $D(\hat{K}_j) \cong D(\hat{K}_j')$ for each $1 \leq j \leq s$.

We may also ask if there a limit on the number of strong inversions a link can have. Kojima [45] has shown that any non-trivial link can only ever have a finite number of strong inversions. In the case of knots, other cases have been determined by Sakuma [79, Proposition 3.1]:

Proposition 1.2.8 (Sakuma, 1985). *Suppose K is a knot admitting n strong inversions.*

1. *If K is a torus knot then $n = 1$.*

2. *If K is hyperbolic then $n = 2$ if it has a cyclic or free period of period 2, and $n = 1$ if it does not.*

Unfortunately, outside of these two classes the situation is nowhere near as simple. As a consequence of Proposition 1.2.7 it is possible for any positive integer n to construct a composite knot which has more than n inverting involutions (c.f. [79, Remark 3.2]). Sakuma has also shown that it is possible to do this for prime satellite knots [82].

We will finish this section on the subject of mirroring a strongly invertible knot. Given a strongly invertible knot (K, h) we observe that h also takes the mirror of K, $\overline{K}$, to itself, and $\mathrm{Fix}(h)$ meets $\overline{K}$ in two points. Hence, we obtain another strongly invertible knot, known as the *strongly invertible mirror* of (K, h), which we denote by $(\overline{K}, \overline{h})$. It follows from the equivalence relation on strongly invertible knots that $(K, h) \cong (\overline{K}, \overline{h})$ if and only if $\overline{K} = f(K)$ for some orientation-preserving homeomorphism f on S^3 (that is, K is amphicheiral) *and* $h = f^{-1}hf$.

For cheiral K, the strongly invertible mirror is clearly a distinct object in its own right. However, this can also be the case for an amphicheiral K too, which is due to the second point requiring f and h to commute. For an example, we return once more to the Figure-8 knot. Notice that the diagrams for $(4_1, h_1)$ and $(4_1, h_2)$ in Figure 1.9 are mirror images of one another; that is, $(\overline{4_1, h_1}) \cong (4_1, h_2)$. However, since $(4_1, h_1)$ and $(4_1, h_2)$ are distinct strongly invertible knots, it must be the case that $(4_1, h_1)$ is not equivalent to its strongly invertible mirror, despite 4_1 being amphicheiral.

Sakuma [79, Proposition 3.4] proved the following relationship between the amphicheirality and strong invertibility of hyperbolic knots.

Proposition 1.2.9 (Sakuma, 1985)**.** *Let K be a hyperbolic, amphicheiral knot which admits at least one strong inversion.*

1. *Suppose that K does not have a free or cyclic period of period 2, and let h be the unique inverting involution. Then $(K, h) \cong (\overline{K}, \overline{h})$.*
2. *Suppose K does have period 2, and let h_1 and h_2 be its two inequivalent inverting involutions. Then $(K, h_1) \cong (\overline{K}, \overline{h_2})$.*

1.2.2 Diagrams of strongly invertible knots

As we have seen, finding a diagram of a strongly invertible knot which exhibits the strong inversion is a non-trivial task. Indeed, a quick browse through Rolfsen's table of knots [77, Appendix C] reveals many instances of knots that are known to admit a strong inversion where the diagram chosen to represent the knot does not feature it. However, for 2-bridge knots Sakuma [79] has developed a method to determine their diagrams that feature the strong inversion.

Definition 1.2.10. Let $L \subset S^3$ be a link. A *bridge presentation* of L is a diagram D_L in which the majority of D_L lies entirely within the plane, with a finite number of 'bridges' containing all the over-crossings of the diagram. The *bridge number* of L is the minimum number of bridges required out of all possible bridge presentations.

In particular, 2-bridge knots are knots with bridge number 2; this is the smallest possible bridge

number a non-trivial knot can have.

A construction due to Schubert assigns to every 2-bridge link a pair of coprime integers (α, β) such that $\alpha > 0$, $|\beta| < \alpha$, and β is odd. The pair of integers is then used to construct a bridge presentation for the link which has bridge number 2. This presentation is referred to as *Schubert's normal form* of a 2-bridge link, and is denoted by $S(\alpha, \beta)$. Furthermore, if α is odd then $S(\alpha, \beta)$ is a knot, and if α is even $S(\alpha, \beta)$ is a two-component link. For a description of how the normal form is formed in practice see [38, Chapter 2].

Schubert [83] completely classified 2-bridge links (cf [38, Theorem 2.1.3]):

1. The 2-bridge knots $S(\alpha, \beta)$ and $S(\alpha', \beta')$ are equivalent if and only if

$$\alpha = \alpha', \ \beta^{\pm 1} \equiv \beta' \pmod{\alpha}.$$

2. The 2-component 2-bridge links $S(\alpha, \beta)$ and $S(\alpha', \beta')$ are equivalent if and only if

$$\alpha = \alpha', \ \beta^{\pm 1} \equiv \beta' \pmod{2\alpha}.$$

For knots, since α and β are both odd, we note that there exists an equivalent 2-bridge knot $S(\alpha, \beta')$, where $\beta' = \beta \pm \alpha$ and β' is even. Sakuma [79] uses a continued fraction expansion of $S(\alpha, \beta')$ in order to construct strongly invertible knot diagrams. Namely, $\frac{\alpha}{\beta}$ has the unique continued fraction

$$\frac{\alpha}{\beta} = a_1 + \cfrac{1}{a_2 + \cfrac{1}{a_3 + \cfrac{1}{\ddots + \cfrac{1}{a_n}}}}$$

where all the a_i *and* n are non-zero even integers. Sakuma denotes this continued fraction by $[a_1, a_2, \ldots, a_n]$.

Remark. This continued fraction is not the same as Conway's normal form for a 2-bridge link, although similar in appearance. To see this, we refer to [38, Chapter 10]; the continued fraction Sakuma uses makes an appearance in Exercise 2.1.14.

Now let $K(\alpha, \beta')$ be the 2-bridge knot with Schubert normal form $S(\alpha, \beta)$. Bankwitz and Schubert proved that 2-bridge knots are invertible [5], and it is also true that they have a cyclic period of period 2 (see [38, Figure 2.17] for a diagram exhibiting it). Suppose $K(\alpha, \beta')$ is a hyperbolic knot; then $K(\alpha, \beta')$ is strongly invertible and Proposition 1.2.8 tells us that $K(\alpha, \beta')$ admits exactly two distinct strong inversions. The templates for these strong inversions appear in [79, Figure 2.5] and are displayed in Figures 1.10 and 1.11; a positive integer α_i means there are α_i copies of $\times$ in the relevant box; a negative α_i means there is $|\alpha_i|$ copies of $\times$ (likewise for c_i).

Proposition 1.2.11 (Sakuma, 1985). *Let $K(\alpha, \beta')$ be a 2-bridge knot as above.*

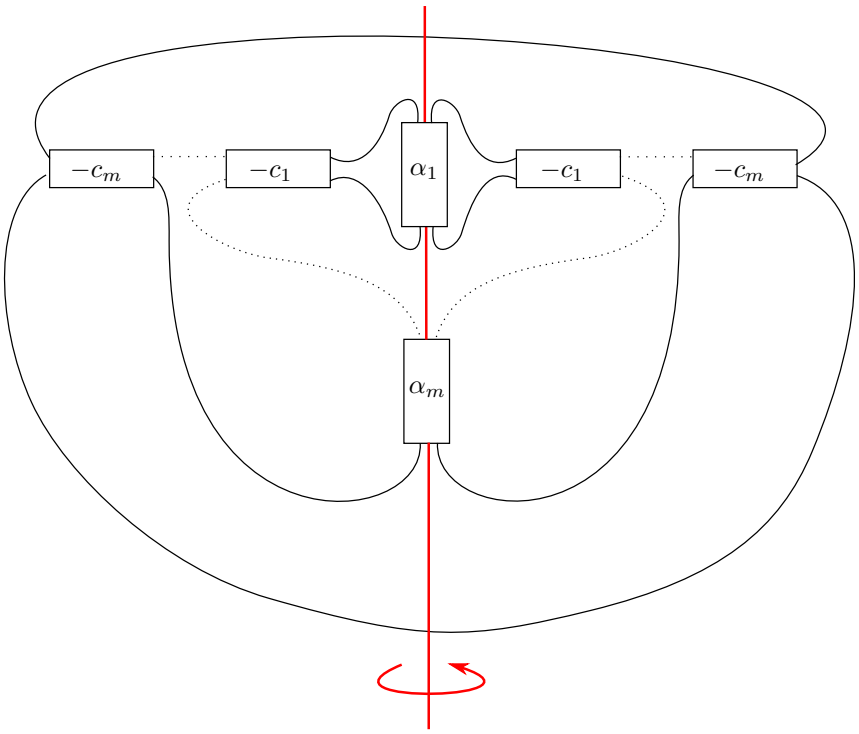

Figure 1.10: Strongly invertible knot diagram for $I_1(\alpha_1, \ldots, \alpha_m; c_1, \ldots, c_m)$

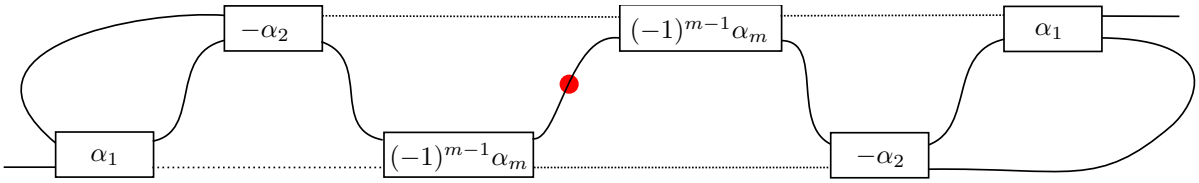

Figure 1.11: Strongly invertible knot diagram for $I_2(\alpha_1, \ldots, \alpha_m)$

1. *Suppose that* $q^2 \not\equiv 1 (mod\ p)$. *Then the two strong inversions on* $K(\alpha, \beta')$ *have diagrams given by* $I_1(a_1, a_3, \ldots, a_{n-1}; \frac{a_2}{2}, \frac{a_4}{2}, \ldots, \frac{a_n}{2})$ *and* $I_1(-a_n, -a_{n-2}, \ldots, -a_2; -\frac{a_{n-1}}{2}, -\frac{a_{n-3}}{2}, \ldots, -\frac{a_1}{2})$

2. *Suppose* $q^2 \equiv 1 (mod\ p)$ *and* $q \not\equiv 1 (mod\ p)$. *Then the two strong inversions on* $K(\alpha, \beta')$ *have diagrams* $I_1(a_1, a_3, \ldots, a_{n-1}; \frac{a_2}{2}, \frac{a_4}{2}, \ldots, \frac{a_n}{2})$ *and* $I_2(a_1, a_2, \ldots, a_{\frac{n}{2}})$

Remark. Actually, the diagram $I_2(\alpha_1, \ldots, \alpha_m)$ is technically not a knot diagram, as it is not a closed curve. In reality the two ends meet, but outside of the plane the diagram is drawn in. This cannot be depicted in the diagram whilst maintaining its symmetry without forming a four-way intersection at the red axis of rotation.

Example 1.2.12. This method was used to construct the two diagrams of the Figure-8 knot in Figure 1.9. The Figure-8 can be expressed as the 2-bridge knot $S(5, 2)$, and has continued fraction expansion $[2, 2]$ (see the Appendix of [79]). Since, $2^2 = 4 \not\equiv 1 (\text{mod } 5)$ we are in case (1) of Proposition 1.2.11, and the two diagrams are $I_1(2; 1)$ and $I_1(-2; -1)$.

Chapter 2

Auxiliary objects of strongly invertible knots

In this chapter we introduce a geometric construction due to Sakuma, which assigns a unique two-component link to every strongly invertible knot, and will investigate some of the properties of these 'Sakuma links'. Then we will describe another construction on strongly invertible knots due to Watson, which assigns a unique sutured tangle to each strongly invertible knot. It turns out that the two constructions can be combined in a sense — which provides us with a diagram of a Sakuma link in which Watson's tangle features. Finally, we will show how Sakuma's construction can be extended to assign further auxiliary objects to strongly invertible knots — these will take the form of tangles and annular knots.

2.1 Sakuma links

We begin with the first of the series of auxiliary objects we can attach to strongly invertible knots. In [79] Sakuma shows it is possible to associate to every strongly invertible knot a unique two-component link with linking number zero, where both components are unknotted. This construction works just as well on framed strongly invertible knots, composite strongly invertible knots (in the sense of Definition 1.2.7), and strongly invertible doubles.

2.1.1 Sakuma's construction

For an oriented strongly invertible knot (K, h), let $\mathcal{N}$ be an equivariant tubular neighbourhood of K, and l be a preferred longitude of $\mathcal{N}$. The requirement for equivariance means that our involution h takes $\mathcal{N}$ to itself (but non-trivially). In addition, we demand that the image of l under h does not intersect l — that is, $h(l) \cap l = \emptyset$. This means we have a pair of disjoint longitudes l and $h(l)$ which are exchanged by the strong inversion. Next, define $p : S^3 \to S^3/h \cong S^3$ to be the projection of S^3 to its quotient space under the involution h, $\mathcal{B} = p(\mathrm{Fix}(h))$, $\mathcal{L} = p(l \cup h(l))$, and claim that $\mathbb{L} = \mathcal{B} \cup \mathcal{L}$ is a link of the class we are interested in: we will henceforth refer to such links as *Sakuma links*.

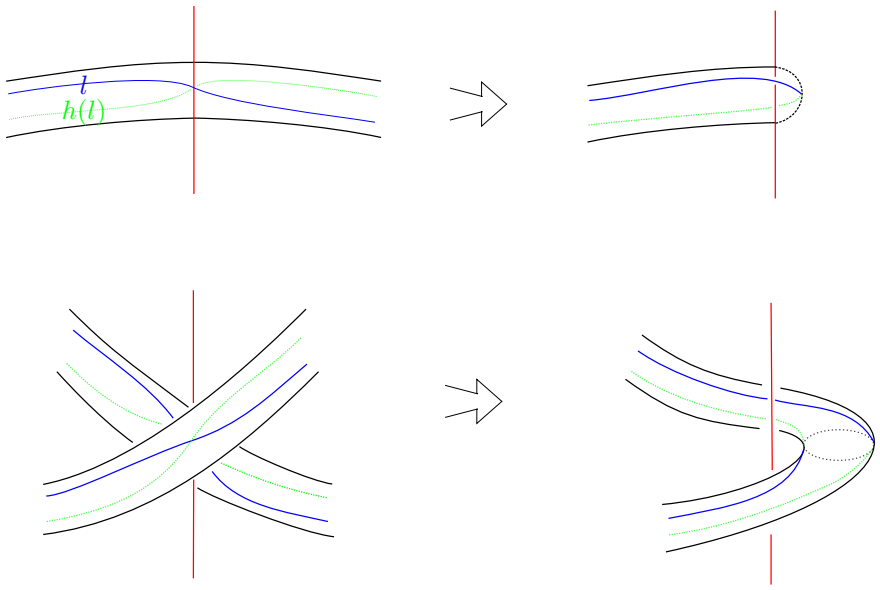

Figure 2.1: Constructing $\mathcal{L}$ from l and $h(l)$

Note that, as $\mathrm{Fix}(h)$ is unaffected by the action of p, $\mathcal{B}$ is still an unknotted circle. For $\mathcal{L}$, since $h(l) \cap l = \emptyset$, the effect of passing to the quotient space is that the two longitudes get glued together at the places where the fixed point set interacts with the knot to produce another copy of S^1. To see an example of this consider Figure 2.1. Here, the blue longitude l and the green longitude $h(l)$ have been drawn in such a way as to show their equivariant nature — l should be viewed as lying on the reader's side of $\mathcal{N}$, while $h(l)$ lies on its far side. Passing to the quotient space in each local case glues the longitudes together as shown.

For an example of Sakuma's construction in action, consider the trefoil with its single strong inversion (c.f. Proposition 1.2.8), $(3_1, h)$ as depicted in Figure 2.2. On the left hand side we have fixed a diagram for $(3_1, h)$, and on the right is a diagram for the two-component link $\mathbb{L}$ obtained from applying Sakuma's construction. A Sakuma link obtained from an equivalent strongly invertible knot is of the same type as $\mathbb{L}$, so any choice from the equivalence class of $(3_1, h)$ is permissible. For completeness we have also included a diagram of $p(K)$, the image of this presentation of the trefoil under the projection (the result of which is an edge of a θ-graph). When we draw diagrams of $\mathbb{L}$ we depict $\mathcal{B}$ as a vertical straight line (passing through the point at infinity) and draw $\mathcal{L}$ as an unknot with two parallel strands that lie entirely on the left or the right of $\mathcal{B}$ (according to taste) aside from in the following cases (see Figure 2.3):

1. The strands form a *clasp* around $\mathcal{B}$, with one strand looping over and back under to meet the other.

2. The strands coil around $\mathcal{B}$.

3. The strands twist about each other.

The first two relate to the two cases where $\mathrm{Fix}(h)$ crosses K:

1. When $\mathrm{Fix}(h)$ meets K.

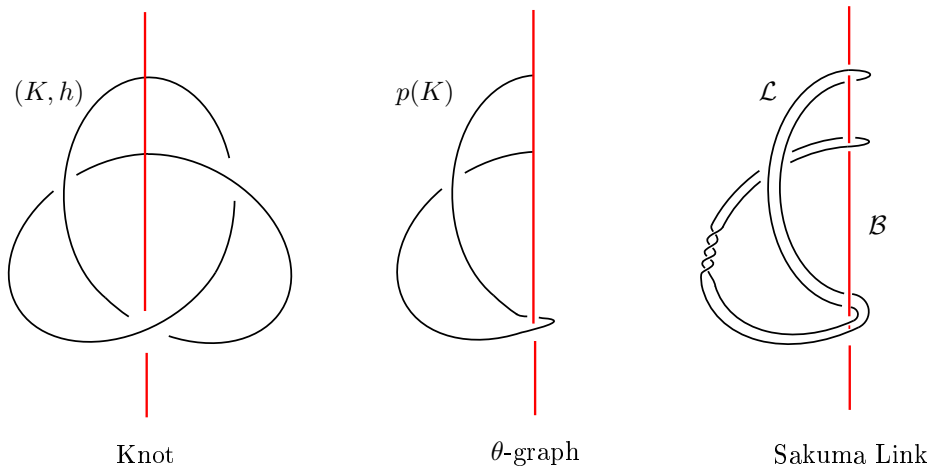

Figure 2.2: Sakuma's construction on $(3_1, h)$

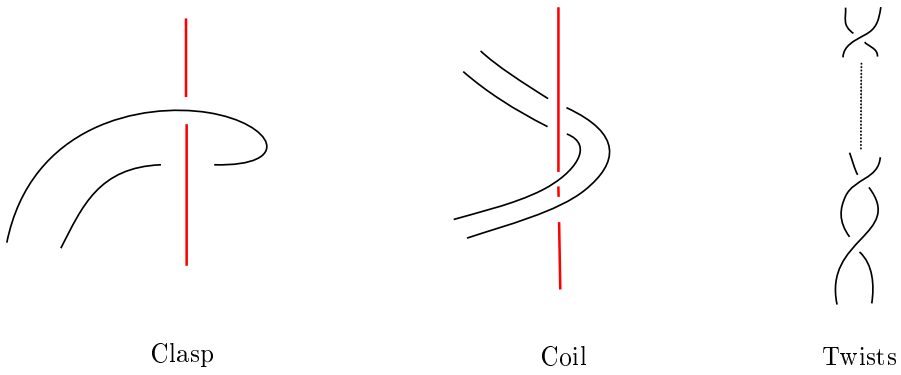

Figure 2.3: Local behaviour of Sakuma links

2. When $\mathrm{Fix}(h)$ passes between two strands of K.

The third case comes about from the framing of the longitude l. Since Sakuma requires that l be a preferred longitude (that is, a longitude with linking number zero), it is sometimes the case that compensatory twists must be put into l. These twists then get carried through the projection to form the twists in $\mathcal{L}$ — for an example see the Sakuma link in Figure 2.2, which was formed from a preferred longitude of the trefoil .

Remark. Notice that in Figure 2.2 we have chosen to draw the clasps of $\mathcal{L}$ so that they are 'oriented' oppositely. By this we mean that the 'upper' clasp has its over strand 'above' (with respect to the y-coordinate of the plane the diagram is drawn in) its parallel neighbour; and the 'lower' clasp has the over strand 'below' its neighbour. This could be changed by flipping one of the clasps over, at the price of changing the number of half twists between the strands. In all that follows, however, we will consider the clasps to be arranged as in Figure 2.2. Recall that the writhe is a property of an oriented knot diagram equal to the number of positive crossings minus the number of negative crossings. For knot diagrams of K with even writhe nothing needs to be changed, but when the writhe is odd (for example in the diagram of the trefoil Figure 2.2

comes from) a flip is needed to arrange the clasps as desired. Sakuma also makes this choice of clasp orientation, as can be seen in [79, Figure 2.1 (b)]. We will refer to such a diagram as the *standard projection diagram* of a Sakuma link, and will denote it $D_{\mathbb{L}}$. By convention, we shall always orient $\mathcal{B}$ with the arrow pointing upwards.

We will now justify why the linking number of $\mathcal{B}$ and $\mathcal{L}$ is zero in a Sakuma link. We firstly note that a coil can never make any contribution to the linking number, due to the fact one strand always travels in the opposite direction to its parallel neighbour. Therefore, the only non-zero linking between $\mathcal{B}$ and $\mathcal{L}$ comes from the clasps, and, since we specified at the beginning that $\mathrm{Fix}(h)$ intersects K in two points, we always have exactly two of them. When the clasps are oriented as specified above there is always an even number of half twists, therefore the clasps have opposite contributions to the linking number which cancel each other out.

2.1.2 Changing the framing

Although Sakuma specifies we use preferred longitudes when forming Sakuma links, we can just as easily ask for the linking number between l and K to be any integer we like. Therefore, it is possible to control exactly how many twists end up in $\mathcal{L}$, which allows us to create an extended family of *framed Sakuma links*. For example, if our diagram $D_{(K,h)}$ has even writhe and we were to take l to be the naive longitude we might first consider — known as the *blackboard framed longitude*, or the *Seifert longitude* — no twists appear in $\mathcal{L}$. Note that the framing of the blackboard longitude depends on the writhe of $D_{(K,h)}$.

However, changing the framing does affect the linking number of the resulting Sakuma link. We can get a two-component link of linking number zero when we take l to be an even framed longitude, and one of linking number ± 2 when l is an odd framed longitude. This follows from the discussion at the end of the previous section: when the clasps are oriented as per our convention an odd number of half twists in $\mathcal{L}$ means the linking number of $\mathbb{L}$ is ± 2, depending on how we decide to orient $\mathcal{L}$.

Definition 2.1.1. Suppose (K, h) is a strongly invertible knot and $n \in \mathbb{Z}$ is the linking number between K and a chosen longitude l. We call the triple (K, h, n) a *framed strongly invertible knot*. Let $\mathbb{L}_n$ be a two-component link obtained from (K, h, n) using Sakuma's construction on l and $h(l)$. We call $\mathbb{L}_n$ a *framed Sakuma link*, and note that $\mathbb{L}_0 := \mathbb{L}$. Two framed strongly invertible knots (K, h, n) and (K', h', n') are equivalent if and only (K, h) and (K', h') are equivalent, and $n = n'$.

Remark. When we talk about Sakuma links in general, without mentioning a specific framing, we mean the standard 0-framed case.

It is beneficial to know when forming a framed Sakuma link from a strongly invertible knot how many half twists will appear in $\mathcal{L}$. We will now make this number precise.

Lemma 2.1.2. *Let (K, h, n) be a framed strongly invertible knot with diagram $D_{(K,h,n)}$, and suppose the writhe of $D_{(K,h,n)}$ is x. Let $\mathbb{L}_n$ be the associated framed Sakuma link, and form the*

standard projection diagram $D_{\mathbb{L}_n}$. Let the number of half twists in $D_{\mathbb{L}_n}$ be denoted by m.

1. *Suppose x is even. Then $m = x - n$.*
2. *Suppose x is odd. If $x < 0$ then $m = x - n - 1$ and if $x > 0$, $m = x - n + 1$.*

Proof. Fix a diagram for (K, h, n) and suppose it has writhe $x \in \mathbb{Z}$. Then $-2x + 2n$ half twists must be added to a blackboard longitude ($-x + n$ on each side of $\mathrm{Fix}(h)$ in order to preserve symmetry under h), where by a negative half twist we simply mean one that has -1 linking number with K.

There are two cases we need to consider.

1. When x is even we end up with $x - n$ half twists in $\mathcal{L}$ with the clasps arranged as per our convention. Note that the sign of the half twists is reversed when we project — this is because the orientation of l is opposite to that of $h(l)$.
2. When x is odd we still have $x - n$ half twists after projecting but one of the clasps needs flipping over in order to arrange them as desired. This either adds another negative half twist if x is negative or adds a positive half twist if x is positive. So we end up with either $x - n - 1$ or $x - n + 1$ half twists.

□

2.1.3 Classifying Sakuma links

We will now formally classify Sakuma links, and prove that Sakuma's construction is indeed a bijection between the set of strongly invertible knots and the set of Sakuma links.

We will begin by recalling some covering space terminology, see for example [28] for further details. Given a topological space X, a covering space is, informally speaking, another topological space made up of multiple copies of X glued together.

Definition 2.1.3. Let X be a topological space. A *covering space* $\widetilde{X}$ is a topological space plus a map $p : \widetilde{X} \to X$ such that for each point $x \in X$ there is an open neighbourhood U of x such that $p^{-1}(U)$ is a union of disjoint open sets each of which is mapped homeomorphically onto U by p. We call $p^{-1}(x)$ a *fibre* over x, and the cardinality of $p^{-1}(x)$ the *degree* of the covering. If the degree, n, is finite we say the covering space $(\widetilde{X}, p)$ is an *n-fold covering space*.

Equally important are examples of spaces that 'almost' cover a space, expect for in a small subset. These are the *branched covering spaces*; we define them formally as follows (c.f. [77, Chapter 10B]).

Definition 2.1.4. Let $\widetilde{M}$ and M be n-manifolds with proper co-dimension 2 sub-manifolds $\widetilde{B} \subset \widetilde{M}$ and $B \subset M$. $\widetilde{M}$ is said to be a *branched covering* of M with *branch sets* $\widetilde{B}$ and B if there exists a surjective map $p : \widetilde{M} \to M$ satisfying:

1. Components of pre-images of open sets of M form a basis for the topology of $\widetilde{M}$.

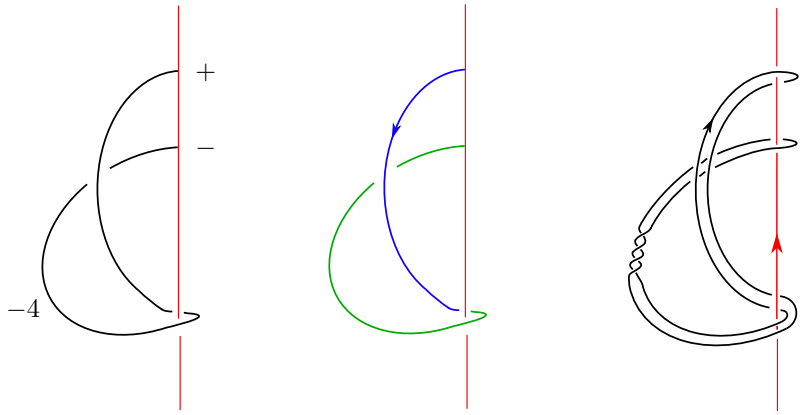

Figure 2.4: A θ-graph and its Sakuma link

2. $p(\widetilde{B}) = B$, $p(\widetilde{M} - \widetilde{B}) = M - B$, and the restriction $p : \widetilde{M} - \widetilde{B} \to M - B$ is a covering space map.

We call the restriction the *associated unbranched covering*, and if it has degree n we say the branched covering is an n-fold branched covering.

All of the branched covering spaces we will encounter will be 2-sheeted. These are referred to as *double branched covers*, and are often denoted by $\Sigma(M, B)$, where M is the base manifold, and B is the downstairs branch set.

We now will prove a lemma which allows us to recover the writhe of a strongly invertible knot diagram from its related θ-graph. Let (K, h, n) be a framed strongly invertible knot with diagram $D_{(K,h,n)}$ and equip this diagram with an orientation. This choice of diagram then necessarily fixes one for its θ-graph, and by an abuse of notation we denote the diagram of the interval corresponding to the image of K under the quotient map p $p(K)$. Next, orient $p(K)$, divide it up into sections, with the divides coming when $p(K)$ coils around $\mathcal{B}$, and colour the sections alternatingly with two colours (see Figure 2.4 for an example).

We notice that there are two ways in which $p(K)$ can coil around $\mathcal{B}$, depending on how the related crossing is arranged in $D_{(K,h,n)}$. We illustrate both cases in Figure 2.5, and label coil and crossing Type I or Type II.

Lemma 2.1.5. *Let (K, h, n), $D_{(K,h,n)}$ and $p(K)$ be as above and orient and colour $p(K)$ as described. Let X be the set of crossings in $p(K)$ between strands of the same colour and Y be the set of crossings between strands of different colours. Let a be the number of Type I coils and b be the number of Type II coils. Then,*

$$Wr\left(D_{(K,h,n)}\right) = 2\left[\sum_{x\in X} sign(x) - \sum_{y\in Y} sign(y)\right] - a + b.$$

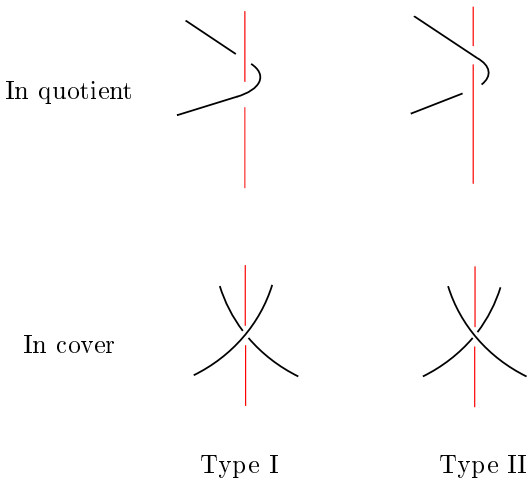

Figure 2.5: Coils and crossings

Proof. We begin by examining how crossings in our diagram $D_{(K,h,n)}$ get encoded in our diagram for $p(K)$ (which we also refer to as $p(K)$). Away from the image of the fixed point set a crossing in $p(K)$ corresponds to two crossings upstairs in $D_{(K,h,n)}$. Furthermore, each coil in $p(K)$ corresponds to a single crossing in $D_{(K,h,n)}$, namely to one that has the fixed point set of h passing through the middle of it. Putting this information together we note that

$$\text{number of crossings in } K = a + b + 2(\text{number of crossings in } p(K)).$$

We now claim that Type I crossings in $D_{(K,h,n)}$ always contribute -1 to $Wr\left(D_{(K,h,n)}\right)$ and Type II crossings always contribute $+1$. Suppose for a contradiction that a Type I crossing contributes $+1$ to $Wr\left(D_{(K,h,n)}\right)$. Then, the strands forming the crossing must be oriented so that the outgoing strands are on opposite sides of the fixed point set. We know they must eventually return to interact with the fixed point set; in particular, we must have one of three possible cases:

- The strands attach to another Type I crossing
- The strands attach to a Type II crossing
- The strands meet at one of the intersection points with the fixed point set

The problem with each of these possibilities is that, due to the symmetry of $D_{(K,h,n)}$, it is impossible to put a consistent orientation on it. The third case can be immediately ruled out, as the strands would then meet oppositely oriented. For the other two cases, since the strands leave on opposite sides they must return to a Type I or Type II crossing from opposite sides. This means that they can only join to another positive Type I crossing or to a negative Type II crossing. But now we are stuck, because a negative Type II crossing presents exactly the same

problem: the outgoing strands cannot join to an intersection point. Hence, we can only have negative Type I crossings in $D_{(K,h,n)}$. The same argument works for positive Type II crossings. Hence, we can only have negative Type I crossings and positive Type II crossings – which explains the last two terms in our writhe formula for $D_{(K,h,n)}$.

We now will examine the contributions made by crossings away from the fixed point set. Observe that at a coil the orientation of $p(K)$ always swaps between matching the orientation on the related strand in $D_{(K,h,n)}$ to opposing it — this is precisely what is encoded by the colouring of $p(K)$. Examining the crossings, we note that the sign of a crossing between two strands of the same colour is always the same as the sign of the related crossing in $D_{(K,h,n)}$, whilst the sign of a crossing between different coloured strands is always opposite to the related sign in $D_{(K,h,n)}$.

Putting everything together gives us the result as claimed. □

Example 2.1.6. As an example, let us see what happens when we apply the lemma to the diagrams in Figure 2.4. The number of Type I coils is 1, the number of Type II coils is 0, the set X is empty and the set Y contains one crossing with sign $+1$. Therefore, the writhe of the diagram of the trefoil which induced the diagram of the θ-graph is:

$$Wr\left(D_{(K,h,n)}\right) = 2(-1) - 1 = -3$$

as expected.

The lemma is used together with the following observation. Given fixed diagrams $D_{(K,h,n)}$, $p(K)$, and $D_{\mathbb{L}_n}$ we can pass from $D_{\mathbb{L}_n}$ to $p(K)$ if we decorate the θ-graph with the extra information found in $D_{\mathbb{L}_n}$. See Figure 2.4 for an example of this observation in practice: the left picture has been decorated with an integer to keep track of the twists (and their sign) in $\mathcal{L}$, as well as plus and minus signs, which tell us how the clasps are arranged.

We now can classify framed Sakuma links.

Proposition 2.1.7. *Let $L = K_1 \cup K_2$ be a two-component oriented link in S^3. Suppose the following two conditions hold:*

L-1 K_1 and K_2 are unknotted.

L-2 Up to ambient isotopies of L, K_2 bounds a properly embedded disc meeting K_1 transversely in exactly two points.

Then L is a framed Sakuma link, that is, there exists some framed strongly invertible knot (K, h, n) such that applying Sakuma's construction returns L.

Proof. We begin by noting that since K_2 is unknotted, it bounds a disc, which we will call S_2. Now, condition L-2 tells us that K_2 forms two clasps around K_1, in the sense of Figure 2.3. We now perform an ambient isotopy on K_1 so that it passes through the point at infinity, so that a diagram of L has K_1 depicted as an axis. Then we take the double branched cover $\Sigma(S^3, K_1)$, which, since K_1 is unknotted, is just another copy of S^3, and consider the lifts of K_2. These will

be two longitudes of a knot K that meets the branch set, the lift of K_1, exactly twice — once for each clasp downstairs. Furthermore, K admits a strong inversion h given by rotating K π radians about the branch set; and the lifts of K_2 are equivariant with respect to this inversion. In order to determine the framing n of the lifts of K_2 we use Lemma 2.1.2 and Lemma 2.1.5.

Hence, (K, h, n) is a framed strongly invertible knot, and has L as its associated framed Sakuma link.

□

While the above result does not explicitly mention the linking number of L, the fact that it is either 0 or ± 2 follows from condition L-2. Following the notation given in [77, Chapter 5D], let us equip S_2 with a bi-collar (S_2, S_2^+, S_2^-) i.e. take $S_2 \times [-1, 1]$ and set $S_2^+ = S_2 \times \{1\}$ and $S_2^- = S_2 \times \{-1\}$. Then exactly one of the following three things must happen:

1. At both intersection points K_1 passes locally from S_2^- to S_2^+.
2. At both intersection points K_1 passes locally from S_2^+ to S_2^-.
3. At one point K_1 passes locally from S_2^- to S_2^+, and at the other from S_2^+ to S_2^-.

This implies the linking number $lk(K_1, K_2)$ must be either 2, -2, or 0 respectively.

Proposition 2.1.8. *There is a bijection between the set of framed strongly invertible knots and the set of framed Sakuma links.*

Proof. Denote by ϕ the map which takes a framed strongly invertible knot to its framed Sakuma link. We will first prove ϕ is well defined, then will prove it is injective. Surjectivity follows from Proposition 2.1.7.

- Let us first prove that ϕ is well defined. Suppose that two framed strongly invertible knots are equivalent i.e. $(K, h, n) \cong (K', h', n')$. We immediately must have $n = n'$, and a homeomorphism $f\colon S^3 \to S^3$ such that $fhf^{-1} = h'$ and $f(K) = K'$. We are looking to construct a homeomorphism $g\colon S^3 \to S^3$ that takes $\mathbb{L}$ to $\mathbb{L}'$.

  We begin by observing that $f(\mathrm{Fix}(h)) = \mathrm{Fix}(h')$, and $f(l) \cup f(h(l))$ is a pair of equivariant preferred longitudes on K'. Also, h and h' define equivalence relations $\sim$ and $\sim'$ on S^3, and p and p' can be thought of as mapping each point x to its respective equivalence classes $[x]_\sim$ and $[x]_{\sim'}$. Given this, we define a map g as follows:

$$\begin{aligned} g\colon\ & S^3 \to S^3 \\ & [x]_\sim \mapsto [f(x)]_{\sim'} \end{aligned}$$

  It is now easy to see that g takes $\mathbb{L}$ to $\mathbb{L}'$ as required.

- Now let us prove that ϕ is injective. Suppose that applying Sakuma's construction to two framed strongly invertible knots (K, h, n), (K', h', n') gives equivalent links downstairs i.e.

there exists a g such that $g(\mathbb{L}_n) = \mathbb{L}'_{n'}$. We want to now show that $(K, h, n) \cong (K', h', n')$.

Let x be a point in the downstairs copy of S^3, and let $\widetilde{x}_1$ and $\widetilde{x}_2$ be its two lifts, with respect to p, in the covering copy of S^3. Likewise, let $\widetilde{g(x)}_1$ and $\widetilde{g(x)}_2$ be the two lifts of $g(x)$ with respect to p'. We note that the strong inversions h and h' exchange the relevant two lifts. We define a map f as follows:

$$\begin{aligned} f\colon\ & S^3 \to S^3 \\ & \widetilde{x}_i \mapsto \widetilde{g(x)}_i \quad i \in \{1, 2\}. \end{aligned}$$

It should be clear that f takes K to K', and $fhf^{-1} = h'$ as required. Furthermore, since f is a homeomorphism, it also preserves the linking number between K and l. Hence, $n = n'$, and we are done.

□

2.1.4 Properties of Sakuma links

While not every two-component link can be a Sakuma link due to the linking number restriction and the fact that both the components are unknotted in a Sakuma link, they still form an interesting subset of the set of two-component links; to the author's knowledge they have not been studied before as a class in their own right.

We now will prove some elementary facts about Sakuma links, in order to give ourselves a clearer image of them. The fact that the projection diagrams for Sakuma links get increasingly more complex in terms of the number of crossings means that computing link invariants is computationally time consuming. However, we can make use of Sakuma's construction. Although it was originally developed in order to prove things about strongly invertible knots, we can use it in the opposite direction; that is, we can use properties about strongly invertible knots to say things about Sakuma links.

Lemma 2.1.9. *Sakuma links are prime.*

Sakuma links are clearly non-trivial and non-split. They are also locally trivial — no factorising sphere exists that can cut a Sakuma link into two distinct prime links.

Given a link it is of interest to determine whether it is hyperbolic, torus or satellite. We next will show the existence of Sakuma links in each of the three sets. To do so, we make use of the following theorem, due to Menasco [55].

Theorem 2.1.10 (Menasco, 1984)**.** *Let $L \subset S^3$ be a link. If L is prime and alternating, and L is not a torus link, then L is hyperbolic.*

Adams, writing in [56, Chapter 1], explains that in order to tell that a prime alternating link is not a torus link we simply need to draw the alternating projection. If the diagram is not a

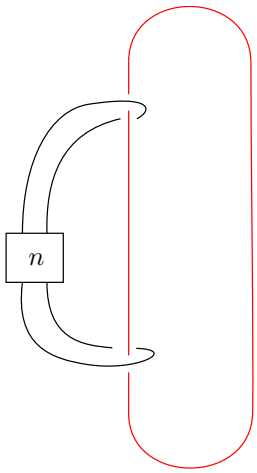

Figure 2.6: Sakuma links associated to $(\mathcal{U}, h_0, n)$

'2-braid', that is, a diagram in which the two strands twist around one another (see [56, Figure 1]) then the link is not a torus link.

We now turn to the family of framed Sakuma links associated to the framed strongly invertible unknots. This family is alternating, as can be seen in Figure 2.6 (up to flipping the clasps), and aside from the cases where $n = \pm 1$, they are not torus links. Theorem 2.1.10 then tells us that they must be hyperbolic. This fact can also be verified by use of SnapPy [16]. The cases in which $n = \pm 1$ can be drawn as 2-braids, and so are torus links.

There is also an infinite family of Sakuma links which are satellite.

Proposition 2.1.11. *Let $K \subset S^3$ be any knot. Then there exists infinitely many framed satellite Sakuma links with companion K.*

Proof. Given a knot K form the framed strongly invertible double $(D(K), h, n)$. Suppose $\mathbb{L}_n$ is the framed Sakuma link associated to $(D(K), h, n)$: it can be easily seen that $\mathbb{L}_n$ is a satellite link with companion K. See Figure 2.7 for an instance where K is the right-handed trefoil — those with an interest in rock climbing may observe that the blue component essentially forms an overhand knot on the bight. □

Remark. Note that we do not require K to be prime in the above proposition. Strongly invertible doubles are defined just as well for composite K.

The above proposition works because the framed Sakuma links associated to framed strongly invertible doubles do not have any coils in their projection diagrams (in the sense of Figure 2.3), which allows for the existence of a factorising sphere. This is an interesting feature of Sakuma links that will affect the possible symmetries they can have. We state exactly which subsets of Sakuma links share this property.

Proposition 2.1.12. *Let $\mathbb{L}_n = \mathcal{B} \cup \mathcal{L}$ be a framed Sakuma link, and consider the standard projection diagram $D_{\mathbb{L}_n}$ that results from Sakuma's construction. Suppose there are no coils in*

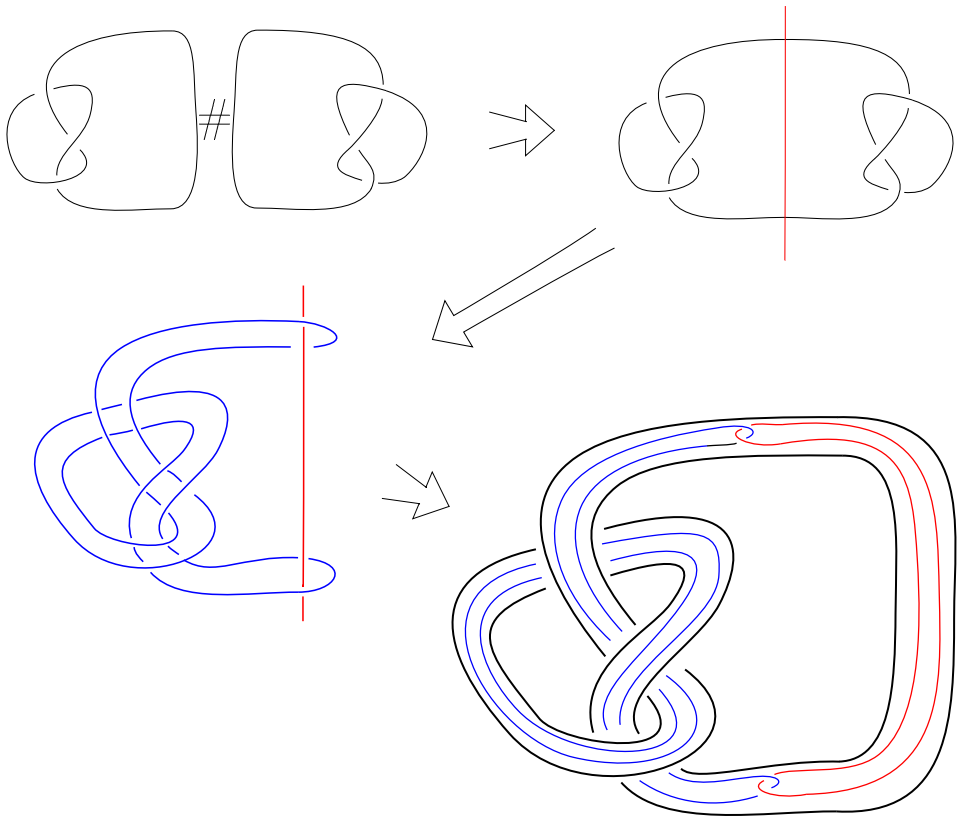

Figure 2.7: A Sakuma link viewed as a satellite link

$\mathcal{L}$. *Then* $\mathbb{L}_n$ *is associated to one of the following:*

1. *A framed strongly invertible unknot* $(\mathcal{U}, h_0, n)$.
2. *A framed strongly invertible double* $(D(K'), h, n)$, *for some prime knot* K'.
3. *A framed equivariant product of strongly invertible doubles,* $(\{\#_{i=1}^{s} D(K_i')\}, h, n)$, *for prime knots* K_i'.

Proof. This can be seen by reversing Sakuma's construction, by taking the double branched cover of the pair (S^3, B). If $\mathcal{L}$ does not coil around $\mathcal{B}$ then its two lifts in $\Sigma(S^3, B)$, i.e. the two longitudes of the strongly invertible knot (K, h, n), cross $\mathrm{Fix}(h)$ exactly twice. This means that K can only cross $\mathrm{Fix}(h)$ twice too; namely, at the two points where K meets $\mathrm{Fix}(h)$. But then we can embed a factorising sphere S into S^3 which meets K at both points of $K \cap \mathrm{Fix}(h)$. Therefore K is a product knot. In light of Lemma 1.2.6 and Theorem 1.2.7, it then follows that either K is either equivalent to a framed strongly invertible unknot, to a framed strongly invertible double, or to a framed equivariant product of strongly invertible doubles. □

We note that every framed Sakuma link described in Proposition 2.1.12 is a satellite link.

We may also be interested in the symmetry properties of Sakuma links. These will be discussed in more detail at the end of the next chapter, when more tools have been made available to us. For now, let us state the necessary criteria for a Sakuma link to be amphicheiral.

Lemma 2.1.13. *Let $\mathbb{L}_n$ be the framed Sakuma link associated to the strongly invertible knot (K, h, n). Then the mirror of $\mathbb{L}_n$ is the framed Sakuma link $\overline{\mathbb{L}}_{-n}$, which is obtained from $(\overline{K, h, -n})$.*

Proof. This follows from Sakuma's construction. Using Lemma 2.1.2 we see that in order to swap the sign of the twist crossings over we need to take $-n$ as the framing on our longitudes. □

Corollary 2.1.14. *Let $\mathbb{L}_n$ be the framed Sakuma link associated to the framed strongly invertible knot (K, h, n). Then $\mathbb{L}_n$ is amphicheiral if and only if $(K, h, n) \cong (\overline{K, h, -n})$; that is, if and only if there exists an orientation preserving homeomorphism f on S^3 such that $f(K) = \overline{K}$, $h = f^{-1}hf$, and $n = 0$.*

Proof. This is a consequence of Sakuma's bijection and the above lemma. □

We can immediately conclude from the above that framed Sakuma links are not amphicheiral, apart from in the standard case where $n = 0$. Even here, we can rule out more candidates. For example, strongly invertible torus knots $(T(p, q), h)$ can never have an amphicheiral Sakuma link, as torus knots are always cheiral. For hyperbolic knots we can combine the corollary with Sakuma's result (Proposition 1.2.9). In order for a Sakuma link $\mathbb{L}$ associated to a hyperbolic amphicheiral strongly invertible knot (K, h) to be itself amphicheiral it must be the case that K admits a single strong inversion — so it cannot have a free or cyclic period of period 2. We observe that in the tables Sakuma provides in the appendix of [79] none of the prime strongly invertible knots with 9 crossings or less have this property.

2.2 Sakuma tangles

An additional family of geometric objects we can associate to strongly invertible knots comes in the form of a collection of tangles.

We will start with the definition of a general tangle (c.f. [50, Section 1], [92, Definition 3]).

Definition 2.2.1. An *n-string tangle* T is a pair (B^3, τ), where B^3 is the 3-ball and τ is a collection of n properly embedded arcs in B^3 with $\tau \cap \partial B^3 = \partial \tau$, along with a potentially empty set of embedded copies of S^1.

There are two differing notions of equivalence for tangles, depending on whether we desire to keep the end points of the arcs fixed or not. If we want the end points free then tangles are considered equivalent up to homeomorphism of the pair (B^3, τ) (or, equivalently up to ambient isotopy of τ within B^3). If we want the end points to be fixed, we also specify that the homeomorphisms (ambient isotopies) fix the boundary of B^3. Their usefulness comes when we want to examine local properties of a knot or link, which allows us to prove things about the links themselves.

We will be primarily concerned with a certain class of tangles, called *sutured tangles*. Sutured tangles arise when instead of using B^3, we take the homeomorphic sutured manifold $D^2 \times I$ (see Figure 2.8). Sutured manifolds are a class of 3-manifolds with boundary, and were first defined by Gabai in [19]. They have been of particular interest in recent years due to the development

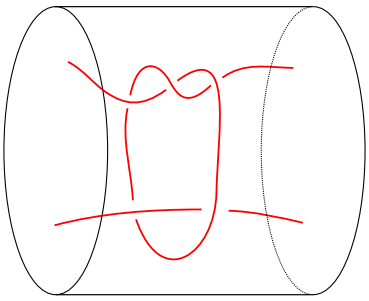

Figure 2.8: A sutured tangle

of homological invariants of sutured objects, some of which we will see in Chapter 4. Sutured manifolds are defined formally as follows.

Definition 2.2.2. A *sutured manifold* (Y, Γ) is a compact, oriented 3-manifold with boundary ∂Y along with a set $\Gamma \subset \partial Y$ of pairwise disjoint annuli $A(\Gamma)$ and tori $T(\Gamma)$. The interior of each component of $A(\Gamma)$ contains a *suture* — an oriented, simple, closed curve which is homologically non-trivial in $A(\Gamma)$. We denote the set of sutures by $s(\Gamma)$.

We can equip $D^2 \times I$ with a sutured structure by taking $A(\Gamma)$ to be the subset $S^1 \times I \cong A$: the suture is usually taken to be the curve $S^1 \times \{\frac{1}{2}\}$. The definition of a sutured tangle is then as follows (cf. [92, Definition 3]).

Definition 2.2.3. An *n-string sutured tangle* T is a pair $(D^2 \times I, \tau)$, where n of the end points of $\partial\tau$ are contained in $D^2 \times \{0\}$ and n are contained in $D^2 \times \{1\}$.

Sutured tangles are considered up to homeomorphisms of $(D^2 \times I, \tau)$ which fix $\partial D^2 \times I$ point-wise (equivalently, up to ambient isotopies of τ which act trivially on $\partial D^2 \times I$ c.f. [22, Definition 5.1]). This is in order to preserve the sutured structure of the manifold $D^2 \times I$. In all that follows all the tangles we will encounter will be sutured; when we henceforth refer to a tangle, we really mean a sutured tangle. Note that this notion of equivalence allows us to move the end points of the tangle around, as long as we keep them within $D^2 \times \{0, 1\}$. We shall depict sutured tangles as a collection of broken arcs in a copy of $I \times I$, where, as for link diagrams, a break indicates a crossing between two strands.

A related family of objects worth mentioning are *braids*. A general n-strand braid B_n consists of n properly embedded strands in $D^2 \times I$, each with one boundary point in $D^2 \times \{0\}$ and one in $D^2 \times \{1\}$, with each strand intersecting every $D^2 \times \{t\}$ $(0 \leq t \leq 1)$ exactly once. As for sutured tangles, we depict braids as a collection of strands lying within $I \times I$; the additional condition means that each strand travels continually from $I \times \{0\}$ to $I \times \{1\}$ without ever turning back on itself. We use a stronger equivalence relation on braids; namely, we specify that ambient isotopies additionally fix $D^2 \times \{0, 1\}$. In pratice, this means the end points of braids are fixed.

Given a braid diagram B_n we can form its closure $\widehat{B_n}$. This is the link diagram formed by joining the end point of each strand $x \times \{0\}$ to the end point $x \times \{1\}$ that lies directly opposite from it without creating any new crossings. A famous theorem of Alexander [1] says that every link in

S^3 can be represented by closing a braid diagram in this way. We can also form the closure of a sutured tangle diagram D_T in the same way; we call the link diagram $D_{\widehat{T}}$ obtained the *braid-like closure* of D_T.

2.2.1 Classifying Sakuma tangles

We look to show that every strongly invertible knot has an associated sutured tangle, which we will call its *Sakuma tangle*. We will first outline a recipe of how to build a Sakuma tangle, then will show how Sakuma tangles are related to Sakuma links. An example of the following recipe (with $k = 2$) can be seen in Figure 2.9.

- Begin by defining a k-string tangle with no closed components that we depict in a copy of $I \times I$ by placing $k-1$ marked points on the top and bottom edges, along with one marked point on each side edge.
- We then form the 2-cable of the tangle, and add a total of m half twists between pairs of strands, where for two strands running vertically in the diagram the crossing $\times$ is represented by $+1$.
- Finally, we attach to both sides of the twisted 2-cable a trivial 2-string tangle, with one strand running to the top edge and the other strand to the bottom edge. Call this tangle diagram D_{T^m}.

We observe that a tangle T^m constructed in this way is a member of an equivalence class. In particular, we can exchange pairs of points in the same $D^2 \times \{0, 1\}$ which are the endpoints of strands that twist around each other, which will change the value of m. The reason we take pains to distinguish representatives from the same tangle is due to the different results we get when closing them up. Let the braid-like closure of T^m be denoted by $\widehat{T^m}$; we note that $\widehat{T^m} \ncong \widehat{T^n}$ if $m \neq n$.

We are now ready to formally characterise the class of Sakuma tangles.

Definition 2.2.4. Let T be a k-string sutured tangle with no closed components and $k \in 2\mathbb{Z}$. Suppose the following two conditions hold:

T-1 The braid-like closure $\widehat{T}$ is unknotted in S^3.

T-2 T admits a construction as above.

Then T is a representative of some Sakuma tangle.

The conditions given in the above definition should be viewed as the tangle counterparts to those found in Proposition 2.1.7. In particular, condition T-1 is intended to correspond to condition L-1, and condition T-2 to condition L-2. This motivates the following result.

Proposition 2.2.5. *Let T^m be a representative of a Sakuma tangle. There exists a unique Sakuma link $\mathbb{L}_n$ associated to T^m, for some $n \in \mathbb{Z}$.*

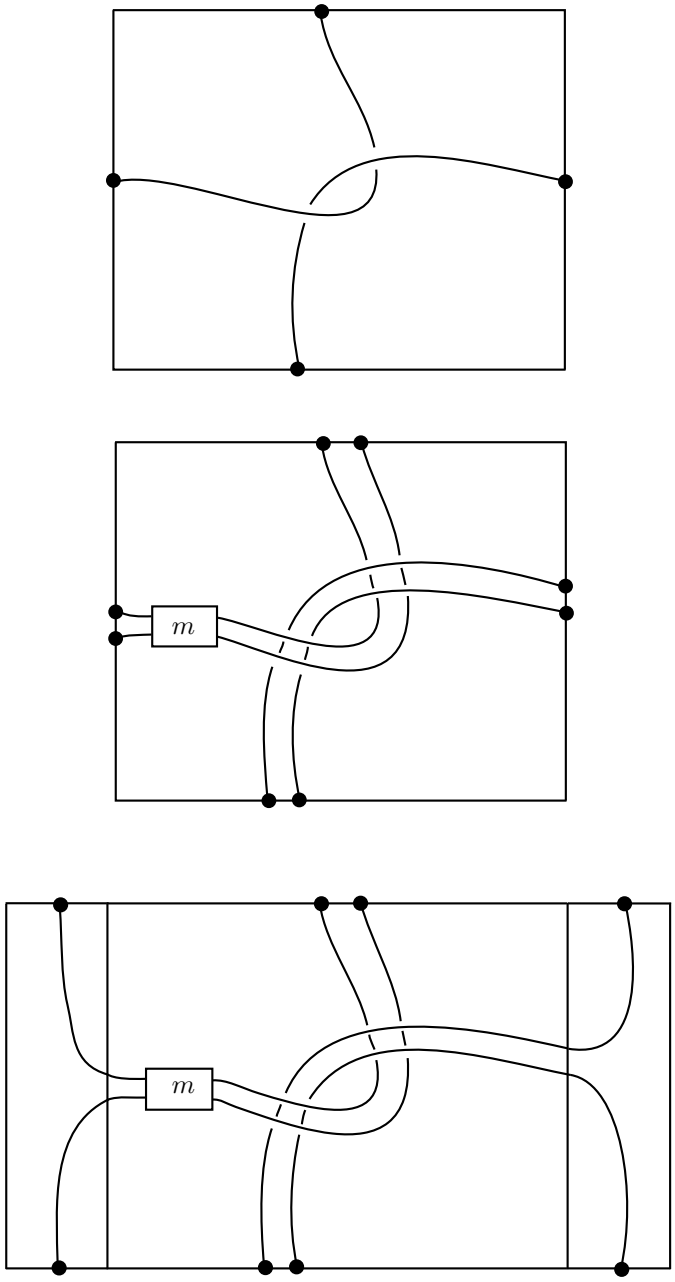

Figure 2.9: Constructing a Sakuma tangle

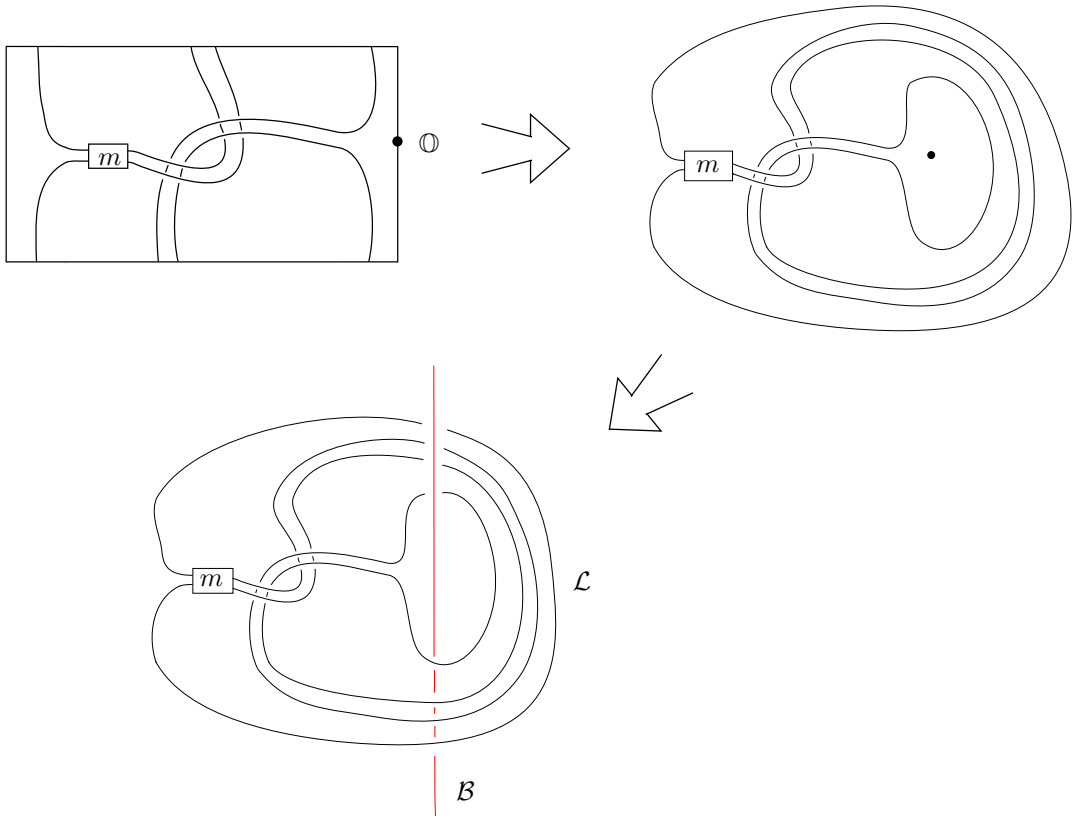

Figure 2.10: Constructing a Sakuma link from a Sakuma tangle

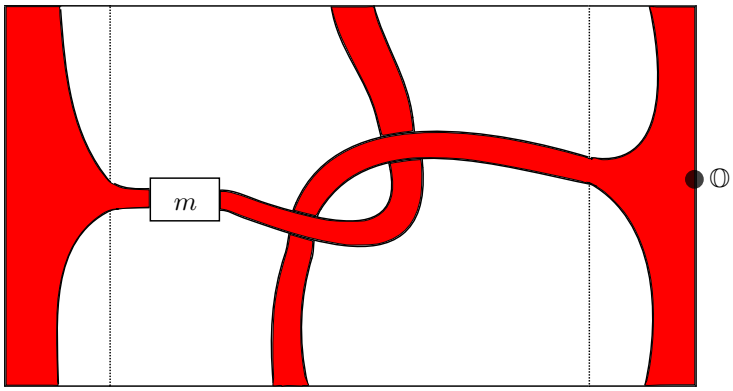

Figure 2.11: The cut open disc S_2 as seen in a Sakuma tangle

Proof. We begin by exhibiting how a Sakuma link can be obtained from a Sakuma tangle, then will show that this link is unique up to link equivalence. See Figure 2.10 for an illustration of the following process.

Suppose T^m has n strands. Fix a diagram D_{T^m}. We first form link diagram from D_{T^m}.

1. Mark a point $\mathbb{O}$ on D_{T^m} at $(1, \frac{1}{2})$. Then form $D_{\widehat{T^m}}$, ensuring that it encloses $\mathbb{O}$. Call this component $\mathcal{L}$.

2. Add an additional component to $D_{\widehat{T^m}}$, which we depict as a vertical axis passing through $\mathbb{O}$ and the point at infinity, and forming exactly $2n$ crossings with $\mathcal{L}$ as suggested in Figure 2.10. Label this component $\mathcal{B}$.

We claim $\mathbb{L}_n = \mathcal{B} \cup \mathcal{L}$ is a Sakuma link i.e. it satisfies both conditions of Proposition 2.1.7.

Firstly, we note that L-1 is satisfied since $\mathcal{B}$ is unknotted by definition, and $\mathcal{L}$ is unknotted by condition T-1.

For L-2, we can find the required disc as follows. Shade in the regions in the tangle diagram bounded by T^m as in Figure 2.11 to get a series of ribbons, with one ribbon widening out at either end. Now we form $D_{\widehat{T^m}}$, and observe that this allows us to glue the ribbons together in such a way as to from a single long disc with a lasso at both ends. Furthermore, $\mathcal{B}$ meets the disc transversely in exactly two points — once at $\mathbb{O}$ and once at the centre of the other lasso — so L-2 is also satisfied. In order to determine the value of n we need to use Lemma 2.1.2 and Lemma 2.1.5 as we did when classifying Sakuma links.

Now suppose T and T' are equivalent Sakuma tangles, and $\mathbb{L}$ and $\mathbb{L}'$ be their associated Sakuma links. Then the ambient isotopy between T and T' induces one between $\mathbb{L}$ and $\mathbb{L}'$, and so $\mathbb{L}$ and $\mathbb{L}'$ are equivalent links. □

Conversely, Sakuma tangles are obtained from Sakuma links very naturally.

Lemma 2.2.6. *Let $\mathbb{L}_n = \mathcal{B} \cup \mathcal{L}$ be a framed Sakuma link. Then there is a unique representative of a Sakuma tangle associated to $\mathbb{L}_n$.*

Proof. We obtain a Sakuma tangle from $\mathbb{L}_n$ by passing to the exterior of $\mathcal{B}$, which is homeomorphic to a solid torus. We cut this solid torus along a meridional disc intersecting $\mathcal{L}$ transversely and unfurl the result — which gives us the 3-manifold $D^2 \times \mathbb{R}$ with $2k$ strands. We see immediately that it satisfies T-2, and since $\mathcal{L}$ is unknotted it also satisfies T-1. Hence, it is a representative of a Sakuma tangle. □

Combining the previous two results gives us a bijection.

Corollary 2.2.7. *There is a one-to-one correspondence between Sakuma links $\mathbb{L}_n$ and tangle representatives of Sakuma tangles T^m.*

We can also compare strongly invertible knots and Sakuma tangles. Since changing the framing of the strongly invertible knot yields a different representative of the same Sakuma tangle, it follows that the two sets are in natural bijection.

Corollary 2.2.8. *There is a one-to-one relationship between strongly invertible knots (K, h) and Sakuma tangles.*

2.3 Watson tangles

In addition to Sakuma's, there is another major construction on strongly invertible knots that we will be utilising. In [91] Watson shows it is possible to associate to every strongly invertible knot another sutured tangle which is distinct from the Sakuma tangle defined in the previous section. However, as we will see, Watson's construction fits very neatly in with Sakuma's.

2.3.1 Watson's construction

Watson begins by considering the exterior of a strongly invertible knot (K, h), which we will denote by $E(K) \cong S^3 \backslash \mathring{\mathcal{N}}(K)$. The strong inversion on K also acts on $E(K)$: we say that $E(K)$ is strongly invertible if there is an involution h on $E(K)$ with 1-dimensional fixed point set intersecting the boundary torus $\left(\partial E(K) \cong \partial \mathring{\mathcal{N}}(K)\right)$ in exactly four points. Clearly $E(K)$ is strongly invertible if and only if K admits a strong inversion.

Next, analogously to Sakuma, we quotient out by the involution h. This produces a manifold $E(K)\backslash h$ homeomorphic to the standard 3-ball B^3. Consider now $\mathrm{Fix}(h)$ as a subset of $E(K)$: it is composed of two strands with all four boundary points lying on the boundary torus. Watson's tangle is defined to be the pair $(E(K)\backslash h, p(\mathrm{Fix}(h))$, where $p : E(K) \to E(K)/h$. The process for the left-hand trefoil is shown in Figure 2.12 — we will follow Watson and depict the strands in the tangle as running horizontally.

Remark. The construction can be easily reversed by taking the double branched cover of a Watson tangle $\Sigma(B^3, \tau)$. This returns us the knot exterior $E(K)$ of a strongly invertible knot (K, h).

An important point to note about Watson's construction is that it makes no use of framed longitudes; as for Sakuma tangles, only one Watson tangle is obtained for each strongly invertible knot.

We now consider Watson's construction in the sutured setting. It turns out that it can be adapted to sutured tangles very easily, as long as we equip $E(K)$ with a sutured structure. See [92, Figure 4] for an example of this in practice. Recall that a sutured n-string tangle is a tangle in $D^2 \times I$ such that n points lie on $D^2 \times \{0\}$ and n other points lie on $D^2 \times \{1\}$. The main difference in the sutured case is that we are restricted in what we can do with the boundary points. In particular, we cannot exchange a point in $D^2 \times \{0\}$ with a point in $D^2 \times \{1\}$ as that would not preserve the sutured structure of $D^2 \times I$. We can, however, exchange a pair of points in the same $D^2 \times \{0, 1\}$, which amounts to adding twists in two strands of τ. We will label the

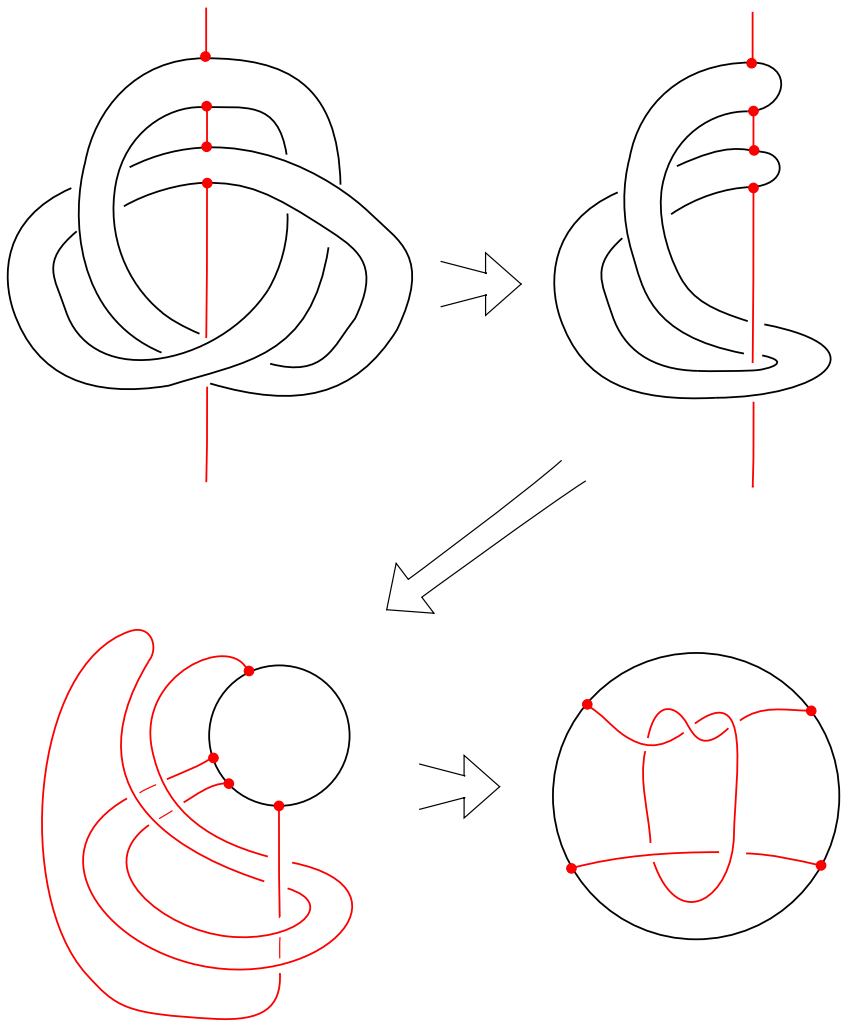

Figure 2.12: Watson's construction

tangle diagram with zero twists D_{T^0}, and, with the convention that $\diagup\!\!\diagdown$ is represented by $+1$, we will refer to the tangle representative with m twists to be D_{T^m}. As for Sakuma tangles, when no specific representative is required, we will simply use D_T.

After we have fixed a representative and chosen a diagram of a Watson tangle T we can obtain a collection of link diagrams by adding in extra strands to connect the endpoints of τ. Firstly, we can join the endpoints in $I \times \{0\}$ and $I \times \{1\}$ together without adding any extra crossings; we will follow Watson's notation and call the link represented by this diagram $T(\frac{1}{0})$. In addition, we can form the braid-like closure of the diagram, and we label the link represented by this diagram $T(0)$. Expanding on this, we can form an infinite family of link diagrams by adding crossings when we attach end points of $I \times \{0\}$ and $I \times \{1\}$ together. With the same convention as above, we define $T(m)$ to be the link represented by the diagram obtained by closing D_T with m crossings. We note that in this notation $T(m) = T^m(0)$.

Remark. Our convention for representing the twist crossings is the opposite to that Watson uses. This is because we will be primarily concerned with the closure $T(\frac{1}{0})$, and in that link the strands τ are oriented in different directions.

Watson proves that his construction is a bijection. Namely,

Proposition 2.3.1 (Watson, 2014)**.** *There is a one-to-one correspondence between strongly invertible knots (K, h) and sutured tangles satisfying the additional property that $T(\frac{1}{0})$ is the unknot.*

2.4 Combining the constructions

So far we have seen two constructions that take as their starting point a strongly invertible knot (K, h) and associate to it a unique auxiliary object. In one case Sakuma shows us how to obtain a two-component link with both components unknotted and linking number zero; in the other Watson obtains a sutured tangle.

Since both constructions begin by quotienting out by the strong inversion, a natural question that arises is whether one construction can be expressed in terms of the other. Said another way, is there a precise geometric connection between Sakuma links and Watson tangles? Completing the relationship suggested by Propositions 2.1.8 and 2.3.1 we have the following.

Proposition 2.4.1. *Let (K, h) be a strongly invertible knot. There is a one-to-one correspondence between tangle representatives of the Watson tangle, T^m and framed Sakuma links $\mathbb{L}_n$.*

Proof. Let us run through Watson's construction on the whole of S^3 this time, and let us add in two framed longitudes with framing n as per Sakuma's instructions. Form the Watson tangle (B^3, τ), take a representative T^m, and consider the exterior of the copy of B^3. This is another copy of B^3, and, furthermore, contains a tangle consisting of two arcs and a single copy of S^1, perhaps with some twists. Figure 2.13 shows the process for the left-handed trefoil. Combining the two tangles in the obvious way, we produce a two-component link with linking number ± 2 or

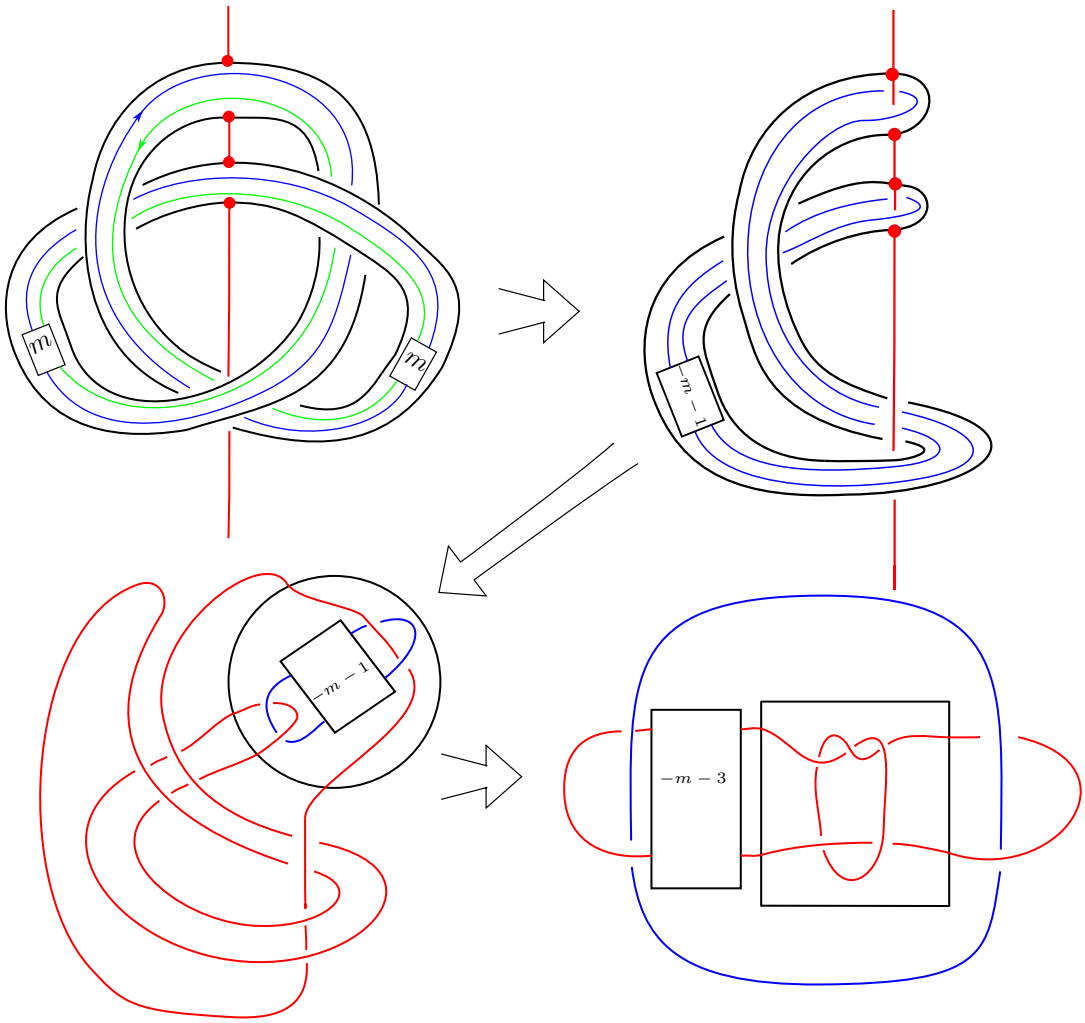

Figure 2.13: Combining Sakuma's and Watson's constructions

0 (depending on the choice of longitude framing). This link is a framed Sakuma link; to determine the precise relationship between m and n we refer to Lemma 2.1.2. □

As a consequence of the above construction we end up with an alternative link diagram for a Sakuma link, which shows precisely the relationship between Sakuma's and Watson's constructions. The Sakuma link is drawn in such a way that the branch set component $\mathcal{B}$ is clearly $T^m(\frac{1}{0})$ for some Watson tangle representative T^m. See Figure 2.13 for an example with the left-handed trefoil — note that for simplicity we have chosen not to draw the pair of longitudes in the first diagram as being equivariant. The extra twists featuring in the final diagram are brought about by the isotopies when passing from the third diagram.

2.5 Annular Sakuma knots

By now we have defined an increasingly large number of auxiliary objects we can equip to strongly invertible knots. We will finish this chapter by squeezing Sakuma's construction just a little more to obtain a final set of objects, which will take the form of a pair of *annular knots*.

2.5.1 Properties of annular links

We briefly mention a few properties of annular links, which are, put simply, links sitting inside the thickened annulus $A \times I$, which we parametrise in cylindrical coordinates by the following:

$$A \times I = \{(r, \theta, z) : r \in [1, 2], \theta \in [0, 2\pi], z \in [0, 1]\} \subset S^3.$$

Annular links are of interest primarily due to their interactions with links in the 3-sphere, as well as with braids. In one direction, annular links can be obtained naturally through braid closures or braid-like closures of any sutured tangle. On the other hand, invariants of annular links have been shown to be related to invariants of 3-manifolds through the use of spectral sequences, which we will return to in Chapter 4. Our motivation for studying them is Sakuma's construction, which will allow us to associate strongly invertible knots with annular knots.

Definition 2.5.1. An n-component *annular link* L, is a disjoint union of n copies of S^1, properly embedded in $A \times I$.

Whilst it is true that all links can be embedded in the annulus, the class of annular links is in some respects larger than the class of links in S^3. On the one hand, we can embed a link trivially into $A \times I$ by placing it entirely within a three ball $B^3 \subset A \times I$; or, alternatively, we can use the fact that the unknot is a companion to every link, which embeds our link in $A \times I$ in a homologically non-trivial way. Following this logic, there are really two notions of the unknot in $A \times I$: a version which is nullhomologous in $H_1(A \times I; \mathbb{Z})$, and a version which corresponds to the generator of $H_1(A \times I; \mathbb{Z})$. We will denote these two unknots by $\mathcal{U}$ and $\widehat{\mathcal{U}}$ respectively — the hat version is so labelled to indicate $\widehat{\mathcal{U}}$ is the closure of the 1-strand braid. Additionally, as we shall see, there are many examples of non-equivalent knots in the annulus that become equivalent when they are embedded in S^3.

Annular links are considered to be equivalent up to ambient isotopy, where we additionally demand the isotopies act trivially on $\partial A \times I$ — that is, they also preserve the sutured structure of $A \times I$. Alternatively, two annular links L and L' are equivalent if there exists an orientation preserving homeomorphism f from $(A \times I, \partial A \times I)$ to itself such that $f(L) = L'$. The standard sutured structure we place on $A \times I$ is $A(\Gamma) = \partial A \times I$ and $s(\Gamma) = \partial A \times \{\frac{1}{2}\}$, but, as $A \times I$ is homeomorphic to the solid torus $D^2 \times S^1$, if we were not interested in the sutured structure we could just as well consider our annular links to be embedded in the solid torus.

Just as for their spherical counterparts, annular knots and links can be depicted through a choice of diagram — the only difference is that annular link diagrams are drawn in an annulus $A \subset \mathbb{R}^2$ instead of in $\mathbb{R}^2$. There also exists a Reidemeister theorem for annular links: two annular links are equivalent if and only if there exists a series of annular Reidemeister moves taking a diagram of one onto a diagram of the other. The moves are exactly the same as in the $\mathbb{R}^2$ scenario, except this time we are not allowed to move a strand over the hole in the annulus, nor over its outside edge.

There also exist similar notions of symmetry for annular links. For example, an unoriented

annular link L is said to be amphicheiral if it is equivalent to its mirror — the link obtained from L by the orientation reversing homeomorphism which reflects $A \times I$ in the plane $z = \frac{1}{2}$. We will be concerned with symmetries of annular knots insofar as their relationship with symmetries of a canonical two-component link we can associate to each annular knot.

Definition 2.5.2. Let $K \subset A \times I \subset S^3$ be an annular knot. Consider the two-component link $L = K \cup \mathcal{B} \subset S^3$, where $\mathcal{B}$ is an unknot consisting of the z-axis and the point at infinity. We call L the *two-component completion* of K.

Since an annular knot can be viewed as lying in the exterior of the additional component in its two-component completion, we can rule out, for example, the amphicheirality of the link if the annular knot is cheiral. The relationship between an annular knot and its two-component completion will additionally show up as a connection between their respective annular and spherical link invariants.

2.5.2 Extending Sakuma's construction

Given a framed Sakuma link we can naturally form a pair of annular knots by viewing one component as lying in the exterior of the other. We use the term *annular Sakuma knot* to refer to either associated annular knot; it should be immediately clear that a framed Sakuma link is precisely the two-component completion of an annular Sakuma knot. By performing this modest extension of Sakuma's construction we obtain a large family of annular knots to which we can apply annular knot invariants. Furthermore, by construction every annular Sakuma knot is unknotted when embedded into S^3, and this has some interesting ramifications when applying certain invariants.

Given the standard projection diagram $D_{\mathbb{L}_n}$ of a framed Sakuma link $\mathbb{L}_n = \mathcal{L} \cup \mathcal{B}$, it is a relatively simple matter to draw a diagram of the 'longitude' annular Sakuma knot $\mathcal{L} \subset S^3 \backslash \mathcal{N}(\mathcal{B})$, as $\mathcal{B}$ appears as an axis (for an example see Figure 2.14). In order to determine a diagram for the 'branch-set' annular knot, however, we need to apply a series of Reidemeister moves as suggested by Figure 2.13.

It is immediate from Proposition 2.1.8 that there is a unique pair of annular Sakuma knots associated to every framed strongly invertible knot. We will now prove that in almost all cases the pair are not equivalent to one other.

Proposition 2.5.3. *Let $\mathbb{L}_n = \mathcal{B} \cup \mathcal{L}$ be a framed Sakuma link, and let $\mathcal{B}$ and $\mathcal{L}$ also denote the two annular knots obtained from $\mathbb{L}_n$. Then $\mathcal{B}$ and $\mathcal{L}$ are equivalent if and only if $\mathbb{L}_n$ is associated to one of the following:*

1. *A framed strongly invertible unknot $(\mathcal{U}, h_0, n)$.*
2. *A framed strongly invertible double $(D(K'), h, n)$, for some prime knot K'.*
3. *A framed equivariant product of strongly invertible doubles, $(\{\#_{i=1}^{s} D(K'_i)\}, h, n)$, for prime knots K'_i.*

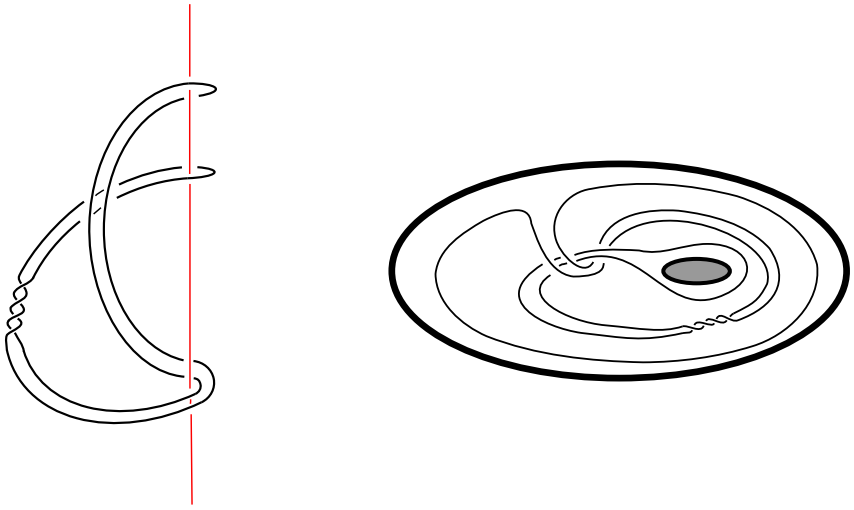

Figure 2.14: A Sakuma link and the annular knot $\mathcal{L} \subset E(\mathcal{B})$

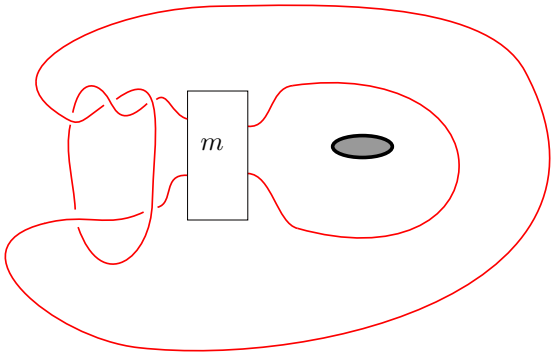

Figure 2.15: An annular Sakuma knot obtained from the Watson tangle T^m

Proof. This Proposition is really just a Corollary of Proposition 2.1.12. The presence of coils makes it impossible to exchange $\mathcal{L}$ and $\mathcal{B}$, and the only framed Sakuma links without coils in their projection diagrams are those listed above. □

Another way to view the two annular Sakuma knots is as annular closures of representatives of the Sakuma tangle and the Watson tangle we encountered previously. Given a sutured tangle T, there is a natural annular knot we can associate to T. We take the braid-like closure $\widehat{T}$ by identifying $D^2 \times \{0\}$ with $D^2 \times \{1\}$ using the identity map. This means in practice we join each point $x \in D^2 \times \{0\}$ to its 'opposite' point $x \in D^2 \times \{1\}$, resulting in a knot in a solid torus, which we can deform in to a thickened annulus by a homeomorphism.

It is clear that given a representative of a Sakuma tangle T^m we can from the braid-like closure to obtain the annular knot $\mathcal{L} \subset A \times I$, where $\mathbb{L}_n = \mathcal{B} \cup \mathcal{L}$ is the related framed Sakuma link. The other annular knot $\mathcal{B} \subset A \times I$ is obtained from a representative of the Watson tangle by applying the same process. See Figure 2.15 for an example.

Perhaps the most commonly studied class of annular knots are those obtained from braid closures

(see for example [20], [4]). Interestingly, the set of annular Sakuma knots is almost entirely disjoint from this set of annular knots, meaning we have a brand new family of annular knots to apply annular link invariants to.

Proposition 2.5.4. *Let K be an annular Sakuma knot that is not associated to $(\mathcal{U}, h_0, \pm 1)$. Then K is not equivalent to a braid closure.*

Proof. For a general k-strand braid B_k, form its closure $\widehat{B_k}$, and consider the two-component completion, L. Since in a braid all strands run from $D^2 \times \{0\}$ to $D^2 \times \{1\}$, when we close all strands in $\widehat{B_k}$ are oriented in the same direction. Hence, the linking number of L is precisely the number of strands in B_k, namely k. Suppose K is equivalent to $\widehat{B_k}$; then it must the case that $k = 2$.

Now, K has an associated framed Sakuma link $\mathbb{L}_n = \mathcal{B} \cup \mathcal{L}$. We form the standard projection diagram $D_{\mathbb{L}_n}$ in which K wraps around a vertical axis. Since $k = 2$, there therefore cannot be any coils present in K when considered as a component of $\mathbb{L}_n$. The two possibilities are then that K is equivalent to $\mathcal{L}$, or that K is equivalent to $\mathcal{B}$.

For the first case, recall Proposition 2.1.12. As a consequence we have that K is associated to some $(\mathcal{U}, h_0, n)$, to some $(D(K), h, n)$, or to a equivariant sum of $(D(K), h, n)$. Out of all these cases, the only time when K is equivalent to a braid closure is when it is associated to $(\mathcal{U}, h_0, \pm 1)$.

In the second case we see that unless $\mathbb{L}_n$ is associated to $(\mathcal{U}, h_0, \pm 1)$ it is never a braid closure, and this is already covered by the first case in light of Proposition 2.5.3. □

Chapter 3

Polynomial invariants of strongly invertible knots

In this chapter we will start to define and calculate invariants of strongly invertible knots. In particular, we will concentrate on invariants which take the form of a polynomial with integer coefficients. There are three such invariants we will focus on: the η-polynomial of Kojima and Yamasaki, the Jones polynomial, and the annular Jones polynomial. The η-polynomial is an invariant of two-component links with linking number zero, and is perhaps best thought of as an invariant in the spirit of the Alexander polynomial, insofar as it is also constructed using infinite cyclic covering spaces. The reader is encouraged to compare the construction of the η-polynomial with that of the Alexander polynomial featured in Rolfsen's book [77, Chapter 7]. The Jones polynomial was constructed by Vaughan Jones in the 1980s, and is an invariant of knots and links in S^3. Today, the Jones polynomial is perhaps one of the most well known link invariants, due to its simple construction, and its ability to detect cheiral links. It remains in vogue primarily due to its relationship to *Khovanov homology*, a homological link invariant whose Euler characteristic is the Jones polynomial. Its annular spin-off, which is an invariant of annular links, was originally constructed as a consequence of independent work by Przytycki [70] and Turaev [90] on skein modules. This allowed the generalisation of the Jones polynomial to links in thickened surfaces, of which the thickened annulus $A \times I$ is one of the simplest examples.

We will apply the three invariants to strongly invertible knots and compare the results, with particular emphasis on their abilities to distinguish strongly invertible knots, detect the trivial strongly invertible knot, and detect the cheirality of a strongly invertible knot. Finally, we will change tack somewhat, and will explain how the three invariants can be used to help determine the intrinsic symmetry group of a framed Sakuma link.

3.1 The η-polynomial

As we mentioned above, the η-polynomial is a link invariant of two-component links with linking number zero, originally defined by Kojima and Yamasaki [46] in the late 1970s. In this section we

will define η for a general two-component link with linking number zero, list some of its properties and features, and apply it to Sakuma links. We will also provide the necessary background on the theory of infinite cyclic covering spaces — which are required to define η.

3.1.1 Infinite cyclic covering spaces

We will expand upon the brief introduction to covering spaces given in Definition 2.1.3. The primary reference for the following definitions is [38, Appendix B].

Definition 3.1.1. Let X be a connected space. An *infinite cyclic cover* of X is a covering space $(\widetilde{X}, p)$ with fibre $\mathbb{Z}$.

The requirement that X is connected is necessary in order for all fibres to be homeomorphic. We call each copy of X contained in $\widetilde{X}$ a *fundamental domain*.

Example 3.1.2. If $X = S^1$ then there exists a covering map $p : \mathbb{R} \to S^1$ given by $p(t) = e^{2\pi i t}$. If we examine the pre-images we see that the fibre of this cover is $\mathbb{Z}$.

Two connected covering spaces $(\widetilde{X_1}, p_1)$ and $(\widetilde{X_2}, p_2)$ of a connected space X are considered equivalent if there exists a homeomorphism $f : \widetilde{X_1} \to \widetilde{X_2}$ such that $p_1 = p_2 f$. When the connected space X is also locally-path connected and semilocally simply-connected (two terms we shall leave undefined, see [28, Chapter 1] for further details) it turns out that the number of connected equivalence classes X has is related to its fundamental group. The following result appears in Hatcher [28, Theorem 1.38].

Theorem 3.1.3 (Classification of connected covering spaces)**.** *Let X be a connected, locally path-connected, and semilocally simply-connected space with basepoint x_0. The equivalence classes of connected covering spaces over X are in bijection with the conjugacy classes of subgroups of $\pi_1(X, x_0)$.*

In all that follows we will assume our connected space X is also locally path-connected and semilocally simply-connected.

Definition 3.1.4. Given a covering $(\widetilde{X}, p)$, let $Homeo_p(\widetilde{X})$ be the subgroup of $Homeo(\widetilde{X})$ consisting of all the homeomorphisms $h : \widetilde{X} \to \widetilde{X}$ such that $ph = p$. We call such homeomorphisms *deck transformations* or *covering transformations*.

Definition 3.1.5. A covering space $(\widetilde{X}, p)$ is called *regular* or *normal* if for every $x \in X$ and for every pair of lifts $\tilde{x}, \tilde{x}'$ of x there is a deck transformation taking $\tilde{x}$ to $\tilde{x}'$.

The term 'normal' arises from a relationship between normal covering spaces and normal subgroups of the fundamental group of the base space.

Theorem 3.1.6. *Let $(\widetilde{X}, p)$ be a connected covering space and let $H = p_*(\pi_1(\widetilde{X})) \subset \pi_1(X)$. Then*

1. *$\widetilde{X}$ is a normal covering space if and only if H is a normal subgroup of $\pi_1(X)$.*

2. $Homeo_p(\widetilde{X})$ is isomorphic to $N(H)/H$, where $N(H)$ is the normaliser of H in $\pi_1(X)$.

In particular, $Homeo_p(\widetilde{X})$ is isomorphic to $\pi_1(X)/H$ if $\widetilde{X}$ is a normal covering.

Definition 3.1.7. Let X be a connected space, Π be an infinite cyclic group generated by t and $\gamma : \pi_1(X) \to \Pi$ be an epimorphism. The *infinite cyclic cover* of X *determined by* γ is the connected, normal covering space $(\widetilde{X}, p)$ such that $p_*(\pi_1(\widetilde{X})) = ker(\gamma) \subset \pi_1(X)$.

By Theorem 3.1.6 and the first isomorphism theorem for groups it then follows that

$$Homeo_p(\widetilde{X}) \cong \pi(X)/p_*(\pi_1(\widetilde{X})) = \pi_1(X)/ker(\gamma) \cong Im(\gamma) = \Pi.$$

Therefore, Π acts freely as the group of deck transformations of $\widetilde{X}$. As $\widetilde{X}$ is a normal covering space we know that for every $x \in X$ and every pair of lifts $\tilde{x}, \tilde{x}'$ there exists a $t^i \in \Pi$ such that $t^i(\tilde{x}) = \tilde{x}'$. To describe the action of Π we first number the fundamental domains of $\widetilde{X}$, then specify that t sends a lift $\tilde{x}$ of $x \in X$ associated to n to the lift of x associated to $n+1$.

Two covering spaces worth mentioning are the *universal covering space* and the *universal abelian covering space*. A connected covering space is said to be *universal*, and is denoted by $(\overline{X}, p)$, if it is a covering space corresponding to the trivial subgroup of $\pi_1(X, x_0)$. The universal covering space has the property that it is a covering space of every other covering space of its base space X.

The universal abelian covering space $(\widehat{X}, p)$ is the covering space associated to the commutator subgroup $[\pi_1(X, x_0), \pi_1(X, x_0)]$. If we quotient $\pi_1(X, x_0)$ with its commutator subgroup then we obtain the abelianisation of $\pi_1(X, x_0)$, which is just the 1st homology group $H_1(X; \mathbb{Z})$. We will in particular be interested in the special case when $H_1(X; \mathbb{Z})$ is isomorphic to an infinite cyclic group — in which case the universal abelian covering space coincides with the infinite cyclic covering space determined by the abelianisation.

We also note that the universal and universal abelian covering spaces coincide if and only if the commutator subgroup is trivial; this is the case in the $(\mathbb{R}, p)$ covering space of S^1 we outlined above, for example.

3.1.2 Definition and properties of η

We now will formally define the η-polynomial. The following description is taken from Kojima and Yamasaki's paper [46].

To define η, we first take a two-component link $L = K_1 \cup K_2 \subset S^3$ with linking number zero. We then consider the complement X_i of one of its components, that is, $X_i = S^3 \backslash K_i$ for $i \in \{1, 2\}$. The homology groups of X_i are the same as those for S^1, which means in particular that $H_1(X_i; \mathbb{Z}) \cong \mathbb{Z}$. This puts us in the special case where the universal abelian covering space $\widehat{X_i}$ of X_i is also an infinite cyclic covering induced by the abelianisation of $\pi_1(X_i)$. It then follows that the group of deck transformations of $\widehat{X_i}$ is isomorphic to $\mathbb{Z}$, or equivalently to an infinite cyclic group $\Pi = \langle t \rangle$.

We then proceed as in [77, Chapter 7]; namely, we use the group of deck transformations to define a module structure on the homology groups of $\widehat{X_i}$ over the group ring $\Lambda = \mathbb{Z}[t, t^{-1}]$. We define an action of Λ on homology elements $\alpha \in H_i(\widehat{X}; \mathbb{Z})$ by $t * \alpha = t\alpha$. Now let $p(t) \in \Lambda$: $p(t)$ can be expressed as

$$p(t) = c_{-r}t^{-r} + \ldots + c_0 + \ldots + c_s t^s.$$

We then define $p(t)\alpha$ to be

$$p(t)\alpha = c_{-r}t^{-r}\alpha + \ldots + c_0\alpha + \ldots + c_s t^s \alpha.$$

We will in particular consider $H_1(\widehat{X_i}; \mathbb{Z})$ as a Λ-module.

The next step is to observe that since the linking number of L is zero the lifts of the other link component K_j and its preferred longitude l_j are a collection of closed curves. Furthermore, each pair of lifts are representatives of the same homology class $[\tilde{l_j}] \in H_1(\widehat{X_i}; \mathbb{Z})$. Now, $H_1(\widehat{X_i}; \mathbb{Z})$ is a torsion module over Λ [57], so there exists a Laurent polynomial $f(t) \in \Lambda$ such that $f(t)[\tilde{l_j}] = 0$. This means that $f(t)\tilde{l_j}$ must bound a disc ζ in $\widehat{X_i}$ by the definition of $H_1(\widehat{X}, \mathbb{Z})$. The formal definition of η is then

$$\eta(L, i, j; t) = \frac{1}{f(t)} \sum_{n=-\infty}^{\infty} Int\left(\zeta, t^n(\widetilde{K_j})\right) t^n$$

where *Int* refers to the intersection number between ζ and a translate $t^n(\widetilde{K_j})$ in $\widehat{X_i}$. Kojima and Yamasaki prove [46, Proposition 1] that η is well-defined; that is, it does not depend on our choice of ζ or $f(t)$.

Some basic properties of η are as follows [46, Proposition 2]:

Proposition 3.1.8 (Kojima-Yamasaki,1979)**.** *The following equalities hold:*

1. $\eta(L, i, j; t) = \eta(L, i, j; t^{-1})$.
2. $\eta(L, i, j, 1) = 0$.

In other words, the η-polynomial is always symmetric and the sum of its coefficients is always zero. We will therefore sometimes denote it by $[a_0, a_1, \ldots, a_n$ as Sakuma does in [79], where $[a_0, a_1, \ldots, a_n$ refers to the polynomial given by $a_0 + \sum_{i=1}^{n} a_i(t^{-i} + t^i)$.

Returning to the definition, it is clear that there are two η-polynomials we can obtain from L depending on which complement we decide to take; we will refer to these as $\eta(L, 1, 2; t)$ and $\eta(L, 2, 1; t)$. In [33, Theorem 4] Jin proves the following theorem which shows a connection between, $\eta(L, 1, 2; t)$ and $\eta(L, 2, 1; t)$.

Theorem 3.1.9 (Jin, 1988)**.** *Let $L = K_1 \cup K_2$ be a link with $lk(K_1, K_2) = 0$ and let $\Delta_L(t_1, t_2)$, $\Delta_1(t)$ and $\Delta_2(t)$ be the Alexander polynomials of L, K_1 and K_2 respectively, which are normalised to satisfy the following symmetry conditions:*

1. $\Delta_i(t^{-1}) = \Delta_i(t)$ *for* $i = 1, 2$,

2. $\Delta(t_1, t_2) = (1 - t_1^{-1})(1 - t_2^{-1})g(t_1, t_2)$ *and* $g(t_1^{-1}, t_2^{-1}) = g(t_1, t_2)$.

Then

$$\eta(L, 1, 2; t) = \pm\frac{(1-t)(1-t^{-1})g(t,1)}{\Delta_1(t)}$$

and

$$\eta(L, 2, 1; t) = \pm\frac{(1-t)(1-t^{-1})g(1,t)}{\Delta_2(t)}$$

Jin notes that if we take the link complement $X_L = S^3 \backslash L$ then the plus and minus signs can be determined from a presentation matrix for $H_1(\widehat{X_L}; \mathbb{Z})$ that allows the computation of the three relevant Alexander polynomials. An immediate consequence of Jin's theorem is the following.

Corollary 3.1.10. *Let $L = K_1 \cup K_2$ be a link as above. Then*

$$\eta(L, 1, 2; t) = \pm\eta(L, 2, 1; t)\frac{g(t,1)}{g(1,t)}\frac{\Delta_2(t)}{\Delta_1(t)}.$$

Therefore, the two η-polynomials differ by a polynomial factor, which can be determined from a presentation matrix for $H_1(\widehat{X_L}; \mathbb{Z})$ and the two Alexander polynomials.

Now let M_L be the closed 3-manifold obtained from S^3 by doing a 0-framed surgery on our link L (that is, the result of removing a tubular neighbourhood of L, then re-gluing, so that a meridional curve is glued to a longitudinal curve). Define $\widetilde{M_{L_i}}$ to be the infinite cyclic cover of M_L determined by the composite homomorphism from $\pi_1(M_L)$ to $\mathbb{Z}$ that first abelianises to $H_1(M_L; \mathbb{Z}) \cong \mathbb{Z} \oplus \mathbb{Z}$, then sends the homology class $[K_i]$ to the generator of $\mathbb{Z}$ and the class $[K_j]$ to zero. Kojima and Yamasaki define the *polynomial of Alexander's type with respect to* K_i to be the determinant of a square presentation matrix of $H_1(\widetilde{M_{L_i}}; \mathbb{Z})$ as a Λ-module, which they denote by $A(M_L, i; t)$. This polynomial is well defined up to multiplication by units of Λ, which are the monomials $\pm t^{\pm i}$. They use this polynomial to obtain the following theorem [46, Theorem 1]:

Theorem 3.1.11 (Kojima-Yamasaki, 1979)**.** *For a tame link $L = K_1 \cup K_2$ whose linking number is zero,*

$$\eta(L, i, j; t) \doteq \frac{A(M_L, i; t)}{\Delta_i(t)}$$

where $\{i, j\} \in \{1, 2\}$, and '$\doteq$' means 'up to multiplication by units' in Λ.

Note that in the case where $i = 1$ and K_1 is unknotted the η-polynomial equals $A(M_L, 1; t)$, up to multiplication by units.

3.1.3 The η-polynomial of a Sakuma link

As we have established a bijection between strongly invertible knots and Sakuma links we can apply the η-polynomial to strongly invertible knots: this was Sakuma's original motivation behind his construction. Pleasingly though, because all Sakuma links have both components unknotted

the calculations are made much simpler. Indeed, Sakuma defines the η-polynomial of a Sakuma link in [79] to be as follows:

Definition 3.1.12. Let $\mathbb{L} = \mathcal{B} \cup \mathcal{L}$ be a Sakuma link obtained from a strongly invertible knot (K, h), and take $K_1 = \mathcal{B}$ and $K_2 = \mathcal{L}$. Then,

$$\eta_{(K,h)}(t) := \eta(\mathbb{L}, 1, 2; t) = \sum_{i=-\infty}^{\infty} \mathrm{lk}\left(\widetilde{l_{\mathcal{L}}}, t^i(\widetilde{\mathcal{L}})\right) t^i.$$

The reason that this definition is equivalent to Kojima and Yamasaki's for Sakuma links comes from observing that, since B is unknotted, the universal abelian cover of $X_{\mathcal{B}}$ is homeomorphic to $\mathbb{R} \times D^2$. As the group $H_1(\mathbb{R} \times D^2; \mathbb{Z}) \cong 0$ the lift $\widetilde{l_{\mathcal{L}}}$ is a trivial homology element, so we can take $f(t) = 1$ in Kojima and Yamasaki's definition. Then we take $\partial\zeta = \widetilde{l_{\mathcal{L}}}$ and

$$\eta(L, 1, 2; t) = \sum_{i=-\infty}^{\infty} Int\left(\zeta, t^i(\tilde{\mathcal{L}})\right) t^i = \sum_{i=-\infty}^{\infty} \mathrm{lk}\left(\widetilde{l_{\mathcal{L}}}, t^i(\widetilde{\mathcal{L}})\right) t^i.$$

Remark. Note that in order to make $l_{\mathcal{L}}$ a preferred longitude compensatory half twists must once again be added.

We observe that a fundamental domain of $\widehat{X_{\mathcal{B}}}$ is precisely a representative of a Sakuma tangle for (K, h); see [79, Figure 2.3(b)] or Figure 3.1 for an example. In addition, for Sakuma links Theorem 3.1.11 implies $\eta(\mathbb{L}, 1, 2; t) \doteq A(M_{\mathbb{L}}, 1; t)$, since $\Delta_1(t) = 1$. Studying the proof of [46, Proposition 4] we see that $\eta(\mathbb{L}, 1, 2; t)$ is exactly the 'a' term that appears in the presentation matrix Kojima and Yamasaki derive for $H_1(\widetilde{M_{L_1}}; \mathbb{Z})$, which for Sakuma links is 1×1.

When calculating η we fix a convention that before we lift $\mathcal{L}$ in $\widehat{X_{\mathcal{B}}}$ we arrange $D_{\mathbb{L}}$ so that the two clasps are at the very top and bottom of the diagram, as shown in Figure 3.1. This follows Sakuma, as can be seen in [79, Figure 2.3(a)].

Example 3.1.13. We take the left-handed trefoil with its single strong inversion $(3_1, h)$, and calculate its η-polynomial. The process of obtaining the Sakuma link and forming the infinite cyclic cover of $S^3 \backslash \mathcal{B}$ is illustrated in Figure 3.1, where the green closed curve is taken to be our chosen lift of $\mathcal{L}$ and the red and blue curves are two of its translates under the action of Λ. Other translates of the green curve are not required, as they all clearly have zero linking number with the lift of the preferred longitude of $\mathcal{L}$ (which is not depicted in the diagram).

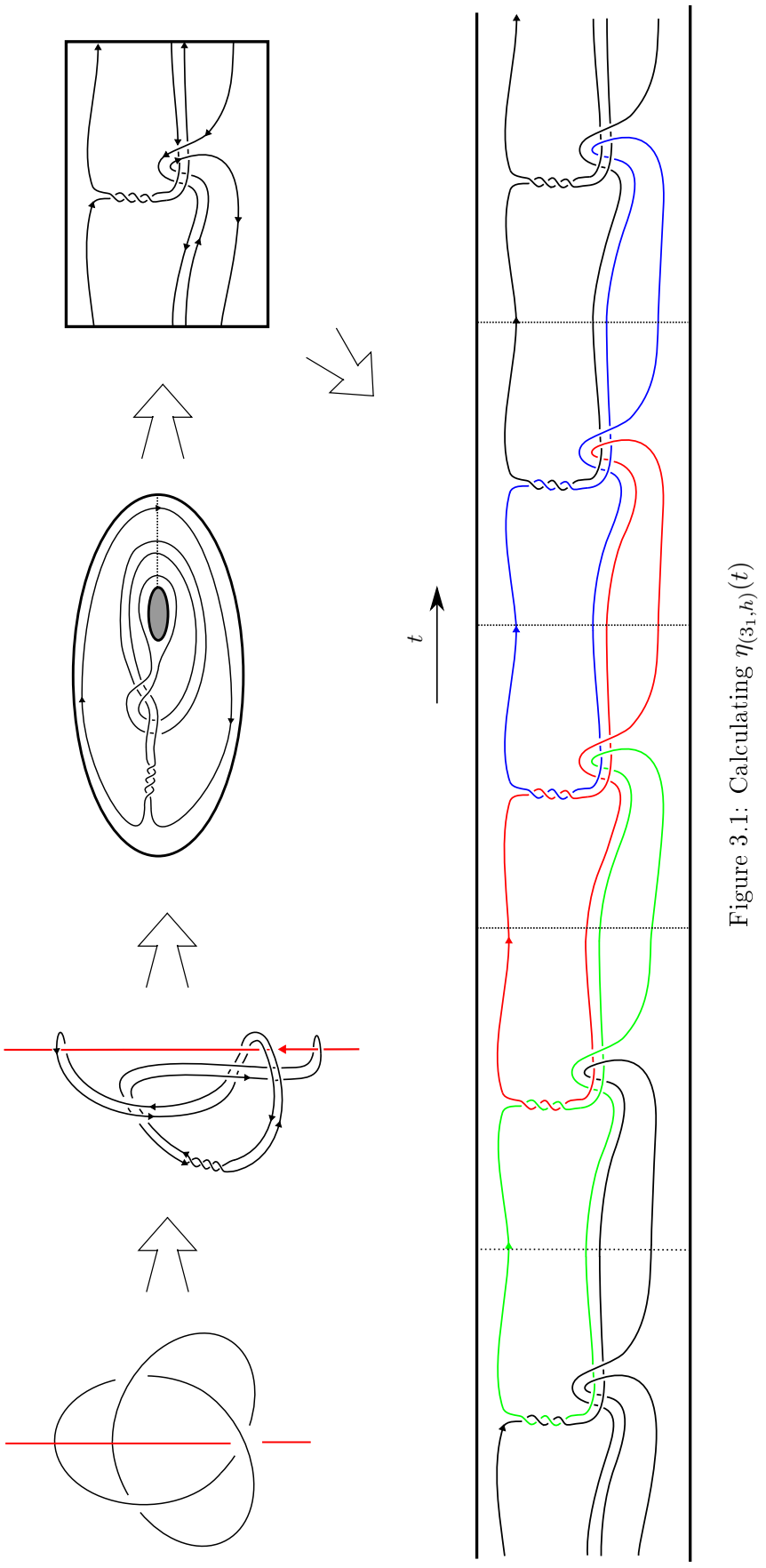

Figure 3.1: Calculating $\eta_{(3_1,h)}(t)$

We calculate the non-zero coefficients of the η-polynomial:

$$\begin{aligned}
\mathrm{lk}\left(\widetilde{l_{\mathcal{L}}}, \widetilde{\mathcal{L}}\right) &= \tfrac{8-4}{2} &= 2\\
\mathrm{lk}\left(\widetilde{l_{\mathcal{L}}}, t(\widetilde{\mathcal{L}})\right) &= \tfrac{4-4}{2} &= 0\\
\mathrm{lk}\left(\widetilde{l_{\mathcal{L}}}, t^2(\widetilde{\mathcal{L}})\right) &= \tfrac{-2}{2} &= -1
\end{aligned}$$

Hence,

$$\eta_{(3_1,h)}(t) = -t^{-2} + 2 - t^2 = [2, 0, -1$$

For Sakuma links η satisfies a few additional properties to those given in Proposition 3.1.8 [79, Theorem II]:

Theorem 3.1.14 (Sakuma, 1985)**.** *$\eta_{(K,h)}(t)$ satisfies the following properties:*

1. $\eta_{(K,h)}(t) = \eta_{(K,h)}(t^{-1})$
2. $\eta_{(K,h)}(1) = 0$
3. $\eta_{(K,h)}(-1) = 0$

In addition, for any Laurent polynomial $f(t)$ with integer coefficients satisfying the above conditions, there exists a strongly invertible knot (K,h) such that $\eta_{(K,h)}(t) = f(t)$.

Proof. We will prove the first three properties. A proof of the final result can be found in [79], which comes from calculating the η-polynomials of the 2-bridge strongly invertible knots we saw earlier.

1. The first property follows directly from the definition of η:

$$\begin{aligned}
\eta_{(K,h)}(t^{-1}) &= \sum_{i=-\infty}^{\infty} \mathrm{lk}\left(\widetilde{l_{\mathcal{L}}}, t^i(\widetilde{\mathcal{L}})\right)(t^{-1})^i\\
&= \sum_{i=-\infty}^{\infty} \mathrm{lk}\left(\widetilde{l_{\mathcal{L}}}, t^i(\widetilde{\mathcal{L}})\right)t^{-i}\\
&= \sum_{i=\infty}^{-\infty} \mathrm{lk}\left(\widetilde{l_{\mathcal{L}}}, t^i(\widetilde{\mathcal{L}})\right)t^{i}\\
&= \eta_{(K,h)}(t)
\end{aligned}$$

2. For the second property we have

$$\eta_{(K,h)}(1) = \sum_{i=\infty}^{\infty} \mathrm{lk}\left(\widetilde{l_{\mathcal{L}}}, t^i(\widetilde{\mathcal{L}})\right).$$

   Now consider a single fundamental domain of $\widehat{X_{\mathcal{B}}}$ and the various lifts of $\mathcal{L}$ and $l_{\mathcal{L}}$ sitting inside it. This consists of pairs of strands running in parallel that enter and exist the domain together, aside from at the top and the bottom where they peel apart to the left and right

of the domain. Now, we label and orient the strands according to the following conventions (which are taken from [79]); see Figure 3.2 for an example.

(a) The top left strand is oriented downwards and has index 0.

(b) Suppose we have already indexed a strand α. Let A be the end point of α and B be the point opposite to A. Let β be the strand that starts from B. Then define index(β) to be index(α) + 1 if B is on the right side of the domain or index(α) − 1 if B is on the left side.

The indexing of the strands encodes information about the translates of $\widetilde{\mathcal{L}}$ that enter and exit the domain. Sakuma also assigns to each crossing p in the fundamental region an index d_p: suppose α is a strand passing over another strand β at p, then $d_p := \text{index}(\alpha) - \text{index}(\beta)$. Each crossing in the fundamental domain stands for a crossing in $\widehat{X_{\mathcal{B}}}$ between $\widetilde{l_{\mathcal{L}}}$ and some translate of $\widetilde{\mathcal{L}}$; the index of a crossing indicates precisely which translate. An important example are the twist crossings: as the strand entering the fundamental domain from the top left has index 0 and the strand leaving at the top right has index 1 it is clear that the twist crossings must have index ± 1.

The linking numbers $\text{lk}\left(\widetilde{l_{\mathcal{L}}}, t^i(\widetilde{\mathcal{L}})\right)$ can be obtained from the indexed crossings. For $i \neq 0$ simply sum the signs of all crossings of index i. For $i = 0$ we also need to take into account the compensatory twists we put into $l_{\mathcal{L}}$ — which have signed sum equal to -2 times the signed sum of the twist crossings in $\mathcal{L}$. Let q be a twist crossing, then

$$\sum_{i=\infty}^{\infty} \text{lk}\left(\widetilde{l_{\mathcal{L}}}, t^i(\widetilde{\mathcal{L}})\right) = \sum_p \text{sign}(p) - \sum_q \text{sign}(q).$$

On the other hand, we can reobtain a diagram for $\mathcal{L}$ from the fundamental domain by gluing the left-hand side of the domain to the right-hand side in the obvious way. There is then a natural correspondence between crossings in the fundamental domain and crossings in the diagram for $\mathcal{L}$. Hence, we have

$$\text{lk}(l_{\mathcal{L}}, \mathcal{L}) = \sum_p \text{sign}(p) - \sum_q \text{sign}(q).$$

But we know that $l_{\mathcal{L}}$ is a preferred longitude of $\mathcal{L}$. Therefore, $\sum_{i=\infty}^{\infty} \text{lk}\left(\widetilde{l_{\mathcal{L}}}, t^i(\widetilde{\mathcal{L}})\right) = 0$ as required.

3. For the third property we have:

$$\begin{aligned}
\eta_{(K,h)}(-1) &= \sum_{i=-\infty}^{\infty} \text{lk}\left(\widetilde{l_{\mathcal{L}}}, t^i(\widetilde{\mathcal{L}})\right)(-1)^i \\
&= \sum_{i \text{ even}} \text{lk}\left(\widetilde{l_{\mathcal{L}}}, t^i(\widetilde{\mathcal{L}})\right) - \sum_{i \text{ odd}} \text{lk}\left(\widetilde{l_{\mathcal{L}}}, t^i(\widetilde{\mathcal{L}})\right) \\
&= -2 \sum_{i \text{ odd}} \text{lk}\left(\widetilde{l_{\mathcal{L}}}, t^n(\widetilde{\mathcal{L}})\right)
\end{aligned}$$

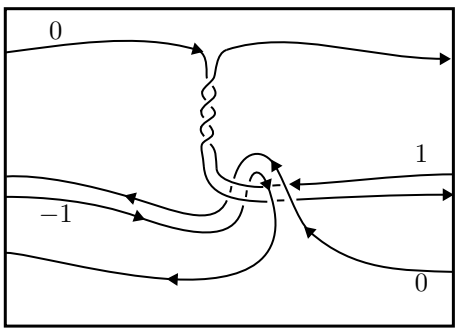

d_p	$\text{sign}(p)$
1	−
−1	−
1	−
−1	−
1	+
2	−
0	−
1	+
−2	−
−1	+
−1	+
0	−

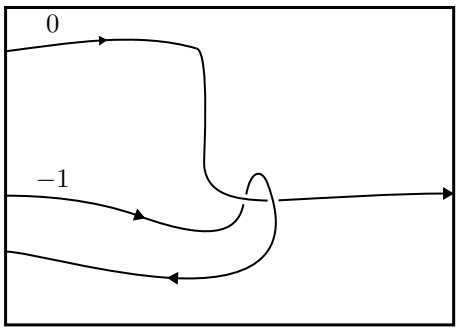

d_p	ϵ_p
1	−
−1	−

$$\widetilde{\eta} = -x_{-1} - x_1$$

Figure 3.2: Indexing crossings in a fundamental and pseudo-fundamental domain

Where the final equality is a consequence of the second property. We will now prove that

$$\sum_{i \text{ odd}} \text{lk}\left(\widetilde{l_{\mathcal{L}}}, t^i(\widetilde{\mathcal{L}})\right) = 0.$$

Consider once more the fundamental domain for $\widehat{X_{\mathcal{B}}}$, and suppose the strands are oriented and indexed as described above. We additionally colour the strands with two colours, beginning with the top left strand, and swapping colours for each strand starting at a point opposite to the end point of an already coloured strand. Examine the crossings between strands of different colours — it should be clear that these are precisely the odd indexed crossings.

On the other hand, if we recall how $\mathcal{L}$ was formed by gluing together l and $h(l)$, it is also true that every instance of $\mathcal{L}$ passing around $\mathcal{B}$ equates to swapping between following a piece of l to following a piece of $h(l)$ or vice versa. It then becomes apparent that all the odd indexed crossings are those between a l piece and a $h(l)$ piece of $\mathcal{L}$. Now, we know that $\text{lk}(l, h(l)) = 0$, so if we sum up all the signs of the odd indexed crossings we must get 0. Therefore, $\sum_{i \text{ odd}} \text{lk}\left(\widetilde{l_{\mathcal{L}}}, t^i(\widetilde{\mathcal{L}})\right) = 0$ and the third property of η then follows.

□

As we saw in Figure 3.1, calculating η by hand requires a certain number of diagrams, and for more complex strongly invertible knots the process becomes time consuming. To combat this, Sakuma developed a faster way to calculate η by working with a 'pseudo-fundamental' domain of the infinite cyclic cover. This is formed by removing half the strands in a fundamental domain, as shown in Figure 3.2. This speeds the calculation up considerably as there are roughly a quarter as many crossings to deal with in a pseudo-fundamental domain. We replicate Sakuma's description of his shortcut:

1. Start with a Sakuma link and construct a fundamental domain of $\widehat{X_{\mathcal{B}}}$, as in Figure 3.1.

2. Construct a pseudo-fundamental domain for the infinite cyclic cover.

3. Assign an index and orientation to each strand in the pseudo-fundamental domain in the same way as for the fundamental domain, starting by indexing the top strand with 0 and orienting it downwards.

4. Assign to each crossing p an *index* d_p as described for crossings in the fundamental domain, and a *signature* $\epsilon_p \in \{+,-\}$ as follows: let α and β be the over-strand and under-strand at p; if β crosses α from left to right set ϵ_p to $+$, and if β crosses α from right to left set ϵ_p to $-$. Note that the signature is therefore the negative of the sign of p.

   Let also $\widetilde{\eta} = \sum_p \epsilon_p x_{d_p}$.

5. Let $\eta'(t)$ be the Laurent polynomial obtained from $\widetilde{\eta}$ by setting $x_i = t^{i-1} - 2t^i + t^{i+1}$. As $\eta'(t)$ is symmetric, it can be expressed as $[b_0, b_1, b_2, \ldots$

6. Then $\eta_{K,h)}(t) = [a_0, a_1, a_2, \ldots$, where

$$a_j = \left\{ \begin{array}{ll} -2\displaystyle\sum_{i\geq 1} b_{2i} & (j=0) \\ -\displaystyle\sum_{i\geq 1} b_{2i+1} & (j=1) \\ b_j & (j\geq 2) \end{array} \right\}$$

The final steps require a little justification. Each crossing in the pseudo-fundamental domain corresponds to four crossings in the fundamental domain, and the indices of the strands are related as indicated in Figure 3.3. The index and signature of the crossing shown in the pseudo-fundamental domain is $+i$. On the other side, the indices and signs of the crossings in the fundamental domain are $-i, +(i+1), +(i-1)$, and $-i$. This explains the substitution of x_i for $t^{i-1} - 2t^i + t^{i+1}$. As a general a_j term ($j \neq \{0,1\}$) can be determined by summing the signs of all crossings with index j in the fundamental domain, the correspondence means that $a_j = b_j$ for $j \neq \{0,1\}$.

Unfortunately though, since the twists in the fundamental domain are not present in the pseudo-fundamental domain it is not possible to obtain the a_0 and a_1 terms purely from working with the pseudo-fundamental domain. However, it is possible to determine them from the b_j terms.

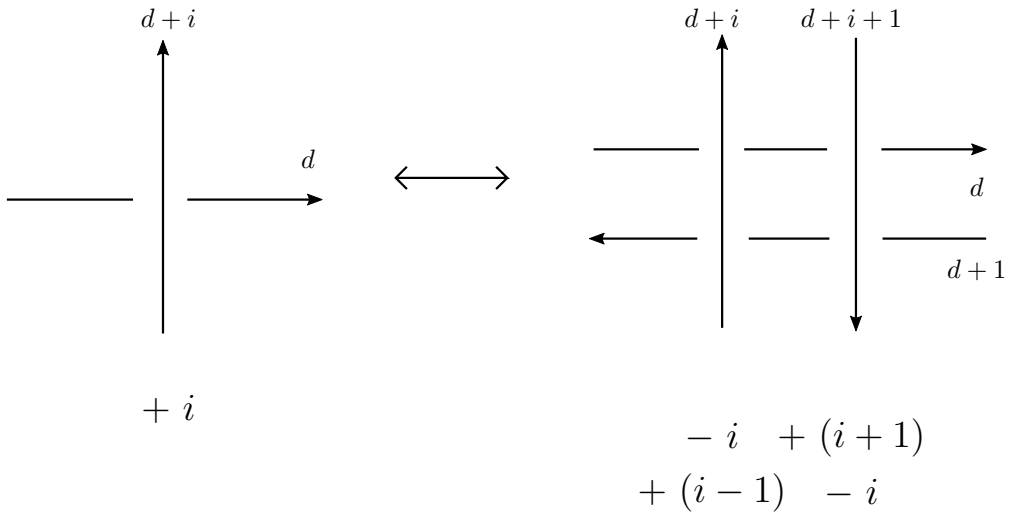

Figure 3.3: Crossing correspondence between fundamental and pseudo-fundamental domains

Recall that $\eta_{(K,h)}(1) = \eta_{(K,h)}(-1) = 0$; this implies that

$$\sum_{i \text{ odd}} \mathrm{lk}\left(\widetilde{l_{\mathcal{L}}}, t^i(\widetilde{\mathcal{L}})\right) = \sum_{i \text{ even}} \mathrm{lk}\left(\widetilde{l_{\mathcal{L}}}, t^i(\widetilde{\mathcal{L}})\right) = 0.$$

The a_0 term can now be calculated:

$$\begin{aligned} \sum_{|i|\geq 0} \mathrm{lk}\left(\widetilde{l_{\mathcal{L}}}, t^{2i}(\widetilde{\mathcal{L}})\right) = 0 \quad &\Longrightarrow \; a_0 = -2\sum_{i\geq 1} a_{2i} \\ &\Longrightarrow \; a_0 = -2\sum_{i\geq 1} b_{2i} \end{aligned}$$

Similarly,

$$\begin{aligned} \sum_{|i|\geq 0} \mathrm{lk}\left(\widetilde{l_{\mathcal{L}}}, t^{2i+1}(\widetilde{\mathcal{L}})\right) = 0 \quad &\Longrightarrow \; 2a_1 = -2\sum_{i\geq 1} a_{2i+1} \\ &\Longrightarrow \; 2a_1 = -2\sum_{i\geq 1} b_{2i+1} \\ &\Longrightarrow \; a_1 = -\sum_{i\geq 1} b_{2i+1} \end{aligned}$$

Example 3.1.15. For an example of Sakuma's shortcut in action, we calculate the η-polynomial of the left-handed trefoil once more. Consider the pseudo-fundamental domain appearing in Figure 3.2. We then have,

$$\begin{aligned} \eta'(t) &= -(t^{-2} - 2t^{-1} + 1) - (1 - 2t + t^2) \\ &= -t^{-2} + 2t^{-1} - 2 + 2t - t^2 \\ &= [-2, 2, -1 \end{aligned}$$

Hence,

$$\eta_{(3_1,h)}(t) = [2, 0, -1$$

as we calculated earlier.

We now discuss the effect of applying η to framed Sakuma links. The process is the same as in the base case, however since we require links of linking number zero we can only define η on even framed strongly invertible knots, that is, on (K, h, n) where n is even.

Definition 3.1.16. Let $(K, h, n), n \in 2\mathbb{Z}$, be a framed strongly invertible knot, and $\mathbb{L}_n = \mathcal{B} \cup \mathcal{L}$ be its framed Sakuma link. Define $\eta_{(K,h,n)}(t)$ by the equality

$$\eta_{(K,h,n)}(t) := \eta(\mathbb{L}_n, 1, 2; t) = \sum_{i=-\infty}^{\infty} \mathrm{lk}\left(\widetilde{l_{\mathcal{L}}}, t^i(\widetilde{\mathcal{L}})\right) t^i.$$

It turns out that knowing η for a zero-framed strongly invertible knot (K, h) is enough to determine it for its whole family of even framed strongly invertible knots (K, h, n).

Proposition 3.1.17. *Let (K, h) be a strongly invertible knot with Sakuma link $\mathbb{L}$, and suppose that $\eta_{(K,h)}(t) = [a_0, a_1, a_2, \ldots$. Then,*

$$\eta_{(K,h,n)}(t) = [a_0 + n, a_1 - \frac{n}{2}, a_2, \ldots$$

where n is an even integer.

Proof. Fix a diagram $D_{(K,h)}$ and suppose it has writhe $x \in \mathbb{Z}$. Suppose we want a longitude l with framing $n \in Z$. Then $-2x+2n$ half twists must be added to a blackboard longitude ($-x+n$ on each side of $\mathrm{Fix}(h)$) in order to preserve symmetry under h.

Recall Lemma 2.1.2. There are two cases we need to consider:

- When x is even nothing needs to be done and we end up with $x - n$ half twists in $D_{\mathbb{L}}$ with the clasps arranged as per our convention.
- When x is odd we still have $x - n$ half twists after projecting but one of the clasps needs flipping over in order to arrange them as desired. This either adds another negative half twist if x is negative or adds a positive half twist if x is positive. So we end up with either $x - n - 1$ or $x - n + 1$ half twists.

Now, the only two terms that are affected by changing the number of half twists in $D_{\mathbb{L}}$ are a_0 and a_1. Changing the numbers of twists changes the writhe of $D_{\mathbb{L}}$, so a different number of compensatory twists need to be added in $l_{\mathcal{L}}$ — this explains a_0. For a_1, this follows because the twists only contribute to a_1 in the lifts.

Let us examine the effect on a_1 first. In all cases we end up an extra $-n$ half twists in $D_{\mathbb{L}}$, therefore our new a_1 term, a_1' is given by $a_1' = a_1 - \frac{n}{2}$.

Now, we observe that a_0 is made up of two parts: self crossings of $\widetilde{\mathcal{L}}$, which get counted twice; and compensatory twists put in to ensure $\widetilde{l_{\mathcal{L}}}$ was preferred. The change in a_0 comes down to the number of extra twists that we put in $D_{\mathbb{L}}$, so it follows that $a_0' = a_0 + n$ as required. □

Example 3.1.18. Take once more the left-handed trefoil with its unique strong inversion as in Figure 3.1, but this time set $n = 2$. This results in six negative twists in $D_{\mathbb{L}}$. Our formula tells us that

$$\eta_{(3_1,h,2)}(t) = [4, -1, -1$$

which can easily be verified by adjusting the diagrams in Figure 3.1.

Next we prove a result about the relationship between the highest non-zero power of t of the η-polynomial and the number of coils in the standard projection diagram.

Lemma 3.1.19. *Let (K, h, n) be a framed strongly invertible knot with Sakuma link $\mathbb{L}_n$ and consider $D_{\mathbb{L}_n}$, the standard projection diagram for $\mathbb{L}_n$. Let x denote the number of coils present in the diagram. Then the largest non-zero power of t in the η-polynomial of $\mathbb{L}_n$ is bounded above by $x + 2$, that is $a_i = 0$ for $i \geq x + 2$.*

Proof. As we have previously seen, in $D_{\mathbb{L}_n}$ every instance of $\mathcal{L}$ looping around $\mathcal{B}$ equates to an instance of $\widetilde{\mathcal{L}}$ passing into the next fundamental domain along. Now, as $\widetilde{\mathcal{L}}$ is a closed curve we know that it can only occupy a finite number of fundamental domains. In the case where $x = 0$ there are only two places where $\mathcal{L}$ loops around $\mathcal{B}$, so $\widetilde{\mathcal{L}}$ can only pass into the next domain and return; hence, it occupies two fundamental domains. Adding a coil increases the 'reach' of $\widetilde{\mathcal{L}}$ in that it occupies an extra fundamental domain, so the total number of fundamental domains occupied is 3; in general, if $\mathcal{L}$ has x coils then $\widetilde{\mathcal{L}}$ will occupy $x + 2$ fundamental domains. Now consider translates of $\widetilde{\mathcal{L}}$, $t^i(\widetilde{\mathcal{L}})$. There can clearly be no linking between $\widetilde{l_{\mathcal{L}}}$ and $t^i(\widetilde{\mathcal{L}})$ for $i \geq x+2$, and the result follows. □

We next consider the other η-polynomial we could take from a framed Sakuma link ($\eta(\mathbb{L}_n, \mathcal{L}, \mathcal{B}; t)$, $n \in 2\mathbb{Z}$ in the terminology of Definition 3.1.12). An important detail to note is that Sakuma has chosen to take $\eta(\mathbb{L}, \mathcal{B}, \mathcal{L}; t)$ instead of $\eta(\mathbb{L}, \mathcal{L}, \mathcal{B}; t)$ to attach to the associated strongly invertible knot. In light of Corollary 3.1.10, however, it would appear $\eta(\mathbb{L}_n, \mathcal{L}, \mathcal{B}; t)$ can tell us nothing that we cannot obtain from $\eta(\mathbb{L}_n, \mathcal{B}, \mathcal{L}; t)$. In addition, it turns out that $\eta(\mathbb{L}_n, \mathcal{L}, \mathcal{B}; t)$ can only ever have three terms: the constant term and the $t^{\pm 1}$ terms.

Proposition 3.1.20. *Suppose $\mathbb{L}_n$, $n \in 2\mathbb{Z}$, is a framed Sakuma link obtained from a framed strongly invertible knot (K, h, n), and suppose that in the standard projection diagram for $\mathbb{L}_n$ $\mathcal{L}$ coils around $\mathcal{B}$, in the sense of Figure 2.3. Then,*

$$\eta(\mathbb{L}_n, 2, 1; t) = a_1 t^{-1} + a_0 + a_1 t \quad a_0, a_1 \in \mathbb{Z}.$$

Proof. Given $D_{\mathbb{L}_n}$ we perform Watson's construction in order to obtain a diagram for $\mathbb{L}_n$ with $\mathcal{L}$

as the axis. In this diagram $\mathcal{B}$ does not coil around $\mathcal{L}$ at all, so a lift of $\mathcal{B}$ in $\widehat{X_{\mathcal{L}}}$ can only occupy a maximum of two fundamental domains. Therefore, $t^i(\widetilde{\mathcal{B}})$ for $i \geq 2$ can not possibly link with $\widetilde{l_{\mathcal{B}}}$, hence $\eta(\mathbb{L}, 2, 1; t)$ can only have three terms. □

Recall Proposition 2.1.12 from the previous chapter. Combining this with the above result than gives us the following.

Corollary 3.1.21. *Suppose $\mathbb{L}_n$, $n \in 2\mathbb{Z}$, is a framed Sakuma link associated one of the following:*

1. *A framed strongly invertible unknot $(\mathcal{U}, h_0, n)$.*
2. *A framed strongly invertible double $(D(K'), h, n)$, for some prime knot K'.*
3. *A framed equivariant product of strongly invertible doubles, $(\{\#_{i=1}^{s} D(K_i')\}, h, n)$, for prime knots K_i'.*

Then $\eta(\mathbb{L}_n, 1, 2; t) = \eta(\mathbb{L}_n, 2, 1; t)$.

Proof. If (K, h, n) is a member of one of the three classes of framed strongly invertible knots listed above then $D_{\mathbb{L}_n}$ does not have any coils, and so has pure exchange symmetry. This means that $\eta(\mathbb{L}_n, 1, 2; t) = \eta(\mathbb{L}_n, 2, 1; t) = a_1 t^{-1} + a_0 + a_1 t$. □

We will conclude this section by returning to the question of which knots admitting strong inversions are amphicheiral.

Proposition 3.1.22 (Sakuma, 1985)**.** *Let (K, h) be a strongly invertible knot and suppose K is hyperbolic and amphicheiral.*

1. *Suppose that K does not have a free or cyclic period of period 2, and let h be the unique inverting involution. Then $(K, h) \cong (\overline{K, h})$, and so $\eta_{(K,h)}(t) = \eta_{(\overline{K,h})}(t) = -\eta_{(K,h)}(t) = 0$.*
2. *Suppose K does have period 2, and let h_1 and h_2 be its two inequivalent inverting involutions. Then $(K, h_1) \cong (\overline{K, h_2})$, and so $\eta_{(K,h_1)}(t) = \eta_{(\overline{K,h_2})}(t) = -\eta_{(K,h_2)}(t)$.*

For a proof see [79].

We can extend the above result to include framed strongly invertible knots.

Corollary 3.1.23. *Let (K, h, n), $n \in 2\mathbb{Z}$ be an even-framed strongly invertible knot and suppose K is hyperbolic and amphicheiral.*

1. *Suppose that K does not have a free or cyclic period of period 2, and let h be the unique inverting involution. Then $(K, h, n) \cong (\overline{K, h, n})$, and so $\eta_{(K,h,n)}(t) = \eta_{(\overline{K,h,n})}(t)$.*
2. *Suppose K does have period 2, and let h_1 and h_2 be its two inequivalent inverting involutions. Then $(K, h_1, n) \cong (\overline{K, h_2, n})$, and so $\eta_{(K,h_1,n)}(t) = \eta_{(\overline{K,h_2,n})}(t)$.*

As a result of the above results, the η-polynomial can be used to detect the cheirality of hyperbolic knots which admit strong inversions. The following examples appear in [79, Example 3.5].

Example 3.1.24. Consider the hyperbolic knots 10_{104} and 10_{155} in the Rolfsen tables [77, Appendix C]:

1. 10_{104} has a unique strong inversion, and from work of Hartley [27] and Murasugi [59], it can be shown that it does not have period 2. However, its η-polynomial is $[2, -1, 1-1$, so it cannot be amphicheiral.

2. 10_{155} has two unique strong inversions, and using [27] it can be shown that it has a free period of period 2. But, the respective η-polynomials of the two strongly invertible knots are 0 and $[-4, 0, 2$, and so 10_{155} cannot be amphicheiral either.

We end this section by applying η to the mirrors of Sakuma links. Recall Lemma 2.1.13 from Chapter 2; for a framed Sakuma link $\mathbb{L}_n$ with framed strongly invertible knot (K, h, n), we saw that its mirror image is the framed Sakuma link given by $\overline{\mathbb{L}}_{-n}$, which has $(\overline{K, h, -n})$ as its framed strongly invertible knot. It then follows from the definition of the η-polynomial that $\eta_{(K,h,n)}(t) = -\eta_{(\overline{K,h,-n})}(t)$, and so if a Sakuma link is amphicheiral its η-polynomial must be zero.

3.2 The Jones polynomial

The next polynomial invariant we will consider is the Jones polynomial — which was first defined by Jones in [34]. The Jones polynomial is an invariant of links in the 3-sphere, and takes the form of a Laurent polynomial with coefficients in $\mathbb{Z}$. In the discussion to follow we will be using a renormalised version of the Jones polynomial, which is the version Khovanov categorified [40] when he defined the Khovanov homology of a link. Just as for the η-polynomial, this invariant can be used to study strongly invertible knots via the framed Sakuma links we constructed in the previous chapter.

3.2.1 Definition of $J(L)$

We start by taking an oriented link L in S^3 and fixing a diagram $D_L \subset \mathbb{R}^2$ for it. One way to obtain the Jones polynomial is by first calculating a related polynomial — the *Kauffman bracket*. The Kauffman bracket was first introduced by Kauffman in [36] and is an invariant of the link diagram, though not of the link itself.

Definition 3.2.1. Let $D_L \subset \mathbb{R}^2$ be a link diagram. The *Kauffman bracket* $\langle D_L \rangle \in \mathbb{Z}[q^{\pm 1}]$, is a Laurent polynomial defined by the following three axioms:

$$\langle \emptyset \rangle = 1 \tag{3.1}$$

$$\langle \bigcirc D_L \rangle = (q + q^{-1}) \langle D_L \rangle \tag{3.2}$$

$$\left\langle \times \right\rangle = \left\langle \asymp \right\rangle - q \left\langle \right\rangle \left\langle \right\rangle \tag{3.3}$$

By scaling the Kauffman bracket by a suitable factor we obtain the Jones polynomial of the link.

Definition 3.2.2. Let $L \subset S^3$ be an oriented link and D_L be a choice of diagram for L with n_+ positive crossings and n_- negative crossings, and let $\langle D_L \rangle$ be the Kauffman bracket of D_L. The *unnormalised Jones polynomial* of L is defined to be

$$\widehat{J}(L)(q) := (-1)^{n_-} q^{n_+ - 2n_-} \langle D_L \rangle.$$

The *Jones polynomial* is then

$$J(L)(q) := \frac{\widehat{J}(L)(q)}{q + q^{-1}}.$$

Remark. The reason we normalise the Jones polynomial is to ensure that the unknot has Jones polynomial equal to 1, rather than $q + q^{-1}$.

Remark. As mentioned earlier, this definition of the Jones polynomial is due to Khovanov, and is actually a rescaled version of the original polynomial as defined by Jones. Jones uses the notation $V(t)$ to describe the polynomial — we can pass between the two versions using the following substitution (c.f. [40]):

$$V(L)(t)\Big|_{\sqrt{t}=-q} = J(L)(q)$$

Another way to express the Jones polynomial is through constructing a *cube of smoothings*, an example of which we have depicted in Figure 3.4. Let $L \subset S^3$ as before and D_L be a diagram for L in $\mathbb{R}^2$. Begin by numbering the crossings of D_L from 1 to n and denote by $\asymp$ and $)($ the 0 and 1-smoothings of a crossing $\times$ respectively. An n-tuple $\alpha \in \{0,1\}^n$ gives us a set of smoothing instructions for D_L: simply smooth the ith crossing according to the ith entry in α. We denote by S_α the result of applying the smoothing instructions given by α, which is nothing more than a collection of disjoint circles in the plane — this is sometimes referred to as a *Kauffman state* of D_L (c.f. [95]). We will denote the set of Kauffman states for D_L by $\mathcal{K}(D_L)$. The phrase 'cube of smoothings' comes from the fact that the Kauffman states can be arranged on the vertices of a hypercube, where each α determines the vertex S_α appears at.

We determine $\langle D_L \rangle$ from a cube of smoothings by attaching to each S_α a term of the form $(-1)^r q^r (q + q^{-1})^u$ and summing; where r is the *height* of the smoothing (the number of 1's that appear in α, also denoted $|\alpha|$) and u is the number of circles appearing in the smoothing. Finally, we multiply $\langle D_L \rangle$ by a normalisation term as before to obtain $J(L)$. This can be expressed more succinctly as follows:

$$J(L)(q,t) = \frac{(-1)^{n_-} q^{n_+ - 2n_-}}{q + q^{-1}} \left[\sum_{r=0}^{n} (-1)^r q^r \left(\sum_{|\alpha|=r} \langle S_\alpha \rangle \right) \right] \tag{3.4}$$

where $\langle S_\alpha \rangle = (q + q^{-1})^u$.

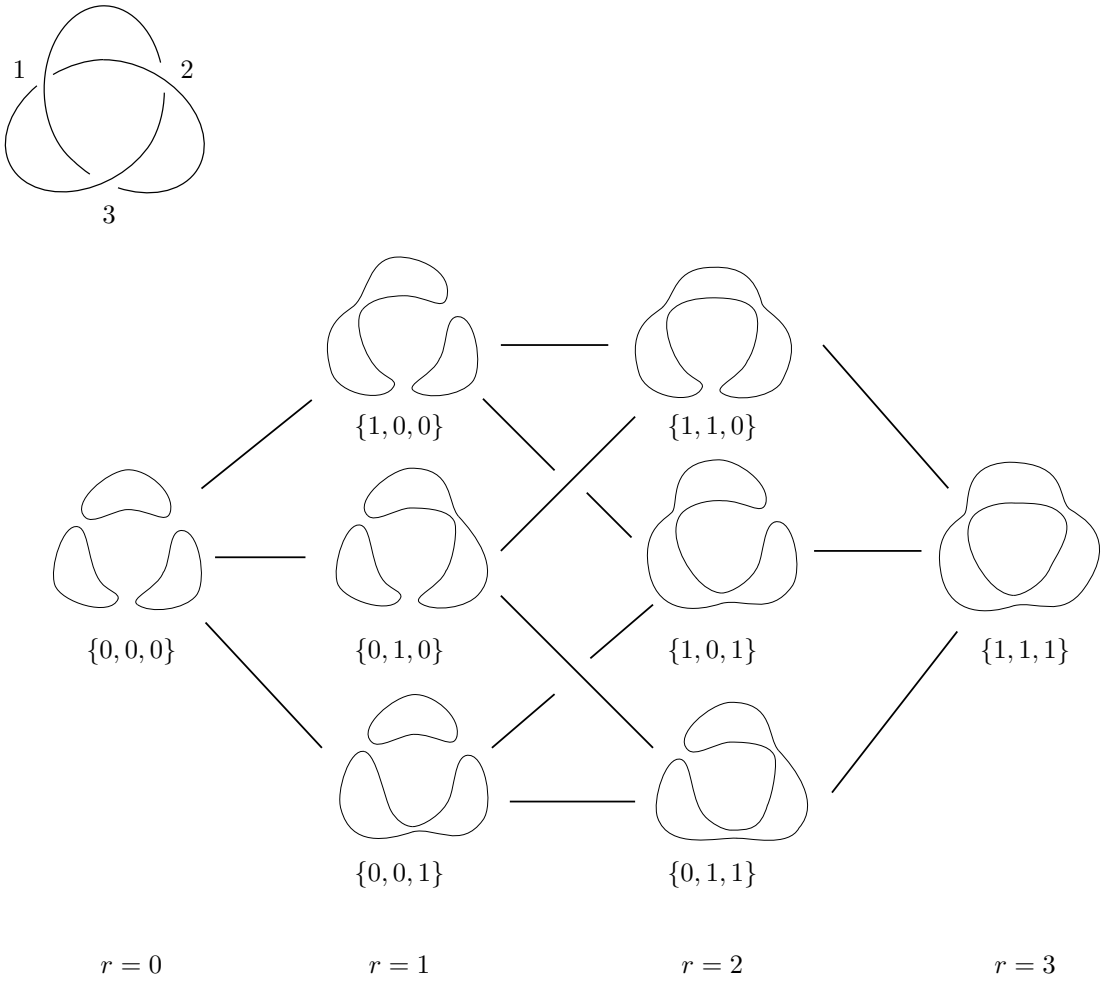

Figure 3.4: Cube of smoothings for a diagram of the trefoil

3.2.2 The Jones polynomial of a Sakuma link

Just as for η, we can use the bijection between strongly invertible knots and Sakuma links in order to apply the Jones polynomial to strongly invertible knots. Given a strongly invertible knot (K, h) with Sakuma link $\mathbb{L}$ we simply define the Jones polynomial of (K, h) to be that of $\mathbb{L}$:

Definition 3.2.3. Let $\mathbb{L}$ be a Sakuma link obtained from a strongly invertible knot (K, h). Then,

$$J_{(K,h)}(q) := J(\mathbb{L})(q).$$

We now have our second polynomial invariant of strongly invertible knots. Just as for η, we can define the Jones polynomial of a framed strongly invertible knot — the advantage here being that all framings are permissible, not just even ones.

Definition 3.2.4. Let (K, h, n) be a framed strongly invertible knot with Sakuma link $\mathbb{L}_n$. Then, we set

$$J_{(K,h,n)}(q) := J(\mathbb{L}_n)(q).$$

In the rest of this thesis we will pass over the Jones polynomial in favour of its annular counterpart, although, as we shall see later on, the two polynomials are closely connected. We will briefly consider, however, a couple of consequences of applying the Jones polynomial to a framed Sakuma link.

For starters, the Jones polynomial is a good detector of amphicheirality. For knots, the Jones polynomial of an amphicheiral knot is palindromic, that is $J(K)(q) = J(K)(q^{-1})$. For links, we have a slightly expanded notion of amphicheirality. Recall that an n-component link L is ϵ-amphicheiral if L is equivalent to L_ϵ, where the n-tuple $\epsilon \in \{+,-\}^n$ indicates whether the orientation of each K_i is preserved or reversed. In this setting, the Jones polynomial of an ϵ-amphicheiral link $J(L)(q)$ is equal to $q^k J(L)(q^{-1})$, where $k \in \mathbb{Z}$ (see, for example, [37, Lemma 3.1]). That is, the coefficients of $J(L)$ are still palindromic, but the powers of q are shifted. Applying this knowledge to framed Sakuma links, $J(\mathbb{L}_n)$ can rule out the presence of ϵ-amphicheiralities of $\mathbb{L}_n$. We use this knowledge to restate Proposition 3.1.22 in terms of the Jones polynomial (recall Proposition 1.2.9 and Corollary 2.1.14).

Corollary 3.2.5. *Let (K,h,n) be a framed strongly invertible knot and suppose K is hyperbolic and amphicheiral.*

1. *Suppose that K does not have a free or cyclic period of period 2, and let h be the unique inverting involution. Then $(K,h,n) \cong (\overline{K,h,n})$, and so $J_{(K,h,n)}(q) = J_{\overline{(K,h,n)}}(q)$ for all n. In particular, when $n=0$ we have $J_{(K,h)}(q) = J_{\overline{(K,h)}}(q) = J_{(K,h)}(q^{-1})$.*
2. *Suppose K does have period 2, and let h_1 and h_2 be its two inequivalent inverting involutions. Then $(K,h_1,n) \cong (\overline{K,h_2,n})$, and so $J_{(K,h_1,n)}(q) = J_{\overline{(K,h_2,n)}}(q)$ for all n. In particular, when $n=0$ we have $J_{(K,h_1)}(q) = J_{\overline{(K,h_2)}}(q) = J_{(K,h_2)}(q^{-1})$.*

Example 3.2.6. Let $K = 4_1$, the Figure-8 knot, and consider its two inequivalent strong inversions as depicted in Figure 1.9. We take 0-framed longitudes for both strongly invertible knots, form the respective Sakuma links, and calculate their Jones polynomials:

$$J_{(4_1,h_1)}(q) = q^{-9} - 3q^{-7} + 4q^{-5} - 3q^{-3} + 3q^{-1} - q + 2q^5 - 2q^7 + 2q^9 - q^{11}$$

$$J_{(4_1,h_2)}(q) = -q^{-11} + 2q^{-9} - 2q^{-7} + 2q^{-5} - q^{-1} + 3q - 3q^3 + 4q^5 - 3q^7 + q^9$$

Note that, since in the $n=0$ setting the Sakuma links are mirrors of one another, the above Jones polynomials are obtained from one another by substituting q for q^{-1}.

Next, a word on unknot detection. The Jones polynomial has been proven not to detect the unlink for n-component links; indeed, infinitely many counterexamples have been shown [17]. However, for two-component links, the families constructed with trivial Jones polynomials are not Sakuma links as their components are not unknots. This leads to the following question:

Question. Does the Jones polynomial detect the strongly invertible unknot? That is, if $\mathbb{L}$ is a Sakuma link such that $J(\mathbb{L})(q) = 0$, is $\mathbb{L}$ the two-component unlink?

While it might seem unlikely that restricting to Sakuma links will turn the Jones polynomial into

an unlink detector, there may well be a constraint on a non-trivial Sakuma link having trivial Jones polynomial coming from the topology of Sakuma links. We will leave this question open for further study.

3.3 The annular Jones polynomial

The next polynomial knot invariant we come across is the *annular Jones polynomial*, an offshoot of the Jones polynomial for links in the thickened annulus $A \times I$. In this section we will define the annular Jones polynomial and apply it to the annular Sakuma knots we encountered at the end of the last chapter.

3.3.1 Definition and constructions

Consider an oriented link L in the thickened annulus $A \times I$ and let D_L be a diagram for L in A. We can then calculate the annular Jones polynomial $AJ(L)$, which is really nothing more than an extension of the standard Jones polynomial $J(L)$ to the annular setting.

First, we define the annular Kauffman bracket.

Definition 3.3.1. Let $D_L \subset A$ be an annular link diagram. The *annular Kauffman bracket* $\langle D_L \rangle_A \in \mathbb{Z}[q^{\pm 1}, t^{\pm 1}]$, is a two-variable Laurent polynomial defined by the following four axioms:

$$\langle \emptyset \rangle_A = 1 \tag{3.5}$$

$$\langle \bigcirc D_L \rangle_A = (q + q^{-1}) \langle D_L \rangle_A \tag{3.6}$$

$$\langle \circledcirc D_L \rangle_A = (qt + (qt)^{-1}) \langle D_L \rangle_A \tag{3.7}$$

$$\left\langle \times \right\rangle_A = \langle \asymp \rangle_A - q \, \langle \rangle \langle \rangle_A \tag{3.8}$$

The third of the above axioms requires further explanation. By $\circledcirc$ we simply mean there exists a circle in the diagram which encloses the hole in the annulus, without implying anything about how D_L interacts with the hole (D_L may well enclose the hole too). For example, if D_L is n nested circles around the hole $\langle D_L \rangle_A = (qt + (qt)^{-1})^n$.

Comparing these formulas with those for the standard Kauffman bracket, we note that the only difference between the two is when we have a circle which is homologically non-trivial in $H_1(A; \mathbb{Z})$; we encode this difference by the variables $t^{\pm 1}$.

We now come to the definition of the annular Jones polynomial.

Definition 3.3.2. Let $L \subset A \times I$ be an oriented link and D_L be a choice of diagram for L with n_+ positive crossings and n_- negative crossings, and let $\langle D_L \rangle_A$ be the annular Kauffman bracket of D_L. The *annular Jones polynomial* is defined to be

$$AJ(L)(q,t) := (-1)^{n_-} q^{n_+ - 2n_-} \langle D_L \rangle_A. \tag{3.9}$$

Lemma 3.3.3. *Let $L \subset A \times I$ be an oriented link with annular Jones polynomial $AJ(L)(q,t)$.*

Then setting t equal to 1 returns the unnormalised Jones polynomial of $L \subset S^3$; that is,

$$AJ(L)(q,1) = \widehat{J}(q).$$

Proof. This follows immediately from the definition of the annular Kauffman bracket, which resolves to the standard Kauffman bracket when we set t equal to 1. Furthermore, if L is the n-component unlink then we obtain $AJ(L)(q,1) = (q+q^{-1})^n$, which is the value of the unnormalised Jones polynomial for $L \subset S^3$. □

What the above lemma really tells us is that setting t equal to 1 in the annular Jones polynomial is the algebraic equivalent of taking our annular link $L \subset A \times I \subset S^3$, forgetting the thickened annulus, and calculating the Jones polynomial of L. This highlights the close relationship between the Jones polynomial and its annular counterpart.

Proposition 3.3.4. *The annular Jones polynomial is an invariant of annular links.*

Proof. We will check that the annular Jones polynomial is invariant under the first two Reidemeister moves — invariance under the third move can be shown using a similar method.

Let $D_L =$  , and suppose D_L has n_+ positive crossings and n_- negative crossings. Then

$$\begin{aligned} AJ(\text{}) &= (-1)^{n_-} q^{n_+ - 2n_-} \langle \text{} \rangle_A \\ &= (-1)^{n_-} q^{n_+ - 2n_-} \left(\langle \text{} \rangle_A - q \langle \text{} \rangle_A \right) \\ &= (-1)^{n_- + 1} q^{n_+ - 2(n_- - 1)} \langle \text{} \rangle_A \\ &= AJ(\text{}). \end{aligned}$$

So AJ is invariant under Reidemeister I moves.

Next, let $D_L =$  . We have

$$\begin{aligned} AJ(\text{}) &= (-1)^{n_-} q^{n_+ - 2n_-} \langle \text{} \rangle_A \\ &= (-1)^{n_-} q^{n_+ - 2n_-} \left(\langle \text{} \rangle_A - q \langle \text{} \rangle_A - q \langle \text{} \rangle_A + q^2 \langle \text{} \rangle_A \right) \\ &= (-1)^{n_-} q^{n_+ - 2n_-} \left(-q \langle \text{} \rangle_A \right) \\ &= (-1)^{n_- + 1} q^{(n_+ - 1) - 2(n_- - 1)} \langle \text{} \rangle_A \\ &= AJ(\text{}). \end{aligned}$$

So AJ is also invariant under Reidemeister II moves. □

We will now outline several useful ways of expressing the annular Jones polynomial. The first is as follows:

$$AJ(L)(q,t) = \sum_m t^m \mathcal{P}_m(q), \tag{3.10}$$

where $\mathcal{P}_m(q) \in \mathbb{Z}[q^{\pm 1}]$.

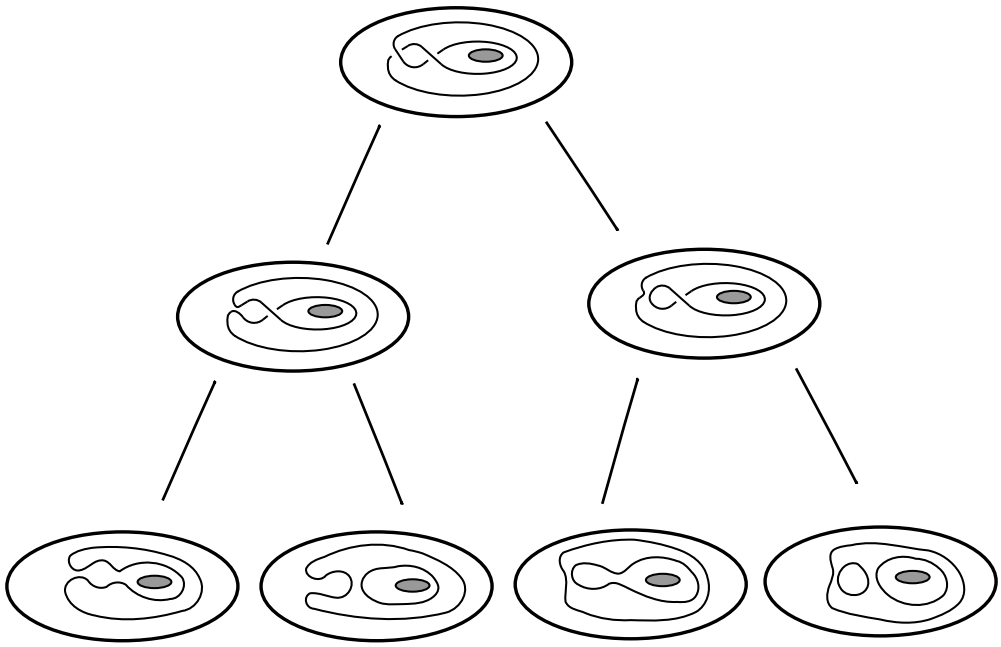

Figure 3.5: Binary tree

Secondly, just as for the Jones polynomial for links in S^3, we can express the annular Jones polynomial using a cube of smoothings. Let $L \subset A \times I$ as before and D_L be a diagram for L in the annulus. Number the crossings of D_L from 1 to n and construct the set of Kauffman states for D_L as in the S^3 setting. This time we calculate $\langle D_L \rangle$ by attaching to each S_α a term of the form $(-1)^r q^r (q+q^{-1})^u (qt+(qt)^{-1})^{k-u}$ and summing; where r is the height of the smoothing, u is the number of circles in the smoothing that are nullhomologous in $H_1(A;\mathbb{Z})$, and $k-u$ is the number of homologically non-trivial circles. Finally, we multiply $\langle D_L \rangle$ by a normalisation term $(-1)^{n_-} q^{n_+ - 2n_-}$ as before to obtain $AJ(L)$. This can be expressed as follows:

$$AJ(L)(q,t) = (-1)^{n_-} q^{n_+ - 2n_-} \left[\sum_{r=0}^{n} (-1)^r q^r \left(\sum_{|\alpha|=r} \langle S_\alpha \rangle_A \right) \right] \tag{3.11}$$

where $\langle S_\alpha \rangle_A = (q+q^{-1})^u (qt+(qt)^{-1})^{k-u}$.

Next, we will describe a *binary tree* construction of the annular Jones polynomial, originally defined by Thistlethwaite [86] for the Jones polynomial of links in S^3. We will be adapting a version as appears in a paper by Wehrli [95], however, as the conventions used fit in better with those used in Khovanov homology (see also [12]). We begin with the observation that the annular Kauffman bracket can be described in the following way:

$$\langle D_L \rangle_A = \sum_{S_\alpha \in \mathcal{K}(D_L)} (-1)^r q^r \langle S_\alpha \rangle_A \tag{3.12}$$

where $|\alpha| = r$. Now, given D_L we can repeatedly use the fourth Kauffman bracket axiom (3.8) to

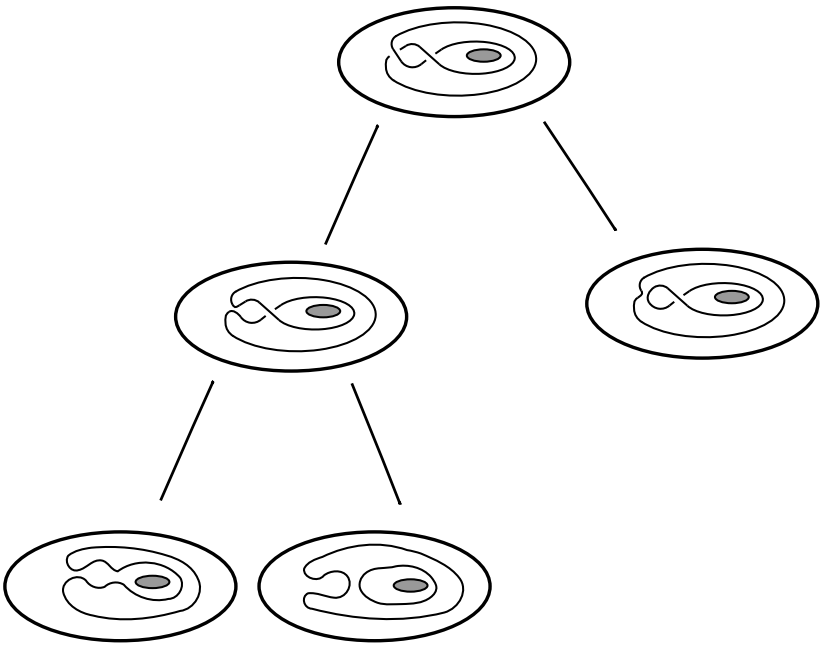

Figure 3.6: Truncated binary tree

reduce D_L into its set of Kauffman states, which allows us to obtain $\langle D_L \rangle_A$; see Figure 3.5 for an example. The order in which we decide to smooth crossings will affect the diagrams that appear at each vertex of the binary tree, but the same Kauffman bracket is returned for any choice of order.

The above method will work for every knot diagram eventually, but, as Wehrli comments, in practice it quickly becomes impractical, as the complexity of (3.12) grows exponentially as n increases. The process is made more efficient, however, if we stop smoothing crossings whenever we obtain a partially smoothed diagram which is equivalent (up to Reidemeister moves) to a member of the following set:

$$\mathcal{Z} = \left\{ \bigcirc,\ \circledcirc, \circledcirc, \ldots, \circledcirc, \ldots \right\} \tag{3.13}$$

This truncates the binary tree, as we now do not have to smooth every crossing (c.f. Figure 3.6). We will refer to such a tree by $\mathcal{T}_{D_L}$.

We can then define a basis for the annular Kauffman bracket as follows:

$$\begin{array}{lcll}
\langle z_0 \rangle_A & := & \langle \bigcirc \rangle_A & = (q + q^{-1}) \\
\langle z_1 \rangle_A & := & \langle \circledcirc \rangle_A & = (qt + (qt)^{-1}) \\
\langle z_2 \rangle_A & := & \langle \circledcirc \rangle_A & = (qt + (qt)^{-1})^2 \\
\vdots & & \vdots & \\
\langle z_m \rangle_A & := & \langle \circledcirc \rangle_A & = (qt + (qt)^{-1})^m \\
\vdots & & \vdots &
\end{array}$$

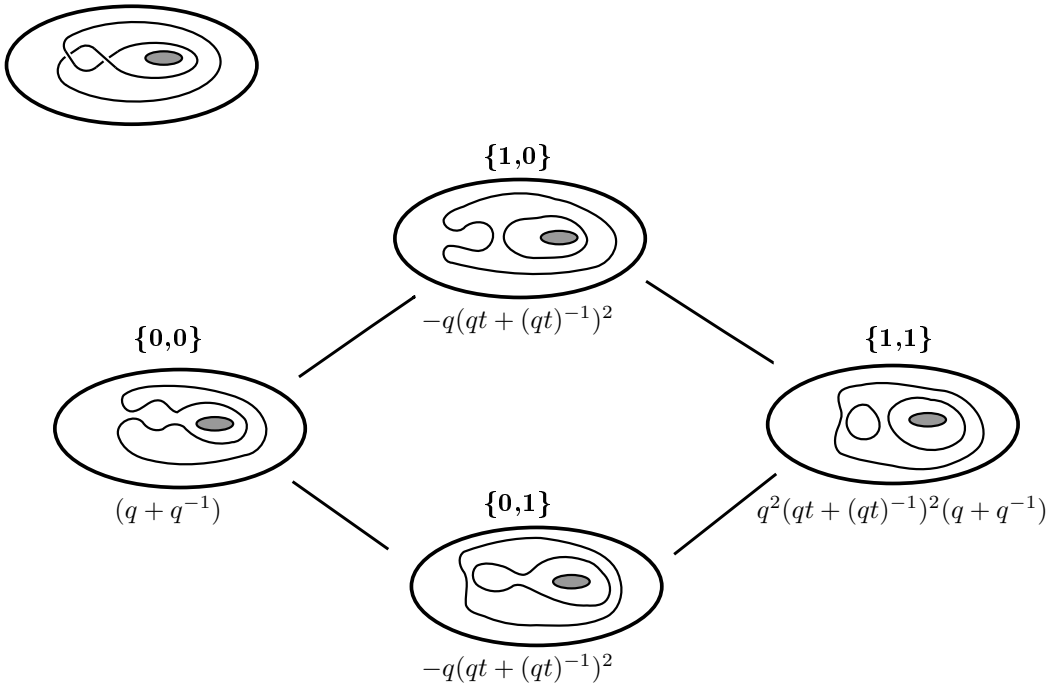

Figure 3.7: Calculating $AJ(K)$

Said more precisely, we have:

$$\langle D_L \rangle_A = \sum_m A_m(q) \langle z_m \rangle_A \tag{3.14}$$

where $A_m(q) \in \mathbb{Z}[q^{\pm 1}]$. Although the truncated tree $\mathcal{T}_{D_L}$ is dependent on the order in which we smooth the crossings of D_L the basis coefficients obtained are ultimately the same regardless of our initial choice of order. This basis can also be used as a basis for the annular Jones polynomial: let n_+ and n_- be the number of positive and negative crossings in D_L. Then,

$$AJ(L)(q,t) = (-1)^{n_-} q^{n_+ - 2n_-} \sum_m A_m(q) \langle z_m \rangle_A \tag{3.15}$$

Example 3.3.5. Consider the annular knot diagram D_K depicted in Figure 3.7. We follow the cube of smoothings procedure to calculate the annular Jones polynomial of the knot. Figure 3.7 includes the cube of smoothings for the knot diagram, with the relevant polynomial term attached to each smoothing. As a result,

$$\begin{aligned} \langle D_K \rangle_A &= (q+q^{-1}) - 2q(qt+(qt)^{-1})^2 + q^2(qt+(qt)^{-1})^2(q+q^{-1}) \\ &= (q+q^{-1}) + (q^3-q)(qt+(qt)^{-1})^2 \\ &= \langle z_0 \rangle_A + (q^3-q)\langle z_2 \rangle_A \end{aligned}$$

and, so

$$\begin{aligned} AJ(K) &= q^{-4}\langle z_0\rangle_A + (q^{-1}-q^{-3})\langle z_2\rangle_A \\ &= t^{-2}(q^{-3}-q^{-5}) + (q^{-5}-q^{-3}+2q^{-1}) + t^2(q-q^{-1}) \end{aligned}$$

We notice that if we were to embed this annular knot into S^3 we would obtain the unknot. Therefore, when we specialise $AJ(K)$ by setting $t = 1$ we expect to obtain the unnormalised Jones polynomial of the unknot: a quick calculation proves that this is indeed the case.

3.3.2 General properties

We will now detail a number of general results about various characteristics of the annular Jones polynomial. In the definition of AJ the role of the homologically non-trivial circles in the various Kauffman states is to decorate AJ with its additional t variable. Intuitively, we might expect the powers of t present in an annular Jones polynomial to be related in some way to how the annular link wraps around the central hole in the annulus. This intuition leads us to the concept of the *wrapping number* of an annular link.

Definition 3.3.6. Let $L \subset A \times I$ be an annular link. The *wrapping number* ω of L is the minimal geometric intersection number of all members of the equivalence class of L with a meridional disc of $A \times I$.

Informally, the wrapping number of an annular link is the number of times a representative of L that has been 'pulled tight' runs around the central hole.

Example 3.3.7. Let B_n be an n-strand braid, and $\widehat{B_n} \subset A \times I$ be its closure. Then $\omega = n$.

Now let $L \subset A \times I$, fix a diagram D_L, and consider a Kauffman state of D_L. A useful technique to divide the circles into the trivial and non-trivial camps is to draw a ray λ in A from the inner edge to the outer edge such that λ avoids all the crossings, then determine the parity of the number of times λ meets a given circle — an odd number means the circle is non-trivial, and an even number means it is trivial. We make use of this technique in the proofs of the next two results.

Lemma 3.3.8. *Let $L \subset A \times I$ be an annular link with wrapping number ω, and consider $AJ(L)(q,t)$ expressed as in* (3.10)*, i.e as*

$$AJ(L)(q,t) = \sum_m t^m \mathcal{P}_j(q).$$

Then ω bounds the powers of t in $AJ(L)(q,t)$ from above; that is $\mathcal{P}_m(q) = 0$ for $|m| > \omega$.

Proof. Let D_L be a diagram of a representative of L which realises the wrapping number of L. This means that if we draw a ray λ in the annulus as described above, λ meets D_L in exactly ω points. Consider $\langle D_L\rangle_A$: the powers of t are entirely dependent on the number of homologically non-trivial circles present in the smoothings of D_L, and the maximum number of these possible in

a smoothing is ω, where each meeting point is contained in a separate non-trivial circle. Therefore, there cannot be any powers of t in which $|m|$ is greater than ω. □

The next lemma tells us that the powers of t in $AJ(L)(q,t)$ are dependent on the parity of the wrapping number — expanding further on the statement 'the t powers encode how L wraps around the hole in the annulus'.

Lemma 3.3.9. *Let $L \subset A \times I$ be an annular link with wrapping number ω. Consider the expression of $AJ(L)(q,t)$ in* (3.10) *i.e as*

$$AJ(L)(q,t) = \sum_m t^m \mathcal{P}_m(q).$$

1. *Suppose ω is even. Then $\mathcal{P}_m(q) = 0$ for all odd m.*
2. *Suppose ω is odd. Then $\mathcal{P}_m(q) = 0$ for all even m.*

Proof. (1) Suppose ω is even and let D_L be a diagram of L which realises ω. Suppose for a contradiction that there exists a non-zero $\mathcal{P}_m(q)$ for m odd. Then there must be a smoothing S_α of D_L in which there are m non-trivial circles. Then there are $\omega - m$ remaining intersection points between a ray λ and D_L to account for, and by assumption these are all contained in trivial circles. But $\omega - m$ is odd, so one circle must contain an odd number of the remaining meeting points. But then this circle is also non-trivial, and we have a contradiction. Hence, $\mathcal{P}_m = 0$ for all odd m. The proof of (2) follows in a similar way. □

The next result follows work of Grigsby and Ni [20] on the annular Khovanov homology of braid closures (see Proposition 4.2.4). Some of their techniques can be applied to the annular Jones polynomial. In particular, the annular Jones polynomial can rule out the possibility of an annular link being equivalent to a braid closure.

Lemma 3.3.10. *Let B_n be an n-strand braid, and let $\widehat{B_n} \subset A \times I$ be its closure. Then $\mathcal{P}_\omega(q) = aq^b$ for integers a, b.*

Proof. Take a diagram for $\widehat{B}$ and consider its cube of smoothings. As Grigsby and Ni note only one smoothing does not 'backtrack'. We attach $(-q)^r(qt + (qt)^{-1})^n$ to this smoothing. Since $\omega = n$, we have $\mathcal{P}_\omega(q) = (-1)^{r+n_-} q^{r+\omega+n_+-2n_-}$ and the result follows. □

We may wonder, due to the evident similarity between the Jones polynomial and the annular Jones polynomial, how many of the properties of J still hold for annular links, and how the two invariants relate to each other. We will explore this idea in a few different directions.

Firstly, we highlight a result due to Pascual [68, Theorem 3] concerning satellite knots. Recall Definition 1.1.16: we denote a satellite knot with pattern $P \subset A \times I$ and companion knot $C \subset S^3$ by $\mathrm{Sat}(P, C)$. Recall also the definition of a n-parallel cable link of a knot C (Definition 1.1.17) — the satellite link with companion C and pattern the torus link $T(0, n)$.

Theorem 3.3.11 (Pascual, 2016). *Let $P \subset A \times I$ be an annular knot, $C \subset S^3$ be a knot in the 3-sphere, $(C; n)$ be the n-parallel cable link of C, and $Sat(P, C)$ be the satellite knot with pattern P and companion knot C. Then,*

$$J(Sat(P,C))(q) = AJ(P)(q,t)\Big|_{z^n = J(C;n)(q)}$$

The proof of the above can be found in [68], albeit stated using slightly different terminology. Due to the fact that the pattern knot is simpler in terms of crossings to the satellite knot formed from it, Pascual's theorem provides us with a way of calculating the Jones polynomial of the satellite that is less expensive computationally. We can make use of this theorem in the Sakuma link setting, since infinitely many Sakuma links are satellite if we perform Sakuma's construction with a strongly invertible double $(D(K), h)$, where $K \subset S^3$ is any knot.

Next we turn our attention to the two-component completions of annular knots. Recall that, given an annular knot $K \subset A \times I$, we can obtain its two-component completion $L = K \cup \mathcal{B} \subset S^3$ by adding an additional unknotted component $\mathcal{B}$ which consists of the z axis and the point at infinity. We investigate the relationship between $AJ(K)(q,t)$ and $J(L)(q)$, using Pascual's theorem as motivation.

Let $L = K \cup \mathcal{B}$ be the two-component completion of an annular knot K. Let D_L be a diagram for L obtained from a diagram of K, D_K, which realises the wrapping number of K by adding in $\mathcal{B}$ as a vertical axis passing through the hole — we will refer to any such D_L as a *preferred* diagram of L. We note that every crossing in D_K has a canonical counterpart in D_L.

We use another binary tree style method to calculate the Kauffman bracket of a preferred D_L. The key difference from the binary trees we use to calculate the ordinary Kauffman bracket is that we will not smooth any crossings between K and $\mathcal{B}$. We define a *partial Kauffman state* of a preferred diagram D_L to be the link obtained as a result of smoothing all other crossings — which are precisely the self-crossings of K. As before, we will truncate the binary tree; we will stop whenever a partially smoothed diagram is Reidemeister equivalent to one of the following:

$\overline{\mathcal{Z}} =$ 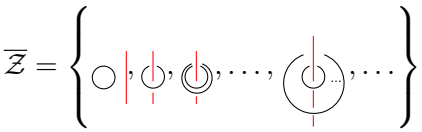 (3.16)

We will refer to such a binary tree by $\mathcal{T}_{D_L}$; for an example see Figure 3.8. We also note there exists a canonical bijection between this set and the set $\mathcal{Z}$ we defined in (3.13).

Lemma 3.3.12. *Let $K \subset A \times I$, and D_K be a diagram of K. Let L be the two-component completion of K and D_L be the preferred diagram of L corresponding to D_K. Number the crossings in D_K and their counterparts in D_L in the same way. Let $\mathcal{T}_{D_K}$ and $\mathcal{T}_{D_L}$ be the truncated binary trees of D_K and D_L obtained by smoothing crossings in the numbered order. Then $\mathcal{T}_{D_K}$ and $\mathcal{T}_{D_L}$ are isomorphic.*

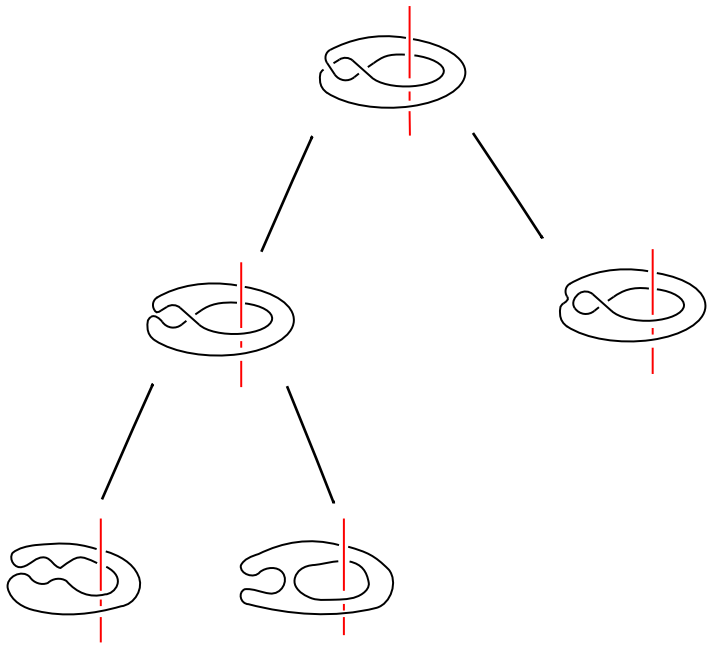

Figure 3.8: A truncated binary tree of partial Kauffman states

Proof. This follows immediately from the definitions: resolving a crossing in D_K is clearly equivalent to resolving its counterpart in D_L. □

Next, we define the following basis for the Kauffman bracket of a preferred diagram of a two-component completion.

$\langle \overline{z}_0 \rangle :=$ 

$\langle \overline{z}_1 \rangle :=$ 

$\langle \overline{z}_2 \rangle :=$ 

$\vdots \qquad \vdots$

$\langle \overline{z}_m \rangle :=$ 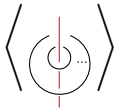

$\vdots \qquad \vdots$

We can immediately observe that for $m > \omega$, $\langle \overline{z}_m \rangle = 0$; this is a consequence of Lemma 3.3.8. The Kauffman bracket of D_L can be written as follows:

$$\langle D_L \rangle = \sum_{m=0}^{\omega} B_m(q) \langle \overline{z}_m \rangle,$$

where $B_m(q) \in \mathbb{Z}[q^{\pm 1}]$. We compare the above basis for $\langle D_L \rangle$ with that obtained for $\langle D_K \rangle_A$ (see (3.14)). Since the two truncated binary trees are isomorphic each $A_m(q)$ is a factor of $B_m(q)$.

There are, however, some extra powers of q in the basis for $\langle D_L \rangle$ which need to be explained. Namely, in order to pass from a diagram appearing in an end vertex of $\mathcal{T}_{D_L}$ to one which is equivalent to some $\overline{z}_m$ some Reidemeister II moves are required; these moves do not show up in the annular setting. For an example of this compare the bottom left vertex in Figure 3.8 with the equivalent vertex in Figure 3.6.

The number of RII moves required is determined by the wrapping number ω.

Lemma 3.3.13. *Let L be a two-component completion of an annular knot K with wrapping number ω, with preferred diagram D_L. Let $\mathcal{T}_{D_K}$ and $\mathcal{T}_{D_L}$ be the two isomorphic truncated binary trees for D_K and D_L, and let S be an end vertex of $\mathcal{T}_{D_L}$. Suppose S is equivalent to $\overline{z}_m$; then the number of RII moves required is $\omega - m$.*

Proof. In D_L strands running around $\mathcal{B}$ are joined together in pairs when we smooth crossings, and form $\frac{\omega - m}{2}$ loops. Each loop needs to be pulled around the axis, which requires two Reidemeister II moves; hence, the total number of RII moves required to transform S into $\overline{z}_m$ is $\omega - m$. □

As as result, we have:

$$\langle D_L \rangle = \sum_{m=0}^{\omega} (-q)^{\omega - m} A_m(q) \langle \overline{z}_m \rangle.$$

Therefore, we have a basis for $\widehat{J}(L)$ as well:

$$\widehat{J}(L)(q) = (-1)^{n_-} q^{n_+ - 2n_-} \sum_{m=0}^{\omega} (-q)^{\omega - m} A_m(q) \langle \overline{z}_m \rangle.$$

Next, we note that the members of the set (3.16) are always connect sums of Hopf links.

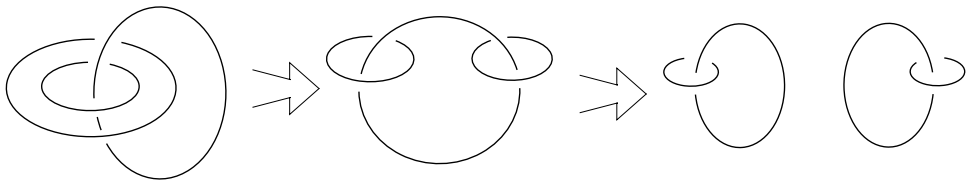

Therefore, the values of $\langle \overline{z}_m \rangle$ can be calculated easily, using an induction argument. We have in particular:

$$\langle \overline{z}_m \rangle = \left\{ \begin{array}{ll} (q^{-1} + q^3)^m (q + q^{-1}) & m \geq 1 \\ (q + q^{-1})^2 & m = 0 \end{array} \right\}$$

We see that $(q + q^{-1})$ is a factor of all $\langle \overline{z}_m \rangle$. Therefore, we can express the Jones polynomial of L as follows:

$$J(L)(q) = (-1)^{n_-} q^{n_+ - 2n_-} \left((-q)^{\omega} A_0(q)(q + q^{-1}) + \sum_{m=1}^{\omega} (-q)^{\omega - m} A_m(q)(q^{-1} + q^3)^m \right) \quad (3.17)$$

This leads us to a result relating $AJ(K)(q,t)$ and $J(L)(q)$.

Theorem 3.3.14. *Let $K \subset A \times I$ be an annular knot with wrapping number ω and two-component completion $L = K \cup \mathcal{B} \subset S^3$. Let D_L be a preferred diagram of L with $n_+^{K,\mathcal{B}}$ positive crossings and $n_-^{K,\mathcal{B}}$ negative crossings between the components K and $\mathcal{B}$. Then,*

$$J(L)(q) = X(q) AJ(K)(q,t)\Big|_{\langle z_0 \rangle_A = (-q)^{\omega}(q+q^{-1}), \langle z_m \rangle_A = (-q)^{\omega - m}(q^{-1}+q^3)^m}$$

where $X(q) = (-1)^{n_-^{K,\mathcal{B}}} q^{n_+^{K,\mathcal{B}} - 2n_-^{K,\mathcal{B}}}$.

Proof. The work has almost all been done. The only thing left is to note, comparing (3.15) and (3.17), that we need to scale by a term corresponding to the uncounted crossings of D_L in D_K, which are precisely those between K and $\mathcal{B}$. The result then follows. □

Example 3.3.15. As a quick example illustrating the formula in action, we will use the link and the annular knot featuring in Figures 3.6 and 3.8. We will orient $\mathcal{B}$ upwards, and orient K in the same way in both D_L and D_K. On the one hand, a direct calculation yields

$$\begin{aligned} J(L)(q) &= q^{-6}\langle D_L \rangle \\ &= q^{-4}(q + q^{-1}) + (q^{-3} - q^{-5})(q^{-1} + q^3)^2. \end{aligned}$$

Whilst, on the other,

$$\begin{aligned} AJ(K)(q,t) &= q^{-4}\langle D_K \rangle_A \\ &= q^{-4}\langle z_0 \rangle_A + (q^{-1} - q^{-3})\langle z_2 \rangle_A. \end{aligned}$$

Finally, we have $(-1)^{n_-^{K,B}} q^{n_+^{K,B} - 2n_-^{K,B}} = (-1)^2 q^{-2} = q^{-2}$, and so

$$J(L)(q) = q^{-2} AJ(K)(q,t)\Big|_{\langle z_0 \rangle_A = q^2(q+q^{-1}), \langle z_2 \rangle_A = (q^{-1}+q^3)^2}$$

as expected.

Lastly, we will consider sensitivity to cheirality. One of the most notable properties of the Jones polynomial is its ability to detect the cheirality of a knot. It turns out that this is property holds for the annular Jones polynomial too.

Proposition 3.3.16. *Let $K \subset A \times I$ be an annular knot. Suppose K is amphicheiral; then $AJ(K)(q,t)$ is palindromic, that is, $AJ(K)(q,t) = AJ(K)(q^{-1}, t^{-1})$.*

Proof. Fix a diagram $D_K \subset A$ for K, and suppose D_K has n_+ positive crossings, and n_- negative

crossings. Recall that $AJ(K)(q,t)$ can be expressed as follows:

$$AJ(K)(q,t) = (-1)^{n_-} q^{n_+ - 2n_-} \left[\sum_{r=0}^{n} (-1)^r q^r \left(\sum_{|\alpha|=r} \langle S_\alpha \rangle_A \right) \right].$$

Now, we consider the mirror image of K, and take $D_{\overline{K}}$. We can express $AJ(\overline{K})(q,t)$ as

$$AJ(\overline{K})(q,t) = (-1)^{n_+} q^{n_- - 2n_+} \left[\sum_{r=0}^{n} (-1)^{n-r} q^{n-r} \left(\sum_{|\alpha|=n-r} \langle S_\alpha \rangle_A \right) \right].$$

Now,

$$AJ(K)(q^{-1},t^{-1}) = (-1)^{n_-} q^{-n_+ + 2n_-} \left[\sum_{r=0}^{n} (-1)^r q^{-r} \left(\sum_{|\alpha|=r} \langle S_\alpha \rangle_A \right) \right]$$

since $\langle S_\alpha \rangle_A$ is palindromic by definition. Suppose K is amphicheiral; then it follows that $AJ(K)(q,t) = AJ(\overline{K})(q,t)$. We compare terms at height $r = i$:

$$\begin{aligned} AJ(K)(q^{-1},t^{-1})_i &= (-1)^{n_- + i} q^{-n_+ + 2n_- - i} \left(\sum_{|\alpha|=i} \langle S_\alpha \rangle_A \right) \\ &= (-1)^{2n_+ + n_- - i} q^{2n_- - n_+ - i} \left(\sum_{|\alpha|=n-i} \langle S_\alpha \rangle_A \right) \\ &= AJ(\overline{K})(q,t)_i. \end{aligned}$$

Summing over i for $1 \leq i \leq n$ gives $AJ(K)(q^{-1},t^{-1}) = AJ(\overline{K})(q,t) = AJ(K)(q,t)$ as required. □

Remark. Interestingly, we do not need the whole of $AJ(K)$ in order to rule out the amphicheirality of an annular knot. If we write $AJ(K)$ as the sum of the $\mathcal{P}_t(q)$ polynomials (recall (3.10)), then if $\mathcal{P}_0(q)$ is not palindromic $AJ(K)$ cannot be palindromic.

3.3.3 The annular Jones polynomial of an annular Sakuma knot

We now look to apply the annular Jones polynomial to the annular Sakuma knots we defined in the previous chapter. The fact that for every strongly invertible knot (K,h) there exists a unique pair of annular Sakuma knots means that the annular Jones polynomial can be considered as an invariant of strongly invertible knots.

Definition 3.3.17. Let (K,h) be a strongly invertible knot with Sakuma link $\mathbb{L} = \mathcal{B} \cup \mathcal{L}$. Define the pair of annular Jones polynomials associated to (K,h) by $AJ_{(K,h)}(\mathcal{B})$ and $AJ_{(K,h)}(\mathcal{L})$.

We can likewise define a pair of annular Jones polynomials for every framing. We note that, as for the Jones polynomial of the Sakuma link, one advantage of the annular Jones polynomial over the η-polynomial is that we can define the annular Jones polynomial for all framed strongly invertible knots, not just those with even framings.

Definition 3.3.18. Let (K, h, n) be a framed strongly invertible knot with framed Sakuma link $\mathbb{L}_n = \mathcal{B} \cup \mathcal{L}$. Define the pair of annular Jones polynomials associated to (K, h, n) by $AJ_{(K,h,n)}(\mathcal{B})$ and $AJ_{(K,h,n)}(\mathcal{L})$.

We next will consider some consequences of the results in the previous section when brought to bear on annular Sakuma knots.

Firstly, we return to Theorem 3.3.14. This tells us not only that the Jones polynomial of a framed Sakuma link $\mathbb{L}_n$ and the annular Jones polynomial of its annular Sakuma knots are closely connected, but that the two annular Jones polynomials are related too. For a framed Sakuma link $\mathbb{L}_n = \mathcal{B} \cup \mathcal{L}$ we obtain:

$$X(q)AJ(\mathcal{L})(q,t)\Big|_{\langle z_0 \rangle_A = (-q)^{\omega_{\mathcal{L}}}(q+q^{-1}),\ldots} = X'(q)AJ(\mathcal{B})(q,t)\Big|_{\langle z_0 \rangle_A = (-q)^{\omega_{\mathcal{B}}}(q+q^{-1}),\ldots} \tag{3.18}$$

In some situations we have an even stronger result; the following should be thought of as the annular Jones version of Corollary 3.1.21.

Proposition 3.3.19. *Let $\mathbb{L}_n = \mathcal{B} \cup \mathcal{L}$ be a framed Sakuma link associated to one of the following:*

1. *A framed strongly invertible unknot $(\mathcal{U}, h_0, n)$.*
2. *A framed strongly invertible double $(D(K'), h, n)$, for some prime knot K'.*
3. *A framed equivariant product of strongly invertible doubles, $(\{\#_{i=1}^{s} D(K_i')\}, h, n)$, for prime knots K_i'.*

Then $AJ(\mathcal{L})(q,t) = AJ(B)(q,t)$.

Next we mention the wrapping numbers of the pair of annular Sakuma knots. As we saw before, the wrapping number of an annular link determines the powers of t which appear in its annular Jones polynomial. For annular Sakuma knots we have:

Corollary 3.3.20. *Let $\mathbb{L}_n = \mathcal{B} \cup \mathcal{L}$ be a framed Sakuma link not equivalent to the two-component unlink, and denote by $\omega_{\mathcal{B}}$ and $\omega_{\mathcal{L}}$ the respective wrapping numbers of $\mathcal{B}$ and $\mathcal{L}$.*

1. *$\omega_{\mathcal{L}}$ is even; hence $AJ(\mathcal{L})$ only contains even powers of t.*
2. *$\omega_{\mathcal{B}} = 2$; hence $AJ(\mathcal{B})$ only contains powers of t equal to $0, \pm 2$.*

Proof. Consider the standard projection diagram $D_{\mathbb{L}_n}$. The number of times $\mathcal{L}$ wraps around $\mathcal{B}$ corresponds to the number of times $\mathcal{L} \subset A \times I$ intersects the meridional disc when we form the annular Sakuma knot. This will always be an even number — a coil provides two intersection points, and the clasps provide one each. Therefore, the wrapping number $\omega_{\mathcal{L}}$ must be even and Lemma 3.3.9 then tells us that only even powers of t can be contained in $AJ(\mathcal{L})$.

For the second part, we note that when $\mathbb{L}_n$ is drawn with $\mathcal{L}$ as the axis, $\mathcal{B}$ only forms clasps with $\mathcal{L}$ and no coils. Furthermore, we cannot remove the clasps in any way, so the minimum

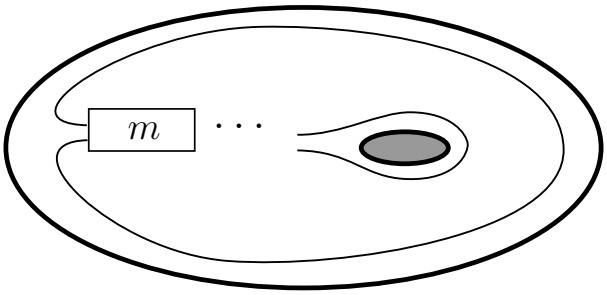

Figure 3.9: Diagram for L_m

intersection number of all possible representatives for $\mathcal{B} \subset A \times I$ with the meridional disc is 2, and so $\omega_{\mathcal{B}} = 2$. Applying Lemma 3.3.9 gives us the result. □

An interesting question, which we leave open, is the following:

Question. Suppose L is an annular Sakuma knot and $AJ_{(K,h)}(L) = q+q^{-1}$. Is $(K,h) \cong (\mathcal{U}, h_0)$?

The answer to the above is yes if for an annular knot K with wrapping number ω, $\mathcal{P}_\omega(q)$ is always non-zero. We note that there is some evidence towards this being the case; every calculation of the annular Jones polynomial obtained by the author to date satisfies the condition.

Given a strongly invertible knot (K,h) we have seen how an infinite family of annular knots can be obtained by changing the framing of the longitude in Sakuma's construction. We next will explain how the annular Jones polynomials of this family are related.

Consider (K,h,n) and fix a family of diagrams for a family of annular Sakuma knots which vary only by the number of twists in a *twist box* (c.f. Figure 3.9). Let D_{L_m} denote a diagram for an annular Sakuma knot L_m which has m twists in its twist box (note that we index L_m by the number of twists in its fixed diagram D_{L_m}). To avoid overly complicating matters we will not explicitly mention the framing required to obtain L_m, but this can be calculated easily enough if desired using Lemma 2.1.2. Our goal is the proof of the following result, which relates the annular Jones polynomial of L_m to that of L_0.

Proposition 3.3.21. *Fix a family of diagrams for a family of annular Sakuma knots as in Figure 3.9 and suppose there are n_+ positive crossings and n_- negative crossings in D_{L_m}, and $\overline{n}_+$, $\overline{n}_-$ in D_{L_0}. Set $c = \overline{n}_- - n_-$. Then:*

When $m > 0$,

$$AJ(L_m)(q,t) = (-1)^{m-c} q^{2m+3c} AJ(L_0)(q,t) + q\left(qt + (qt)^{-1}\right)^2 \sum_{i=0}^{m-1} (-1)^i q^{2i}$$

When $m < 0$

$$AJ(L_m)(q,t) = (-1)^{-c} q^{-m+3c} AJ(L_0)(q,t) + q^{-1}\left(qt + (qt)^{-1}\right)^2 \sum_{i=0}^{-m-1} (-1)^i q^{-2i}$$

Proof. The proof will rely on repeated use of the Kauffman bracket skein relation axiom (3.8) on D_{L_m}.

Firstly, suppose $m > 0$. Then $\times$ is smoothed, and we obtain 1-smoothing $\langle \asymp \rangle_A$, which is precisely $\langle D_{L_{m-1}} \rangle_A$, and 0-smoothing $\langle \rangle \langle \rangle_A$, which is the bracket for a two-component annular link (equivalent to the two-component annular unlink with both components non-trivial), which we will denote by $D_{\widehat{L}_{m-1}}$. Repeated application of (3.8) leaves us with the following:

$$\begin{aligned}
\langle D_{L_m} \rangle_A &= \left\langle D_{\widehat{L}_{m-1}} \right\rangle_A - q \left\langle D_{L_{m-1}} \right\rangle_A \\
&= (-q)^0 \left\langle D_{\widehat{L}_{m-1}} \right\rangle_A + (-q)^1 \left\langle D_{\widehat{L}_{m-2}} \right\rangle_A + (-q)^2 \left\langle D_{L_{m-2}} \right\rangle_A \\
&\quad \vdots \\
&= (-q)^m \langle D_{L_0} \rangle_A + \sum_{i=0}^{m-1} (-q)^i \left\langle D_{\widehat{L}_{m-1-i}} \right\rangle_A
\end{aligned}$$

At this point the job is not quite done, as we also need to scale the annular Kauffman bracket in order to obtain the annular Jones polynomial, namely

$$AJ(L_m)(q,t) = (-1)^{n_-} q^{n_+ - 2n_-} \langle D_{L_m} \rangle_A$$

where n_- and n_+ are the number of positive and negative crossings in D_{L_m}. We multiply everything by $(-1)^{n_-} q^{n_+ - 2n_-}$, and convert the Kauffman brackets of D_{L_0} and $D_{L_{m-1-i}}$ to their respective annular Jones polynomials. This will leave behind some residue powers of $(-q)$, which we now calculate.

Firstly,

$$\begin{aligned}
(-1)^{n_-} q^{n_+ - 2n_-} \langle D_{L_0} \rangle_A &= (-1)^{-c} q^{m+3c} (-1)^{\overline{n}_-} q^{\overline{n}_+ - 2\overline{n}_-} \langle D_{L_0} \rangle_A \\
&\quad (-1)^{-c} q^{m+3c} AJ(L_0)
\end{aligned}$$

Also,

$$\begin{aligned}
(-1)^{n_-} q^{n_+ - 2n_-} \left\langle D_{\widehat{L}_{m-1-i}} \right\rangle_A &= q^{i+1} (-1)^{n_-} q^{n_+ - 1 - i - 2n_-} \left\langle D_{\widehat{L}_{m-1-i}} \right\rangle_A \\
&= q^{i+1} AJ(\widehat{L}_{m-1-i}) \\
&= q^{i+1} \left(qt + (qt)^{-1} \right)^2
\end{aligned}$$

Combining everything gives,

$$\begin{aligned}
AJ(L_m)(q,t) &= (-1)^{m-c} q^{2m+3c} AJ(L_0) + \sum_{i=0}^{m-1} (-q)^i q^{i+1} \left(qt + (qt)^{-1} \right)^2 \\
&= (-1)^{m-c} q^{2m+3c} AJ(L_0) + q \left(qt + (qt)^{-1} \right)^2 \sum_{i=0}^{m-1} (-1)^i q^{2i}
\end{aligned}$$

When $m < 0$ the only things that changes are that $\langle D_{\widehat{L}_{m+1}} \rangle_A$ is now the 1-smoothing, and $\langle D_{L_{m+1}} \rangle_A$ is now the 0-smoothing, which alters the powers of $(-q)$. Otherwise, the argument

proceeds as above to get the claimed result. □

Remark. The above result is particularly useful when running Mathematica calculations, since we can calculate for the annular Sakuma knot with zero twists, then use the proposition to scale the answer as necessary. For strongly invertible knot diagrams where the writhe is large and 0-framed longitudes are desired, considerable time savings can be made using this two-step technique.

Next we prove a version of [79, Proposition 3.4] for the annular Jones polynomial.

Corollary 3.3.22. *Let (K, h, n) be a framed strongly invertible knot and suppose K is hyperbolic and amphicheiral.*

1. *Suppose that K does not have a free or cyclic period of period 2. Let h be the unique inverting involution and $\mathbb{L}_n = \mathcal{B} \cup \mathcal{L}$ be the framed Sakuma link of (K, h, n). Then we have $(K, h, n) \cong (\overline{K, h, n})$, and so*

$$AJ_{(K,h,n)}(\mathcal{L})(q,t) = AJ_{(\overline{K,h,n})}(\mathcal{L})(q,t)$$

and

$$AJ_{(K,h,n)}(\mathcal{B})(q,t) = AJ_{(\overline{K,h,n})}(\mathcal{B})(q,t)$$

for all n. In particular, for $n = 0$

$$AJ_{(K,h)}(\mathcal{L})(q,t) = AJ_{(\overline{K,h})}(\mathcal{L})(q,t) = AJ_{(K,h)}(\mathcal{L})(q^{-1},t^{-1})$$

and

$$AJ_{(K,h)}(\mathcal{B})(q,t) = AJ_{(\overline{K,h})}(\mathcal{B})(q,t) = AJ_{(K,h)}(\mathcal{B})(q^{-1},t^{-1}).$$

2. *Suppose K does have a free or cyclic period of period 2. Let h_1 and h_2 be its two inequivalent inverting involutions, and $\mathbb{L}_{n,i} = \mathcal{B}_i \cup \mathcal{L}_i$ be the framed Sakuma link of (K, h_i, n). Then $(K, h_1, n) \cong (\overline{K, h_2, n})$, and so*

$$AJ_{(K,h_1,n)}(\mathcal{L}_1)(q,t) = AJ_{(\overline{K,h_2,n})}(\mathcal{L}_2)(q,t)$$

and

$$AJ_{(K,h_1,n)}(\mathcal{B}_1)(q,t) = AJ_{(\overline{K,h_2,n})}(\mathcal{B}_2)(q,t)$$

for all n. In particular, for $n = 0$

$$AJ_{(K,h_1)}(\mathcal{L}_1)(q,t) = AJ_{(\overline{K,h_2})}(\mathcal{L}_2)(q,t) = AJ_{(K,h_2)}(\mathcal{L}_2)(q^{-1},t^{-1})$$

and

$$AJ_{(K,h_1)}(\mathcal{B}_1)(q,t) = AJ_{(\overline{K,h_2})}(\mathcal{B}_2)(q,t) = AJ_{(K,h_2)}(\mathcal{B}_2)(q^{-1},t^{-1})$$

Proof. This follows as a consequence of Sakuma's original result, Corollary 2.1.14 and Proposition 3.3.16. □

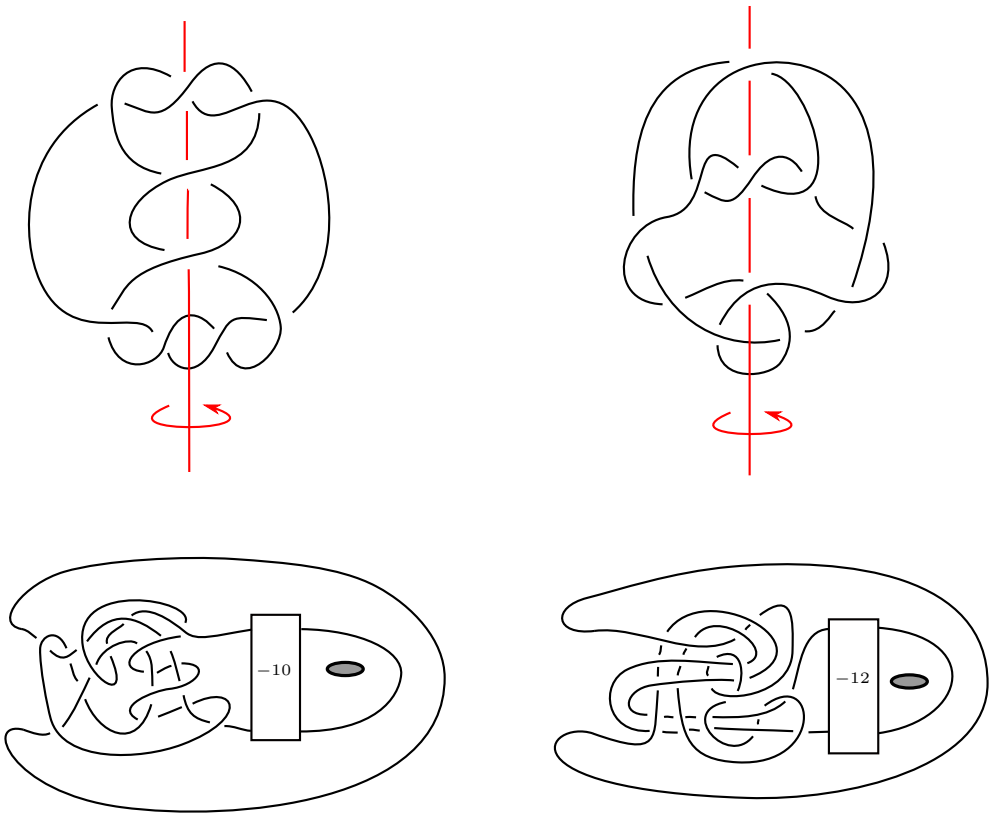

Figure 3.10: $(9_9, h_1)$ (left), $(9_9, h_2)$ (right) and one of their respective annular Sakuma knots

We will end with some examples and computations. The following examples were chosen due to their appearance in [92], where Watson's $\varkappa$ invariant is shown to exhibit certain advantages over the η-polynomial. All accompanying figures were taken from [92], and all calculations were computed using a Mathematica program written by the author.

Example 3.3.23. Consider the two strongly invertible knots $(9_9, h_1)$ and $(9_9, h_2)$. These have been shown to have the same η-polynomial [79]. We calculate the annular Jones polynomials $AJ_{(9_9,h_1)}(\mathcal{B})$ and $AJ_{(9_9,h_2)}(\mathcal{B})$ and record their respective $\mathcal{P}_0(q)$ polynomials:

$$\begin{aligned}(9_9, h_1): \quad & -q^{-29} + 3q^{-27} - 5q^{-25} + 5q^{-23} - 2q^{-21} - 3q^{-19} + 6q^{-17} - 5q^{-15} - 4q^{-11} - 6q^{-9} \\ & +4q^{-7} - q^{-5} - q^{-3} + 2q^{-1} \\ (9_9, h_2): \quad & -q^{-33} + 2q^{-31} - 2q^{-29} - 2q^{-27} + 8q^{-25} - 11q^{-23} + 4q^{-21} + 10q^{-19} - 22q^{-17} \\ & +22q^{-15} - 11q^{-13} - 3q^{-11} + 11q^{-9} - 10q^{-7} + 6q^{-5} - 3q^{-3} + 2q^{-1}\end{aligned}$$

These distinguish the two strongly invertible knots, and therefore the full annular Jones polynomials must do as well.

Next, we compare our invariants' sensitivity to cheirality.

Example 3.3.24. 8_{20} admits a single strong inversion, which is depicted in Figure 3.11. The η-polynomial of $(8_{20}, h)$ is 0 [79], and so cannot say anything about the cheirality of 8_{20}. A direct

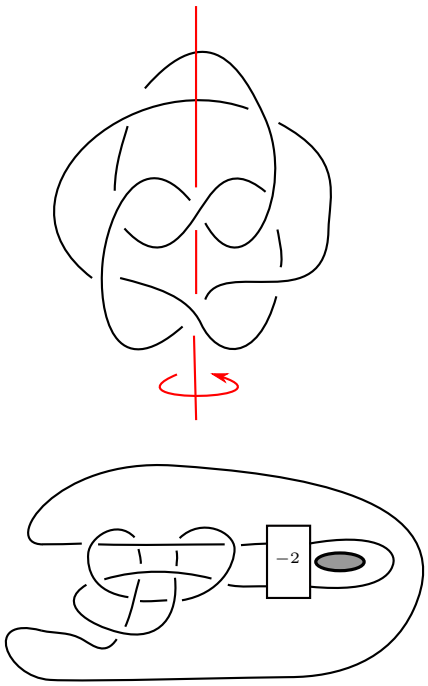

Figure 3.11: $(8_{20}, h)$ and one of its annular Sakuma knots

calculation for $AJ_{(8_{20},h)}(\mathcal{B})$ returns

$$AJ_{(8_{20},h)}(\mathcal{B})(q,t) = \left\{ \begin{array}{l} \mathcal{P}_{-2}(q) : -q^{-15} + 2q^{-13} - 2q^{-11} + q^{-9} + q^{-7} - 3q^{-5} + 3q^{-3} - q^{-1} \\ \mathcal{P}_{0}(q) : q^{-15} - 2q^{-13} + 3q^{-11} - 3q^{-9} + q^{-7} + 2q^{-5} - 4q^{-3} + 5q^{-1} - 2q + q^{3} \\ \mathcal{P}_{2}(q) : -q^{-11} + 2q^{-9} - 2q^{-7} + q^{-5} + q^{-3} - 3q^{-1} + 3q - q^{3} \end{array} \right\}$$

which is clearly not palindromic. Corollary 3.3.22 then says that 8_{20} cannot be amphicheiral.

The three knots $(10_{48},\ 10_{71},\ 10_{104})$ appearing in the next example are of particular interest since, as Watson remarks [92], they are cheiral knots for which the cheirality cannot be detected by either the Jones polynomial, the signature, or even Khovanov homology. Furthermore, the Khovanov homology of 10_{71} and 10_{104} is the same. Watson proves [92, Proposition 25] that each of them admit a single strong inversion — we apply the annular Jones polynomial to each of $(10_{48}, h)$, $(10_{71}, h)$, and $(10_{104}, h)$.

Example 3.3.25. Consider $(10_{48}, h)$. This time, we calculate $AJ_{(10_{48},h)}(\mathcal{B})$ and just state $\mathcal{P}_0(q)$:

$$\mathcal{P}_0(q) = q^{-19} - 4q^{-17} + 8q^{-15} - 10q^{-13} + 7q^{-11} + 2q^{-9} - 11q^{-7} + 16q^{-5} - 13q^{-3} + 6q^{-1} - 4q^{3} + 3q^{5} - q^{7}.$$

This is not palindromic, and so Corollary 3.3.22 says 10_{48} cannot be amphicheiral.

Example 3.3.26. Now consider $(10_{71}, h)$. Once more, we calculate $AJ_{(10_{71},h)}(\mathcal{B})$ and state $\mathcal{P}_0(q)$:

$$\mathcal{P}_0(q) = -q^{-25} + 2q^{-23} - 3q^{-21} + 2q^{-19} + q^{-17} - 4q^{-15} + 6q^{-13} - 4q^{-11} + 2q^{-9} + q^{-7} - q^{-5} + q^{-1}.$$

Hence, 10_{71} is not amphicheiral.

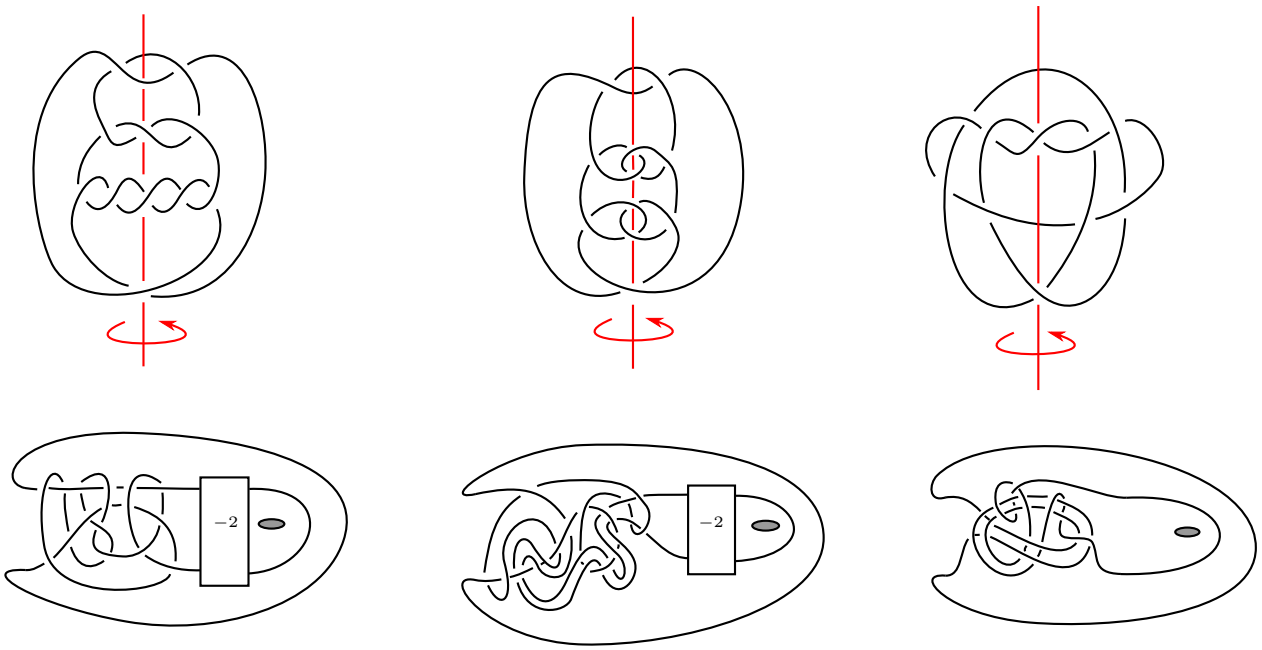

Figure 3.12: (left to right) $(10_{48}, h)$, $(10_{71}, h)$, $(10_{104}, h)$, and one of their annular Sakuma knots

Example 3.3.27. Consider $(10_{104}, h)$. Here, $\mathcal{P}_0(q)$ is:

$$\mathcal{P}_0(q) = \begin{array}{l} q^{-15} - 2q^{-13} + 2q^{-11} + q^{-9} - 4q^{-7} + 5q^{-5} - 7q^{-1} + 12q - 7q^3 - 3q^5 \\ +10q^7 - 10q^9 + 4q^{11} + 2q^{13} - 4q^{15} + 3q^{17} - q^{19} \end{array}$$

Hence, as before, 10_{104} is not amphicheiral.

We note additionally,

Theorem 3.3.28. *Consider the strongly invertible knots* $(10_{71}, h)$ *and* $(10_{104}, h)$. *We have on the one hand* $AJ_{(10_{71},h)}(\mathcal{B}) \neq AJ_{(10_{104},h)}(\mathcal{B})$, *whilst on the other* $Kh(10_{71}) \cong Kh(10_{104})$.

The above theorem is surprising as we have uncovered an instance where a polynomial invariant tells us something a categorified invariant cannot.

3.4 Comparing η and AJ

In this section we prove a result comparing the η and annular Jones polynomials of an infinite family of torus knots. The motivation behind our choice of these knots came from observing that in the tables of η-polynomials Sakuma includes in the appendix of [79] the entries for the trefoil (a.k.a $T(-3,2)$) and the cinquefoil (a.k.a $T(-5,2)$) are the same. This could perhaps be written off as a coincidence, but for the fact that the η-polynomials of $T(-7,2)$ and $T(-9,2)$ are also the same. We will first prove a result showing that this behaviour holds for consecutive pairs of torus knots $T(-m,2)$ and $T(-m-2,2)$ ($m \geq 3$ and odd), then will show, interestingly, that the annular Jones polynomial distinguishes all the members of the family.

Recall [79, Proposition 3.1] that torus knots have a unique strong inversion. Moreover, all torus

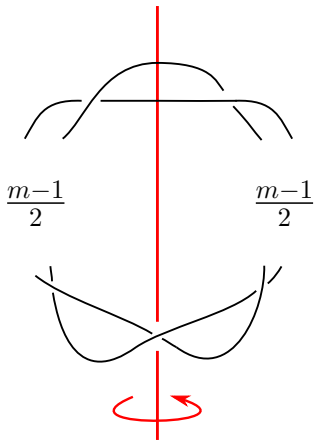

Figure 3.13: A diagram of $T(-m,2)$ with its single strong inversion

knots are cheiral, so a strongly invertible torus knot $(T(p,q),h)$ is never equivalent to its strongly invertible mirror $(\overline{T(p,q),h}) \cong (T(-p,q),h)$. The results for the annular Jones and η polynomials for the mirrors can be obtained easily, however, by substituting t for t^{-1} and q for q^{-1} in the first case, and multiplying by -1 in the second.

Let us first calculate the η-polynomials of this family. To do this we will utilise Sakuma's shortcut on the diagram of $(T(-m,2),h)$ in Figure 3.13, the process of which we saw earlier. Consider Figure 3.14: there are two separate cases we need to calculate — when $\frac{m-2}{2}$ is odd and when it is even. Here $\frac{m-2}{2}$ simply stands for the number of twists, recording nothing about their sign.

Let us first suppose $\frac{m-2}{2}$ is odd. We calculate the values of d_p and ϵ_p for all the crossing points p in the pseudo-fundamental domain, which are as follows:

	d_p	ϵ_p
p_1	1	$-$
p_2	-1	$-$
$\vdots$	$\vdots$	$\vdots$
$p_{\frac{m-1}{2}}$	1	$-$
$p_{\frac{m-1}{2}+1}$	-1	$-$

Then,

$$\tilde{\eta} = \underbrace{x_1 - x_{-1} - \ldots - x_1}_{\frac{m-1}{2}} - x_{-1}$$

and

$$\eta'(t) = \underbrace{-(1-2t+t^2) - (t^{-2}-2t^{-1}+1) - \ldots - (1-2t+t^2)}_{\frac{m-1}{2}} - (t^{-2}-2t^{-1}+1).$$

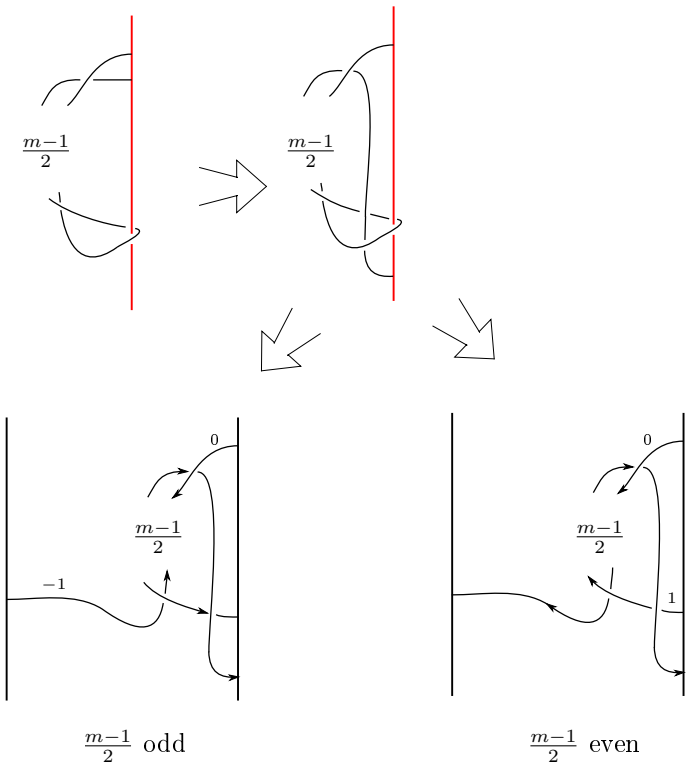

Figure 3.14: Using Sakuma's η shortcut on $(T(-m,2),h)$

Now set $2x = \frac{m-1}{2} + 1$. In Sakuma's notation, $\eta'(t)$ is then

$$\eta'(t) = [-2x, 2x, -x$$

which means

$$\eta(t) = [2x, 0, -x.$$

Now suppose $\frac{m-2}{2}$ is even.

	d_p	ϵ_p
p_1	-1	$-$
p_2	1	$-$
$\vdots$	$\vdots$	$\vdots$
$p_{\frac{m-1}{2}}$	1	$-$
$p_{\frac{m-1}{2}+1}$	0	$+$

Then,

$$\tilde{\eta} = \underbrace{x_{-1} - x_1 \ldots - x_1}_{\frac{m-1}{2}} + x_0$$

and

$$\eta'(t) = \underbrace{-(t^{-2} - 2t^{-1} + 1) - (1 - 2t + t^2) - \ldots - (1 - 2t + t^2)}_{\frac{m-1}{2}} + (t^{-1} - 2 + t).$$

Now set $2z = \frac{m-1}{2}$.

$$\eta'(t) = [-(2z+2), 2z+1, -z$$

So,

$$\eta(t) = [2z, 0, -z$$

The above calculations lead to the following.

Proposition 3.4.1. *$\eta_{(T(-m,2),h)}(t) = \eta_{(T(-m-2,2),h)}(t)$ for $m = 4k-1$, $(k \geq 1)$.*

Proof. If $m = 4k-1$ for some positive integer k, then $\frac{m-1}{2} = \frac{4k-2}{2} = 2k-1$ is odd. Then $2x = 2k$, and

$$\eta_{(T(-m,2),h)}(t) = [2k, 0, -k$$

Now we substitute $m+2$ for m in the even case. We have $2z = \frac{(m+2)-1}{2}$ and $m+2 = 4k+1$, so $\frac{m+1}{2} = 2k$. Then, $2z = 2k$ and

$$\eta_{(T(-m-2,2),h)}(t) = [2k, 0, -k$$

as required. □

The above result tells us that there are infinitely many pairs of torus knots which are not distinguished by the η-polynomial. Additionally, since $\eta_{\overline{(T(-m,2),h)}}(t) = -\eta_{(T(m,2),h)}(t)$ we also have the following.

Corollary 3.4.2. *$\eta_{(T(m,2),h)}(t) = \eta_{(T(m+2,2),h)}(t)$ for $m = 4k-1$, $(k \geq 1)$.*

Now let us calculate the annular Jones polynomials of our family of strongly invertible torus knots. If we apply the construction and consider the 'longitude' annular Sakuma knot, that is $\mathcal{L} \subset A \times I$, we obtain the family of annular knots with diagrams as depicted in Figure 3.15, which we will refer to by $\mathcal{L}_{T(-m,2)}$.

Consider $D_{\mathcal{L}_{T(-m,2)}}$. The crossings are grouped into three different sets:

- A set of $m+1$ twist box crossings.
- A set $2m-2$ crossings grouped into $\frac{m-1}{2}$ 'hash-tags'.
- A final set of four crossings, which also form a hash-tag.

Also included in the diagram is a ray λ drawn in red and the four arcs λ meets labelled as a, b, c, d. We see that λ meets only these four arcs an odd number of times, so the only powers of t that can appear in $AJ(\mathcal{L}_{T(-m,2)})(q,t)$ are those for $-4 \leq j \leq 4$ (this follows from the same argument used in Lemma 3.3.8). In addition, the maximum number of non-trivial circles that any Kauffman state of $D_{\mathcal{L}_{T(-m,2)}}$ can have is four.

Lemma 3.4.3. *Consider the annular knot diagram for $\mathcal{L}_{T(-m,2)}$ as shown in Figure 3.15, and suppose $\alpha \in \{0,1\}^{3m+3}$ is some tuple that produces exactly four non-trivial circles in the related*

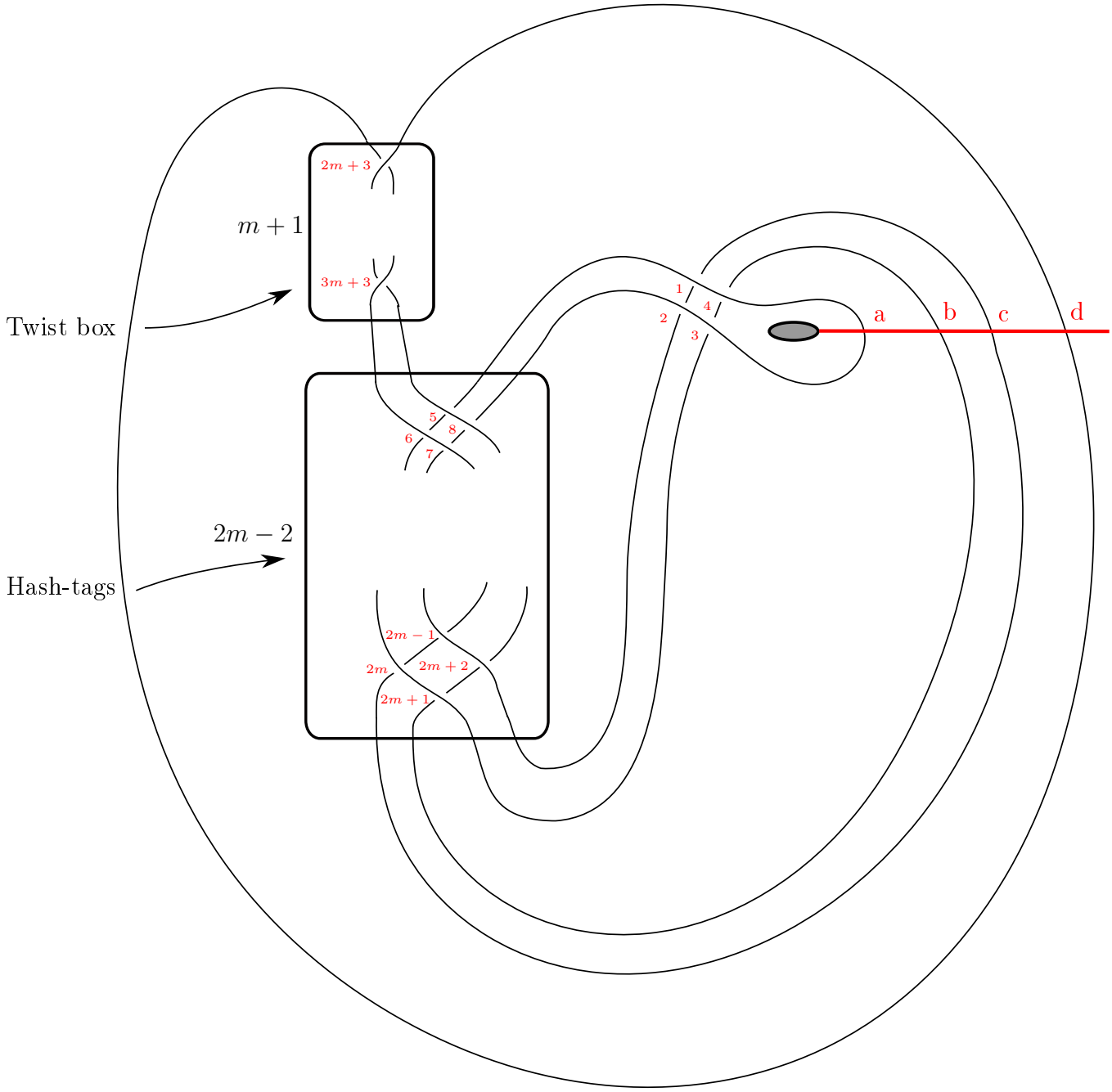

Figure 3.15: An annular Sakuma knot diagram for $(T(-m,2),h)$

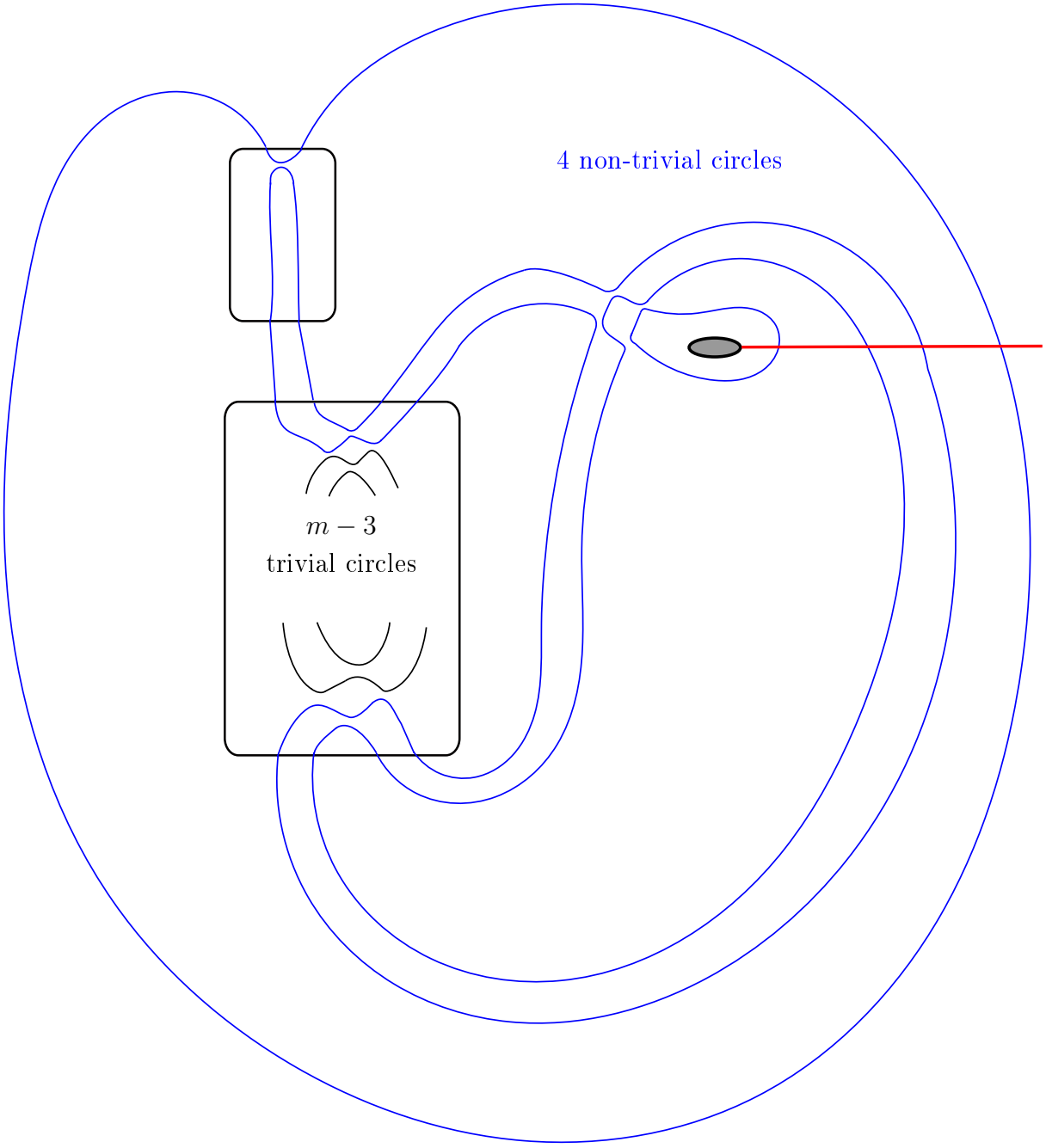

Figure 3.16: A Kauffman state for $D_{\mathcal{L}_{T(-m,2)}}$

Kauffman state S_α. Then the arcs labelled a, b, c, d in Figure 3.15 must all feature in distinct non-trivial circles in S_α.

Proof. Suppose for a contradiction that two of a, b, c, d feature in the same circle in S_α. Then λ intersects this circle an even number of times, which means the circle must be trivial. But then the number of non-trivial circles must be less than 4, which is a contradiction.

Now suppose any three of a, b, c, d are in the same circle. Then this circle is non-trivial, and in addition the circle containing the remaining arc is also non-trivial. But now no more non-trivial circles can exist, which is again a contradiction. Hence, each of the labelled arcs must be contained in a separate non-trivial circle. □

Now we come to the main calculation. We will prove that the annular Jones polynomial is sufficient to distinguish every member of the family of $\mathcal{L}_{T(-m,2)}$, and so every strongly invertible knot $(T(-m,2),h)$. The strategy we will follow will be to show that for $m \geq 3$ there is always a term in $AJ(\mathcal{L}_{T(-m-2,2)})(q,t)$ that is not in $AJ(\mathcal{L}_{T(-m,2)})(q,t)$. More precisely, we will show that the term containing the smallest power of q in the $\mathcal{P}_{-4}(q)$ polynomial is not in $AJ(\mathcal{L}_{T(-m,2)})(q,t)$.

Proposition 3.4.4. *Let $m \geq 3$ be an odd integer. Then the term containing the smallest power of q appearing in $\mathcal{P}_{-4}(q)$ for $AJ(\mathcal{L}_{T(-m,2)})(q,t)$ is $-q^{-4m-1}$.*

Proof. As before, we fix a diagram for $\mathcal{L}_{T(-m,2)}$ as shown in Figure 3.15, number its crossings as shown and fix an orientation. We will first exhibit a family of Kauffman states for $D_{\mathcal{L}_{T(-m,2)}}$ that all contribute towards the coefficient of the smallest power of q in $\mathcal{P}_{-4}(q)$; then will show that the sum of their contributions leaves us with a -1 coefficient.

Let $\alpha \in \{0,1\}^{3m+3}$ and S_α be the related Kauffman state. Define c_α to be the number of circles appearing in S_α, and recall that $|\alpha|$ is the 'height' of α; that is, $|\alpha| = \sum_i \alpha_i$, where α_i is the ith entry. The task now before us is to uncover all the Kauffman states S_α subject to the following conditions:

i) S_α has four non-trivial circles.

ii) The value $c_\alpha - |\alpha|$ is the maximum possible.

The first condition is required as we are considering a term in $\mathcal{P}_{-4}(q)$, and the second condition comes from the fact that when we calculate AJ we scale up by $|\alpha|$. We will proceed by starting with α equal to the all-zero smoothing ($\alpha_i = 0$ for all $0 \leq i \leq 3m+3$) then will determine which entries need to be changed to 1's in order to satisfy the two conditions. Note that the all-zero Kauffman state does not satisfy the two conditions itself, because it does not contain any non-trivial circles.

We begin by considering the first four crossings. In order to satisfy condition i) Lemma 3.4.3 tells us that a, b, c, d must be in distinct circles in S_α. Out of the 2^4 possibilities we have for smoothing these four crossings, the only ones that satisfy Lemma 3.4.3 are $\{0,0,0,0,\ldots\}$, $\{0,0,1,0,\ldots\}$, and $\{0,1,1,0,\ldots\}$. We will proceed by taking $\{0,1,1,0,\ldots\}$ as the smoothing instructions for

the first four crossings; we will eventually show that the other two possibilities give a smaller value of $c_\alpha - |\alpha|$. After performing these four smoothings we have 1 non-trivial smoothing, and $|\alpha| = 2$.

The next set of crossings we will examine are the $2m-2$ crossings that appear in the hash-tag crossing box. If we smooth all of these crossings with the 0-smoothing we obtain $m-3$ trivial circles, and get an extra non-trivial smoothing. We now have $m-1$ circles, two of which are non-trivial, and $|\alpha| = 2$.

The final set of $m+1$ crossings appear in the twist box. If we smooth them all with a 0-smoothing we do not obtain enough non-trivial circles, so at least one of the crossings must be smoothed with a 1-smoothing. We now have $m+1$ circles, four of which are non-trivial, and $|\alpha| = 3$, so $c_\alpha - |\alpha| = m-2$.

We note that the value of $c_\alpha - |\alpha|$ is less than $m-2$ if we were to change the first four entries of α to $\{0,0,0,0,\ldots\}$ or $\{0,0,1,0,\ldots\}$. In both of these cases the two non-trivial circles containing the arcs b and c must pass through the hash-tag crossing box. However, this must necessarily give a smaller number of trivial circles than we previously obtained, and, furthermore, we need additional 1-smoothings. Hence, the value of $c_{\alpha'} - |\alpha'|$ must be smaller than $c_\alpha - |\alpha|$ for the smoothing $S_{\alpha'}$ where the first four entries in α' are $\{0,0,0,0,\ldots\}$ or $\{0,0,1,0,\ldots\}$.

We now note that each additional 1 entry in the $m+1$ twist box crossings increases the number of circles by one each time, as an extra trivial circle is added. We also obtain an additional trivial circle if we set $\alpha_5 = 1$. For each of these changes the value of $c_\alpha - |\alpha|$ is unchanged, and we therefore obtain a family of smoothings given by:

$$\mathcal{S} := \{0,1,1,0,\epsilon_1,0,\ldots,0,\epsilon_2,\epsilon_3,\ldots,\epsilon_{m+2}\},$$

where $\epsilon_i \in \{0,1\}$ and at least one $\epsilon_i = 1$. This is precisely the family of smoothings we are looking for. An example of an S_α is shown in Figure 3.16. The four non-trivial circles are drawn in here in blue, and for this α all ϵ_i are zero except for ϵ_2.

The next step is to determine what the contribution to $\mathcal{P}_{-4}(q)$ is from each of the Kauffman states in $\mathcal{S}$. The power of q in each contribution is

$$-(m-2) + n_+ - 2n_- = -m + 2 + (m+1) - 2(2m+2) = -4m - 1,$$

where n_+ and n_- are the number of positive and negative crossings in the diagram of $\mathcal{L}_{T(-m,2)}$. However the coefficient for a contribution switches between 1 and -1, as we also need to scale by $(-1)^{|\alpha|}$. We will now show that the sum of the contributions from $\mathcal{S}$ is non-zero.

Now, $|\mathcal{S}| = 2^{m+2} - 1$: we have a choice of replacing each ϵ_i with a 0 or a 1 as long as at least one of the ϵ is replaced with a 1; the only choice that is not allowed is therefore the all-zero replacement. Ignoring this for a moment, out of the 2^{m+2} choices for α half of them have an even number of 1 entries and half have an odd number of 1 entries. Therefore, for half the choices of α $(-1)^{|\alpha|}$ is odd and for the other half it is even. Hence, the values of $(-1)^{|\alpha|}q^{-4m-1}$ for $\alpha \in \mathcal{S}$

cancel in pairs, but because the all-zero replacement (which has an even number of 1 entries) is not allowed we end up with a $-q^{-4m-1}$ which is left uncancelled, as required. □

Corollary 3.4.5. *$AJ(\mathcal{L}_{T(-m,2)})(q,t) \neq AJ(\mathcal{L}_{T(-m-2,2)})(q,t)$ for all $m \geq 3$. Hence, the annular Jones polynomial distinguishes every member of the family of torus knots $T(-m,2)$, $m \geq 3$.*

Recall that the annular knot $\mathcal{L}_{T(-m,2)}$ has as its mirror the annular knot $\overline{\mathcal{L}_{T(-m,2)}} \cong \mathcal{L}_{T(m,2)}$, and

$$AJ(\mathcal{L}_{T(-m,2)})(q^{-1},t^{-1}) = AJ(\overline{\mathcal{L}_{T(-m,2)}})(q,t) = AJ(\mathcal{L}_{T(m,2)})(q,t).$$

The next result follows immediately from this and the above Corollary.

Corollary 3.4.6. *$AJ(\mathcal{L}_{T(m,2)})(q,t) \neq AJ(\mathcal{L}_{T(m+2,2)})(q,t)$ for all $m \geq 3$. Hence, the annular Jones polynomial distinguishes every member of the family of torus knots $T(m,2)$, $m \geq 3$.*

3.5 The intrinsic symmetry group of a Sakuma link

We will end this chapter with a different application of the invariants we have seen so far. Namely, we will use the η, Jones, and annular Jones polynomials to study the symmetry properties of framed Sakuma links via their intrinsic symmetry groups. Recall that for a two-component link L its intrinsic symmetry group $Sym^*(L)$ is a subgroup of the following finite group:

$$\Gamma(L) = \mathbb{Z}/2\mathbb{Z} \times ((\mathbb{Z}/2\mathbb{Z} \times \mathbb{Z}/2\mathbb{Z}) \rtimes S_2),$$

where S_2 is the 2 element permutation group. This is a non-abelian group which is isomorphic to $\mathbb{Z}/2\mathbb{Z} \times D_4$, and has 16 elements.

For two-component links, Berglund et al. [11] have developed a general strategy for determining the intrinsic symmetry group. On the one hand, they exhibit some symmetries via explicit isotopies to bound the order of $Sym^*(L)$ from below. In the majority of cases these symmetries are elements that invert one or both components, that is, are elements of the form $(\epsilon_0, \epsilon_1, \epsilon_2, p)$ with one or both of ϵ_1 and ϵ_2 equal to -1. In addition to this, they also seek to rule out the existence of other elements of $\Gamma(L)$ in the intrinsic symmetry group, which allows them to bound the order of $Sym^*(L)$ from above. The methods they employed for this task tend to follow the same general template: first picking some link invariant, then using it to show that $L^\gamma \ncong L$ for some $\gamma \in \Gamma(L)$. Invariants they favoured ranged in complexity; from numerical invariants such as the linking number and the self-writhe (for alternating links), through to polynomial invariants like the Jones polynomial.

When looking to calculate the intrinsic symmetry group of a framed Sakuma link $\mathbb{L}_n$ we can start by exploiting their geometric properties. Firstly, the element $(1,1,1,(12))$ (the pure exchange symmetry) can be ruled out of the vast majority of intrinsic symmetry groups. The following is an immediate consequence of Proposition 2.1.12.

Corollary 3.5.1. *Let $\mathbb{L}_n$ be a framed Sakuma link. Then $\mathbb{L}_n$ has pure exchange symmetry if and only if $\mathbb{L}_n$ is associated to a framed unknot, a framed strongly invertible double, or to a framed*

equivariant product of strongly invertible doubles.

We note that the presence of a pure exchange symmetry for even framed Sakuma links can be ruled out using the η-polynomial and for all framings using the annular Jones polynomial. Recall Corollary 3.1.21: it is clear that if $\mathbb{L}_n$ has pure exchange $\eta(\mathbb{L}_{2n}, 1, 2; t)$ must equal $\eta(\mathbb{L}_{2n}, 2, 1; t)$, and so if they are not equal no pure exchange symmetry can be present. This logic can be applied just as well to the annular Jones polynomial — if $AJ_{(K,h,n)}(\mathcal{L}) \neq AJ_{(K,h,n)}(\mathcal{B})$ then $\mathbb{L}_n$ has no pure exchange symmetry.

We now will describe the intrinsic symmetry group of all framed Sakuma links constructed from different framings on the strongly invertible unknot. The following lemmas are due to Berglund's team [11].

Lemma 3.5.2 (Berglund, Cantarella, ..., 2012)**.** *Let L be a two-component link in S^3, and $Sym^*(L)$ be its intrinsic symmetry group.*

1. *If the linking number of L is non-zero, then $Sym^*(L) < \Sigma_{8,2}$.*
2. *For L alternating, if the self-writhe is non-zero then $Sym^*(L) < \Sigma_{8,1}$.*
3. *For L alternating, if the linking number and self-writhe are non-zero then $Sym^*(L) < \Sigma_{4,1}$.*

The group $\Sigma_{8,2}$ is defined to be all elements of $\Gamma(L)$ of the form $\{(\epsilon_0, \epsilon_1, \epsilon_2, p) : \epsilon_0\epsilon_1\epsilon_2 = 1\}$; Berglund et al. refer to it as 'even operations and pure exchange'. The group $\Sigma_{8,1}$ is given by elements of the form $\{(1, \epsilon_1, \epsilon_2, p)\}$, and $\Sigma_{4,1}$ can be described by $\{(1, \epsilon_1, \epsilon_2, p) : \epsilon_1 = \epsilon_2\}$.

Berglund et al. find the intrinsic symmetry groups of five framed Sakuma links, which in Rolfsen notation are: $0_1^2, 4_1^2, 5_1^2, 6_3^2, 7_3^2$ and 8_6^2. They are constructed from the strongly invertible unknot with framings $0, -1, -2, -3, -4$ and -5, respectively. We use their methods to prove the following, which is a modest extension of their results.

Proposition 3.5.3. *Let $\mathbb{L}_n$ be a framed Sakuma link obtained from $(\mathcal{U}, h, n)$, where $\mathcal{U}$ is the unknot, and $n \in \mathbb{Z}$.*

- *If $n = 0$ then $Sym^*(\mathbb{L}_n) = \Sigma(0_1^2) = \Gamma(L)$.*
- *If $n \neq 0$ is even then $Sym^*(\mathbb{L}_n) = \Sigma_{8,1}$.*
- *If n is odd then $Sym^*(\mathbb{L}_n) = \Sigma_{4,1}$.*

Proof. The case when $n = 0$ appears in [11], so let us assume $n \neq 0$ and deal with each case separately.

Suppose n is even and negative. In [11, Figure B3] it is shown that 5_1^2 and 7_3^2 (a.k.a the Sakuma links obtained from $(\mathcal{U}, h_0, -2)$ and $(\mathcal{U}, h_0, -4)$) possess a pure inversion, that is, an element in their intrinsic symmetry groups of the form $(1, -1, -1, e)$. It is clear that in general the Sakuma link associated to $(\mathcal{U}, h_0, n)$ will also have this symmetry. We combine this with the fact that all the links we are considering are purely exchangeable to get $\Sigma_{4,1} < Sym^*(\mathbb{L}_n)$. We then note

that in all cases the self-writhe of $\mathbb{L}_n$ is non-zero (recall that all Sakuma links obtained from unknots are alternating), so part (2) of Lemma 3.5.2 tells us that $Sym^*(\mathbb{L}_n) < \Sigma_{8,1}$. Next, we observe that [11, Figure B4] shows the existence of $(1,-1,1,e)$ in $\Sigma(7_3^2)$, and it is again clear that in general this element will always be in $Sym^*(\mathbb{L}_n)$. However, $(1,-1,1,e)$ is not an element of $\Sigma_{4,1}$, which means $Sym^*(\mathbb{L}_n) = \Sigma_{8,1}$. Since the pair of Sakuma links obtained from $(\mathcal{U}, h_0, n)$ and $(\mathcal{U}, h_0, -n)$ are not equivalent the result holds for n positive too.

Now suppose n is odd and negative. We again use [11, Figure B3] to note that every Sakuma link we are considering has a pure inversion — therefore $\Sigma_{4,1} < Sym^*(\mathbb{L}_n)$. Now, every link in this family has linking number non-zero, and for all links aside from $(\mathcal{U}, h_0, -1)$ the self-writhe is non-zero: we apply part (3) of Lemma 3.5.2 to get for these links $Sym^*(\mathbb{L}_n) = \Sigma_{4,1}$; we again note that the result holds for n positive too. Finally, we see that Berglund et al. have proved that for $n = \pm 1$ $Sym^*(L)$ is also $\Sigma_{4,1}$. □

We will end by briefly exploring various tactics we can use in order to put some bounds on the size of the intrinsic symmetry group of a general framed Sakuma link. Since we will not be exhibiting any explicit symmetries, we will not be able to completely determine $Sym^*(\mathbb{L}_n)$ as Bergland et al. do for their links; nonetheless, by using nothing more complicated computationally than the polynomial invariants we have encountered, many elements of $\Gamma(L)$ can be shown not to be elements of $Sym^*(\mathbb{L}_n)$.

Firstly, if the link is not one of three classes of framed Sakuma link that appear in Corollary 3.5.1 we can immediately rule out pure exchange symmetries, and indeed, all elements where $p = (12)$. As stated earlier, the η-polynomial can rule out these elements for even n if $\eta(\mathbb{L}_n, \mathcal{L}, \mathcal{B}; t) \neq \eta(\mathbb{L}_n, \mathcal{B}, \mathcal{L}; t)$, as can the annular Jones polynomial for all n if $AJ_{(K,h,n)}(\mathcal{L}) \neq AJ_{(K,h,n)}(\mathcal{B})$.

We now turn to elements in which $\epsilon_0 = -1$. The Jones polynomial is the natural invariant to choose in order to rule out these elements, however, we can also use the annular Jones polynomial. If a framed Sakuma link is amphicheiral, then its two annular Sakuma knots must also be amphicheiral; hence, if the annular Jones polynomial of an annular Sakuma knot is not palindromic, then the framed Sakuma link cannot be amphicheiral.

An even easier invariant that can be employed for this is the linking number — if a framed Sakuma has non-zero linking number it cannot be amphicheiral, so $(-1,1,1,e)$ can be ruled out for all odd framings. Conversely, when the linking number is zero we can make use of the η-polynomial. The following result is due to Jiang, Li, Wang and Wu [32, Theorem 4.2].

Theorem 3.5.4 (Jiang, Li, Wang, Wu, 2012)**.** *Suppose $L = K_1 \cup K_2$ is an oriented link in S^3 with zero linking number. If $\eta(L,1,2;t) \neq 0$ then L is absolutely cheiral. Moreover, if $\eta(L,1,2;t) \neq \eta(L,2,1;t)$ then L is set-wise cheiral.*

By 'absolutely cheiral' we mean there are no elements in $Sym^*(L)$ of the form $(-1,\epsilon_1,\epsilon_2,e)$, and 'set-wise cheiral' that we also exclude elements in which $p = (12)$.

Finally, we come to elements of Γ_2 in which $\epsilon_0 = 1$ and either one or both of ϵ_1 and ϵ_2 equal

-1. Although it is true that the Jones polynomial of a knot in S^3 is the same regardless of which orientation we choose to take, for links the story is different. Changing the orientation of a component of, for example a two-component link, changes the number of positive and negative crossings between the components. This difference is picked up by the Jones polynomial in the final scaling term, hence, we can use $J(\mathbb{L})$ to rule out $(1, -1, 1, e)$ and $(1, 1, -1, e)$. Changing both orientations means that the number of positive and negative crossings is unchanged, however, so $(1, -1, -1, e)$ cannot be ruled out by using $J(\mathbb{L})$.

Remark. Due to our ability to generate an infinite family of framed Sakuma links from each strongly invertible knot the intrinsic symmetry groups of a vast collection of two-component links can be obtained almost for free once an initial group is determined, as we showed in our proof for the framed Sakuma links constructed from the unknot.

Chapter 4

Homological invariants of strongly invertible knots

In this chapter we will continue to construct invariants of strongly invertible knots via the quotient objects obtained in Sakuma's and Watson's constructions. This time we concern ourselves with invariants taking the form of a homology theory, all of which are various derivatives of Khovanov homology. Khovanov homology was first defined by Mikhail Khovanov [40] in the late 1990s, and revolutionised the study of knots and links. The basic idea is to construct a bi-graded chain complex from the set of complete smoothings of a link diagram, the homology of which turns out to be an invariant of the link. Furthermore, by design the Euler characteristic of Khovanov homology is the Jones polynomial of the link — as a result Khovanov homology is said to *categorify* the Jones polynomial.

The main advantage of working with homological invariants over polynomial invariants is that there tends to be more structure present in the categorified world, and this can be exploited in order to exhibit additional qualities of invariants — the primary example being unknot detection [47]. In particular, we can make use of spectral sequences between Khovanov and Heegaard-Floer homology theories, the first of which was due to Ozsváth and Szabó [66]. The downside of all this extra structure, however, is that homological invariants are much harder, and more time consuming, to compute, forcing us to often work in the polynomial world.

We will look at five invariants of strongly invertible knots in the course of this chapter: Khovanov homology, annular Khovanov homology, $\varkappa$, $\varkappa_A$, and tangle Khovanov homology — $\varkappa_A$ being a conjectured new invariant, which is best viewed as an annular offshoot of Watson's $\varkappa$ [92]. Just as for the polynomial invariants we considered in the previous chapter, we will be evaluating the invariants' abilities to detect the unknot, distinguish strong inversions, and detect the cheirality of the underlying knot.

4.1 Khovanov homology

In this first section we will recall the definition of Khovanov homology, and will use it to study strongly invertible knots via Sakuma links. The go-to reference when learning about Khovanov homology for the first time is Dror Bar-Natan's excellent summary [9] of Khovanov's seminal paper.

4.1.1 Construction

The construction of Khovanov homology we will outline here is taken from Bar-Natan's paper. We start by taking a link L in the 3-sphere, make a choice of diagram D_L for it and number the crossings from 1 to n, then form the cube of smoothings of D_L in exactly the same way as we did for the Jones polynomial in the previous chapter. However, instead of attaching a polynomial term to a Kauffman state S_α (with $\alpha \in \{0,1\}^n$), we attach a vector space over a choice of base field $\mathbb{F}$.

The basic 'unit' of our vector spaces is denoted V: it is two-dimensional, and is generated by the elements v_+ and v_-. To a Kauffman state S_α with $|\alpha| = r$ and c circles we attach the vector space $V_\alpha^{\otimes c}$. We follow Rasmussen's notation [73] by defining a $\mathbb{Z}$-grading, denoted by p, on V: $p(v_+) := 1$ and $p(v_-) := -1$. The p grading is extended to $V^{\otimes c}$ in the natural way, namely:

$$p(v_1 \otimes v_2 \otimes \ldots \otimes v_k) = p(v_1) + p(v_2) + \ldots + p(v_k).$$

The edges of the cube of smoothings can be viewed as cobordisms between Kauffman states. Taking this viewpoint further, we adopt Grigsby and Wehrli's terminology [23] and call another Kauffman state $S_{\alpha'}$ an *immediate successor* of S_α if α' is obtained from α by replacing a single 0 with a 1, that is, $\alpha_i = 0$, $\alpha'_i = 1$ for some $1 \leq i \leq n$, and $\alpha_j = \alpha'_j$ for all $j \neq i$. We observe that the edge cobordisms take a Kauffman state S_α to all its possible immediate successors. The cobordisms between two Kauffman states come in two types: either two copies of S^1 merge, or a single copy splits in two. We associate to each cobordism taking S_α to $S_{\alpha'}$ a map between the vector spaces $V_\alpha^{\otimes c}$ and $V_{\alpha'}^{\otimes c'}$. We define a merge map m and a split map Δ as follows:

	$V \otimes V \longleftrightarrow V$
m	$v_+ \otimes v_+ \mapsto v_+$
	$v_+ \otimes v_- \mapsto v_-$
	$v_- \otimes v_+ \mapsto v_-$
	$v_- \otimes v_- \mapsto 0$
Δ	$v_+ \mapsto v_+ \otimes v_- + v_- \otimes v_+$
	$v_- \mapsto v_- \otimes v_-$

(4.1)

The maps associated to the two types of cobordism are then defined to be the identity on all copies of V attached to circles not participating in the cobordism, and m or Δ on those that are split or merged. If we are working over a field $\mathbb{F}$ which is not $\mathbb{Z}/2\mathbb{Z}$ then minus signs need to

be added to certain edge maps, which are necessary in order for the differential of the Khovanov chain complex to satisfy $d \circ d = 0$. More precisely, for a edge map $d_{\alpha;\alpha'}$ between two vector space $V_{\alpha}^{\otimes c}$ and $V_{\alpha'}^{\otimes c'}$ we denote by $\epsilon(\alpha;\alpha')$ the number of 1s to the left of the changed 0 in α (i.e the sum of all the α_j $(j < i)$, where α_i is the position of the changed 0 in α). If $\epsilon(\alpha;\alpha')$ is an odd number then we add a minus sign to $d_{\alpha;\alpha'}$.

From here we can define the *Khovanov bracket* of D_L. This is chain complex formed by taking the direct sum of all the vector spaces at the same height, with differentials given by the sum of all the relevant edge maps. We denote the Khovanov bracket of D_L by $[\![D_L]\!]$; this should be viewed as the analogue of the Kauffman bracket in the categorified setting. Like the Kauffman bracket (recall (3.3)), the Khovanov bracket can be described by three axioms, which are as follows:

$$[\![\emptyset]\!] = 0 \to \mathbb{F} \to 0 \tag{4.2}$$

$$[\![\bigcirc D_L]\!] = V \otimes [\![D_L]\!] \tag{4.3}$$

$$[\![\times]\!] = \mathcal{F}(0 \to [\![)(]\!] \to [\![)]\!](]\!]\{1\} \to 0) \tag{4.4}$$

The third axiom is the mapping cone on the two chain complexes $[\![)(]\!]$ and $[\![)]\!](]\!]$, which is referred to by Bar-Natan as the 'flatten' operation on double chain complexes (hence the use of $\mathcal{F}$). We will return to this axiom, and will explain precisely what we mean by a mapping cone in an upcoming section.

Elements $v \in V^{\otimes c}\{r\}$ have two gradings associated to them. The first is the *homological grading*, which is defined as $s(v) = |v| - n_-$, where $|v| = r$ is the height of v and n_- is the number of negative crossings in D_L. The homological grading determines the position of v in the Khovanov chain complex, that is, the degree of the abelian group it is contained within.

The second grading is obtained from the p grading we have already seen. From this, we define the *quantum grading* of v to be $q(v) = p(v) + |v| + n_+ - 2n_-$, where n_+ is the number of positive crossings in D_L. The crucial thing about the quantum grading, and indeed, the reason we shift the p grading in the first place, is that the maps m and Δ preserve it.

Next, the Khovanov chain complex can be obtained. We simply shift the Khovanov bracket in both degrees, which is should be thought of as the categorified analogue of obtaining $\widehat{J}(L)$ from $\langle D_L \rangle$ by multiplying by $(-1)^{n_-}q^{n_+-2n_-}$. The Khovanov chain complex $CKh(L)$ is defined by $[\![D_L]\!][n_-]\{n_+ - 2n_-\}$, where the square bracket indicates a shift in homological grading, and the curly brackets a shift in quantum grading. It turns out, remarkably, that the cohomology of this chain complex, $Kh^*(L)$ does not depend on our choice of diagram, and so is a link invariant.

Theorem 4.1.1 (Khovanov, 1999)**.** *Let L be an oriented link in S^3. The Khovanov homology of L, $Kh^*(L)$ is a link invariant.*

Another, more concise way, to express the Khovanov homology of a link is to write it in terms of its underlying abelian group (this is used, for example, by Grigsby and Wehrli in [23]). To do

this we take the direct sum of all the $V^{\otimes c}$, accounting for the grading shifts (which we omit here for simplicity):

$$CKh(L) = \left(\bigoplus_{\alpha} V_{\alpha}^{\otimes c} \right).$$

The differential ∂_{Kh} can be expressed as the sum

$$\partial_{Kh} = \sum_{\alpha;\alpha'} (-1)^{\epsilon(\alpha;\alpha')} d_{\alpha;\alpha'}$$

taken over all pairs α, α', where α' is an immediate successor of α. We then can write

$$Kh^*(L) \cong H^*\Big(CKh(L), \partial_{Kh}\Big). \tag{4.5}$$

We often express the Khovanov homology of a link in terms of its *Poincaré polynomial*.

Definition 4.1.2. Let $L \subset S^3$ be a link with Khovanov homology $Kh^*(L)$ over a field $\mathbb{F}$. The Poincaré polynomial of $Kh^*(L)$ is the following two-variable Laurent polynomial:

$$\mathcal{P}(Kh^*(L)) := \sum_{i,j} s^i q^j \dim_{\mathbb{F}}(Kh^{i,j}(L)),$$

where $Kh^{i,j}(L)$ is the graded piece of $Kh^*(L)$ with homological grading i and quantum grading j. We call s the *homological variable* and q the *quantum variable*.

The Poincaré polynomial is closely related to the Jones polynomial of the link, that is:

$$\chi_q(Kh^*(L)) := \sum_{i,j} (-1)^i q^j \dim_{\mathbb{F}}\big(Kh^{i,j}(L)\big) = \widehat{J}(L) \tag{4.6}$$

The above equation is what is meant when we say Khovanov homology 'categorifies' the Jones polynomial.

We end this background section by mentioning a natural refinement of Khovanov homology, again due to Khovanov [41], which deals with a particular sub-complex of the Khovanov chain complex $CKh(L)$. The homology of this sub-complex is referred to as *reduced* Khovanov homology $\widetilde{Kh}^*(L)$, and is set up in such a way that its Euler characteristic is the Jones polynomial — not the unnormalised version.

The chain complex for reduced Khovanov homology differs from the 'full-fat' version by the addition of a basepoint x on one of the components of D_L. We form the reduced Khovanov chain complex $\widetilde{CKh}^*(D_L)$ from the cube of smoothings for D_L exactly how we would in the standard case, except that this time we attach a 1-dimensional vector space $\langle v_+ \rangle$ to all circles which contain x. We retain the usual merge and split maps for cobordisms not involving x, and define them to be as follows for those which do involve x.

	$V \otimes V \longleftrightarrow \langle v_+ \rangle$	$\langle v_+ \rangle \otimes V \longleftrightarrow V$
m	$v_+ \otimes v_+ \mapsto v_+$ $v_+ \otimes v_- \mapsto 0$ $v_- \otimes v_+ \mapsto 0$ $v_- \otimes v_- \mapsto 0$	$v_+ \otimes v_+ \mapsto v_+$ $v_+ \otimes v_- \mapsto v_-$
Δ	$v_+ \mapsto v_+ \otimes v_- + v_- \otimes v_+$	$v_+ \mapsto v_+ \otimes v_-$ $v_- \mapsto 0$

The differential $\widetilde{\partial_{Kh}}$ is then expressed as

$$\widetilde{\partial_{Kh}} = \sum_{\alpha;\alpha'} (-1)^{\epsilon(\alpha;\alpha')} \widetilde{d_{\alpha;\alpha'}}$$

taken over all pairs α, α', where α' is an immediate successor of α, and $\widetilde{d_{\alpha;\alpha'}}$ is as in the standard case but with the new notions of the split and merge maps.

We can then define the reduced Khovanov homology as follows:

$$\widetilde{Kh}^*(L) \cong H^*\Big(\widetilde{CKh}^*(D_L)\{-1\}, \widetilde{\partial_{Kh}}\Big) \tag{4.7}$$

The shift of -1 in the quantum grading is done to ensure that the reduced Khovanov homology of the unknot is $\mathbb{F}[0,0]$.

As stated above, the 'take-home' feature of reduced Khovanov homology can be seen in its Euler characteristic:

$$\chi_q(\widetilde{Kh}^*(L)) := \sum_{i,j} (-1)^i q^j \dim_{\mathbb{F}}\big(\widetilde{Kh^{i,j}}(L)\big) = J(L) \tag{4.8}$$

That is, the reduced Khovanov homology is the categorification of the standard Jones polynomial.

If L is a knot, then its reduced Khovanov homology does not depend on the choice of basepoint. For links, however, choosing a different component on which to place the basepoint can affect it (see [41]), unless we work over $\mathbb{Z}/2\mathbb{Z}$. Shumakovitch [84] proved the following:

Theorem 4.1.3 (Shumakovitch, 2004)**.** *Let $L \subset S^3$ be an oriented link. Then*

$$Kh^*(L;\mathbb{Z}/2\mathbb{Z}) \cong \widetilde{Kh}^*(L;\mathbb{Z}/2\mathbb{Z})[0,-1] \oplus \widetilde{Kh}^*(L;\mathbb{Z}/2\mathbb{Z})[0,1].$$

In particular, $\widetilde{Kh}^*(L;\mathbb{Z}/2\mathbb{Z})$ does not depend on the choice of component for the base point.

This result highlights additional advantages of working with $\mathbb{Z}/2\mathbb{Z}$ coefficients.

4.1.2 The skein exact sequence

As promised, we now return to the third Khovanov bracket axiom (4.4). The following explanation was taken mostly from Le Gros' Masters' thesis [49, Chapter 4.5]. Given a crossing in a link diagram, we can smooth the crossing in two ways, and consider the three Khovanov brackets $[\![\times]\!]$, $[\![)(]\!]$, and $[\![)(]\!]$. As we will see, it turns out that the three are related by a short exact sequence, and we can apply a result from homological algebra to obtain a long exact sequence in their homologies. This long exact sequence is known as the *skein exact sequence*.

First we require the following, classic result, which can be found in any good textbook on homological algebra (see, for example [78, Theorem 10.42]).

Theorem 4.1.4. *Consider the short exact sequence of chain complexes:*

$$0 \to A^* \to B^* \to C^* \to 0$$

There exists natural homomorphisms $\delta^n : H^n(C) \to H^{n+1}(A)$ such that the homology groups form a long exact sequence.

We begin by constructing the short exact sequence. Suppose $L \subset S^3$ is an oriented link, and D is a choice of diagram for L with n crossings, n_+ of which are positive and n_- are negative. We consider a crossing $\times$ in D, and denote by D_0 and D_1 the diagrams of the 0 and 1-smoothings. We now consider the Khovanov brackets of the triple D, D_0, D_1, letting d^i being the ith differential in $[\![D]\!]$, and d_0^i and d_1^i the ith differentials in $[\![D_0]\!]$ and $[\![D_1]\!]$. Recall the construction of $[\![D]\!]$ from the cube of smoothings of D. Since D_0 and D_1 have been obtained from D by smoothing a crossing, every Kauffman state in their respective cubes also features in the cube for D. However, it should be noted that the cube for D_1 starts at height 1 and ends at height n, so some extra shifting is required in order to express the chain groups of $[\![D_1]\!]$ as subgroups of $[\![D]\!]$. In particular, the chain groups comprising $[\![D]\!]$ can be expressed as the following:

$$[\![D]\!]^i = \left\{ \begin{array}{ll} [\![D_0]\!]^i & i = 0 \\ [\![D_0]\!]^i \oplus [\![D_1]\!]^{i-1}\{1\} & 0 < i < n \\ [\![D_1]\!]^{i-1}\{1\} & i = n \end{array} \right\}$$

This decomposition of $[\![\times]\!]$ is exactly what is meant by the third Khovanov bracket axiom, albeit expressed in a slightly different way. Observe that the differential d^i in $[\![D]\!]$ is in general the sum of d_0^i, d_1^{i-i} and an extra term going from $[\![D_0]\!]$ to $[\![D_1]\!]$. From this we obtain a short exact sequence of the Khovanov brackets:

$$0 \to [\![D_1]\!][1]\{1\} \hookrightarrow [\![D]\!] \twoheadrightarrow [\![D_0]\!] \to 0$$

This short exact sequence can be shifted as usual to obtain a short exact sequence in the Khovanov chain complexes, however there are two cases to consider, when $\times$ is positive and when it is negative.

First, let us assume $\times$ is positive. Then the orientation of D is preserved in the 0-smoothing, but not in the 1-smoothing. Let us therefore pick an orientation on the components of D_1 and define an integer c as follows:

$$c = \text{number of negative crossings in } D_1 - \text{number of negative crossings in } D.$$

Now, D_0 has $n_+ - 1$ positive crossings and n_- negative crossings, and D_1 has $(n-1)-(c+n_-)$ positive crossings and $c+n_-$ negative crossings. We therefore need to shift $[\![D_0]\!]$ by $-n_-$ in the i grading and $(n_+ - 1) - 2n_-$ in the j grading, and $[\![D_1]\!]$ by $-(c+n_-)$ in the i grading and $(n-1)-(c+n_-)-2(c+n_-) = n_+ - 2n_- - 3c - 1$ in the j grading to obtain $CKh(D_0)$ and $CKh(D_1)$. However, we need to shift everything by $[-n_-]\{n_+ - 2n_-\}$ in order to obtain $CKh(D_L)$. This means there is extra shifting required in $CKh(D_0)$ and $CKh(D_1)$.

$$\begin{aligned} [\![D_1]\!]^{i-1,j-1}[-n_-]\{n_+ - 2n_-\} &= [\![D_1]\!]^{i-c-1,j-1-3c-1}[-c-n_-]\{n_+ - 2n_- - 3c - 1\} \\ &= CKh^{i-c-1,j-1-3c-2}(D_1) \end{aligned}$$

$$\begin{aligned} [\![D_0]\!]^{i,j}[-n_-]\{n_+ - 2n_-\} &= [\![D_0]\!]^{i,j-1}[-n_-]\{n_+ - 2n_-\} \\ &= CKh^{i,j-1}(D_0) \end{aligned}$$

The short exact sequence in CKh is then:

$$0 \to CKh(D_1)[-c-1]\{-3c-2\} \hookrightarrow CKh(D) \twoheadrightarrow CKh(D_0)\{-1\} \to 0,$$

which then induces the following long exact sequence in homology:

$$\cdots \longrightarrow Kh^{i-c-1,j-3c-2}(L_1) \longrightarrow Kh^{i,j}(L) \longrightarrow Kh^{i,j-1}(L_0) \xrightarrow{\gamma} Kh^{i-c,j-3c-2}(L_1) \longrightarrow Kh^{i+1,j}(L) \longrightarrow Kh^{i+1,j-1}(L_0) \longrightarrow \cdots$$

Now let us assume $\times$ is negative. This time D_1 inherits the orientation of D. Pick an orientation on D_0 and define c' as

$$c' = \text{number of negative crossings in } D_0 - \text{number of negative crossings in } D.$$

We follow the same process as above to obtain a similar, but subtly different, short exact sequence in CKh:

$$0 \to CKh(D_1)\{1\} \hookrightarrow CKh(D) \twoheadrightarrow CKh(D_0)[-c']\{-3c'-1\} \to 0,$$

and obtain another long exact sequence in homology:

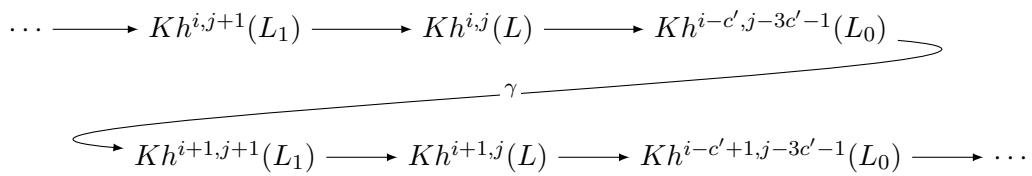

Remark. The skein exact sequence works in exactly the same way in the reduced setting — in fact we may simply exchange each Khovanov group for its reduced counterpart in the above sequences with no further work necessary.

The primary application of the skein exact sequence is to express the Khovanov homologies of a link in terms of the Khovanov homologies of simpler pieces. We will use it in particular when comparing the annular Khovanov homologies of annular Sakuma knots obtained from the same family of framed Sakuma links.

4.1.3 Khovanov homology and strongly invertible knots

Khovanov homology is the first homological invariant we can apply to strongly invertible knots. For a strongly invertible knot (K, h) we form the Sakuma link $\mathbb{L}$ and calculate $Kh^*(\mathbb{L})$, which is clearly an invariant of (K, h).

Definition 4.1.5. Let (K, h) be a strongly invertible knot with Sakuma link $\mathbb{L}$. Then set $Kh^*(K, h) := Kh^*(\mathbb{L})$.

As for the η-polynomial, Jones polynomial, and annular Jones polynomials, we can define Khovanov homology of a framed Sakuma link.

Definition 4.1.6. Let (K, h, n) be a framed strongly invertible knot with Sakuma link $\mathbb{L}_n$. Then we set $Kh^*(K, h, n) := Kh^*(\mathbb{L}_n)$.

It is known that Khovanov homology detects the two-component unlink [29]. Since the trivial strongly invertible knot $(\mathcal{U}, h_0)$ has as its Sakuma link the two-component unlink we immediately have the following:

Corollary 4.1.7. *Let (K, h) be a strongly invertible knot with Sakuma link $\mathbb{L}$. Then,*

$$(K, h) \cong (\mathcal{U}, h_0) \iff dim_{\mathbb{F}}(Kh^*(\mathbb{L})) = 4.$$

That is, Khovanov homology detects the strongly invertible unknot.

The above result is significant for us as this is the first invariant we have outlined that detects the trivial strongly invertible knot. In the previous chapter we saw that the η-polynomial does not detect $(\mathcal{U}, h_0)$, and it is an open question whether the Jones and annular Jones polynomials do. This fact is reflective of the existing progress on unlink detection in general — where categorified invariants have, broadly speaking, been shown to detect unlinks, whilst their decategorified counterparts, on the whole, have not.

Like its decategorified counterpart, Khovanov homology is a good detector of cheirality. The following is due to Khovanov [40, Corollary 11]:

Lemma 4.1.8. *Let $K \subset S^3$ be a knot. Suppose K is amphicheiral; then $Kh^*(K)$ is palindromic, that is, $Kh^{i,j}(K) \cong Kh^{-i,-j}(K)$ for all (i,j).*

Because of its sensitivity to cheirality, we can reproduce [79, Proposition 3.4] for Khovanov homology too. However, as the statement is almost identical to the versions we have seen before (for example Corollary 3.2.5), we will leave it up to the reader to construct the result.

In the rest of this chapter we will pass over Khovanov homology in favour of its lesser known annular cousin.

4.2 Annular Khovanov homology

We will now move on to the variant of Khovanov homology for links in thickened annuli defined by Asaeda, Przytycki, and Sikora in [2]. The construction of *annular Khovanov homology* is very similar to that of links in the 3-sphere — the main difference comes from equipping the chain complex with an additional third grading, which encodes information about how the link wraps around the central hole. It turns out that the new k grading is non-increasing with respect to the Khovanov differential, which allows us to apply tools from homological algebra to form another, related chain complex — the homology of which is annular Khovanov homology. The two homology theories are related by a *spectral sequence*, the theory of which we will briefly recap. Finally, we will apply annular Khovanov homology to the annular Sakuma knots we constructed earlier, and will prove that annular Khovanov homology also detects the strongly invertible unknot.

4.2.1 Filtrations and spectral sequences

Here we recap the concept of a *spectral sequence*, a powerful tool used by homological algebraists. The content in this section is taken from Chow's article [14] and McCleary's book [53], which should be consulted for proofs and further reading. In everything that follows we will work with cochain complexes of finite dimensional vector spaces over fields, as this is the setting we find ourselves in with Khovanov homology; however, everything can be defined just as well for chain complexes and for complexes of modules over rings. We will also from now on drop the 'co' prefix, in keeping with the general looseness that this is used in Khovanov homology (which is technically a cohomology theory).

Spectral sequences arise when we are able to equip a chain complex with a $\mathbb{Z}$-grading that 'plays nicely' with the complex's differential. The ideal scenario is that of a *graded chain complex*, which allows us to split each chain group into graded slices, each of which are preserved by the differential. More precisely, for a cochain complex (C^*, δ) given by

$$\cdots \xrightarrow{\delta} C^{i-1} \xrightarrow{\delta} C^i \to C^{i+1} \xrightarrow{\delta} \cdots$$

which is equipped with a grading, so that each C_i can be expressed as

$$C^i = \bigoplus_p C^{i,p} \ ,$$

the complex is graded if $\delta(C^{i,p}) \subset C^{i+1,p}$ for all i and p. This means that the homology of the whole chain complex is the same as the sum of the homologies of each slice, that is

$$H^*\Big(C^*, \delta\Big) = \bigoplus_{p=1}^{n} H^*\Big(C^{*,p}, \delta\Big).$$

When we have a graded chain complex we find it is often computationally less expensive to calculate the homologies of each slice than that of the whole complex at once.

In practice, however, when we are able to define an extra grading on a chain complex we often do not have anything nearly as nice as a graded chain complex. More likely, what results is a *filtered chain complex*, in which the grading induces a *filtration* — a nested sequence of sub-complexes which is preserved by the differential. For example,

$$0 = C^{i,0} \subseteq C^{i,1} \subseteq \cdots \subseteq C^{i,n} = C^i$$

where, $\delta(C^{i,p}) \subset C^{i+1,p}$ for all i and p. In this situation we say that the differential is *non-increasing* in the p grading. Note that δ may well take elements of $C^{i,p}$ to elements of $C^{i+1,p}$ with a lower p grading due to the nested nature of the sub-complexes — this is a key distinction from the graded chain complex case we had before.

From here we can form what is known as the *associated graded complex*. In order to do this we form a series of quotient spaces from each nested sequence, defining

$$E_0^{i,p} := C^{i,p}/C^{i,p-1}$$

so that

$$C^i = \bigoplus_p E_0^{i,p}.$$

We then observe that when the differential δ is applied to each $E_0^{i,p}$ it induces a chain map δ_0 which preserves the p grading — two elements of $C^{i,p}$ that differ by an element of $C^{i,p-1}$ get mapped to elements of $C^{i+1,p}$ that differ by an element of $C^{i+1,p-1}$. The associated graded chain complex of (C^*, δ) is then the chain complex

$$\Big(\bigoplus_p E_0^{i,p}, \delta_0\Big),$$

which has isomorphic chain groups to (C^*, δ), but a possibly different differential. This fact means that we cannot assume that the homology of (C^*, δ) is equal to sum of the homologies of the slices of $\Big(\bigoplus_p E_0^{i,p}, \delta_0\Big)$, although the latter can be viewed as an approximation to the former.

In fact, the homology of the associated graded chain complex is the first stage of a sequence which converges to the homology of (C^*, δ) — this sequence is known as *spectral sequence*. The homology of the associated chain complex is denoted by E_1^*, and is referred to as the first 'page' of the spectral sequence, whilst the homology of (C^*, δ) is usually denoted in the literature by E_∞^*. The first page can be viewed as a chain complex by defining a new differential δ_1, which instead of preserving the p grading drops it by 1 — that is it takes $E_1^{i,p}$ to $E_1^{i+1,p-1}$. Taking the homology gives us the second page of the sequence, and the process continues until E_∞^* is obtained. It is important to note that the dimensions of the underlying vector spaces of each page are non-increasing — adding in additional pieces of δ can only remove basis elements.

We now change tack slightly, by defining a notion of equivalence for filtered chain complexes. This definition appears in [24, Definition 2.6], with a slight change of notation.

Definition 4.2.1. Let C_1 and C_2 be two filtered chain complexes. We say that C_1 and C_2 are *filtered quasi-isomorphic*, and write $C_1 \simeq C_2$, if there exists a third filtered chain complex C', and filtered chain maps

$$\phi_j : C_j \to C',$$

such that

$$\phi_j : E_i(C_j) \to E_i(C')$$

is an isomorphism for all $i \in \mathbb{Z}_+, j \in \{1, 2\}$.

Two general chain complexes are said to be quasi-isomorphic if they have isomorphic homology groups — the above definition simply allows for the extra filtration information.

Spectral sequences are particularly powerful when used to relate two homology theories. Indeed, in recent years there have been many results which utilise a spectral sequence between Khovanov-style homology theories on the one hand, and *Heegaard-Floer*-style theories on the other. Furthermore, the most commonly used method to prove a Khovanov style homology theory detects the unknot is to find a spectral sequence to an invariant that is already known to detect it — this is the methodology used originally by Kronheimer and Mrowka [47] when they proved the Khovanov homology detects the unknot. Spectral sequences have featured in work of, for example, Grigsby and Wehrli [22], [23], [24], [25], Baldwin [3], and Roberts [76], [75], as well as many others.

4.2.2 Construction

To calculate annular Khovanov homology of an annular link L we first take a diagram $D_L \subset A$ and form the cube of smoothings in the usual fashion. We observe that the circles present in a general complete smoothing S_α can be divided into two sets: those that enclose the central hole, and those that do not. Continuing on from the construction of the annular Jones polynomial we refer to the sets of circles as 'non-trivial' and 'trivial' respectively.

We then proceed as before and attach a vector space to each circle: to a trivial circle we attach a copy of V as in the S^3 setting, and to a non-trivial circle we attach a 2-dimensional vector

space W over $\mathbb{F}$ generated by w_+ and w_-. As ungraded vector spaces V and W are isomorphic, and we specify in addition that their p gradings are also the same. The difference comes from an additional grading — the *annular k grading*, which we now define. Suppose that a Kauffman state S_α consists of circles $K_1, \ldots, K_u, K_{u+1}, \ldots, K_c$ (where u is the number of trivial circles) which are associated to vector spaces $V_1, \ldots, V_u$ and $W_{u+1}, \ldots, W_c$. Then,

$$\begin{aligned} k(v_{\pm_i}) &:= 0 \\ k(w_{\pm_i}) &:= \pm 1 \end{aligned}$$

The k grading of a basis vector $v_{\pm_1} \otimes \ldots \otimes v_{\pm_u} \otimes w_{\pm_{u+1}} \otimes \ldots \otimes w_{\pm_c}$ is defined exactly how we would expect:

$$\begin{aligned} v_{\pm_1} \otimes \ldots \otimes v_{\pm_u} \otimes w_{\pm_{u+1}} \otimes \ldots \otimes w_{\pm_c} &= k(v_{\pm_1}) + \ldots + k(v_{\pm_u}) + k(w_{\pm_{u+1}}) + \ldots + k(w_{\pm_c}) \\ &= k(w_{\pm_{u+1}}) + \ldots + k(w_{\pm_c}). \end{aligned}$$

With this additional grading we construct the triply graded Khovanov chain complex $CAKh^*(D_L)$ (note that the underlying abelian groups of $CAKh^*(D_L)$ and $CKh^*(D_L)$ are isomorphic, provided we discard the k grading). To define the differentials on $CAKh^*(D_L)$ we recall the definition of the Khovanov differential, and examine its effect on the k grading of a basis element. Observe first that there are three kinds of splitting and merging behaviour between trivial circles and non-trivial circles.

1. Two trivial circles can merge into a single trivial circle and a trivial circle can split into two trivial circles.

2. A trivial circle and a non-trivial circle can merge into a non-trivial circle and a non-trivial circle can split into a trivial circle and a non-trivial circle.

3. Two non-trivial circles can merge into a trivial circle and a trivial circle can split into two non-trivial circles.

In each of the three cases the Khovanov differential either preserves the k grading, or lowers it by 2. That is, we can express ∂_{Kh} as the following:

$$\partial_{Kh} = \partial_0 + \partial_{-2}$$

where ∂_0 is the piece that preserves the k grading, and ∂_{-2} is the piece that lowers it by 2. For completeness we include their effects on all three gradings (i, j, k):

$$\begin{aligned} deg(\partial_0) &= (1, 0, 0) \\ deg(\partial_{-2}) &= (1, 0, -2) \end{aligned}$$

As a consequence of this observation the k grading induces a filtration on the Khovanov chain complex, so we can form the associated graded chain complex. In this setting we do this by slicing up each group in the Khovanov chain complex into slices of each k degree, then form a

series of chain complexes with ∂_0 as the differential. Taking the homology of each slice and direct summing gives us annular Khovanov homology, which we denote by $AKh^*(L)$.

In practice, an easier way to arrive at AKh is to instead use ∂_0 in the annular Khovanov chain complex and take the homology. This short-cuts the whole process of taking the homology of each slice of the associated chain complex and direct summing. In other words,

$$AKh^*(L) \cong H^*\Big(CAKh(D_L), \partial_0\Big)$$

The table below (4.9) appears in Kesse's Bachelor's thesis [39] and details the differential ∂_0. In the first case nothing needs to be done as all k gradings are 0, however in the second and third cases minor adjustments need to be made in order for the k grading to be preserved.

	(1) $V \otimes V \longleftrightarrow V$	(2) $V \otimes W \longleftrightarrow W$	(3) $W \otimes W \longleftrightarrow V$
m	$v_+ \otimes v_+ \mapsto v_+$ $v_+ \otimes v_- \mapsto v_-$ $v_- \otimes v_+ \mapsto v_-$ $v_- \otimes v_- \mapsto 0$	$v_+ \otimes w_+ \mapsto w_+$ $v_+ \otimes w_- \mapsto w_-$ $v_- \otimes w_+ \mapsto 0$ $v_- \otimes w_- \mapsto 0$	$w_+ \otimes w_+ \mapsto 0$ $w_+ \otimes w_- \mapsto v_-$ $w_- \otimes w_+ \mapsto v_-$ $w_- \otimes w_- \mapsto 0$
Δ	$v_+ \mapsto v_+ \otimes v_- + v_- \otimes v_+$ $v_- \mapsto v_- \otimes v_-$	$w_+ \mapsto v_- \otimes w_+$ $w_- \mapsto v_- \otimes w_-$	$v_+ \mapsto w_+ \otimes w_- + w_- \otimes w_+$ $v_- \mapsto 0$

(4.9)

We can define the Poincaré polynomial of annular Khovanov homology:

$$\mathcal{P}(AKh^*(L)) := \sum_{i,j,k} s^i q^j t^k \dim_{\mathbb{F}}\big(AKh^{i,j,k}(L)\big)$$

One thing to note is that annular Khovanov homology is the categorified version of the annular Jones polynomial that we saw earlier. That is,

$$\chi_{q,t}(AKh^*(L)) := \sum_{i,j,k} (-1)^i q^j t^k \dim_{\mathbb{F}}\big(AKh^{i,j,k}(L)\big) = AJ(L)(q,t) \tag{4.10}$$

where, similarly to the standard Khovanov case, $AKh^{i,j,k}(L)$ refers to the homogeneous piece of $AKh^*(L)$ in grading (i,j,k).

Example 4.2.2. For an example we return to the annular knot we first saw in Example 3.3.5. Let $\mathbb{F} = \mathbb{Z}/2\mathbb{Z}$ and consider the cube of smoothings featured in Figure 4.1. Note that we have chosen to number the circles from the inside out, so that, for example, the leftmost copy of V or W attached to each smoothing corresponds to the innermost circle in the smoothing. From this cube we form the Khovanov bracket $[\![D_K]\!]$:

$$[\![D_K]\!]: \quad 0 \longrightarrow V[0]\{0\} \xrightarrow{\delta_1} (W^{\otimes 2} \oplus W^{\otimes 2})[1]\{1\} \xrightarrow{\delta_2} (W \otimes V \otimes W)[2]\{2\} \longrightarrow 0$$

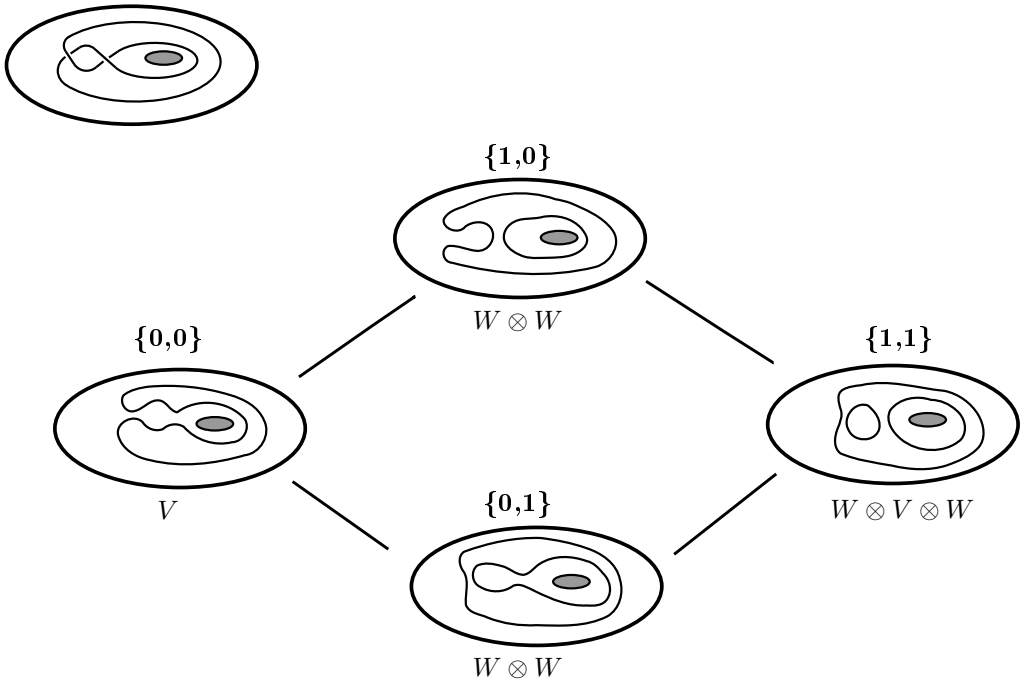

Figure 4.1: Calculating AKh

In this example $n = 2$, $n_+ = 0$, and $n_- = 2$, so to obtain the annular Khovanov chain complex we shift the homological degree by -2 and the quantum degree by -4:

$$CKh(D_K): \quad 0 \to V[-2]\{-4\} \xrightarrow{\delta_1} (W^{\otimes 2} \oplus W^{\otimes 2})[-1]\{-3\} \xrightarrow{\delta_2} (W \otimes V \otimes W)[0]\{-2\} \to 0$$

The action of the annular Khovanov differential ∂_0 is as follows:

δ_1		
v_+	$\mapsto$	$(w_+ \otimes w_- + w_- \otimes w_+, w_+ \otimes w_- + w_- \otimes w_+)$
v_-	$\mapsto$	0

δ_2		
$(w_+ \otimes w_+, 0)$	$\mapsto$	$w_+ \otimes v_- \otimes v_+$
$(w_+ \otimes w_-, 0)$	$\mapsto$	$w_+ \otimes v_- \otimes w_-$
$(w_- \otimes w_+, 0)$	$\mapsto$	$w_- \otimes v_- \otimes w_+$
$(w_- \otimes w_-, 0)$	$\mapsto$	$w_- \otimes v_- \otimes w_-$
$(0, w_+ \otimes w_+)$	$\mapsto$	$w_+ \otimes v_- \otimes w_+$
$(0, w_+ \otimes w_-)$	$\mapsto$	$w_+ \otimes v_- \otimes w_-$
$(0, w_- \otimes w_+)$	$\mapsto$	$w_- \otimes v_- \otimes w_+$
$(0, w_- \otimes w_-)$	$\mapsto$	$w_- \otimes v_- \otimes w_-$

And so the $AKh^*(K)$ groups are:

$$\begin{aligned} AKh^{-2,*,*}(K) &\cong \mathbb{Z}/2\mathbb{Z}[-2,-5,0] \\ AKh^{-1,*,*}(K) &\cong \mathbb{Z}/2\mathbb{Z}[-1,-1,2] \oplus \mathbb{Z}/2\mathbb{Z}[-1,-3,0] \oplus \mathbb{Z}/2\mathbb{Z}[-1,-5,-2] \\ AKh^{0,*,*}(K) &\cong \mathbb{Z}/2\mathbb{Z}[0,1,2] \oplus \mathbb{Z}/2\mathbb{Z}[0,-1,0] \oplus \mathbb{Z}/2\mathbb{Z}[0,-1,0] \oplus \mathbb{Z}/2\mathbb{Z}[0,-3,-2] \end{aligned}$$

Where $[i,j,k]$ indicates a grading shift of (i,j,k). The Poincaré polynomial is then

$$\mathcal{P}(AKh^*(K)) = s^{-2}q^{-2} + s^{-1}q^{-1}t^2 + s^{-1}q^{-3} + s^{-1}q^{-5}t^{-2} + qt^2 + 2q^{-1} + q^{-3}t^{-2},$$

and we observe that by setting $s = -1$ we obtain the annular Jones polynomial we calculated in Example 3.3.5:

We can also display annular Khovanov homology groups in a table. We will use the Poincaré polynomial of AKh, and place it in a table with horizontal axis the homological grading, vertical axis the quantum grading, and the annular grading appearing in each box as a power of t. In this example the table looks like:

q\s	−2	−1	0
−5	1	t^{-2}	
−3		1	t^{-2}
−1		t^2	2
1			t^2

4.2.3 Properties and applications

In this section we will detail some key characteristics of annular Khovanov homology, and will mention a number of spectral sequences which converge from annular Khovanov homology to another homology theory.

As annular Khovanov homology categorifies the annular Jones polynomial it shares the properties we mentioned in the previous chapter. For example, the wrapping number of an annular link determines the possible k gradings present in its annular Khovanov homology:

Lemma 4.2.3. *Let $L \subset A \times I$ be an annular link with wrapping number ω. Then $AKh^{i,j,k}(L) \cong 0$ for all k such that $|k| > \omega$. Furthermore,*

1. *Suppose ω is even. Then $AKh^{i,j,k}(L) \cong 0$ for all odd k.*
2. *Suppose ω is odd. Then $AKh^{i,j,k}(L) \cong 0$ for all even k.*

We mentioned in the previous chapter that Grigsby and Ni proved a result about the annular Khovanov homology of braid closures [20, Corollary 1.2]. Their result is stronger than the version we proved for the annular Jones polynomial (Lemma 3.3.10), as it uses extra information present in annular Khovanov homology — see [20] for further details.

Proposition 4.2.4 (Grigsby-Ni, 2011). *Let $L \subset A \times I$ be an annular link with wrapping number ω. Then the group*

$$AKh(L,\omega) := \bigoplus_{i,j} AKh^{i,j,\omega}(L),$$

is isomorphic to $\mathbb{F}$ if and only if L is equivalent to a closed braid.

For example, the annular knot featured in Example 4.2.2 has

$$AKh(K,2) \cong \mathbb{Z}/2\mathbb{Z}[0,1,2] \oplus \mathbb{Z}/2\mathbb{Z}[-1,-1,2]$$

and so is not equivalent to a braid closure.

Additionally, Baldwin and Grigsby [4, Theorem 1] have proven a result about AKh and its ability to detect the trivial n-strand braid.

Theorem 4.2.5 (Baldwin-Grigsby, 2015). *Let B_n be an n-string braid, and let $\mathbb{1}$ be the trivial n-string braid. If $AKh^*(\widehat{B_n}) \cong AKh^*(\widehat{\mathbb{1}})$, then $B_n = \mathbb{1}$.*

Also, as it contains the annular Jones polynomial, and due to its relationship with Khovanov homology, annular Khovanov homology can be used to detect the cheirality of an annular knot.

Lemma 4.2.6. *Let $K \subset A \times I$ be an annular knot. Suppose K is amphicheiral; then $AKh^*(K)$ is palindromic, that is, $AKh^{i,j,k}(K) \cong AKh^{-i,-j,-k}(K)$ for all (i,j,k).*

Next, we will mention a number of spectral sequences which converge from annular Khovanov homology to another homology theory, with the aim of placing annular Khovanov homology within a wider mathematical framework.

Firstly, we make explicit the relationship between annular and regular Khovanov homology. In the last section we saw how the annular Khovanov homology of an annular link L can be expressed in terms of the Khovanov chain complex of $L \subset S^3$ by using the k grading preserving piece of the Khovanov differential, ∂_0. If we then include the piece that drops the k grading by two, ∂_{-2}, and take the homology of $AKh^*(L)$ with respect to it then we re-obtain $Kh^*(L)$. In the terminology of spectral sequences, therefore, annular Khovanov homology converges to Khovanov homology. This is simply the homological counterpart of the relationship between $AJ(L)$ and $\widehat{J}(L)$ we observed in the previous chapter.

Example 4.2.7. Consider again the AKh calculation in Example 4.2.2. When we take the homology of $AKh^*(L)$ with respect to ∂_{-2} some cancellation occurs. In total three pairs of generators cancel: $\mathbb{Z}/2\mathbb{Z}[-2,-5,0]$ with $\mathbb{Z}/2\mathbb{Z}[-1,-5,-2]$, $\mathbb{Z}/2\mathbb{Z}[-1,-3,0]$ with $\mathbb{Z}/2\mathbb{Z}[0,-3,-2]$, and $\mathbb{Z}/2\mathbb{Z}[-1,-1,2]$ with $\mathbb{Z}/2\mathbb{Z}[0,-1,0]$. This leaves us with $\mathbb{Z}/2\mathbb{Z}[0,1,2]$ and $\mathbb{Z}/2\mathbb{Z}[0,-1,0]$, and throwing away the k grading gives $\mathbb{Z}/2\mathbb{Z}[0,1]$ and $\mathbb{Z}/2\mathbb{Z}[0,-1]$, which is the Khovanov homology of the unknot in S^3, as expected.

Next, we discuss the connection between annular Khovanov homology and an offshoot of Heegaard-Floer homology, known as *sutured Floer homology*. The first indication that such a relationship existed was due to Roberts. Given a link L in the complement of an unknot $B \subset S^3$ he proved

in [76] the existence of a spectral sequence between $AKh^*(L)$ and a variant of the knot Floer homology of $\widetilde{B} \subset \Sigma(S^3, L)$. Grigsby and Wehrli [23, Theorem 2.1] proved that this variant was in fact isomorphic to the sutured Floer homology as defined by Juhász [35]. In Grigsby and Wehrli's notation, the result reads as follows:

Theorem 4.2.8 (Grigsby-Wehrli, 2009)**.** *Let $L \subset A \times I$ be a link in the product sutured manifold $A \times I$. Then there is a spectral sequence whose E_1 term is $AKh^*(\overline{L})$ and whose E_∞ term in $SFH(\Sigma(A \times I, L))$.*

We will keep the details of this spectral sequence, including the filtration gradings, deliberately vague. In all the results we will go on to prove we will only require the existence of this spectral sequence, as we will mainly concern ourselves with the Khovanov end. We will remark, however, that the spectral sequence yields more invariants than just AKh and SFH. As Grigsby and Wehrli explain in [24, Remark 3.9], arguments of Roberts [75, Sec. 7] and Baldwin [3] can be used to show that the filtered chain complex that features in the spectral sequence admits a sequence of invariants — one for each page of the spectral sequence — up to filtered quasi-isomorphism.

For annular Sakuma knots we may well ask ourselves what exactly the 3-manifolds $\Sigma(A \times I, L)$ are. Let (K, h) be a strongly invertible knot with Sakuma link $\mathbb{L} = \mathcal{B} \cup \mathcal{L}$ and annular Sakuma knots $\mathcal{L}, B \subset A \times I$. When $L = B$ we can simply reverse Sakuma's construction. That is, $\Sigma(A \times I, B)$ is $S^3 \backslash \big(\mathcal{N}(l) \cup \mathcal{N}(h(l))\big)$, where l and $h(l)$ are the pair of equivariant longitudes of K used in Sakuma's construction. Interestingly, in the case where we have two distinct strong inversions on the same knot, (K, h_1), (K, h_2), we note that $\Sigma(A \times I, B_1) \cong \Sigma(A \times I, B_2)$, which means that $AKh(\mathcal{L}_1)$ and $AKh(\mathcal{L}_2)$ have the same E_∞ page in Grigsby and Wehrli's spectral sequence. In other words, applying the spectral sequence means we lose track of the strong inversions.

For the annular knot $\mathcal{L}$ we first express $\mathbb{L}$ as the two-component completion of $B \subset A \times I$. Then, as $A \times I$ is homeomorphic to the exterior of B, the double branched cover with branch set $\mathcal{L}$ is simply the exterior of the two-component link depicted in Figure 4.2.

Remark. We have been somewhat lax in the above discussion, as we have neglected all mention of the sutured structure on $\Sigma(A \times I, L)$. Recall that the sutured structure on $A \times I$ is given by $A(\Gamma) = \partial A \times I$ and $s(\Gamma) = \partial A \times \{\frac{1}{2}\}$. Reconceptualising $A \times I$ as the exterior of the other link component L', in the double branched cover we end up with two sutures on the exterior of each lift of L', so $\Sigma(A \times I, L)$ has four sutures in total.

Finally, we briefly detail the Lee spectral sequence between Khovanov homology and Khovanov-Lee homology, and how this can be adapted to the annular setting. Lee in [48] defines a deformation of Khovanov homology, in which the Khovanov differential ∂_{Kh} is altered and the resulting homology is taken. Analogously to the annular case, the Lee differential ∂_{Lee} lowers the quantum grading, which induces a spectral sequence from Kh to Kh_{Lee}. The spectral sequence from Khovanov homology to Khovanov-Lee homology was exploited by Rasmussen [73], who used it to define his famous s invariant.

Grigsby, Licata, and Wehrli [21] have applied Lee's ideas to the annular setting. They show how annular Khovanov homology converges to Khovanov-Lee homology by defining a $\mathbb{Z} \oplus \mathbb{Z}$ filtration on the Khovanov chain complex. They then extended Rasmussen's ideas, by defining a series of s-type invariants for an annular link, which they denote by d_t, $t \in [0, 2]$.

Theorem 4.2.9 (Grigsby-Licata-Wehrli, 2016)**.** *Let $L \subset A \times I$ be an annular link, let o be an orientation on L, and let $t \in [0, 2]$.*

1. *$d_t(L, o)$ is an oriented annular link invariant.*
2. *$d_{1-t}(L, o) = d_{1+t}(l, o)$ for all $t \in [0, 1]$.*
3. *$d_0(L, o) = d_2(L, o) = s(L, o) - 1$.*
4. *Viewed as a function, $[0, 2] \to \mathbb{R}$, $d_t(l, o)$ is piecewise linear.*

Remark. Whilst rich in structure, the d_t invariant is hard to calculate. The only calculations to date have been done on a Mathematica program written by Scott Morrison (see [21]), but this only takes annular links formed from braid closures as its input. As a result, we will pass over the d_t invariant, remarking only that adapting Morrison's program to annular Sakuma knots would be an interesting direction in which to take Sakuma's construction further.

4.2.4 Annular Khovanov homology and strongly invertible knots

Just in the decategorified setting, we can apply annular Khovanov homology to strongly invertible knots via the extended version of Sakuma's construction. Here we formally define the annular Khovanov homology of a strongly invertible knot, and apply some of the results covered in the previous section to annular Sakuma knots.

Definition 4.2.10. Let (K, h) be a strongly invertible knot with Sakuma link $\mathbb{L} = \mathcal{B} \cup \mathcal{L}$. We define the pair of annular Khovanov homologies associated to (K, h) by $AKh^*_{(K,h)}(\mathcal{B})$ and $AKh^*_{(K,h)}(\mathcal{L})$.

We also define annular Khovanov homology on framed strongly invertible knots.

Definition 4.2.11. Let (K, h, n) be a framed strongly invertible knot with framed Sakuma link $\mathbb{L}_n = \mathcal{B} \cup \mathcal{L}$. We define the pair of annular Khovanov homologies associated to (K, h, n) by $AKh^*_{(K,h,n)}(\mathcal{B})$ and $AKh^*_{(K,h,n)}(\mathcal{L})$.

One of the most interesting features of the annular Khovanov homology of a strongly invertible knot is that, because both annular knots are unknotted when embedded into S^3, the annular Khovanov homology always collapses to something two dimensional when we apply the spectral sequence to Khovanov homology — see for instance Example 4.2.7. As previous noted, this property is the homological analogue of a property of the annular Jones polynomial, namely, the fact that the annular Jones polynomial specialises to the unnormalised Jones polynomial of the unknot when the annular variable is set to 1 — see Example 3.3.5.

Next we specify the effect of the wrapping number on the annular Khovanov homology of an

annular Sakuma knot. Recall that the wrapping number of an annular Sakuma knot is always even, and for the 'branch-set' knots it equals two. We then have:

Corollary 4.2.12. *Let $\mathbb{L}_n = \mathcal{B} \cup \mathcal{L}$ be a framed Sakuma link not equivalent to the two-component unlink. Then,*

1. $AKh^{i,j,k}(\mathcal{B}) \cong 0$ *for* $k \notin \{0, \pm 2\}$.
2. $AKh^{i,j,k}(\mathcal{L}) \cong 0$ *for odd* k.

Proof. This follows from Lemma 4.2.3 and Corollary 3.3.20. □

Recall that the set of annular Sakuma knots is almost entirely distinct from the set of braid closures (Proposition 2.5.4). As a consequence of this fact, and of Proposition 4.2.4, it follows that:

Corollary 4.2.13. *Let $L \subset A \times I$ be an annular Sakuma knot with wrapping number ω that is not associated to $(\mathcal{U}, h_0, \pm 1)$. Then $dim(AKh(L, \omega)) \neq 1$.*

In light of annular Khovanov homology's sensitivity to cheirality there also exists a version of [79, Proposition 3.4] for annular Khovanov homology. As for Khovanov homology we will omit the statement, but it is easily deducible from the various versions we included in Chapter 3.

4.2.5 Strongly invertible unknot detection

In this section we will show that annular Khovanov homology detects the strongly invertible unknot. In all that follows take the field $\mathbb{F}$ to be $\mathbb{Z}/2\mathbb{Z}$.

We require a few supporting results. The first is due to Grigsby and Wehrli [23, Proposition 2.24] — here is a slightly altered and abridged version for our purposes.

Proposition 4.2.14 (Grigsby-Wehrli, 2009)**.** *Let $K \subset A \times I$ be an annular link with two-component completion $L = K \cup \mathcal{B}$. Let $p(K) = (lk(K, \mathcal{B})$ mod 2). Then,*

$$SFH\big(\Sigma(A \times I, K)\big) \cong \left\{ \begin{array}{ll} \widehat{HFK}\big(\Sigma(S^3, K), \widetilde{\mathcal{B}}\big) \otimes \Theta & \text{if } p(K) = 1 \\ \widehat{HFK}\big(\Sigma(S^3, K), \widetilde{\mathcal{B}}\big) & \text{if } p(K) = 0 \end{array} \right\}$$

where Θ is a bigraded, dimension 2 vector space over $\mathbb{Z}/2\mathbb{Z}$.

Next is a result due to Ni; we will state the version appearing in [62, Proposition 1.4].

Proposition 4.2.15 (Ni, 2006)**.** *Suppose L is an n-component link in S^3. If the rank of its knot Floer homology $\widehat{HFK}(L)$ is 2^{n-1}, then L is the n-component unlink.*

Finally, we prove a last supporting lemma:

Lemma 4.2.16. *Let $\mathbb{L} = \mathcal{B} \cup \mathcal{L}$ be a Sakuma link constructed from a strongly invertible knot (K, h). Consider $\widetilde{\mathcal{B}} \subset \Sigma(S^3, \mathcal{L})$, the lift of $\mathcal{B}$ in the double branched cover of S^3 over $\mathcal{L}$. Suppose $\widetilde{\mathcal{B}}$ is the two-component unlink. Then $\mathbb{L}$ is the two-component unlink, and hence $(K, h) \cong (\mathcal{U}, h_0)$.*

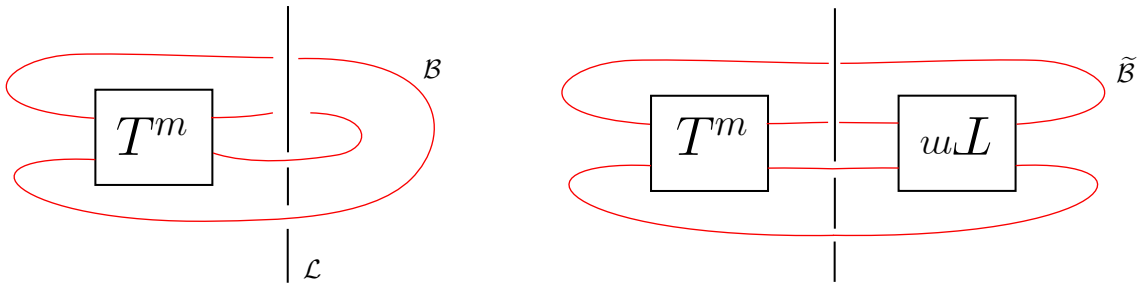

Figure 4.2: A Sakuma link $\mathbb{L} = \mathcal{B} \cup \mathcal{L}$ (left), and $\widetilde{\mathcal{B}} \subset \Sigma(S^3, \mathcal{L})$ (right)

Proof. Sakuma links can be drawn as shown in the left of Figure 4.2, where T^m is a representative of Watson's tangle associated to (K, h) with m twists, as per our convention. Then, since $\mathcal{L}$ is an unknot, $\Sigma(S^3, \mathcal{L}) \cong S^3$, and $\widetilde{\mathcal{B}}$ is a two-component link. It follows that $\widetilde{\mathcal{B}}$ can be drawn as in the right side of Figure 4.2, where by the upside-down T^m we simply mean the tangle T^m rotated π radians about an axis through the plane of the diagram.

Now suppose $\widetilde{\mathcal{B}}$ is the two-component unlink. This means that T^m must be equivalent to the trivial tangle, with two separated strands running in parallel from $D^2 \times \{0\}$ to $D^2 \times \{1\}$. Putting this tangle into the diagram of the Sakuma link, it immediately follows that $\mathbb{L}$ must also be the two-component unlink as required. □

Now comes the main theorem:

Theorem 4.2.17. *Let $\mathbb{L} = \mathcal{B} \cup \mathcal{L}$ be a Sakuma link, and let $\mathcal{U}$ be the homologically trivial unknot in $A \times I$.*

1. *Suppose $AKh^*(\mathcal{L}) \cong AKh^*(\mathcal{U}) \cong \mathbb{F}[0,1,0] \oplus \mathbb{F}[0,-1,0]$. Then $\mathbb{L}$ is the two-component unlink and $\mathcal{L} \cong \mathcal{U}$.*

2. *Suppose $AKh^*(\mathcal{B}) \cong AKh^*(\mathcal{U}) \cong \mathbb{F}[0,1,0] \oplus \mathbb{F}[0,-1,0]$. Then $\mathbb{L}$ is the two-component unlink and $\mathcal{B} \cong \mathcal{U}$.*

Proof. We first turn to Proposition 4.2.14. We know that for all $\mathbb{L}$ the linking number is 0 or ± 2, so we have $p(\mathcal{L}) = p(\mathcal{B}) = 0$.

Consider $\mathcal{U} \subset A \times I$, and let $L = \mathcal{U} \cup \mathcal{B}$ be its two-component completion, which is the two-component unlink. We also have $p(\mathcal{U}) = 0$, so Proposition 4.2.14 tells us that

$$SFH(\Sigma(A \times I, \mathcal{U})) \cong \widehat{HFK}(\Sigma(S^3, \mathcal{U}), \widetilde{\mathcal{B}}).$$

Now, since $\mathcal{U} \subset S^3$ is unknotted, $\Sigma(S^3, \mathcal{U}) \cong S^3$, and $\widetilde{\mathcal{B}}$ is the two-component unlink. Hence, we can apply Ni's result to obtain

$$\begin{aligned} \widehat{HFK}(\Sigma(S^3, \mathcal{U}), \widetilde{\mathcal{B}}) &\cong \widehat{HFK}(S^3, \mathcal{U} \cup \mathcal{U}) \\ &\cong \mathbb{F} \oplus \mathbb{F}. \end{aligned}$$

Putting everything together we have

$$SFH(\Sigma(A \times I, \mathcal{U})) \cong \mathbb{F} \oplus \mathbb{F}.$$

1. Consider $\mathcal{L} \subset A \times I$ and suppose $AKh^*(\mathcal{L}) \cong \mathbb{F} \oplus \mathbb{F}$. We have $\Sigma(S^3, \mathcal{L}) \cong S^3$, and $\widetilde{\mathcal{B}}$ is a two-component link with diagram as in Figure 4.2.

   Now apply the spectral sequence detailed in Theorem 4.2.8 between annular Khovanov homology and sutured Floer homology. It follows

   $$SFH(\Sigma(A \times I), \mathcal{L}) \subseteq \mathbb{F} \oplus \mathbb{F}$$

   If $SFH(\Sigma(A \times I), \mathcal{L}) \cong \mathbb{F}$ then $\widehat{HFK}(S^3, \widetilde{B}) \cong \mathbb{F}$. But then Ni's result tells us $\widetilde{\mathcal{B}}$ is the unknot, which is a contradiction, as we know $\widetilde{\mathcal{B}}$ is a two-component link. Hence, $SFH(\Sigma(A \times I), \mathcal{L}) \cong \mathbb{F} \oplus \mathbb{F}$, and $\widetilde{\mathcal{B}}$ is then the two-component unlink. Lemma 4.2.16 then tells us that $\mathbb{L}$ is also the two-component unlink.

2. Now consider $\mathcal{B} \subset A \times I$ and suppose $AKh^*(\mathcal{B}) \cong \mathbb{F} \oplus \mathbb{F}$. Once more $\Sigma(S^3, \mathcal{B}) \cong S^3$, and $\widetilde{\mathcal{L}}$ is the pair of equivariant longitudes on a tubular neighbourhood of some strongly invertible knot (K, h) that featured in Sakuma's construction.

   Applying the spectral sequence, and using the same logic as above means that the pair of longitudes $l \cup h(l)$ is the two-component unlink. But then $(K, h) \cong (\mathcal{U}, h_0)$, and $\mathbb{L}$ is therefore the two-component unlink.

□

Hence,

Corollary 4.2.18. *Annular Khovanov homology detects the strongly invertible unknot.*

In some respects this result should come as no surprise, given the track record of Khovanov style homology theories to detect unknots. Nevertheless, the above proof is interesting in the sense that we essentially get two unknot detection results for the price of one: on the one hand we show that if an annular Sakuma knot has the same annular Khovanov homology as the homologically trivial unknot then it is equivalent to it; on the other, we use this relation to prove a result about Sakuma links and strongly invertible knots in S^3.

4.2.6 Annular skein exact sequence

Next, we will return to the skein exact sequence and use it to pass between annular Sakuma knots that differ by a change of framing. This is really just the categorified version of the work we did on the annular Jones polynomial in the previous chapter.

Now, in the annular setting the short exact sequence in the Khovanov bracket can be decomposed into its k graded sub-sequences with no loss of data, since the maps are all k grading preserving.

Hence, we can also decompose the skein exact sequence into its k-graded subsequences. For example, when a positive crossing in D_L is smoothed we have:

$$\cdots \longrightarrow AKh^{i-c-1,j-3c-2,k}(L_1) \longrightarrow AKh^{i,j,k}(L) \longrightarrow AKh^{i,j-1,k}(L_0) \xrightarrow{\gamma} AKh^{i-c,j-3c-2,k}(L_1) \longrightarrow AKh^{i+1,j,k}(L) \longrightarrow AKh^{i+1,j-1,k}(L_0) \longrightarrow \cdots$$

Now, as we did in the previous chapter, take a family of annular Sakuma knots and fix a family of diagrams for them which differ only by the number of twists in a twist box (see Figure 3.9); we denote the diagrams D_{L_m}, where $m \in \mathbb{Z}$ refers to the signed number of twist box crossings. We will now explain how the annular Khovanov homologies of the family of Sakuma links are related by applying the skein exact sequence to their diagrams.

In the first case let $m > 0$. Let $\times$ be the left-most twist crossing in D_{L_m}, so the 0-smoothing is $)($ and the 1-smoothing is $\asymp$. We observe that applying the 1-smoothing gives us $D_{L_{m-1}}$ and the 0-smoothing gives a diagram for a two-component annular link equivalent to a pair of non-trivial, unlinked unknots — as in the previous chapter, we shall denote this link diagram by $D_{\widehat{L}_{m-1}}$. We note also that in this case c, which is the number of negative crossings in $D_{L_{m-1}}$ minus the number of negative crossings in D_{L_m}, is zero. This means the skein exact sequence is then:

$$\cdots \longrightarrow AKh^{i-1,j-2,k}(L_{m-1}) \longrightarrow AKh^{i,j,k}(L_m) \longrightarrow AKh^{i,j-1,k}(\widehat{L}_{m-1}) \xrightarrow{\gamma} AKh^{i,j-2,k}(L_{m-1}) \longrightarrow AKh^{i+1,j,k}(L_m) \longrightarrow AKh^{i+1,j-1,k}(\widehat{L}_{m-1}) \longrightarrow \cdots$$

Let's start filling in some of the slots in this sequence. The annular Khovanov homology of $\widehat{L}_{m-1}$ is four dimensional, with the following generators:

$$AKh^*(\widehat{L}_{m-1}) \cong \mathbb{F}[0,2,2] \oplus \mathbb{F}^{\oplus 2}[0,0,0] \oplus \mathbb{F}[0,-2,-2]$$

This means that for $(i-1, j-1, k)$ and $(i, j-1, k)$ not equal to $(0,0,0)$,$(0,2,2)$ or $(0,-2,-2)$ the skein exact sequence simplifies:

$$\cdots \longrightarrow 0 \longrightarrow AKh^{i-1,j-2,k}(L_{m-1}) \xrightarrow{\cong} AKh^{i,j,k}(L_m) \longrightarrow 0 \longrightarrow \cdots$$

As a result, the annular Khovanov homology for L_m contains the majority of the annular Khovanov homology of L_{m-1} as a direct summand, albeit with a shift in gradings. The remaining terms can be found by setting $(i-1, j-1, k)$ equal to $(0,0,0)$, $(0,2,2)$, and $(0,-2,-2)$ in the skein exact sequence.

1. Firstly, let $(i-1, j-1, k)$ equal $(0,0,0)$. The relevant piece of the skein exact sequence is:

$$0 \longrightarrow AKh^{-1,-1,0}(L_{m-1}) \xrightarrow{\alpha} AKh^{0,1,0}(L_m) \xrightarrow{\beta} \mathbb{F}^{\oplus 2}[0,0,0] \xrightarrow{\gamma} AKh^{0,-1,0}(L_{m-1}) \xrightarrow{\delta} AKh^{1,1,0}(L_m) \longrightarrow 0$$

There are three possibilities, depending on the image of γ:

(a) $Im(\gamma) = \mathbb{F}^{\oplus 2}$

(b) $Im(\gamma) = \mathbb{F}$

(c) $Im(\gamma) = 0$

This gives three possibilities for the values of $AKh^{0,1,0}(L_m)$ and $AKh^{1,1,0}(L_m)$:

(a) $AKh^{-1,-1,0}(L_{m-1}) \cong AKh^{0,1,0}(L_m)$

$AKh^{0,-1,0}(L_{m-1}) \cong AKh^{1,1,0}(L_m) \oplus \mathbb{F}^{\oplus 2}$

(b) $AKh^{-1,-1,0}(L_{m-1}) \oplus \mathbb{F} \cong AKh^{0,1,0}(L_m)$

$AKh^{0,-1,0}(L_{m-1}) \cong AKh^{1,1,0}(L_m) \oplus \mathbb{F}$

(c) $AKh^{-1,-1,0}(L_{m-1}) \oplus \mathbb{F}^{\oplus 2} \cong AKh^{0,1,0}(L_m)$

$AKh^{0,-1,0}(L_{m-1}) \cong AKh^{1,1,0}(L_m)$

2. Next, let $(i-1, j-1, k)$ equal $(0,2,2)$. We now have:

$$0 \longrightarrow AKh^{-1,1,2}(L_{m-1}) \xrightarrow{\alpha} AKh^{0,3,2}(L_m) \xrightarrow{\beta} \mathbb{F}[0,2,2] \xrightarrow{\gamma} AKh^{0,1,2}(L_{m-1}) \xrightarrow{\delta} AKh^{1,3,2}(L_m) \longrightarrow 0$$

This time there are two possibilities this time for $Im(\gamma)$: $Im(\gamma) = \mathbb{F}$ and $Im(\gamma) = 0$. They result in:

(a) $AKh^{-1,1,2}(L_{m-1}) \cong AKh^{0,3,2}(L_m)$

$AKh^{0,1,2}(L_{m-1}) \cong AKh^{1,3,2}(L_m) \oplus \mathbb{F}$

(b) $AKh^{-1,1,2}(L_{m-1}) \oplus \mathbb{F} \cong AKh^{0,3,2}(L_m)$

$AKh^{0,1,2}(L_{m-1}) \cong AKh^{1,3,2}(L_m)$

3. Finally, let $(i-1, j-1, k)$ equal $(0,-2,-2)$. We have:

$$0 \longrightarrow AKh^{-1,-3,-2}(L_{m-1}) \xrightarrow{\alpha} AKh^{0,-1,-2}(L_m) \xrightarrow{\beta} \mathbb{F}[0,-2,-2] \xrightarrow{\gamma} AKh^{0,-3,-2}(L_{m-1}) \xrightarrow{\delta} AKh^{1,-1,-2}(L_m) \longrightarrow 0$$

There are again two possibilities of $Im(\gamma)$: $Im(\gamma) = \mathbb{F}$ and $Im(\gamma) = 0$. They result in:

(a) $AKh^{-1,-3,-2}(L_{m-1}) \cong AKh^{0,-1,-2}(L_m)$

$AKh^{0,-3,-2}(L_{m-1}) \cong AKh^{1,-1,-2}(L_m) \oplus \mathbb{F}$

(b) $AKh^{-1,-3,-2}(L_{m-1}) \oplus \mathbb{F} \cong AKh^{0,-1,-2}(L_m)$

$AKh^{0,-3,-2}(L_{m-1}) \cong AKh^{1,-1,-2}(L_m)$

The next thing to do is to apply the skein exact sequence repeatedly in order to express $AKh^*(L_m)$ in terms of $AKh^*(L_0)$. We start by noting that for $(i-1, j-1, k)$ and $(i, j-1, k)$ not equal to $(0,0,0)$,$(0,2,2)$ or $(0,-2,-2)$ we obtain:

$$\cdots \longrightarrow 0 \longrightarrow AKh^{i-m,j-2m,k}(L_0) \xrightarrow{\cong} AKh^{i,j,k}(L_m) \longrightarrow 0 \longrightarrow \cdots$$

That is, $AKh^*(L_m)$ contains the majority of $AKh^*(L_0)$ as a direct summand, but shifted in (i,j,k) gradings by $(m, 2m, 0)$. Further progress is hampered somewhat, since we do not know in general the connecting homomorphisms γ, nor any specific homology groups. We note, however, that we can substitute L_0 for L_{m-1} in the troublesome pieces of the exact sequence, which gives, for example:

$$0 \longrightarrow AKh^{-m,1-2m,0}(L_0) \xrightarrow{\alpha} AKh^{0,1,0}(L_m) \xrightarrow{\beta} \mathbb{F}^{\oplus 2}[0,0,0] \xrightarrow{\gamma} AKh^{-m+1,1-2m,0}(L_0) \xrightarrow{\delta} AKh^{1,1,0}(L_m) \longrightarrow 0$$

We then observe that, since AKh^* is always finite dimensional, if we take a sufficiently large m, $AKh^{-m,1-2m,0}(L_0)$ and $AKh^{-m+1,1-2m,0}(L_0)$ will be zero, which puts us in the case where $Im(\gamma) = 0$. Overall, this means that adding an extra twist when $m \gg 0$ will simply add in a four dimensional vector space — $\mathbb{F}^{\oplus 2}[0,1,0] \oplus \mathbb{F}[0,3,2] \oplus \mathbb{F}[0,-1,-2]$ — and bump everything else up by a grading shift of $(1,2,0)$.

Example 4.2.19. Perhaps an example will make the admittedly rather intense collection of sequences appear more illuminating. We will look at the single family of annular Sakuma knots $\mathcal{U}_m$ associated to the strongly invertible unknot $(\mathcal{U}, h_0)$, which are depicted in Figure 4.3. Using results obtained from *AKh.m*, a Mathematica program written by the author, we claim that $AKh^*(L_m)$ can be expressed as follows:

We will prove the claim by induction. When $m = 1$ the claim holds by a direct calculation. Assume it holds for $m = m'$. Now take $m = m' + 1$. From the discussion above we know that

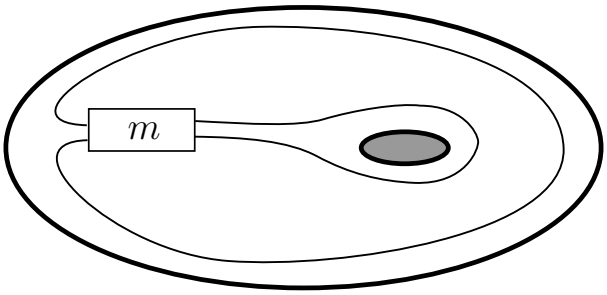

Figure 4.3: Diagram for $\mathcal{U}_m$

$\mathbf{q}\backslash\mathbf{s}$	0	1	2	$\cdots$	$\cdots$	$m-1$	m
-1	t^{-2}						
1	2	t^{-2}					
3	t^2	2	$\ddots$				
5		t^2	$\ddots$	$\ddots$			
$\vdots$			$\ddots$	$\ddots$			
$\vdots$				$\ddots$		t^{-2}	
$2m-1$						1	
$2m+1$						t^2	1

Table 4.1: Annular Khovanov homologies for $\mathcal{U}_m$, $m > 0$

for $(i-1, j-1, k)$ and $(i, j-1, k)$ not equal to $(0,0,0)$,$(0,2,2)$ or $(0,-2,-2)$ it must be the case that $AKh^{i-1,j-2,k}(L_{m'}) \cong AKh^{i,j,k}(L_{m'+1})$. In these three awkward cases we use the inductive hypothesis, which leaves us with $Im(\gamma) = 0$ each time. The claim therefore holds for $m = m' + 1$ too, and so it holds for all $m > 0$.

Returning to the general situation, we will briefly mention the case when $m < 0$. The details are very similar to the $m > 0$ case, so we will spare the sanity of the reader and jump straight to the key points. For a negative crossing $\times$, the 0-smoothing is $\asymp$ and the 1-smoothing is $)($. The skein exact sequence in this case has general form:

$$\cdots \longrightarrow AKh^{i,j+1,k}(\widehat{L}_{m+1}) \longrightarrow AKh^{i,j,k}(L_m) \longrightarrow AKh^{i+1,j+2,k}(L_{m+1})$$
$$AKh^{i+1,j+1,k}(\widehat{L}_{m+1}) \xrightarrow{\delta} AKh^{i+1,j,k}(L_m) \longrightarrow AKh^{i+2,j+2,k}(L_{m+1}) \longrightarrow \cdots$$

For $(i, j+1, k)$ and $(i+1, j+1, k)$ not equal to $(0,0,0)$, $(0,2,2)$ or $(0,-2,-2)$ we obtain:

$$\cdots \longrightarrow 0 \longrightarrow AKh^{i,j,k}(L_m) \xrightarrow{\cong} AKh^{i+1,j+2,k}(L_{m+1}) \longrightarrow 0 \longrightarrow \cdots$$

1. Let $(i+1, j+1, k)$ equal $(0,0,0)$. $Im(\delta)$ is either $\mathbb{F}^{\oplus 2}$, $\mathbb{F}$ or 0:

   (a) $AKh^{0,1,0}(L_{m+1}) \cong AKh^{-1,-1,0}(L_m)$

$$AKh^{1,1,0}(L_{m+1}) \oplus \mathbb{F}^{\oplus 2} \cong AKh^{0,-1,0}(L_m)$$

(b) $AKh^{0,1,0}(L_{m+1}) \oplus \mathbb{F} \cong AKh^{-1,-1,0}(L_m)$

$$AKh^{1,1,0}(L_{m+1}) \cong AKh^{0,-1,0}(L_m) \oplus \mathbb{F}$$

(c) $AKh^{0,1,0}(L_{m+1}) \cong AKh^{-1,-1,0}(L_m) \oplus \mathbb{F}^{\oplus 2}$

$$AKh^{1,1,0}(L_{m+1}) \cong AKh^{0,-1,0}(L_m)$$

2. Let $(i+1, j+1, k)$ equal $(0, 2, 2)$. $Im(\delta)$ is either $\mathbb{F}$ or 0:

(a) $AKh^{0,3,2}(L_{m+1}) \cong AKh^{-1,1,2}(L_m)$

$$AKh^{1,3,2}(L_{m+1}) \oplus \mathbb{F} \cong AKh^{0,1,2}(L_m)$$

(b) $AKh^{0,3,2}(L_{m+1}) \cong AKh^{-1,1,2}(L_m) \oplus \mathbb{F}$

$$AKh^{1,3,2}(L_{m+1}) \cong AKh^{0,1,2}(L_m)$$

3. Let $(i+1, j+1, k)$ equal $(0, -2, -2)$. $Im(\delta)$ is either $\mathbb{F}$ or 0:

(a) $AKh^{0,-1,-2}(L_{m+1}) \cong AKh^{-1,-3,-2}(L_m)$

$$AKh^{1,-1,-2}(L_{m+1}) \oplus \mathbb{F} \cong AKh^{0,-3,-2}(L_m)$$

(b) $AKh^{0,-1,-2}(L_{m+1}) \cong AKh^{-1,-3,-2}(L_m) \oplus \mathbb{F}$

$$AKh^{1,-1,-2}(L_{m+1}) \cong AKh^{0,-3,-2}(L_m)$$

Example 4.2.20. We will finish off the previous example by determining $AKh^*(L_m)$ when $m < 0$. Using another induction argument we obtain the following table:

$\mathbf{q}\backslash\mathbf{s}$	m	$m+1$	$m+2$	$\cdots$	$\cdots$	-1	0
$2m-1$	1	t^{-2}					
$2m+1$		1	t^{-2}				
$2m+3$		t^2	2	$\ddots$			
$2m+5$			t^2	$\ddots$	$\ddots$		
$\vdots$				$\ddots$	$\ddots$	t^{-2}	
$\vdots$					$\ddots$	2	t^{-2}
-1						t^2	2
1							t^2

Table 4.2: Annular Khovanov homologies for $\mathcal{U}_m$, $m < 0$

4.2.7 Framed unknot detection

Next, we will apply the skein exact sequence for annular Khovanov homology to the problem of unknot detection. Thanks to Corollary 4.2.18 we know that that annular Khovanov homology

detects the 0-framed strongly invertible unknot, but can we do any better? That is, can AKh detect any more of the framed strongly invertible unknots?

For a general annular Sakuma knot L_m (either $\mathcal{L}_m$ or $\mathcal{B}_m$), with, say $m > 0$, recall that the skein exact sequence tells us that adding an extra positive twist bumps the majority of the terms up by a grading shift of $(1, 2, 0)$. This means that the basis element of $AKh^*(L_m)$ with the highest i grading is not contained in $AKh^*(L_{m-1})$, so annular Khovanov homology distinguishes every L_m for $m > 0$ (similarly, it distinguishes every L_m for $m < 0$).

We recall a classical result from homological algebra known as the *Five lemma* ([78, Exercise 8.52]).

The Five Lemma. *Consider the commutative diagram of abelian groups, and suppose each row is an exact sequence:*

$$\begin{array}{ccccccccc} A & \xrightarrow{f} & B & \xrightarrow{g} & C & \xrightarrow{h} & D & \xrightarrow{j} & E \\ \downarrow{\scriptstyle l} & & \downarrow{\scriptstyle m} & & \downarrow{\scriptstyle n} & & \downarrow{\scriptstyle p} & & \downarrow{\scriptstyle q} \\ A' & \xrightarrow{r} & B' & \xrightarrow{s} & C' & \xrightarrow{t} & D' & \xrightarrow{u} & E' \end{array}$$

Suppose that m and p are isomorphisms, l is an epimorphism, and q is a monomorphism. Then n is an isomorphism.

Next comes the result:

Theorem 4.2.21. *Let D_{L_m} and $D_{\mathcal{U}_n}$ be two families of diagrams associated to a family of annular Sakuma knots L_m and the family of annular Sakuma knots $\mathcal{U}_n$ associated to the strongly invertible unknot. Suppose that $AKh^*(L_m) \cong AKh^*(\mathcal{U}_n)$, then $L_m \cong \mathcal{U}_n$.*

Proof. We will prove the result for $n \geq 0$ using induction. The proof for $n \leq 0$ runs in exactly the same way, but the skein exact sequences are slightly different.

First, let $n \geq 0$.

When $n = 0$, if $AKh^*(L_m) \cong AKh^*(\mathcal{U}_0)$ then Corollary 4.2.18 tells us that $L_m \cong \mathcal{U}_0$, so the statement holds for the base case.

Suppose that the statement holds for $n = x$, that is, $AKh^*(L_m) \cong AKh^*(\mathcal{U}_x)$ implies that $L_m \cong \mathcal{U}_x$. For $n = x+1$ we apply the skein exact sequence on both D_{L_m} and $D_{\mathcal{U}_{x+1}}$ simultaneously, which produces the following diagram:

$$\begin{array}{ccccccccc} \cdots \to AKh^{i,j+2,k}(L_{m+1}) & \longrightarrow & AKh^{i,j+1,k}(\widehat{L_m}) & \longrightarrow & AKh^{i,j,k}(L_m) & \longrightarrow & AKh^{i+1,j+2,k}(L_{m+1}) & \longrightarrow & AKh^{i+1,j+1,k}(\widehat{L_m}) \to \cdots \\ a\uparrow & & b\uparrow & & c\uparrow & & d\uparrow & & e\uparrow \\ \cdots \to AKh^{i,j+2,k}(\mathcal{U}_{x+1}) & \longrightarrow & AKh^{i,j+1,k}(\widehat{\mathcal{U}_x}) & \longrightarrow & AKh^{i,j,k}(\mathcal{U}_x) & \longrightarrow & AKh^{i+1,j+2,k}(\mathcal{U}_{x+1}) & \longrightarrow & AKh^{i+1,j+1,k}(\widehat{\mathcal{U}_x}) \to \cdots \end{array}$$

We immediately note that b and e are isomorphisms, since $\widehat{L_m} \cong \widehat{\mathcal{U}_x}$. Now, suppose that $AKh^*(L_{m+1}) \cong AKh^*(\mathcal{U}_{x+1})$, so in particular a and d are also isomorphisms. Then the Five

Lemma tell us c is an isomorphism too, and by the inductive hypothesis we have $L_m \cong \mathcal{U}_x$. Therefore, $L_{m+1} \cong \mathcal{U}_{x+1}$ and the statement holds for $n = x+1$. Hence, it holds for all $n \geq 0$. □

The above theorem tells us that annular Khovanov homology is a powerful tool, capable of detecting all framings on the strongly invertible unknot.

4.3 Watson's $\varkappa$ and its annular sidekick

The purpose of this section is to introduce an additional Khovanov-style invariant of strongly invertible knots, $\varkappa$, which was first defined by Watson [92]. As we shall see, $\varkappa$ takes the form of a $\mathbb{Z}$ graded, finite-dimensional vector space, and is extracted from the Khovanov homologies of the family of links obtained by closing up a representative of a Watson tangle. Watson's motivation when defining $\varkappa$ was to develop further applications of the graded information present in Khovanov homology. In recent years structural properties of Khovanov homology have given rise to a number of results of interest to the wider field of low-dimensional topology — for instance, Rasmussen's proof of the Milnor conjecture using the s invariant [73], or Kronheimer and Mrowka's proof that Khovanov homology detects the unknot [47]. Moreover, in the two aforementioned instances the structure exploited is not present in the Jones polynomial — which gives strong justification for studying the inner workings of Khovanov homology over its polynomial sibling.

Interestingly, Watson's $\varkappa$ differs from the invariants we have encountered thus far, as it is defined only on strongly invertible knots, with no alterations coming from a change of framing. On the other hand, its construction from a collection of Khovanov homology groups means it inherits many desirable qualities from Khovanov homology, namely, that of unknot detection and sensitivity to cheirality.

We then will bring Watson's ideas to bear on annular Sakuma knots. It turns out that a similar methodology can be applied to the collection of annular Sakuma knots we obtain from a strongly invertible knot, and in particular a $\varkappa$-like vector space can be obtained from their annular Khovanov homologies, which we will denote by $\varkappa_A$. Just as annular Khovanov homology has an additional grading coming from the annular data, so too does $\varkappa_A$ — it is in particular a $\mathbb{Z} \oplus \mathbb{Z}$ graded vector space. We have been unable to successfully prove $\varkappa_A$ is an invariant of strongly invertible knots, and only conjecture that it is.

4.3.1 Inverse and direct limits

The vector spaces $\varkappa$ and $\varkappa_A$ depend on some additional tools from homological algebra, which we will now detail. The key reference for this section is Rotman's textbook [78, Chapter 7].

The twin concepts we will utilise are *inverse limits* and *direct limits*. They are calculated from *inverse systems* and *direct systems*, which informally are collections of R-modules, which are indexed, along with a collection of maps between them; in inverse systems the maps always lower the indexing, and in direct systems they always raise them. The two limits should be thought

of as constructions which, in a sense, 'glue' the R-modules in the relevent system together. More specifically, the inverse limit generalises intersections; whilst the direct limit generalises unions.

Let's make the above more precise.

Definition 4.3.1. Let I be a partially ordered set, A_i be an I-indexed family of R-modules, and $f_{i,j}$ be a family of R-module maps for all $i \geq j$ such that:

1. $f_{i,i}$ is the identity of A_i for all $i \in I$
2. $f_{i,k} = f_{j,k} f_{i,j}$ for all $i \geq j \geq k$.

The pair $\{A_i, f_{i,j}\}$ is called an *inverse system* over I.

If we are given an inverse system we can form the *inverse limit*.

Definition 4.3.2. Let $\{A_i, f_{i,j}\}$ be an inverse system of R-modules over a partially ordered set I. The *inverse limit* consists of a pair $(\underset{\leftarrow}{A_i}, \alpha_i)$, where $\underset{\leftarrow}{A_i}$ is an R-module and $\{\alpha_i : \underset{\leftarrow}{A_i} \to A_i\}$ is a family of R-module maps such that:

1. $f_{i,j}\alpha_i = \alpha_j$ whenever $i \geq j$
2. For every pair (X, ι_i) such that $\iota_i : X \to A_i$ and $f_{i,j}\iota_i = \iota_j$ for all $i \geq j$ there exists a unique map $\sigma : X \to \underset{\leftarrow}{A_i}$ such that the following diagram commutes:

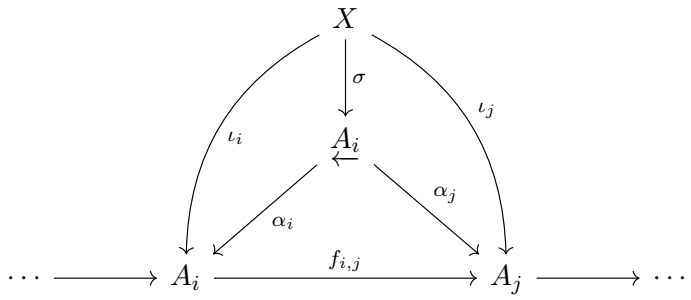

For explicit calculations the above definition is not particularly useful. However, it is possible to describe the inverse limit more concretely. The proof of the next result appears in Rotman [78, Proposition 7.90].

Proposition 4.3.3. *The inverse limit of any inverse system $\{A_i, f_{i,j}\}$ of R-modules over a partially ordered set I exists. Furthermore, let p_i be the projection of the direct product $\prod_i A_i$ to A_i and L be the submodule of $\prod_i A_i$ given by*

$$L = \{\underline{a} \in \prod_i A_i : a_j = f_{i,j}(a_i)\ \forall i \geq j\}.$$

Then the direct limit can be expressed as (L, α_i), where $\alpha_i = p_i|L$.

In other words, an element of the inverse limit can be viewed as a sequence of elements, one from

each A_i, such that for all $i \geq j$, $a_j = f_{i,j}(a_i)$.

Next, we formally define direct systems and direct limits. Although similar in appearance to inverse systems and limits, there are a few key differences in their construction.

Definition 4.3.4. Let I be a partially ordered set, B_i be an I-indexed family of R-modules, and $g_{i,j}$ be a family of R-module maps for all $i \leq j$ such that:

1. $g_{i,i}$ is the identity of B_i for all $i \in \mathbb{Z}$
2. $g_{i,k} = g_{j,k} g_{i,j}$ for all $i \leq j \leq k$.

The pair $\{B_i, g_{i,j}\}$ is called a *direct system* over I.

Definition 4.3.5. Let $\{B_i, g_{i,j}\}$ be a direct system of R-modules over a partially ordered set I. The *direct limit* consists of a pair $(\underrightarrow{B_i}, \beta_i)$, where $\underrightarrow{B_i}$ is an R-module and $\{\beta_i : B_i \to \underrightarrow{B_i}, i \in \mathbb{Z}\}$ is a family of R-module maps such that:

1. $\beta_j g_{i,j} = \beta_i$ whenever $i \leq j$
2. For every pair (Y, ϕ_i) such that $\phi_i : B_i \to Y$ and $\phi_i = \phi_j g_{i,j}$ for all $i \leq j$ there exists a unique map $\zeta : \underrightarrow{B_i} \to Y$ such that the following diagram commutes:

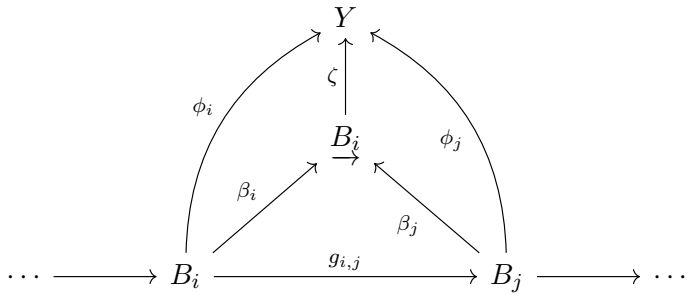

As Rotman notes, the notation for a direct limit is somewhat deficient as it does not detail the maps of the corresponding direct system, which do affect the direct limit. However, this is standard notational practice.

As for inverse limits, the above definition is not particularly useful when we are required to make an explicit calculation. However, it is possible to describe the direct limit in a few alternative ways. The next result appears in Rotman [78, Proposition 7.94].

Proposition 4.3.6. *The direct limit of any direct system $\{B_i, g_{i,j}\}$ of R-modules over a partially ordered index set I exists. Furthermore, let λ_i be the injection of B_i into the sum $\bigoplus_i B_i$ and S be the submodule of $\bigoplus_i B_i$ generated by all elements of the form $\lambda_j(f_{i,j}(b_i)) - \lambda_i(b_i)$. Then the direct limit can be expressed as $(\underrightarrow{B_i}, \beta_i)$, where*

$$\underrightarrow{B_i} \cong \bigoplus_i B_i / S$$

and $\beta_i : b_i \mapsto \lambda_i(b_i) + S$.

Alternatively, we can use the above result to view the direct limit in terms of an equivalence relation. Namely,

$$\underset{\rightarrow}{B_i} \cong \bigoplus_i B_i / \sim$$

where $b_i \sim b_j$ if there exists a k such that $g_{i,k}(b_i) = g_{j,k}(b_j)$, and $\beta_i : b_i \mapsto [b_i]_\sim$.

We will also require some extra theory regarding the relationship between direct limits and short exact sequences. Firstly, we introduce a method of relating two direct systems over the same index set.

Definition 4.3.7. Let $\{A_i, f_{i,j}\}$ and $\{B_i, g_{i,j}\}$ be direct systems over the same index set I. A *transformation* $r : \{A_i, f_{i,j}\} \to \{B_i, g_{i,j}\}$ is an indexed family of maps

$$r = \{r_i : A_i \to B_i\}$$

such that the following diagram commutes for all $i \leq j$:

$$\begin{array}{ccc} A_i & \xrightarrow{f_{i,j}} & A_j \\ \downarrow{\scriptstyle r_i} & & \downarrow{\scriptstyle r_j} \\ B_i & \xrightarrow{g_{i,j}} & B_j \end{array}$$

A transformation $r : \{A_i, f_{i,j}\} \to \{B_i, g_{i,j}\}$ induces a map $\underset{\rightarrow}{r} : \underset{\rightarrow}{A_i} \to \underset{\rightarrow}{B_i}$. We will not explicitly define this induced map, but the details can be found in Rotman.

Definition 4.3.8. Let I be a partially ordered set. We say I is *directed* if for every pair $i, j \in I$ there exists a $k \in I$ such that $i \leq k$ and $j \leq k$.

In the case where the index set is directed the direct limit preserves short exact sequences. The following result appears in Rotman [78, Proposition 7.100].

Proposition 4.3.9. *Let I be a directed set, and let $\{A_i, f_{i,j}\}$, $\{B_i, g_{i,j}\}$, and $\{C_i, h_{i,j}\}$ be direct systems over I. If $r : \{A_i, f_{i,j}\} \to \{B_i, g_{i,j}\}$ and $s : \{B_i, g_{i,j}\} \to \{C_i, h_{i,j}\}$ are transformations, and if*

$$0 \to A_i \xrightarrow{r_i} B_i \xrightarrow{s_i} C_i \to 0$$

is exact for all $i \in I$, then there is a short exact sequence

$$0 \to \underset{\rightarrow}{A_i} \to \underset{\rightarrow}{B_i} \to \underset{\rightarrow}{C_i} \to 0.$$

4.3.2 $\varkappa$ invariant

We now come to Watson's construction of the $\varkappa$ invariant. All proofs of the results in this section can be found in Watson's paper [92].

To calculate $\varkappa$ we begin by taking a strongly invertible knot (K, h) and constructing its Watson tangle T. We then fix a diagram D_T and consider the collection of link diagrams $D_{T(m)}$ obtained by closing D_T with various amounts of extra twists. Depict D_T as in Figure 2.8 and orient both strands in the same direction, from $I \times \{0\}$ to $I \times \{1\}$. This choice of orientation means that $\times$ is a positive crossing — note that this is different to the situation we had in the previous chapter with annular Sakuma knots, as there the strands in the smoothed crossing were oriented in opposite directions.

Next, we calculate the reduced Khovanov homologies of each $T(m)$ over $\mathbb{Z}/2\mathbb{Z}$, and apply the skein exact sequence for $m > 0$ when $\times$ is smoothed. The 0-smoothing $\asymp$ is simply $D_{T(m-1)}$, and the 1-smoothing $)($ is equivalent to the two-component unlink $D_{T(\frac{1}{0})}$ we get when joining the end points in $I \times \{0\}$ together and the end points in $I \times \{1\}$ together; we will denote this link diagram by $D_{X(m-1)}$. Observe that $D_{X(m-1)}$ does not inherit the orientation from $D_{T(m-1)}$.

Suppose there are n_- negative crossings in $D_{T(m)}$ with a braid-like orientation on the strands and c_T negative crossings when the orientation on one strand is reversed. The value of c, the number of negative crossings in $D_{X(m-1)}$ minus the number in $D_{T(m)}$, is

$$c = (c_T + m - 1) - n_-$$

and the long exact sequence is:

$$\cdots \longrightarrow \widetilde{Kh}^{i-c-1,j-3c-2}(X(m-1)) \longrightarrow \widetilde{Kh}^{i,j}(T(m)) \xrightarrow{f_m} \widetilde{Kh}^{i,j-1}(T(m-1))$$
$$\longrightarrow \widetilde{Kh}^{i,j-2}(X(m-1)) \longrightarrow \widetilde{Kh}^{i+1,j}(T(m)) \xrightarrow{f_m} \widetilde{Kh}^{i+1,j-1}(T(m-1)) \longrightarrow \cdots$$

Now we will do the case when m is negative. This time we smooth $\times$, which has 0-smoothing $)($ and 1-smoothing $\asymp$. The value of c' is

$$c' = c_T - (n_- + m)$$

and the long exact sequence is:

$$\cdots \longrightarrow \widetilde{Kh}^{i,j+1}(T(m+1)) \xrightarrow{f_{m+1}} \widetilde{Kh}^{i,j}(T(m)) \longrightarrow \widetilde{Kh}^{i-c',j-3c'-1}(X(m+1))$$
$$\longrightarrow \widetilde{Kh}^{i+1,j+1}(T(m+1)) \xrightarrow{f_{m+1}} \widetilde{Kh}^{i+1,j}(T(m)) \longrightarrow \widetilde{Kh}^{i-c'+1,j-3c'-1}(X(m+1)) \longrightarrow \cdots$$

We extract from the skein exact sequence an inverse system of $\mathbb{Z}/2\mathbb{Z}$ vector spaces over $\mathbb{Z}$. Set $A_m = \widetilde{Kh}^*(T(m))$, and $f_m : \widetilde{Kh}^*(T(m)) \to \widetilde{Kh}^*(T(m-1))$ for $m \in \mathbb{Z}$. The collection of groups

and maps $\{A_m, f_m\}$ forms an inverse system — the map $f_{m,n}$ is defined to be the composition $f_n f_{n+1} \dots f_{m-1} f_m$. We note additionally that the maps f_m preserve the homological grading, and so the inverse system is $\mathbb{Z}$ graded.

We then form the inverse limit of this inverse system, and denote the underlying vector space by $\underleftarrow{Kh}(T)$. Watson proves that this vector space is an invariant of the Watson tangle [92, Proposition 4], and hence of its strongly invertible knot (K, h).

Proposition 4.3.10 (Watson, 2014)**.** *The vector space $\underleftarrow{Kh}(T)$ is a $\mathbb{Z}$ graded invariant of the sutured tangle T, up to isomorphism.*

Unfortunately, it turns out that $\underleftarrow{Kh}(T)$ is not in general finite-dimensional. To remedy this Watson defines the $\varkappa$ invariant as follows:

Definition 4.3.11. Let (K, h) be a strongly invertible knot and $\underleftarrow{Kh}(T)$ be as above. Consider the subspace $\mathbf{K} \subset \underleftarrow{Kh}(T)$ consisting of all sequences $\underline{a}$ such that $a_i = 0$ for $i \ll 0$. Denote the quotient of $\underleftarrow{Kh}(T)/\mathbf{K}$ by $\varkappa(K, h)$.

Watson then proves that $\varkappa(K, h)$ is a finite dimensional vector space, and is also an invariant of strong inversions [92, Proposition 11].

Proposition 4.3.12 (Watson, 2014)**.** *The vector space $\varkappa(K, h)$ is a finite dimensional $\mathbb{Z}$ graded invariant of the strongly invertible knot (K, h), up to isomorphism.*

Remark. We should re-emphasise at this point that $\varkappa$ does not depend at all on longitudes framings of (K, h), since they are all subsumed within its definition — it is therefore an honest invariant of strongly invertible knots.

Due to the Khovanov-style nature of $\varkappa$ it is natural to ask whether it carries the usual properties of unknot detection and sensitivity to cheirality.

Theorem 4.3.13 (Watson, 2014)**.** *Let (K, h) be a strongly invertible knot. Then $\varkappa(K, h) = 0$ if and only if K is the unknot.*

Proposition 4.3.14 (Watson, 2014)**.** *Let (K, h) be a strongly invertible knot, and consider its strongly invertible mirror $(\overline{K}, \overline{h})$. Then $\varkappa^i(K, h) \cong \varkappa^{-i}(\overline{K}, \overline{h})$.*

Example 4.3.15. Let (K, h) be the right-handed trefoil with its unique strong inversion. Watson calculates $\varkappa(K, h)$:

$$\varkappa(K, h) \cong \mathbb{Z}/2\mathbb{Z}[-5] \oplus \mathbb{Z}/2\mathbb{Z}[-3] \oplus \mathbb{Z}/2\mathbb{Z}[-2] \oplus \mathbb{Z}/2\mathbb{Z}[0].$$

Hence, we obtain the following for the strongly invertible mirror:

$$\varkappa(\overline{K}, \overline{h}) \cong \mathbb{Z}/2\mathbb{Z}[0] \oplus \mathbb{Z}/2\mathbb{Z}[2] \oplus \mathbb{Z}/2\mathbb{Z}[3] \oplus \mathbb{Z}/2\mathbb{Z}[5].$$

As a consequence of Proposition 4.3.14 and [79, Proposition 3.4], in certain cases $\varkappa$ is palindromic.

Corollary 4.3.16 (Watson, 2014). *Let K be an amphicheiral knot and suppose that h is a unique strong inversion on K. Then $(K,h) \cong (\overline{K},h)$ and so $\varkappa^i(K,h) \cong \varkappa^{-i}(K,h)$.*

4.3.3 $\varkappa_A$ invariant

Now we turn our attention back to the annular setting, and examine the families of annular Sakuma knots obtained by changing the framing of the longitudes in Sakuma's construction.

As we did in Chapter 3, we construct a family of annular Sakuma knots and fix a family of diagrams for them, which we denote D_{L_m}. As the members of D_{L_m} are related by the skein exact sequence in their annular Khovanov homologies, we find ourselves in a similar situation to Watson.

We reproduce the annular skein exact sequences once more:

For $m > 0$:

$$\cdots \longrightarrow AKh^{i-1,j-2,k}(L_{m-1}) \xrightarrow{g_{m-1}} AKh^{i,j,k}(L_m) \longrightarrow AKh^{i,j-1,k}(\widehat{L}_{m-1})$$
$$AKh^{i,j-2,k}(L_{m-1}) \xrightarrow{g_{m-1}} AKh^{i+1,j,k}(L_m) \longrightarrow AKh^{i+1,j-1,k}(\widehat{L}_{m-1}) \longrightarrow \cdots$$

For $m < 0$:

$$\cdots \longrightarrow AKh^{i,j+1,k}(\widehat{L}_{m+1}) \longrightarrow AKh^{i,j,k}(L_m) \xrightarrow{g_m} AKh^{i+1,j+2,k}(L_{m+1})$$
$$AKh^{i+1,j+1,k}(\widehat{L}_{m+1}) \longrightarrow AKh^{i+1,j,k}(L_m) \xrightarrow{g_m} AKh^{i+2,j+2,k}(L_{m+1}) \longrightarrow \cdots$$

Now set $B_m = AKh^*(L_m)$ and let $g_m : AKh^*(L_m) \to AKh^*(L_{m+1})$ be the map from the skein exact sequence. We observe that the pair $\{B_m, g_m\}$ forms a direct system of $\mathbb{F}$ vector spaces over $\mathbb{Z}$ — the map $g_{m,n}$ is simply defined to be the composition $g_n g_{n-1} \dots g_{m+1} g_m$.

We note that this time the g_m maps do not preserve the i grading. We therefore define a new $\mathbb{Z}$ grading r — for a basis element $x \in AKh^*(L_m)$ we set

$$r(x) = 2i(x) - j(x)$$

and observe that this grading is preserved by the g_m maps. The r grading records the diagonal a basis element lies in in the s/q plots we have been using to record AKh, and thus should be thought of as the counterpart of the δ grading Watson uses in [92]. This diagonal grading is a standard viewpoint from which to study Khovanov homology; see for example work of Shumakovitch [84]. We note additionally that the k grading is also preserved by the maps g_m, and so the direct system is $\mathbb{Z} \oplus \mathbb{Z}$ graded — if we wish to emphasise this information we will write $\{B_m^{r,k}, g_m\}$.

In general we do not know the precise values for the g_m maps. However, by using the analysis

of the skein exact sequence we provided earlier, we find that they are either an isomorphism, a surjection, or an injection. Moreover, there are only a few options for what their kernels and images can be. Namely, a g_m map is exactly one of the following:

1. Isomorphism
2. Surjection with kernel $\mathbb{F}$
3. Surjection with kernel $\mathbb{F} \oplus \mathbb{F}$
4. Injection with cokernel $\mathbb{F}$
5. Injection with cokernel $\mathbb{F} \oplus \mathbb{F}$

As a result, if we know what $B_m^{r,k}$ and $B_{m+1}^{r,k}$ are then the value of $\dim(B_{m+1}^{r,k}) - \dim(B_m^{r,k})$, which will be one of $\{-2,-1,0,1,2\}$, tells us exactly which one of the five options g_m is.

In certain circumstances we require even less information to determine g_m.

Lemma 4.3.17. *Let $g_m : B_m^{r,k} \to B_{m+1}^{r,k}$ be as above.*

- *For $r \notin \{\pm 1, \pm 3\}$ g_m is an isomorphism.*
- *For $k \notin \{0, \pm 2\}$ g_m is an isomorphism.*

Proof. Recall that for $m > 0$ and $(i-1, j-1, k)$, $(i, j-1, k)$ not equal to $(0,0,0)$,$(0,2,2)$ or $(0,-2,-2)$; and for $m < 0$ and $(i, j+1, k)$, $(i+1, j+1, k)$ not equal to $(0,0,0)$, $(0,2,2)$ or $(0,-2,-2)$ the exact sequence simplifies and g_m is an isomorphism. In other words, for $r \notin \{\pm 1, \pm 3\}$ and for $k \notin \{0, \pm 2\}$ g_m is an isomorphism. □

We next form the direct limit of $\{B_m, g_m\}$, which we denote $(\underrightarrow{AKh}, \beta_m)$. In all that follows we will view the direct limit as

$$\underrightarrow{AKh} \cong \bigoplus_{m \in \mathbb{Z}} B_m / \sim$$

where $b_m \sim b_n$ if there exists an $x \in \mathbb{Z}$ such that $g_{m,x}(b_m) = g_{n,x}(b_n)$, and $\beta_m : b_m \mapsto [b_m]_\sim$. Since the g_m maps preserve the $\mathbb{Z} \oplus \mathbb{Z}$ grading it is immediate that the vector space $\underrightarrow{AKh}$ is also $\mathbb{Z} \oplus \mathbb{Z}$ graded.

Conjecture. *Let (K, h) be a strongly invertible knot. The vector space $\underrightarrow{AKh}$ is a $\mathbb{Z} \oplus \mathbb{Z}$ graded invariant of (K, h).*

The author suspects that the above result is true, but has been unable to prove it successfully.

We find that, as Watson did for his invariant, $\underrightarrow{AKh}$ is not finite dimensional. This is because adding an extra twist when $m \gg 0$ simply adds a four dimensional vector space to B_m, namely $\mathbb{F}^{\oplus 2}[-1,0] \oplus \mathbb{F}[-3,2] \oplus \mathbb{F}[1,-2]$. These new generators will be representatives of distinct equivalence classes, which will not have any representatives in any of the previous $B_m^{r,k}$. This observation motivates our definition for $\varkappa_A$.

Definition 4.3.18. Let (K,h) be a strongly invertible knot with direct system $\{B_m, g_m\}$ and direct limit $(\underrightarrow{AKh}, \beta_m)$ as above. Define $\varkappa_A$ as follows:

$$\varkappa_A(K,h) := \{[b] \in \underrightarrow{AKh} : [b] \in Im(\beta_m)\ \forall m \in \mathbb{Z}\}$$

Said another way, $\varkappa_A$ is all the equivalence classes in the direct limit with a non-zero representative in *every* B_m. When we need to specify which family of annular knots we are calculating with, we will write $\varkappa_A(K,h,\mathcal{B})$ or $\varkappa_A(K,h,\mathcal{L})$.

Conjecture. *The vector space $\varkappa_A(K,h)$ is a finite dimensional $\mathbb{Z}\oplus\mathbb{Z}$ graded invariant of strongly invertible knots. In particular,*

$$dim(\varkappa_A) \leq \min_{m\in\mathbb{Z}}\ dim(B_m).$$

Although we have not been able to prove $\varkappa_A$ is an invariant, we will show that it is finite dimensional. Recall that β_m sends each $b_m \in B_m$ to its equivalence class $[b_m]$. Therefore, since every B_m is a finite dimensional vector space it follows that the images of the β_m maps are also finite dimensional. As $\varkappa_A$ cannot contain any more distinct equivalence classes than those in the image of a β_m, we have $\dim(\varkappa_A) \leq \dim(B_m)$ for every $m \in \mathbb{Z}$ and the result follows.

Remark. Like $\varkappa$, $\varkappa_A$ has the framing information from the strongly invertible knot subsumed into its construction. Philosophically, one way in which to view $\varkappa_A$ is as a construction which determines the pieces common to all $AKh(L_m)$ groups, ignoring generators which are added or removed as m increases.

In order to determine $\varkappa_A$ for an actual example, we express the $AKh(L_m)$ groups for each value of m in a table, where numerical entries stand for copies of $\mathbb{F}$, and a power of t indicates the k gradings of each copy of $\mathbb{F}$. We do not explicitly include the g_m maps in the table, however, as we noted before, they are either isomorphisms, surjections, or injections, and their kernels and images can be determined by calculating $\dim(B^{r,k}_{m+1}) - \dim(B^{r,k}_m)$.

As we know the g_m maps are surjective, injective, or both, we know that a graded copy of $\mathbb{F}$ in a row is either sent to a similarly graded copy of $\mathbb{F}$ in the row above, or is sent to 0. In the first case, the two generators are in the same equivalence class in $\underrightarrow{AKh}$; whilst in the second the generator is equivalent to 0. As a consequence of these observations we can use the table to view the equivalence classes in $\underrightarrow{AKh}$ — the 'path' a generator takes through the table, that is, its collection of its images under the g_m maps, represents an equivalence class. It is important to note, however, that the same equivalence class can represented by multiple paths, as multiple generators in the same $B^{r,k}_m$ might be equivalent. In particular, in order to determine $\varkappa_A$ from the table we look for equivalence classes with a representative in every B_m — in other words, for graded copies of $\mathbb{F}$ which are present in every row.

Example 4.3.19. Take the strongly invertible unknot $(\mathcal{U}, h_0)$, and let $\mathcal{U}_m$ be its single family of annular Sakuma knots. From Examples 4.2.19 and 4.2.20 we know the annular Khovanov homology groups for every $\mathcal{U}_m$, and we display a few of them in a section of the table.

$B_m \backslash r$	-3	-1	1	3
$\vdots$				
B_2	$2t^2$	4	$2t^{-2}$	0
B_1	t^2	2	t^{-2}	0
B_0	0	1	1	0
B_{-1}	0	t^2	2	t^{-2}
B_{-2}	0	$2t^2$	4	$2t^{-2}$
$\vdots$				

Table 4.3: Annular Khovanov homologies comprising $\varkappa_A(\mathcal{U}, h)$

Examining the table, we see there are no graded copies of $\mathbb{Q}$ which are present in every row. Hence, there are no equivalence classes in $\underrightarrow{AKh}$ with a non-zero representative in every B_m, and so $\varkappa_A(\mathcal{U}, h_0) = 0$.

Remark. Recall the spectral sequence from AKh to Kh obtained by taking homology with respect to the remaining piece of the Khovanov differential ∂_{-2}. As every annular Sakuma knot is unknotted in S^3 we can observe for each m how B_m collapses to something 2-dimensional. The Khovanov homology of the unknot has r gradings ± 1, and so after running the spectral sequence there must be a generator remaining in the $r = 1$ column, and one in the $r = -1$ columnn. Also, $\deg(\partial_{-2}) = (1, 0, -2)$, so ∂_{-2} raises the r grading by 2. Using these two pieces of information we can see the action of ∂_{-2} on the AKh generators in each row: in general it takes a power of t^k in column r, and sends it to a power of t^{k-2} in column $r + 2$.

In the following two examples the tabulated annular Khovanov homologies were calculated by $AKh.m$ — we then conjecture that the B_m groups follow the pattern as suggested by the tabulated groups. The results of the two examples, therefore, should only be taken as educated guesses.

Example 4.3.20. Consider $(3_1, h)$, the trefoil with its unique strong inversion. Form the various Sakuma links $\mathbb{L} = \mathcal{B} \cup \mathcal{L}$ and consider the family of 'branch-set' annular Sakuma knots $\mathcal{B}_m$ depicted in Figure 4.4. The annular Khovanov homologies of a selection of $\mathcal{B}_m$ are outlined in the table below — for values of m outside those tabulated we conjecture that the values of B_m

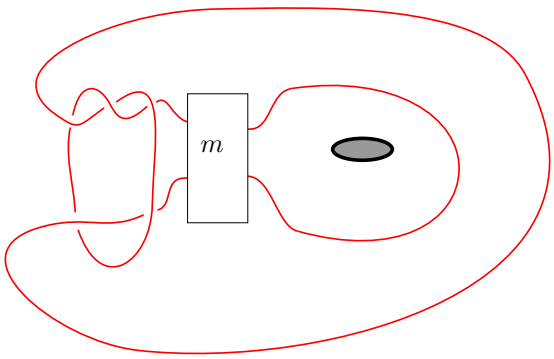

Figure 4.4: 'Branch-set' annular Sakuma knots associated to $(3_1, h)$

continue as suggested by the table.

$B_m \backslash r$	-3	-1	1	3
$\vdots$				
B_5	$3t^2$	$4t^2+6$	$8+3t^{-2}$	$4t^{-2}$
B_4	$2t^2$	$4t^2+4$	$8+2t^{-2}$	$4t^{-2}$
B_3	t^2	$4t^2+2$	$8+t^{-2}$	$4t^{-2}$
B_2	0	$4t^2+1$	9	$4t^{-2}$
B_1	0	$5t^2$	10	$5t^{-2}$
B_0	0	$6t^2$	12	$6t^{-2}$
B_{-1}	0	$7t^2$	14	$7t^{-2}$
B_{-2}	0	$8t^2$	16	$8t^{-2}$
$\vdots$				

Table 4.4: Annular Khovanov homologies comprising $\varkappa_A(3_1, h, \mathcal{B})$

We can easily see which copies of $\mathbb{Q}$ are present in every row. Hence,

$$\varkappa_A(3_1, h, \mathcal{B}) \cong \mathbb{Q}^{\oplus 4}[-1, 2] \oplus \mathbb{Q}^{\oplus 8}[1, 0] \oplus \mathbb{Q}^{\oplus 4}[3, -2].$$

Example 4.3.21. We also calculate $\varkappa_A(3_1, h, \mathcal{L})$, where the family $\mathcal{L}_m$ is depicted in Figure 4.5. As before, for values of m outside those tabulated we conjecture that the values of B_m continue as suggested by the table.

$B_m \backslash r$	-5	-3	-1	1	3
$\vdots$					
B_3	$2t^4$	$9t^2$	$2t^2+14$	$4+9t^{-2}$	$2t^{-2}+2t^{-4}$
B_2	$2t^4$	$8t^2$	$2t^2+12$	$4+8t^{-2}$	$2t^{-2}+2t^{-4}$
B_1	$2t^4$	$7t^2$	$2t^2+10$	$4+7t^{-2}$	$2t^{-2}+2t^{-4}$
B_0	$2t^4$	$6t^2$	$2t^2+9$	$5+6t^{-2}$	$2t^{-2}+2t^{-4}$
B_{-1}	$2t^4$	$6t^2$	$3t^2+8$	$6+6t^{-2}$	$3t^{-2}+2t^{-4}$
B_{-2}	$2t^4$	$6t^2$	$4t^2+8$	$8+6t^{-2}$	$4t^{-2}+2t^{-4}$
$\vdots$					

Table 4.5: Annular Khovanov homologies comprising $\varkappa_A(3_1, h, \mathcal{L})$

Interestingly, in this example we have higher k gradings appearing, as well as an extra r grading. Lemma 4.3.17 tells us that g_m is an isomorphism on those $B_m^{r,k}$, and so the equivalence classes of $\underrightarrow{AKh}$ with these gradings must be in $\varkappa_A$. Once more, we read off the values of $\varkappa_A$:

$$\begin{aligned}\varkappa_A(3_1, h, \mathcal{L}) \cong \quad & \mathbb{Q}^{\oplus 2}[-5, 4] \oplus \mathbb{Q}^{\oplus 6}[-3, 2] \oplus \mathbb{Q}^{\oplus 8}[-1, 0] \oplus \mathbb{Q}^{\oplus 2}[-1, 2] \oplus \\ & \mathbb{Q}^{\oplus 6}[1, -2] \oplus \mathbb{Q}^{\oplus 4}[1, 0] \oplus \mathbb{Q}^{\oplus 2}[3, -2] \oplus \mathbb{Q}^{\oplus 2}[3, -4]\end{aligned}$$

We conclude this section by touching upon some interesting properties of $\varkappa_A$.

First we consider the effect of $\varkappa_A$ on strongly invertible mirrors. Due to the construction of $\varkappa_A$

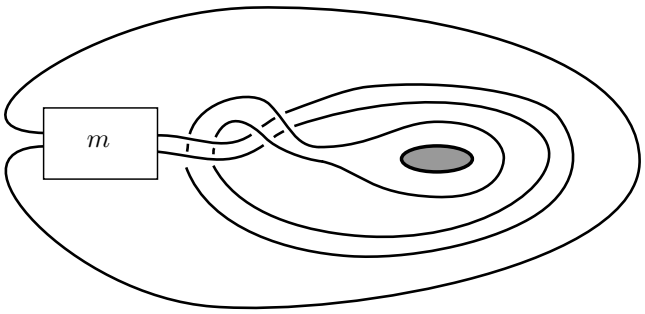

Figure 4.5: 'Longitude' annular Sakuma knots associated to $(3_1, h)$

from the direct limit of annular Khovanov homology groups, we should expect $\varkappa_A$ to behave in a similar fashion on the mirror images of a family of annular Sakuma links. We conjecture the following result, which is simply Proposition 4.3.14 adapted for $\varkappa_A$.

Conjecture. *Let (K, h) be a strongly invertible knot, and consider its strongly invertible mirror $(\overline{K}, h)$. Then $\varkappa^{r,k}(K, h) \cong \varkappa^{-r,-k}(\overline{K}, h)$.*

An immediate corollary of the above conjecture concerns amphicheiral strongly invertible knots with a unique strong inversion; the following is simply Corollary 4.3.16 for $\varkappa_A$.

Conjecture. *Let K be an amphicheiral knot, and suppose that h is a unique strong inversion on K. Then $(K, h) \cong (\overline{K}, h)$ and so $\varkappa_A^{r,k}(K, h) \cong \varkappa_A^{-r,-k}(K, h)$ for all r, k.*

For the remainder of the section we shall assume that $\varkappa_A$ is an invariant of strongly invertible knots, and will end with yet another unknot detection proof. Due to its close relationship with $\varkappa$, we would expect $\varkappa_A$ to also be able to detect the strongly invertible unknot $(\mathcal{U}, h_0)$ — this turns out to indeed be the case. Before we state the proof we require a few supporting results.

Corollary 4.3.22. *Let (K, h) be a strongly invertible knot and L_m be a family of annular Sakuma knots. Suppose that $\varkappa_A(K, h, L) = 0$. Then for all $B_m^{r,k}$ the r gradings are supported only in $r \in \{\pm 1, \pm 3\}$, and the k gradings are supported only for $k \in \{0, \pm 2\}$.*

Proof. This follows from Lemma 4.3.17. We know that for $B_m^{r,k}$ with $r \notin \{\pm 1, \pm 3\}$ and $k \notin \{0, \pm 2\}$ the g_m maps are isomorphisms. Hence, any generator of a $B_m^{r,k}$ with $r \notin \{\pm 1, \pm 3\}$ or $k \notin \{0, \pm 2\}$ is present in all rows of our table, and hence represents a non-zero element of $\varkappa_A(K, h, L)$. But now we have a contradiction, and so there can be so such generators in any $B_m^{r,k}$. □

Lemma 4.3.23. *Let L be an annular Sakuma knot, and let x be a generator of $AKh^*(L)$ with gradings (r, k) where k is non-zero. Then there is a generator x' with gradings $(r + 2k, -k)$.*

Proof. On the level of chain complexes, a generator x of the annular Khovanov chain complex can be paired with another generator x', which we define to be the generator obtained by swapping all v_+s for v_-s and w_+s for w_-s, and vice versa. Suppose x has k grading κ; then x' has k grading

$-\kappa$. We note that the i gradings of x and x' are the same, and their j gradings differ by 2κ. Hence, their r gradings differ by -2κ.

Now, we claim if x is a representative of a homology class of AKh, then so is x'. By considering the ∂_0 piece of the Khovanov differential (4.9), we see that if a basis element is in the kernel of ∂_0 and we change a w_+ to a w_- or vice versa the resulting element is also in the kernel. Hence, if $x \in Ker(\partial_0)$, then so is x'. Furthermore, we see also that if x is not in the image of ∂_0, then neither is x'. Therefore, if x is a representative of a homology class, then so is x'. □

Theorem 4.3.24. *Let (K,h) be a strongly invertible knot and L_m be a family of annular Sakuma knots. Suppose $\varkappa_A(K,h,L) = 0$. Then $L_m = \mathcal{U}_m$, and therefore $(K,h) \cong (\mathcal{U}, h_0)$.*

Proof. We start by applying Lemma 4.3.22, so we know that the r gradings of the $B_m^{r,k}$ are supported only for $r \in \{\pm 1, \pm 3\}$, and the k gradings are only supported for $k \in \{0, \pm 2\}$.

Next we claim that there are no generators in any B_m with (r,k) gradings $(3,0)$ or $(-3,0)$. If there were there would have to be generators with gradings $(5,-2)$ and $(-5,2)$ in order for B_m to collapse to the Khovanov homology of the unknot in S^3, but we have shown there are no such r gradings permissable. For similar reasons, there are no generators with gradings $(3,2)$ or $(-3,-2)$.

We next turn to the skein exact sequence. We restate, in our new notation, the two options for the relationships between $B_{m-1}^{1,-2}$ and $B_m^{1,-2}$ and $B_{m-1}^{3,-2}$ and $B_m^{3,-2}$.

1. $B_{m-1}^{1,-2} \cong B_m^{1,-2}$

   $B_{m-1}^{3,-2} \cong B_m^{3,-2} \oplus \mathbb{F}$

2. $B_{m-1}^{1,-2} \oplus \mathbb{F} \cong B_m^{1,-2}$

   $B_{m-1}^{3,-2} \cong B_m^{3,-2}$

Now, as $\varkappa_A(K,h,L) = 0$, there must be an $M \in \mathbb{Z}$ for which $B_M^{3,-2}$ is zero for the first time, as once $B_m^{3,-2}$ becomes 0 it must stay 0 forever. That is, $B_m^{3,-2}$ is zero for all $m \geq M$ and is non-zero for all $m < M$. This puts us in the second of the above options, and so the dimension of $B_m^{1,-2}$ must therefore increase by 1 for every $m \geq M$.

Next, we note that $\dim(B_{M-1}^{3,-2}) - \dim(B_M^{3,-2}) = 1$. If not then $B_m^{3,-2}$ must be zero for all m, which means that $B_m^{1,-2}$ must be non-zero for all m, and we have non-zero elements of $\varkappa_A$. As a result, we are in the first of the above options, and so $\dim(B_{M-1}^{1,-2}) - \dim(B_M^{1,-2}) = 0$. Therefore, in order for $\varkappa_A(K,h,L)$ to be zero, it must be the case that $B_m^{1,-2} = 0$ for all $m \leq M$. Applying Lemma 4.3.23 to the generators of B_M then tells us that $B_M^{-3,2} = 0$ and $B_M^{-1,2} = 0$.

We now consider the generators of B_M. We have just shown that there are no generators with non-zero k gradings for B_M, and hence, that there are no generators with r gradings ± 3. Since B_M must collapse to the Khovanov homology of the unknot in S^3 when the spectral sequence is

applied, it has to be the case that $B_M \cong \mathbb{F}[1,0] \oplus \mathbb{F}[-1,0]$. We then apply Theorem 4.2.17, which tells us $L_M \cong \mathcal{U}_0$, and the result follows. □

4.4 Tangle Khovanov homology

The final invariant of strongly invertible knots we will consider is yet another form of Khovanov homology — this time for k-string sutured tangles. We will apply this invariant to the pair of tangles we obtain from each strongly invertible knot: the Sakuma tangle and the Watson tangle. In this section we set our base field $\mathbb{F}$ to be $\mathbb{Z}/2\mathbb{Z}$.

4.4.1 Construction

Tangle Khovanov homology was first defined by Khovanov in [42]. Its initial construction follows the spirit of Khovanov homology for knots and links in S^3, but problems arise when we try and obtain a chain complex from the cube of resolutions. We reproduce Bar-Natan's words in [10], where he explains the problem, and Khovanov's response to it:

"...Khovanov homology theory does not lend itself naturally to an extension to tangles. In order to define the chain spaces ones needs to count the cycles in each smoothing, and this number is not known unless all 'ends' are closed, ie, unless the tangles is really a link...Khovanov solves the problem by taking the chain space of a tangle to be the direct sum of all chain spaces of all possible closures of that tangle".

Bar-Natan himself offers a different approach, by working on the level of smoothings and cobordisms for as long as possible before moving to the world of vector spaces and vector space maps. In order to avoid going deep into the necessary terminology, however, we will use another construction of tangle Khovanov homology provided by Grigsby and Wehrli in [22] specifically for k-string sutured tangles. This is admittedly a restriction to a subclass of tangles, but for our purposes this is all we need, since Sakuma tangles and Watson tangles are all members of this subclass. Grigsby and Wehrli's approach results in an isomorphic theory to what Khovanov defined, but is somewhat easier to grasp, and does not require the heavy algebraic machinery Khovanov wheels out. Furthermore, it is closer in spirit to the way we have seen the various Khovanov homologies defined thus far.

Begin by taking a sutured k-string tangle $T = (D^2 \times I, \tau)$ and fixing an orientation and a diagram for it with say, n crossings, which we denote $D_T \subset I \times I$. Next, number the crossings, and, just as for knots and links, form a cube of smoothings for D_T. We note that a general complete smoothing S_α for $\alpha \in \{0,1\}^n$ is a collection of circles contained in $I \times I$ and intervals which have their end points at $\{0,1\} \times I$. Suppose there are c circles and x intervals, and label them $T_1, \dots T_{c+x}$, so that $T_1, \dots T_c$ are the circles, and $T_{c+1}, \dots T_{c+x}$ are the intervals. We say the smoothing *backtracks* if there exists an interval T_i, $c \leq i \leq c+x$, such that $\partial T_i \subset \{0\} \times I$ *or* $\{1\} \times I$, that is, if at least one of the intervals starts and ends at the same end of $I \times I$.

Next, we attach to a smoothing a $\mathbb{Z}/2\mathbb{Z}$ vector space $V(S_\alpha)$

$$V(S_\alpha) := \left\{ \begin{array}{ll} 0 & \text{if } S_\alpha \text{ backtracks} \\ \Lambda^*(Z(S_\alpha)) & \text{otherwise} \end{array} \right\}$$

Where $Z(S_\alpha)$ is a vector space generated by the circle components $[T_1], \ldots, [T_c]$, and $\Lambda^*(Z(S_\alpha))$ is the exterior algebra of $Z(S_\alpha)$. We identify $Z(S_\alpha)$ with the quotient

$$Z(S_\alpha) = Span_{\mathbb{Z}/2\mathbb{Z}}([T_1], \ldots, [T_{c+x}])/[T_{c+1}] \sim \ldots \sim [T_{c+x}] \sim 0$$

which means the exterior algebra can simply be thought of as a polynomial algebra over $\mathbb{Z}/2\mathbb{Z}$ in formal variables $[T_1], \ldots, [T_c]$ with the relations $[T_i]^2 = 0$ for $i \leq c$ and $[T_i] = 0$ for $i > c$. We also write

$$\Lambda^*(Z(S_\alpha)) = \Lambda^0(Z(S_\alpha)) \oplus \Lambda^1(Z(S_\alpha)) \oplus \ldots \oplus \Lambda^c(Z(S_\alpha)),$$

where $\Lambda^0(Z(S_\alpha)) = \mathbb{Z}/2\mathbb{Z}$, $\Lambda^1(Z(S_\alpha)) = Z(S_\alpha)$, and $\Lambda^d(Z(S_\alpha))$ is generated by all possible products of d generators of $Z(S_\alpha)$ (so there are $\binom{c}{d}$ generators of $\Lambda^d(Z(S_\alpha))$.

Before we define the chain complex groups and maps we will mention the two gradings which are placed on elements of the vector space $V(S_\alpha)$. Firstly we have the homological grading, which is exactly the same in this setting as it was in the classical case for knots and links in S^3. Namely, given a element $a \in V(S_\alpha)$

$$i(a) := -n_- + |\alpha|,$$

where n_- is the number of negative crossings in D_T, and $|\alpha|$ is the height of α (the number of 1 entries). Next is the quantum grading. Suppose that $a \in \Lambda^d(Z(S_\alpha)) \subset V(S_\alpha)$, then:

$$j(a) := \dim_{\mathbb{Z}/2\mathbb{Z}}(Z(S_\alpha)) - 2d + n_+ - 2n_- + |\alpha|.$$

Remark. We keep with our conventions for the 0 and 1-smoothings, which are the opposite to those used by Grigsby and Wehrli. Hence, we have swapped n_+ and n_- in the above definitions from what they define in [22].

Next, we define some maps on the edges of our cube of smoothings. Just as before, an immediate successor of a complete smoothing S_α is another complete smoothing $S_{\alpha'}$ in which α' is obtained from α by replacing a single 0 entry with a 1 entry.

In the case where two circles T_i and T_j merge together we define the merge map m to be composite

$$V(S_\alpha) \xrightarrow{\pi} V(S_\alpha)/[T_i] \sim [T_j] \xrightarrow{\cong} V(S_{\alpha'}).$$

When a circle splits into two, the split map Δ is

$$V(S_\alpha) \longrightarrow V(S_{\alpha'})/[T_i] \sim [T_j] \xrightarrow{\gamma} V(S_{\alpha'})$$

where $\gamma(a) := ([T_i] + [T_j])a$.

It turns out that the maps preserve this quantum grading, and raise the homological grading by one (again, this is really a cohomological theory). The Tangle Khovanov homology of T is then defined to be:

$$TKh^*(T) \cong H^*\Big(\bigoplus_{\alpha} V(S_\alpha), D\Big).$$

4.4.2 Spectral sequences

Next, we will mention some results regarding the relationship between tangle Khovanov homology and some of the other invariants we've come across, with a particular emphasis on annular Khovanov homology.

Firstly, Grigsby and Wehrli in [22, Proposition 5.20] prove the existence of a spectral sequence from tangle Khovanov homology to the sutured Floer homology of the double branched cover of $D^2 \times I$ with branch set τ.

Theorem 4.4.1 (Grigsby-Wehrli, 2009)**.** *Let $T = (D^2 \times I, \tau)$ be an k-string, sutured tangle. Then there exists a spectral sequence which has E_1 page $TKh^*(\overline{T})$, and E_∞ page $SFH(\Sigma(D^2 \times I, \tau))$.*

This result is the analogue of their result for annular Khovanov homology and sutured Floer homology (Theorem 4.2.8), and highlights the similarity between AKh and TKh. That they should be connected at all should be intuitive for, if $L \subset A \times I$ is an annular link, we can obtain a sutured tangle by cutting through $A \times I$ along a meridional disc and unfurling the result. As we did for annular links, we will keep the exact nature of this spectral sequence, including the gradings used for the filtration, deliberately vague. That being said, we will remark that once more the filtered quasi-isomorphism type of the chain complex (recall Definition 4.2.1). is independent of the choice of diagram, and every page of the spectral sequence is an invariant of T (see [24, Remark 3.9] for more information).

Expanding on the above comment, Grigsby and Wehrli have additionally proved a series of results that show the spectral sequence between tangle Khovanov homology and sutured Floer homology "behaves well under certain natural geometric operations" [24]. For a k-string sutured tangle T and annular link L let $\mathcal{F}(T)$ and $\mathcal{F}(L)$ denote the filtered chain complexes featuring in the two spectral sequences to sutured Floer homology. Grigsby and Wehrli then prove the following three theorems; the figures accompanying which are all taken from [24].

Theorem 4.4.2 (Grigsby-Wehrli, 2010)**.** *Let $T = (D^2 \times I, \tau)$ be a k-string sutured tangle, and let T' be the tangle obtained from T by adjoining a trivial strand separated from τ by a properly-embedded I-invariant disc F as in Figure 4.6. Then*

$$\mathcal{F}(T) \simeq \mathcal{F}(T').$$

That is, the filtered chain complexes of T and T' are quasi-isomorphic.

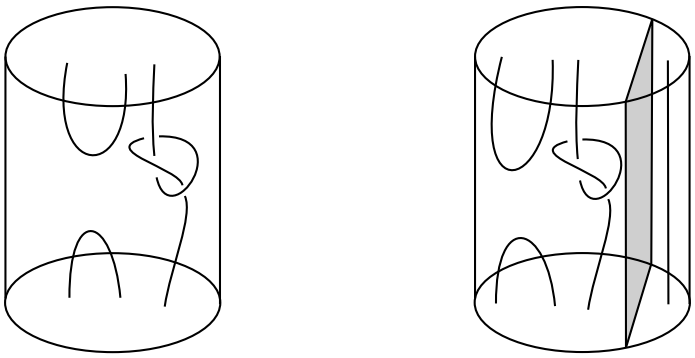

Figure 4.6: Adjoining a trivial strand to a k-string sutured tangle to form a $k+1$-string sutured tangle

Additionally, there is a relationship between the tangle Khovanov homology of two tangles and that of the tangle formed by stacking them on top of one another:

Theorem 4.4.3 (Grigsby-Wehrli, 2010)**.** *Let T_i, $i \in \{1,2\}$ be two k-string sutured tangles, and let $T_1 + T_2$ be any k-string tangle obtained by stacking a diagram of T_1 on top of a diagram of T_2, as in Figure 4.7. Then*

$$\mathcal{F}(T_1 + T_2) \simeq \mathcal{F}(T_1) \otimes \mathcal{F}(T_2).$$

Finally, Grigsby and Wehrli prove the following relationship between AKh and TKh:

Theorem 4.4.4 (Grigsby-Wehrli, 2010)**.** *Let $L \subset A \times I$ be an isotopy class representative of an annular link with diagram D_L, and let $\lambda \subset A$ be a properly embedded oriented arc representing a non-trivial element of $H_1(A, \partial A)$ such that λ intersects D_L transversely. Let $T = (D^2 \times I, \tau)$ be the k-string sutured tangle obtained by decomposing along the surface $\lambda \times I$, endowed with the product orientation.*

Then the spectral sequence

$$TKh^*(\overline{T}) \rightsquigarrow SFH(\Sigma(D^2 \times I, \tau)$$

is a direct summand of the spectral sequence

$$AKh^*(\overline{L}) \rightsquigarrow SFH(\Sigma(A \times I, L)).$$

That is, $\mathcal{F}(T)$ is filtered quasi-isomorphic to a direct summand of $\mathcal{F}(L)$. Furthermore, the direct summand is trivial if there exists some $L' \subset A \times I$ isotopic to L satisfying

$$|(\lambda \times I) \pitchfork L'| < |(\lambda \times I) \pitchfork L|.$$

Essentially, the above theorem states that by cutting A along a suitable ray λ, we obtain a digram for a tangle whose tangle Khovanov homology is a direct summand of the annular Khovanov homology of the annular link. If the link diagram is not one that realises the wrapping number ω of L, then the direct summand is trivial.

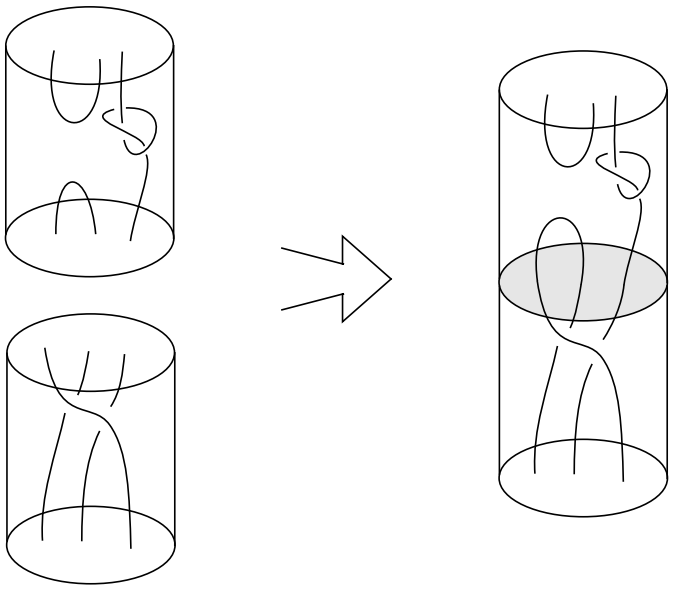

Figure 4.7: Stacking k-string sutured tangles

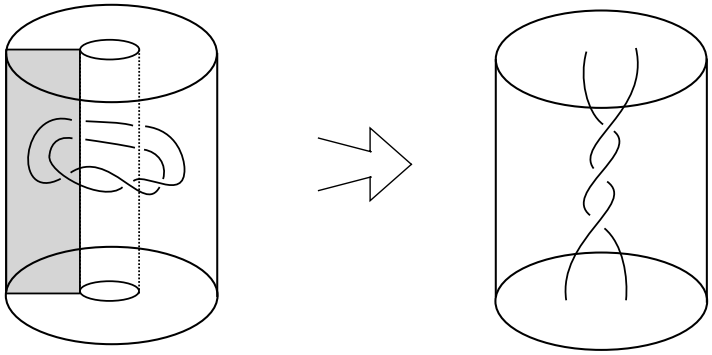

Figure 4.8: Cutting an annular link to obtain a k-string sutured tangle

4.4.3 Application to strongly invertible knots

We will end this chapter by applying tangle Khovanov homology to the two classes of tangles we obtain from strongly invertible knots, using the constructions provided by Sakuma and Watson. The following discussion barely even scratches the surface of the potential applications to the theory of strongly invertible knots tangle Khovanov homology can have, however we hope to give enough motivation from the couple of results we do prove to encourage further study.

We note that, since only one Sakuma tangle and Watson tangle arise from a strongly invertible knot, their tangle Khovanov homologies are, like $\varkappa$ and $\varkappa_A$, invariants which are not altered by a change of framing.

First, let's examine the tangle Khovanov homology of the Sakuma tangles. Interestingly, Sakuma tangles are, in a sense, 'loose enough' for Grigsby and Wehrli's decomposition theorem to be applied to the filtered Khovanov chain complex.

Proposition 4.4.5. *Let (K, h) be a non-trivial strongly invertible knot, and let T be a representative of the Sakuma tangle for (K, h). Let T' be the tangle in Figure 4.9. Then, $\mathcal{F}(T)$ is filtered*

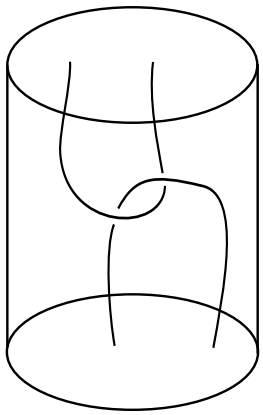

Figure 4.9: A 2-string sutured tangle

quasi-isomorphic to $\mathcal{F}(T')$.

Proof. We will proof the result algorithmically, with our starting place the construction of T as specified in Chapter 1. See Figure 4.10 for an example of the following.

1. Begin by separating all pairs of parallel strands which run from $D^2 \times \{0\}$ to $D^2 \times \{1\}$ in T from the rest of the tangle, removing any twists between the strands. Using Theorem 4.4.2, they can all be removed from T to obtain a tangle T_1 which has a quasi-isomorphic filtered complex $\mathcal{F}(T_1)$.

2. We are then left with four strands which from the clasps around the hole in the braid-like closure. Two of these start and end at the same side, and two start and end at different sides. Separate the two strands that start and end at different sides and remove them. This leaves us with a tangle equivalent to T', and Theorem 4.4.2 tells us $\mathcal{F}(T)$ is filtered quasi-isomorphic to $\mathcal{F}(T')$ as required.

□

As a consequence of the above result we see that, for one thing, tangle Khovanov homology is not a particularly useful invariant if we want to distinguish Sakuma tangles. Sakuma tangles are simply not sufficiently 'tangled' to give a wide enough range of vector spaces. Perhaps more interesting, however, is the fact that the value of $SFH(\Sigma(T))$ must be the same for all Sakuma tangles that do not arise from the trivial strongly invertible knot. This suggests a potential relationship between the double branched covers of Sakuma tangles, which is interesting since we do not have much geometric intuition about what the 3-manifold $\Sigma(D^2 \times I, \tau)$ is for a general Sakuma tangle. We will say no more about this potential connection, simply remarking that this may pose an interesting question for further study.

For Watson tangles, however, the geometric picture for the double branched cover is much clearer. Given a representative of a Watson tangle $T = (D^2 \times I, \tau)$ we can simply reverse Watson's construction. That is, the 3-manifold $\Sigma(D^2 \times I, \tau)$ is nothing more than the knot exterior of the original strongly invertible knot. Suppose $K \subset S^3$ is a knot which admits two distinct strong

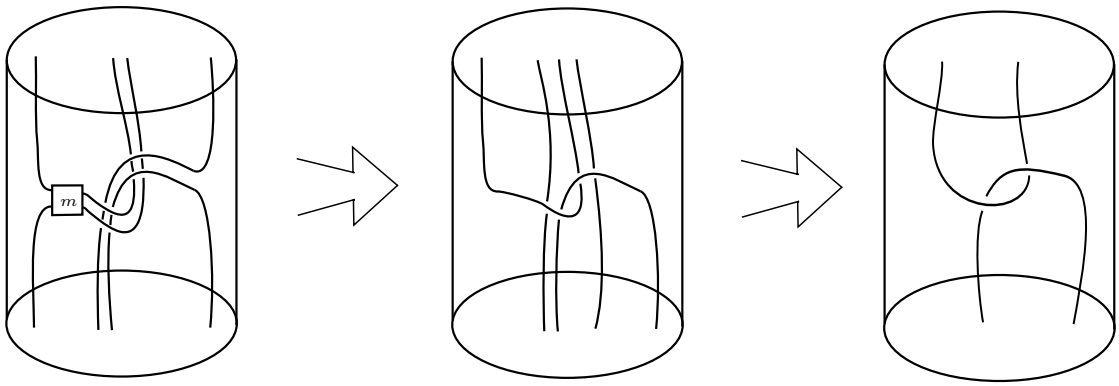

Figure 4.10: Decomposing a Sakuma tangle

inversions h_1 and h_2. Form the Watson tangles of (K, h_1) and (K, h_2), which we shall label T_1 and T_2 respectively. We then note that $TKh^*(T_1)$ and $TKh^*(K_2)$ must both converge to $SFH(S^3\backslash\mathcal{N}(K))$, which means that, just as in the annular setting, by employing the spectral sequence we lose all information about the strong inversions.

Our last result is, perhaps predictably, a final unknot detection result. We first state the following theorem of Juhász, which can be found in [35, Proposition 9.2]:

Proposition 4.4.6 (Juhász, 2006)**.** *If Y is a closed connected oriented 3-manifold and $L \subset Y$ is an oriented link then*

$$\widehat{HFL}(L) \cong SFH\left(Y\backslash\mathcal{N}(L)\right) \otimes \mathbb{Z}/2\mathbb{Z}.$$

If L is a knot then

$$\widehat{HFK}(Y, K) \cong SFH\left(Y\backslash\mathcal{N}(K)\right).$$

Now comes the final theorem:

Theorem 4.4.7. *Let (K, h) be a strongly invertible knot, and let $T_{(K,h)}$ be its Watson tangle. Suppose $TKh^*(T_{(K,h)}) \cong TKh^*(T_{(\mathcal{U},h_0)})$, where $T_{(\mathcal{U},h_0)}$ is the Watson tangle associated to $(\mathcal{U}, h_0)$. Then $(K, h) \cong (\mathcal{U}, h_0)$.*

Proof. Applying the Grigsby-Wehrli spectral sequence we obtain

$$SFH\left(\Sigma(T_{(K,h)}\right) \cong SFH\left(\Sigma(T_{(\mathcal{U},h_0)}\right).$$

Next, we use the fact that $\Sigma(T_{(K,h)}) \cong S^3\backslash\mathcal{N}(K)$ along with Juhász's result

$$\begin{array}{lll} \implies & SFH\left(Y\backslash\mathcal{N}(K)\right) & \cong \quad SFH\left(Y\backslash\mathcal{N}(\mathcal{U})\right) \\ \implies & \widehat{HFK}(Y, K) & \cong \quad \widehat{HFK}(Y,\mathcal{U}). \end{array}$$

But, we know that Knot Floer homology detects the unknot (see [65]), so $K \cong \mathcal{U}$ and the result follows. □

Chapter 5

Conclusion

Over the course of this thesis applying Sakuma's construction has provided us with an increasingly large number of invariants of strongly invertible knots. It seems necessary, therefore, to conclude with a summary of the different invariants we have defined, and discuss some potential directions for further study.

5.1 Executive summary

Initially we had two invariants of strongly invertible knots: the η-polynomial, and $\varkappa$. To these we have added five more: the Jones polynomial, the annular Jones polynomial, Khovanov homology, annular Khovanov homology, and tangle Khovanov homology. We have also conjectured a sixth: $\varkappa_A$.

The main distinction between the invariants is whether they take the form of a polynomial or a homology theory. Traditionally, since categorified invariants contain more structure than polynomial invariants, they are better at distinguishing knots, and give rise to more applications. It would be natural, therefore, to assume that homological invariants should be better at distinguishing strongly invertible knots than polynomial invariants; certainly, a polynomial invariant will never be able to provide more information than its categorified version. However, quite remarkably, we have shown that a polynomial invariant can in certain cases do things a homological invariant cannot. In particular, the annular Jones polynomial has shown to have certain advantages over Khovanov homology when considering strongly invertible knots, as we showed in Theorem 3.3.28. There are further divisions we could make within the homological invariants as well; for example, the $\varkappa$ and $\varkappa_A$ invariants are more complex than a single Khovanov homology or annular Khovanov homology calculation, due to their construction from inverse and direct limits. This means that they take longer to calculate, but do contain more information as a consequence.

We can also classify the invariants by the auxiliary object they are defined on, and, related to this point, whether or not they are sensitive to the choice of longitude framing in Sakuma's construction. The three main auxiliary objects that we have are used are Sakuma links, annular

Sakuma knots, and Watson tangles — although in order to calculate the $\varkappa$ and $\varkappa_A$ invariants we actually require the family of closures of a Watson tangle, and a family of annular Sakuma knots. In terms of the complexity of the process involved to obtain them, Sakuma links require the least amount of work, whilst Watson tangles and the branch-set annular Sakuma knots require the most. On the other hand, if we do choose to perform the additional isotopies to obtain the Watson tangle and annular Sakuma knots, the $\varkappa$, $\varkappa_A$, and TKh invariants do not have any dependence on the framing of the longitudes, which makes them potentially more straightforward to deal with.

Additionally, we have made attempts to compare invariants, most notably the annular Jones polynomial with the η-polynomial. We proved in Corollary 3.4.5 that there exist infinitely many pairs of strongly invertible knots which have identical η-polynomials but different annular Jones polynomials. In light of this result, as well as the presence of the additional variable in the annular Jones polynomial, it seems reasonable to claim, albeit cautiously, that the annular Jones polynomial is a superior invariant, by which we mean there are no pairs of strongly invertible knots with the same annular Jones but different η-polynomials.

Given the differences outlined above, a natural question to ask is which is the optimum invariant for studying strongly invertible knots. The simple answer would be that it ultimately comes down to personal preference. Sometimes using an easier to calculate polynomial invariant may be all we require, whilst, alternatively the situation may demand that we work with a computationally expensive homological invariant. It is worth bearing in mind, however, that all the homological invariants we have encountered detect the strongly invertible unknot, whilst it remains unclear whether a polynomial invariant can. An additional factor we may wish to take into account is whether we desire an invariant which has no dependence on longitude framing; it may well be that having specific longitude framings gives us too much information, when all we require is an honest invariant of strongly invertible knots. The outcome of this cost-benefit analysis will vary from situation to situation — there is unfortunately no single 'master invariant' that is both quick to calculate and applicable in all situations.

5.2 Next steps

Where do we go from here? On the whole the scope of this thesis has been broad rather then deep, and as such there are a number of directions future work could take. For one thing, there are a few loose ends still to take care of on the level of the polynomial invariants — see, for example, the unknown entries in Table 5.1. In addition, we could choose to investigate our homological invariants further, $\varkappa_A$ is only conjectured to be an invariant, or apply more — for instance the d_t invariant of Grigsby, Licata, and Wehrli [21].

In addition, three areas of potential interest are the following:

Categorifying η

As we noted in Chapter 3, the η-polynomial is an invariant closely related to the Alexander polynomial. Both invariants are defined using infinite cyclic covering spaces, and, moreover, Kojima and Yamasaki proved an explicit formula relating the two (recall Theorem 3.1.11). The Alexander polynomial has been shown to be the Euler characteristic of Knot Floer homology [72] [64], and so we can ask if we can construct a homology theory which categorifies the η-polynomial. Such a theory is likely to be some variation of Link Floer homology [52].

Spectral sequences

In Theorem 3.3.14 we proved a relationship between the annular Jones polynomial of an annular knot, and the Jones polynomial of its two-component completion. It seems reasonable to ask whether there exists a similar relationship on the categorified level.

Conjecture. *Let $K \subset A \times I$ be an annular knot, and $L = K \cup \mathcal{B} \subset S^3$ be its two-component completion. There exists a spectral sequence which has E_1 page $AKh(K)$, and E_∞ page $\widetilde{Kh}(L)$.*

We remark that the above connection is a natural one to investigate. For instance, we can obtain a huge class of two-component completions by taking K to be a braid closure and $\mathcal{B}$ to be the braid axis. We could then ask, assuming the conjecture, if any information about braids can be extracted from the spectral sequence. Another set of examples are obtained by taking a link and viewing it as lying in the exterior of one of its meridians — in which case the wrapping number of the annular link will always be equal to 1.

A related question follows from Pascual's theorem (Theorem 3.3.11) regarding the relationship between the Jones polynomial of a satellite knot and the annular Jones polynomial of its pattern. It would again seem likely that there exists a similar relationship in the categorified world. We conjecture:

Conjecture. *Let $P \subset A \times I$ be an annular knot, $C \subset S^3$ be a knot and $Sat(P, C)$ be the satellite knots with pattern P and companion knot C. There exists a spectral sequence which has E_1 page $AKh(P)$ and E_∞ page $Kh(Sat(P, C))$.*

There is also scope for further work on Grigsby and Wehrli's spectral sequence between annular Khovanov homology and sutured Floer homology. In particular, Friedl, Juhász, and Rasmussen [18] have defined a decategorified version of sutured Floer homology, which is best thought of as a generalisation of the Alexander polynomial to sutured manifolds. It would be interesting if a explicit connection could be found on the decategorified level, between the annular Jones polynomial and their invariant.

Quotient objects from symmetries

In this thesis we have utilised Sakuma's construction to obtain various families of quotient objects to associate to a strongly invertible knot. Recalling the other rigid symmetries of knots we saw in Chapter 1 we can ask whether there exist similar geometric constructions for other symmetries, and if so, whether we can apply invariants of strongly invertible knots to their quotient

objects.

As we mentioned in the introduction, for periodic knots we can quotient out by the periodic symmetry to obtain an annular knot. This construction has featured, for example, in work of Murasugi [59], [61], Yokota [99], and Przytycki [71] comparing polynomial invariants of periodic links with those of their quotient links. In more recent times there have been efforts to do the same for homological invariants, and *equivariant* homology theories have been developed which use the periodic symmetry to build a homology theory with additional structure. For example, see work by Chbili [13], Politarczyk [69], and Borodzik and Politarczyk [8]. In addition, Zhang [100] has studied the annular setting and discovered connections between the annular Khovanov homology of a periodic link and its quotient, when both are viewed as lying in the exterior of the axis of rotation.

In light of the above, a potentially naive question is then:

Question. Can an equivariant homology theory be defined using strong inversions?

There is also potential for further study of periodic knots as well. We say a periodic symmetry is *full* if the quotient knot is equivalent to the unknot. An interesting fact about full periodic symmetries is that their number is bounded; Boileau and Paoluzzi [7] have proved that a prime non-trivial knot can only have a maximum of two full periodic symmetries. Full periodic symmetries have been shown to be connected to other interesting features of knots; for example, the presence of full periodic symmetries of a knot is related to the branched coverings of S^3 over it. We say a knot K has an n-twin if there exists a knot $K' \ncong K$ such that the n-fold branched covers over K and K' are isomorphic; Zimmerman [101] has proved the following result.

Theorem 5.2.1 (Zimmerman, 1998)**.** *Let $K \subset S^3$ be a hyperbolic knot and $n \geq 3$. Then K has an n-twin if and only if K has a full periodic symmetry f of order n, and the quotient link $K/f \cup Fix(f)/f$ does not have pure exchange symmetry.*

Full periodic symmetries naturally give rise to two-component links with both components unknotted — simply take the quotient knot and the axis of rotation to be the two components. We can therefore attach to full periodic knots invariants of links and annular knots in the same way we have done for strongly invertible knots. In particular, we may wonder what, if anything, can annular Khovanov homology say about full periodic knots.

In addition to strong inversions and periodic symmetries we also have periodic symmetries which realise the amphicheirality of a knot. Recall that these periodically amphicheiral symmetries are periodic maps of (S^3, K) which reverse the orientation of S^3 and either preserve or reverse the orientation of K. A natural question to ask is whether or not we can play the same game with these symmetries, that is:

Question. Let $K \subset S^3$ be a knot with periodic ($\pm$)amphicheiral symmetry f. Is there a natural quotient object K/f one can associate with the pair (K, f)?

An example of a map which realises a (+)amphicheiral symmetry of a knot is the twisted ro-

tation symmetry that appears in Luo's paper [51]. This would be a good candidate to start investigating.

If the above question can be answered positively, then an additional line of inquiry concerns the symmetry group.

Question. Let $K \subset S^3$ be a knot with symmetry group $Sym(K)$. Can every element of $Sym(K)$ be characterised via a unique quotient object?

Invariant	Polynomial/ Homology theory	Auxiliary Object	Sensitive to framing change?	Unknot detector?	Sensitive to cheirality?
η	P	Sakuma link	Y	N	Y
J	P	Sakuma link	Y	?	Y
AJ	P	Annular Sakuma knot	Y	?	Y
Kh	H	Sakuma link	Y	Y	Y
AKh	H	Annular Sakuma knot	Y	Y	Y
$\varkappa$	H	Watson Tangle	N	Y	Y
$\varkappa_A$	H	Framed annular Sakuma knots	N	Y	?
TKh	H	Watson tangle	N	Y	Y

Table 5.1: Table of invariants covered and some of their key properties

Appendix A

AKh.m Manual

Here we provide a brief description of the Mathematica package *AKh.m*, the first incarnation of which was written by the author in August 2016 using Mathematica 9.0.1.0 on Windows (64-bit). The package provides a means of calculating the annular Khovanov homology of an annular link, and is based heavily upon Bar-Natan's initial 'categorification.m' package — which calculates the Khovanov homology of a link in S^3. A further credit should go to Joseph MacColl, who kindly provided the `KhTable` and `condense` commands, which express the Poincaré polynomial in table format. The program itself works well for links with a small number of crossings, but is somewhat ponderous when put to task on annular Sakuma knots — no doubt a much faster alternative can be written by someone with more programming expertise!

AKh.m requires the KnotTheory' package in order to run, which can be found on the Knot Atlas website [43]. At the time of writing *AKh.m* can calculate *AKh* over $\mathbb{Q}$ and $\mathbb{Z}/p\mathbb{Z}$ for prime p, however an update to also include $\mathbb{Z}$ coefficients is in the works.

We also should mention a Mathematica program 'KhBraids', written by Hunt, Kesse, Licata, and Morrison [31]. This program calculates a closely related annular link invariant, which recovers both annular Khovanov homology and Khovanov homology as specialisations. Their program runs only on annular knots obtained from braid closures, however is considerably more powerful than *AKh.m*.

A.1 Planar Diagram notation for annular links

To calculate the annular Khovanov homology of an oriented annular link L we first require a choice of diagram D_L. In order to describe this diagram in a way intelligible to computers we use *planar diagram notation*. Start by labelling the strands of D_L from 1 to n, increasing the labels by 1 as we pass through a crossing. This provides us with a way to articulate the crossings of D_L in terms of the four strand numbers which comprise it: suppose the incoming under-strand is labelled by i, and, moving anti-clockwise around the crossing, the other three strands are labelled j, k, and l respectively; we then label the crossing $X[i, j, k, l]$. Repeating this procedure gives us a description of the crossings of D_L.

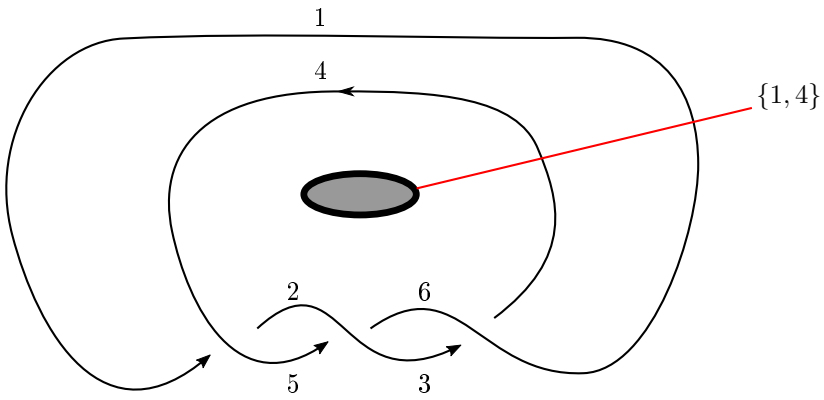

$X[1,5,2,4]$ $X[5,3,6,2]$ $X[3,1,4,6]$

Figure A.1: Annular PD notation

Next, we require a method of describing the position of the hole in the annulus in relation to D_L. This is done by drawing in a ray λ from the inner edge of A to the outer edge which misses all crossings in D_L, then listing the strands λ crosses. For an example, consider the diagram of the right-handed trefoil expressed as a braid closure in Figure A.1 — the complete annular planar diagram notation for this knot is $X[1,5,2,4], X[5,3,6,2], X[3,1,4,6]$ and $\{1,4\}$.

Remark. Note that if we leave the ray list empty then we are effectively describing the planar diagram of D_L lying in $\mathbb{R}^2$ instead of A.

A.2 A guided tour of *AKh.m*

Let's take a stroll through the commands contained within *AKh.m*. Consider once more the annular knot K featured in Figure A.1. We open up Mathematica and load *AKh.m*:

```
In[1]:= << AKh`
```

We can then describe the crossings of K in PD notation:

```
In[2]:= K = PD[X[1, 5, 2, 4], X[5, 3, 6, 2], X[3, 1, 4, 6]];
```

The first three commands in the package count the number of crossings, the number of positive crossings, and the number of negative crossings.

```
NumberOfCrossings [L_PD] := Count[L, X[i_, j_, k_, l_]]

NumberOfPositiveCrossings [L_PD] :=
 Count[L, X[i_, j_, k_, l_] /; j - l == 1 || l - j > 1]

NumberOfNegativeCrossings [L_PD] :=
 Count[L, X[i_, j_, k_, l_] /; l - j == 1 || j - l > 1]
```

```
In[3]:= NumberOfPositiveCrossings[K]

Out[3]= 3
```

`Smoothings` makes a list of all the possible smoothings for our link.

```
Smoothings[L_PD] := Module[{length, types}, length = NumberOfCrossings[L];
  types = Tuples[{0, 1}, length]]

In[4]:= Smoothings[K]

Out[4]= {{0, 0, 0}, {0, 0, 1}, {0, 1, 0},
       {0, 1, 1}, {1, 0, 0}, {1, 0, 1}, {1, 1, 0}, {1, 1, 1}}
```

`Circles` has two possible inputs. When PD notation and a choice of smoothing instructions are entered it produces a list of all the circles in that smoothing, along with all the strands that comprise each circle. When PD notation and a set of smoothing instructions with a single star are entered `Circles` replaces the star with a 0 and a 1, evaluates both, then expresses them either side of an arrow $\rightarrow$.

```
Circles[L_PD, a : {(0 | 1) ...}] :=
 Module[{i, j, k, l},
  ConnectedComponents[
   Graph[DeleteDuplicates[
     Flatten[(Thread[{List @@ L, a}] /.
        {{X[i_, j_, k_, l_], 0} -> {{i, j}, {k, l}},
         {X[i_, j_, k_, l_], 1} -> {{i, l}, {j, k}}}), 1],
     SameQ[#1, #2] || SameQ[#1, Reverse@#2] &]]]]
Circles[L_PD, a_List] :=
 Module[{list}, list = Thread[{List @@ L, a}];
  Circles[L, a /. {"*" -> 0}] -> Circles[L, a /. {"*" -> 1}]]

In[5]:= Circles[K, {0, 0, 0}]

Out[5]= {{2, 4, 6}, {1, 5, 3}}

In[6]:= Circles[K, {"*", 0, 0}]

Out[6]= {{2, 4, 6}, {1, 5, 3}} → {{1, 2, 3, 4, 5, 6}}
```

`CubeOfSmoothings` produces a list of all the complete smoothings of our link with the strands that comprise each circle.

```
CubeOfCircles[L_PD] :=
 Module[{types}, types = Smoothings[L]; Circles[L, #] & /@ types]

In[7]:= CubeOfCircles[K]

Out[7]= {{{2, 4, 6}, {1, 5, 3}}, {{1, 2, 3, 4, 5, 6}},
       {{1, 2, 3, 4, 5, 6}}, {{1, 5, 4, 2}, {3, 6}}, {{1, 2, 3, 4, 5, 6}},
       {{2, 5, 6, 3}, {1, 4}}, {{1, 4, 3, 6}, {2, 5}}, {{3, 6}, {2, 5}, {1, 4}}}
```

`SortCircles` also has two possible inputs. When a list of circles and the ray information are entered it counts the intersections mod 2, and then sorts each circle as either trivial or non-trivial (by which we mean trivial in the first homology group of the annulus). When two lists of circles

separated by an arrow are entered it does the same thing on each side of the arrow.

```
SortCircles[b_List, c_List] :=
 Times @@
  Table[If[Mod[Length[Intersection[b[[n]], c]], 2] == 0,
    trivial[Min[b[[n]]]], nontrivial[Min[b[[n]]]]],
   {n, Length[b]}]
SortCircles[expr_, c_List] :=
 SortCircles[DeleteCases[expr[[1]],
    Alternatives @@ Intersection[expr[[1]], expr[[2]] ] ], c] ->
  SortCircles[DeleteCases[expr[[2]],
    Alternatives @@ Intersection[expr[[1]], expr[[2]] ] ], c]
```

```
In[8]:= SortCircles[{{2, 4, 6}, {1, 5, 3}}, {1, 4}]
Out[8]= nontrivial[1] nontrivial[2]
```

If there is no ray information then `SortCircles` always returns trivial circles...

```
In[9]:= SortCircles[{{2, 4, 6}, {1, 5, 3}}, {}]
Out[9]= trivial[1] trivial[2]
```

The `V` command forms a list of basis elements for the vector space that we attach to a smoothing. `QuantumDegree` and `AnnularDegree` calculate the j and k gradings respectively for a given basis element. It is also possible to search for basis elements with specified j and k gradings.

```
QuantumDegree[expr_] :=
 Count[expr, _vp, {0, 1}] - Count[expr, _vm, {0, 1}]

AnnularDegree[expr_] :=
 Count[expr, vp[_, n], {0, 1}] - Count[expr, vm[_, n], {0, 1}]

V[L_PD, a_List, c_List] :=
 List @@
  Expand[SortCircles[Circles[L, a], c] /.
    {trivial[x_] -> ((vp[x, t]) + (vm[x, t])),
     nontrivial[x_] -> ((vp[x, n]) + (vm[x, n])) } ]
V[L_PD, a_List, c_List, deg_Integer, deg2_Integer] :=
 Select[V[L, a, c],
  ((deg == QuantumDegree[#] + (Plus @@ a)) &&
     (deg2 == AnnularDegree[#])) & ]
```

```
In[10]:= V[K, {0, 0, 0}, {1, 4}]
Out[10]= {vm[1, n] vm[2, n], vm[2, n] vp[1, n], vm[1, n] vp[2, n], vp[1, n] vp[2, n]}

In[11]:= QuantumDegree[vm[1, n] vm[2, n]]
Out[11]= -2

In[12]:= AnnularDegree[vm[1, n] vm[2, n]]
Out[12]= -2

In[13]:= V[K, {0, 0, 0}, {1, 4}, 0, 0]
Out[13]= {vm[2, n] vp[1, n], vm[1, n] vp[2, n]}
```

Next we define the vector space maps:

```
d[L_PD, a_List, b_List] := SortCircles[Circles[L, a], b] /. {
(trivial[x_] trivial[y_] -> trivial[z_]) ->
    {vp[x, t] vp[y, t] -> vp[z, t], vp[x, t] vm[y, t] -> vm[z, t],
     vm[x, t] vp[y, t] -> vm[z, t], vm[x, t] vm[y, t] -> 0},
(trivial[z_] -> trivial[x_] trivial[y_]) ->
    {vp[z, t] -> vp[x, t] vm[y, t] + vm[x, t] vp[y, t],
     vm[z, t] -> vm[x, t] vm[y, t]},
(trivial[x_] nontrivial[y_] -> nontrivial[z_]) ->
    {vp[x, t] vm[y, n] -> vm[z, n], vm[x, t] vp[y, n] -> 0,
     vp[x, t] vp[y, n] -> vp[z, n], vm[x, t] vm[y, n] -> 0},
(nontrivial[z_] -> trivial[x_] nontrivial[y_]) ->
    {vp[z, n] -> vm[x, t] vp[y, n],
     vm[z, n] -> vm[x, t] vm[y, n]},
(nontrivial[x_] nontrivial[y_] -> trivial[z_]) ->
    {vp[x, n] vm[y, n] -> vm[z, t],
     vm[x, n] vp[y, n] -> vm[z, t], vp[x, n] vp[y, n] -> 0,
     vm[x, n] vm[y, n] -> 0},
(trivial[z_] -> nontrivial[x_] nontrivial[y_]) ->
    {vp[z, t] -> vp[x, n] vm[y, n] + vm[x, n] vp[y, n],
     vm[z, t] -> 0}
}

In[14]:= d[K, {"*", 0, 0}, {1, 4}]
Out[14]= {vm[2, n] vp[1, n] → vm[1, t], vm[1, n] vp[2, n] → vm[1, t],
          vp[1, n] vp[2, n] → 0, vm[1, n] vm[2, n] → 0}
```

We form the groups in the Khovanov bracket complex by direct summing the vector spaces as usual.

```
KhBracket[L_PD, c_List, r_Integer, deg___, deg2___] :=
If[r < 0 || r > Length[L], {0}, Join @@
(((v[#]) V[L, #, c, deg, deg2]) & /@
     Permutations[Join[Table[0, {Length[L] - r}],
       Table[1, {r}]]])]
```

```
In[15]:= KhBracket[K, {1, 4}, 0]

Out[15]= {v[{0, 0, 0}] vm[1, n] vm[2, n], v[{0, 0, 0}] vm[2, n] vp[1, n],
       v[{0, 0, 0}] vm[1, n] vp[2, n], v[{0, 0, 0}] vp[1, n] vp[2, n]}
```

Now we shift the i and j degreesl. The function `CC` demands we specify our degrees too, so we actually end up with the homogeneous component of $CAKh$ with degrees $(i, j, k) = (r, deg, deg2)$.

```
CC[L_PD, c_List, r_Integer, deg_Integer, deg2_Integer] :=
KhBracket[L, c, r + NumberOfNegativeCrossings[L],
  deg - NumberOfPositiveCrossings[L] +
   2 NumberOfNegativeCrossings[L], deg2]

In[16]:= CC[K, {1, 4}, 0, 3, 0]

Out[16]= {v[{0, 0, 0}] vm[2, n] vp[1, n], v[{0, 0, 0}] vm[1, n] vp[2, n]}
```

The next commands are concerned with forming the annular Khovanov differential by summing the edge morphisms and adding minus signs as appropriate.

```
ReplaceHead[expr_] :=
Expand[sign = 1;
  Table[ If[expr[[1, 1, i]] == 0,
    sign ReplacePart[expr, {1, 1, i} -> 1], sign = -1 sign; 0],
   {i, Length[expr[[1, 1]]]}]]

ReplaceBody[L_PD, b_List][expr_] :=
d[L, #, b] & /@
  Table[ReplacePart[expr, {1, 1, i} -> "*"][[1, 1]],
   {i, 1, Length[(expr)[[1, 1]]]}]

differential[L_PD, b_List][expr_] :=
 Module[{ReplaceOne, ReplaceStar},
  ReplaceOne = ReplaceHead[expr];
  ReplaceStar = ReplaceBody[L, b][expr];
  Total[MapThread[#1 /. #2 &, {ReplaceOne, ReplaceStar}]]]
differential[L_PD, b_List][0] := 0

In[17]:= differential[K, {1, 4}][v[{0, 0, 0}] vm[2, n] vp[1, n]]

Out[17]= v[{0, 0, 1}] vm[1, t] + v[{0, 1, 0}] vm[1, t] + v[{1, 0, 0}] vm[1, t]
```

We're getting close! The next thing to do is to calculate the ranks of the homology groups. This is done by finding the dimension of the images of the differentials, then using the rank -nullity theorem to find the dimensions of their kernels. This is also where the option of different coefficients appears for the first time (provided by the `opts` variable).

```
Options[Betti] = {Modulus -> Infinity}
Rank[L_PD, a_List, r_Integer, deg_Integer, deg2_Integer,
  opts___] := (
modulus = If[{opts} === {}, Modulus /. Options[Betti],
    Modulus /. {opts}];
Off[Solve::svars];
b0 = CC[L, a, r, deg, deg2];
L1 = Length[b1 = CC[L, a, r + 1, deg, deg2]];
equations =
   (# == 0) & /@
    (Expand[differential[L, a][#] & /@ b0] /.
      MapThread[Rule, {b1, variables = Array[b, L1]}]);
rk = Which[b0 === {0} || b1 === {0}, 0, b0 === {} || b1 === {},
    0, modulus === Infinity,
    MatrixRank[
     Normal[CoefficientArrays[equations, variables]][[2]]],
modulus =!= Infinity,
    MatrixRank[
     Normal[CoefficientArrays[equations, variables]][[2]],
     Modulus -> modulus]
];
On[Solve::svars];
rk
)

Betti[L_PD, a_List, r_Integer, deg_Integer, deg2_Integer,
  opts___] :=
Module[{z},

  z = If[CC[L, a, r, deg, deg2] === {0} ||
     CC[L, a, r, deg, deg2] === {}, 0,
    Length[CC[L, a, r, deg, deg2]] -
     Rank[L, a, r, deg, deg2, opts] -
     Rank[L, a, r - 1, deg, deg2, opts]];
Print[StringForm["Betti[``,``,``] = ``", r, deg, deg2, z]]; z]
```

In[18]:=
```
Betti[K, {1, 4}, 0, 3, 0]
```

```
Betti[0,3,0] = 1
```

Out[18]=
```
1
```

Now that we can calculate ranks of the homology groups, the final thing to do is to include the grading information and determine the Poincaré polynomial of AKh.

```
qtBetti[L_PD, a_List, r_Integer, opts___] :=
(qdegs =
    If[KhBracket[L, a, r + NumberOfNegativeCrossings [L]] === {0},
    0,
    Union[
     QuantumDegree /@ KhBracket[L, a,
        r + NumberOfNegativeCrossings [L]] +
      NumberOfPositiveCrossings [L] -
      NumberOfNegativeCrossings [L] + r] ];
tdegs =
    If[KhBracket[L, a, r + NumberOfNegativeCrossings [L]] === {0},
    0,
    Union[AnnularDegree /@
      KhBracket[L, a, r + NumberOfNegativeCrossings [L]]] ];
(Flatten[Outer[Betti[L, a, r, #1, #2, opts] (q^#1) (t^#2) &,
     {qdegs}, {tdegs}], 3]) )

AKh[L_PD, a_List, opts___] :=
 Expand[Sum[Total[s^r qtBetti[L, a, r, opts]],
   {r, -NumberOfNegativeCrossings [L],
    Length[L] - NumberOfNegativeCrossings [L] } ] ]
```

We can now calculate the annular Khovanov homology of K!

```
In[19]:= AKh[K, {1, 4}]

Betti[0,1,-2] = 1
Betti[0,1,0] = 0
Betti[0,1,2] = 0
Betti[0,3,-2] = 0
Betti[0,3,0] = 1
Betti[0,3,2] = 0
Betti[0,5,-2] = 0
Betti[0,5,0] = 0
Betti[0,5,2] = 1
Betti[1,3,0] = 0
Betti[1,5,0] = 1
Betti[2,3,0] = 0
Betti[2,5,0] = 1
Betti[2,7,0] = 0
Betti[3,3,0] = 0
Betti[3,5,0] = 0
Betti[3,7,0] = 0
Betti[3,9,0] = 1

Out[19]= q^3 + q^5 s + q^5 s^2 + q^9 s^3 + q/t^2 + q^5 t^2
```

The default setting for $AKh.m$ is to calculate AKh with rational coefficients, however it also

works for fields $\mathbb{Z}/p\mathbb{Z}$ for prime p. For example, when $p = 2$ the calculation is as follows:

```
In[20]:= AKh[K, {1, 4}, Modulus → 2]

         Betti[0,1,-2] = 1
         Betti[0,1,0] = 0
         Betti[0,1,2] = 0
         Betti[0,3,-2] = 0
         Betti[0,3,0] = 1
         Betti[0,3,2] = 0
         Betti[0,5,-2] = 0
         Betti[0,5,0] = 0
         Betti[0,5,2] = 1
         Betti[1,3,0] = 0
         Betti[1,5,0] = 1
         Betti[2,3,0] = 0
         Betti[2,5,0] = 1
         Betti[2,7,0] = 1
         Betti[3,3,0] = 0
         Betti[3,5,0] = 0
         Betti[3,7,0] = 1
         Betti[3,9,0] = 1
```

$$\text{Out[20]=}\quad q^3 + q^5 s + q^5 s^2 + q^7 s^2 + q^7 s^3 + q^9 s^3 + \frac{q}{t^2} + q^5 t^2$$

The final few commands allow us to display the Poincaré polynomial in a table.

```
KhTable[kh_] :=
Module[{poly = kh, qShift, tShift, gridPoly, body, head},
qShift = -(Exponent[poly, q, Min]);
  tShift = -(Exponent[poly, s, Min]);
gridPoly = Expand[poly * (q ^ qShift) * (s ^ tShift)];
body = CoefficientList[gridPoly, {q, s}];
head = {Table[i, {i, -qShift, Exponent[poly, q, Max]}],
    Table[i, {i, -tShift, Exponent[poly, s, Max]}]};
Grid[Prepend[Flatten /@ Transpose[{head[[1]], body}],
    PadLeft[head[[2]], Length@body[[1]] + 1, ""]], Frame -> All]
]
```

```
condense[table_] :=
Module[{t = table, n, min, eTable, head},
n = t[[1, -1, 1]] / 2;
min = t[[1, 2, 1]];
If[min <= 0, n++;
n += Abs[min] / 2];
eTable = Table[t[[1, 2 i]], {i, 1, n + 1}];
head = Range[t[[1, 1, 2]], t[[1, 1, -1]]];
PrependTo[head, "q\s"];
PrependTo[eTable, head];
Grid[eTable, Frame -> All] ]

AKhTable[L_PD, a_List, opts___] :=
 condense[KhTable[AKh[L, a, opts]]]
```

In[21]:=
```
AKhTable[K, {1, 4}]
```

```
Betti[0,1,-2] = 1
Betti[0,1,0] = 0
Betti[0,1,2] = 0
Betti[0,3,-2] = 0
Betti[0,3,0] = 1
Betti[0,3,2] = 0
Betti[0,5,-2] = 0
Betti[0,5,0] = 0
Betti[0,5,2] = 1
Betti[1,3,0] = 0
Betti[1,5,0] = 1
Betti[2,3,0] = 0
Betti[2,5,0] = 1
Betti[2,7,0] = 0
Betti[3,3,0] = 0
Betti[3,5,0] = 0
Betti[3,7,0] = 0
Betti[3,9,0] = 1
```

Out[21]=

q\s	0	1	2	3
1	$\frac{1}{t^2}$	0	0	0
3	1	0	0	0
5	t^2	1	1	0
7	0	0	0	0
9	0	0	0	1

We note, as a concluding remark, that leaving the ray information empty returns us the Khovanov homology of our link when embedded in S^3:

In[22]:= **AKhTable[K, {}]**

```
Betti[0,1,0] = 1
Betti[0,3,0] = 1
Betti[0,5,0] = 0
Betti[1,3,0] = 0
Betti[1,5,0] = 0
Betti[2,3,0] = 0
Betti[2,5,0] = 1
Betti[2,7,0] = 0
Betti[3,3,0] = 0
Betti[3,5,0] = 0
Betti[3,7,0] = 0
Betti[3,9,0] = 1
```

Out[22]=

q\s	0	1	2	3
1	1	0	0	0
3	1	0	0	0
5	0	0	1	0
7	0	0	0	0
9	0	0	0	1

Bibliography

[1] James W. Alexander, *A lemma on systems of knotted curves*, Proceedings of the National Academy of Sciences, 9(3):93-95, 1923

[2] Marta M. Asaeda, Józef H. Przytycki and Adam S. Sikora, *Categorification of the Kauffman bracket skein module of I-bundles over surfaces* Algebraic & Geometric Topology, 4(2):1177-1210, 2004

[3] John A. Baldwin, *On the spectral sequence from Khovanov homology to Heegaard Floer homology*, International Mathematics Research Notices, 2011(15):3426-3470, 2011

[4] John A. Baldwin and J. Elisenda Grigsby, *Categorified invariants and the braid group*, Proceedings of the American Mathematical Society, 143(7):2801-2814, 2015

[5] Carl Bankwitz and Hans Georg Schumann, *Über viergeflechte*, Abhandlungen aus dem Mathematischen Seminar der Universität Hamburg, 10(1):263-284, 1934

[6] John Berge, *Some knots with surgeries yielding lens spaces*, Unpublished manuscript

[7] Michel Boileau and Luisa Paoluzzi, *On cyclic branched coverings of prime knots*, Journal of Topology, 1(3):557-583, 2008

[8] Maciej Borodzik and Wojciech Politarczyk *Khovanov homology and periodic links*, arXiv:1807.08795, 2017.

[9] Dror Bar-Natan, *On Khovanov's categorification of the Jones polynomial*, Algebraic & Geometric Topology, 2(1):337-370, 2002

[10] Dror Bar Natan, *Khovanov's homology for tangles and cobordisms*, Geometry & Topology, 9(3):1443-1499, 2005

[11] Michael Berglund, Jason Cantarella, Meredith Perrie Casey, Ellie Dannenberg, Whitney George, Aja Johnson, Amelia Kelly, Al LaPointe, Matt Mastin, Jason Parsley, Jacob Rooney, Rachel Whitaker, *Intrinsic symmetry groups of links with 8 and fewer crossings*, Symmetry, 4(1):143-207, 2012

[12] Abhijit Champanerkar and Ilya Kofman, *Spanning trees and Khovanov homology*, Proceedings of the American Mathematical Society, 137(6):2157-2167, 2009

[13] Nafaa Chbili, *Equivariant Khovanov homology associated with symmetric links*, arXiv:math/0702359, 2007

[14] Timothy Y. Chow *You could have invented spectral sequences*, Notices of the AMS, 53:15-19, 2006

[15] Peter R. Cromwell, *Knots and links*, Cambridge University Press, 2004

[16] M. Culler, N. M. Dunfield, M. Goerner, and J. R. Weeks, *SnapPy, a computer program for studying the geometry and topology of 3-manifolds*, `http://snappy.computop.org`

[17] Shalom Eliahou, Louis H. Kauffman, and Morwen B. Thistlethwaite, *Infinite families of links with trivial Jones polynomial*, Topology, 42(1):155-169, 2003

[18] Stefan Friedl, András Juhász and Jacob Rasmussen, *The decategorification of sutured Floer homology*, Journal of Topology, 4(2):431-478, 2011

[19] David Gabai, *Foliations and the topology of 3-manifolds*, Journal of Differential Geometry, 18(3):445-503, 1983

[20] J.Elisenda Grigsby and Yi Ni, *Sutured Khovanov homology distinguishes braids from other tangles*, arXiv:1305.2183v2, 2013

[21] J.Elisenda Grigsby, Anthony M. Licata, and Stephan M. Wehrli, *Annular Khovanov-Lee homology, braids, and cobordisms*, arXiv:1612.05953, 2016

[22] J.Elisenda Grigsby and Stephan M. Wehrli, *On the coloured Jones polynomial, sutured Floer homology, and knot Floer homology*, Advances in Mathematics, 223(6):2114-2165, 2010

[23] J.Elisenda Grigsby and Stephan M. Wehrli, *Khovanov homology, sutured Floer homology, and annular links*, Algebraic & Geometric Topology, 10(4):2009-2039, 2010

[24] J.Elisenda Grigsby and Stephan M. Wehrli, *On the naturality of the spectral sequence from Khovanov homology to Heegaard Floer homology*, International Mathematics Research Notices, 21:4159-4210, 2010

[25] J.Elisenda Grigsby and Stephan M. Wehrli, *On gradings in Khovanov homology and sutured Floer homology*, Topology and geometry in dimension three, 560:111-128, 2011

[26] Richard Hartley *Knots and Involutions*, Mathematische Zeitschrift, 171(2):175-185, 1980

[27] Richard Hartley, *Knots with free period*, Canadian Journal of Mathematics, 33(1):91-102, 1981

[28] Allen Hatcher, *Algebraic Topology*, Cambridge University Press, 2002

[29] Matthew Hedden and Yi Ni, *Manifolds with small Heegaard Floer ranks*, Geometry & Topology, 14(3):1479-1501, 2010

[30] Shawn R. Henry and Jeffrey R. Weeks, *Symmetry groups of hyperbolic knots and links*, Journal of Knot Theory and Its Ramifications, 1(2):185-201, 1992

[31] Hilary Hunt, Hannah Kesse, Anthony Licata, Scott Morrison, *Computing annular Khovanov homology*, arXiv:1505.04484, 2015

[32] Boju Jiang, Xiao-Song Lin, Shicheng Wang and Ying-Qing Wu, *Achirality of knots and links*, Topology and its Applications, 199:185-208, 2002

[33] Gyo Taek Jin, *On Kojima's η-function of links*, Differential Topology, 14-30, 1988

[34] Vaughan F. R. Jones. *A polynomial invariant for knots via Von Neumann algebras*, Bulletin of the American Mathematical Society, 12:103-112, 1985

[35] András Juhász, *Holomorphic discs and sutured manifolds*, Algebraic & Geometric Topology, 6(3):1429-1457, 2006

[36] Louis H. Kauffman, *State models and the Jones polynomial*, Topology, 26(3):395-407, 1987

[37] Teruhisa Kadokami, *Amphicheiral links with special properties II*, Journal of Knot Theory and its Ramifications, 21(6):1250047, 2012

[38] Akio Kawauchi, *A Survey of Knot Theory*, Birkhäser Verlag, 1996

[39] Hannah Kesse, *Current algebras, categorification and annular Khovanov homology* Bachelor's Thesis (ANU): avaliable at: `https://tqft.net/web/research/students/HannahKeese/thesis.pdf`, 2014

[40] Mikhail Khovanov, *A categorification of the Jones polynomial*, arXiv:math/9908171, 1999

[41] Mikhail Khovanov, *Patterns in knot cohomology, I.*, Experimental mathematics, 12(3): 365-374, 2003

[42] Mikhail Khovanov, *Categorifications of the colored Jones polynomial* Journal of Knot Theory and its Ramifications, 14(1):111-130, 2005

[43] *The Knot Atlas*, `http://katlas.org/wiki/Main_Page`

[44] Kouzi Kodama and Makoto Sakuma, *Symmetry groups of prime knots up to 10 crossings*, Knots 90:323-340, Walter de Gruyter, 1990

[45] Sadayoshi Kojima, *Finiteness of symmetries on* 3*-manifolds*, Transformation groups and representation theory: 1-5, Kyoto University Research Institute for Mathematical Sciences, 1983

[46] Sadayoshi Kojima and Masayuki Yamasaki, *Some new invariants of links*, Inventiones mathematicae, 54(3):213-228, 1979

[47] Peter B. Kronheimer, and Tomasz S. Mrowka, *Khovanov homology is an unknot detector*, Publications mathématiques de l'LHÉS, 113(1):97-208, 2011

[48] Eun Soo Lee, *An endomorphism of the Khovanov invariant*, Advances in Mathematics, 197(2):554-586, 2005

[49] Giovanna Le Gros, *The Khovanov homology of knots*,
Master's Thesis (Victoria University of Wellington): avaliable at:
`http://hdl.handle.net/10063/4901`, 2015

[50] W.B. Raymond Lickorish, *Prime knots and tangles*, Transactions of the American Mathematical Society, 267(1):321-332, 1981

[51] Feng Luo, *Actions of finite groups on knot complements*, Pacific Journal of Mathematics, 154(2):317-329, 1992

[52] Ciprian Manolescu, Peter Ozsváth, Zoltán Szabó, and Dylan P. Thurston, *On combinatorial link Floer homology*, Geometry & Topology, 11(4):2339-2412, 2007

[53] John McCleary, *A user's guide to spectral sequences*, Cambridge University Press, 2001

[54] Yoshihiko Marumoto, *Relations between some conjectures in knot theory*, Mathematics seminar notes, Kobe University, 5(3):377-388, 1977

[55] William Menasco, *Closed incompressible surfaces in alternating knot and link complements*, Topology, 23(1):37-44, 1984

[56] William Menasco and Morwen Thistlethwaite (editors), *Handbook of knot theory*, Elsevier, 2005

[57] John Milnor, *Infinite cyclic coverings*, Conference on the Topology of Manifolds, Prendle, Weber and Schmidt, 115-133, 1968

[58] John W. Morgan and Hyman Bass, *The Smith Conjecture*, Pure and Applied Mathematics 112, 1984.

[59] Kunio Murasugi, *On periodic knots*, Commentarii Mathematici Helvetici, 46(1):162-174, 1971

[60] Kunio Murasugi, *Jones polynomials and classical conjectures in knot theory. II*, Mathematical Proceedings of the Cambridge Philosophical Society, 102(2):317-318, 1987

[61] Kunio Murasugi, *Jones polynomials of periodic links* Pacific Journal of Mathematics, 131(2):319-329, 1988

[62] Yi Ni, *Homological actions on sutued Floer homology*, arXiv:1010.2808, 2010

[63] Richard P. Osborne, *Knots with Heegaard genus 2 complements are invertible*, Proceedings of the American Mathematical Society, 81(3):501-502, 1981

[64] Peter Ozsváth and Zoltán Szabó, *Holomorphic disks and knot invariants*, Advances in Mathematics, 1(186):58-116, 2004

[65] Peter Ozsváth and Zoltán Szabó, *Holomorphic disks and genus bounds*, Geometry &. Topology, 8(1):311-334, 2004

[66] Peter Ozsváth and Zoltán Szabó, *On the Heegaard Floer homology of branched double-covers*, Advances in Mathematics, 194(1):1-33, 2005

[67] Luisa Paoluzzi and Makoto Sakuma, *Prime amphicheiral knots with free period 2*, arXiv:1804.03188, 2018

[68] Adrián Jiménez Pascual, *On Lassos and the Jones polynomial of satellite knots*, Master's Thesis (University of Tokyo), arXiv:1501.01734v2, 2015

[69] Wojciech Politarczyk, *Equivariant Khovanov homology of periodic links*, arXiv:1504.00376, 2015

[70] Józef H. Przytycki, *Skein modules of* 3*-manifolds*, Bulletin of the Polish Academy of Sciences: Mathematics, 39(1-2):91-100, 1991

[71] Józef H. Przytycki, *Symmetric knots and billiard knots*, arXiv:math/0405151, 2004

[72] Jacob Rasmussen, *Floer homology and knot complements*, arXiv:math/0306378, 2003

[73] Jacob Rasmussen, *Khovanov homology and the slice genus*, Inventiones mathematicae, 182(2):419-447, 2010

[74] Kurt Reidemeister, *Elementare begrundung der knotentheorie*, Abhandlungen aus dem Mathematischen Seminar der Universität Hamburg, 5(1):24-32, 1927

[75] Lawrence P. Roberts, *Notes on the Heegaard-Floer link surgery spectral sequence*, arXiv:0808.2817, 2008

[76] Lawrence P. Roberts, *On knot Floer homology in double branched covers*, Geometry & Topology, 17(1): 413-467, 2013

[77] Dale Rolfsen, *Knots and Links*, Publish or Perish, 1976

[78] Joseph J. Rotman, *Advanced Modern Algebra*, American Mathematical Society, 2010

[79] Makoto Sakuma, *On strongly invertible knots*, Algebraic and Topological Theories..., 176-196, 1985

[80] Makoto Sakuma, *Uniqueness of symmetries of knots*, Mathematische Zeitschrift, 192(2):225-242, 1986

[81] Makoto Sakuma, *Non-free-periodicity of amphicheiral hyperbolic knots* Homotopy Theory and Related Topics, 189-194, 1987

[82] Makoto Sakuma, *Realisation of the symmetry groups of links*, Transformation Groups, 291-306, 1989

[83] Horst Schubert, *Knoten mit zwei Brücken*, Mathematische Zeitschrift, 65(1):133-170, 1956

[84] Alexander Shumakovitch, *Torsion of the Khovanov homology*, arXiv:math/0405474, 2004

[85] Peter G. Tait, *On knots I, II, III*, Scientific Papers(1), Cambridge, 273-347, 1898

[86] Morwen B. Thistlethwaite, *A spanning tree expansion of the Jones polynomial*, Topology, 26(3):297-309, 1987

[87] Morwen B. Thistlethwaite, *Kauffman's polynomial and alternating links*, Topology, 27(3):311-318, 1988

[88] William P. Thurston, *Three-dimensional geometry and topology*, Princeton University Press, 1997

[89] Hale F. Trotter, *Non-invertible knots exist*, Topology, 2(4):275-280, 1963

[90] Vladimir G. Turaev, *The Conway and Kauffman modules of the solid torus*, Journal of Soviet Mathematics, (52):2799-2805, 1990

[91] Liam Watson, *Surgery obstructions from Khovanov homology*, Selecta Mathematica, 18(2):417-472, 2012

[92] Liam Watson, *Khovanov homology and the symmetry group of a knot*, Advances in Mathematics, 313:915-946, 2017

[93] Liam Watson, *Instagram.com: @mathonmydeskrightnow*, Available at: `https://www.instagram.com/mathonmydeskrightnow/` [Accessed 25 Jul. 2018].

[94] Jeffery R. Weeks, *Convex hulls and isometries of cusped hyperbolic 3-manifolds*, Topology and its Applications, 52(2):127-149, 1993

[95] Stephan Wehrli, *A spanning tree model for Khovanov homology*, Journal of Knot Theory and its Ramifications, 17(12):1561-1574, 2008

[96] Charles A. Weibel, *An introduction to homological algebra*, Cambridge university press, 1995

[97] Wilbur Whitten, *Symmetries of links*, Transactions of the American Mathematical Society, 135:213-222, 1969

[98] Wilbur Whitten, *Inverting Double Knots*, Pacific Journal of Mathematics, 97(1):209-216, 1981

[99] Yoshiyuki Yokota, *The Kauffman polynomial of periodic knots*, Topology, 32(2):309-324, 1993

[100] Melissa Zhang, *A rank inequality for the annular Khovanov homology of 2-periodic links* Algebraic & Geometric Topology, 18(2):1147-1194, 2018

[101] Bruno Zimmerman, *On hyperbolic knots with homeomorphic cyclic branched coverings* Mathematische Annalen, 311(4):665-673, 1998